Numerical Modelling of the behaviour of stone and composite stone columns in soft soils

Stuart Law

Thesis submitted for the Degree of Doctor of Philosophy in the School of Energy, Geoscience, Infrastructure and Society,

Heriot-Watt University

March 2015

Electronic E-thesis

Numerical Modelling of the behaviour of stone and composite stone columns in soft soils

Stuart Law

Abstract

The use of stone columns as a means of ground improvement has been in use for over 40 years in the United Kingdom and Europe. Their primary purpose is to reduce settlement, reduce consolidation time and increase the bearing capacity of soils. Currently the technique is applied to a variety of soil types, cohesive and granular. Soft cohesive soils have shown a tendency towards higher settlements due to the inability of the soil to restrain the lateral movement or bulging of stone columns.

Current analytical design methods are based upon the unit concept which considers a stone column to be part of an infinite array of columns. Such methods have proved useful when designing large arrays such as those utilised beneath embankments or large rafts. Columns within the group are restrained equally on all sides and held in the same vertical stress conditions. However, at the edge of large (wide) load areas and in smaller foundation configurations columns are not generally restrained on all sides by other columns and must rely on the soil to provide restraint in the outward facing directions. The behaviour of small foundation configurations is more complex due to this lack of restraint with columns subject to deformation at lower stress levels than those in infinite arrays.

This dissertation is concerned with the behaviour of stone columns and proposed composite stone columns installed in soft clay. This research compares the behaviour of small foundations supported by stone columns to behaviour within an infinite array of columns. Specifically the settlement and deformation behaviour of stone columns are considered to identify the main deformation mechanisms and to examine the effect of key design parameters and soft cohesive soils on column performance. A new form of composite stone column was then examined numerically to assess the potential for enhanced column behaviour and settlement reduction.

PLAXIS 3D Foundation is utilised with column behaviour represented by the Mohr-Coulomb Perfect Plasticity model and the Hardening Soil model adopted to model soil behaviour. The soft soil profile adopted in this research is the well characterised Bothkennar soft clay site which was formerly the UK geotechnical test bed. The influence of key stone column design parameters, area ratio, column length, column

confinement and arrangement, column stiffness, column strength, installation effects and the effect of stiff crust thickness was examined for a combination of foundation types with 432 numerical sensitivity studies conducted.

The results reveal that area ratio and column length have a significant impact on the settlement performance of stone columns. Increasing the area ratio was found to reduce the restraint provided by neighbouring columns leading to increased settlement. Increasing column length was found to reduce settlement. When columns were modelled with low area ratios increasing column length had a greater effect on settlement reduction than at higher ratios.

The design parameters of area ratio and column length are established as the controlling parameters for the mode of deformation. The mode of deformation was examined utilising settlement inferred deformation ratios (compression and punching) with comparison to total shear strain plots and stress states in the column. Two primary modes of deformation, bulging and punching (including sub-type termed 'block failure') were inferred. Punching failure was inferred for short columns by high punching ratios and low compression ratios with a concentration of shear strain observed at the base of the floating columns. A sub-type of punching, block failure, was inferred from low compression and low punching ratios for closely spaced columns with low area ratios in which the columns act as one unit punching into the underlying soil. Bulging failure was inferred by low punching ratios and high compression ratios coupled with a concentration of shear strain in upper region of the columns. The magnitude of bulging was found to be at its most severe for high area ratios. Bulging as a mode of failure occurred for column length to diameter ratios greater than 4 and area ratios greater than 8. Bulging was found to occur at the weakest of the soil profile which coincides with the top of the lower Carse clay.

Consideration was given to a method of reducing the potential for lateral column deformation or bulging by the use of a novel composite column. The deformational characteristics of a stone column were identified for a composite of granular and the experimental Protomix materials. Laboratory testing was carried out to gain an understanding of the cohesive, stiffness and unconfined compressive strength properties of the composite before simulation studies were performed on key design parameters such as area ratio, column length, column confinement and arrangement for a combination of foundation types with 108 numerical analysis sensitivities conducted.

The inclusion of a cohesive 'binder' material in the bulging zone was found to reduce settlement for all foundation configurations. Similarly to stone columns area ratio and column length were found to be the design parameters which influenced the results most.

The composite stone columns (CSC) offered higher settlement reduction than traditional stone columns (SC). It was discovered that CSC with an area ratio of 8 were able to achieve the same settlement improvement factor as those with a ratio of 3.5 which suggests the columns could offer the same settlement control but with large column spacing's making their use more economical.

The settlement inferred deformation ratios (compression and punching) were studied while monitoring the total shear strain field cross sections to examine if composite stone columns would behave similarly to a stone column. It was noted that the same modes of deformation of punching (including block failure) and bulging failure were observed. The increased stiffness in the bulging zone saw the transfer of bulging type effects to a depth below the composite treated zone. It was only observed for high area ratios. The improved settlement behaviour of CSC compared to SC is due to the treatment of the bulging zone by CSC and improved column restraint at depth provided by the soil. Punching failure was found to have a higher magnitude and occur to a deeper depth of 3.6 m compared to SC depth of 2.4 m due to the addition of the composite material. The modes of deformation observed for SC were also observed for the new novel CSC columns. This suggests that the same type of foundations can be used and so avoid the need for reinforcement of the foundations as used with piled foundations.

"Nothing happens to any man that he is not formed by nature to bear"

Marcus Aurelius Antoninus Augustus

In memory of those that I have lost and the many challenges that have been overcome. I now live my life for those who have given me so much love and happiness.

Stuart Law

Acknowledgements

I wish to thank my university supervisor, Professor Peter K. Woodward for the opportunity to carry out the investigations detailed in this thesis. His support and encouragement during this research has been greatly appreciated.

I wish to thank my industry supervisor David Preece CEng for the opportunity to carry out the investigations detailed in this thesis. His support and encouragement during this research has been greatly appreciated. I would also like to thank Marc Evans, Technical Director of Pennine Vibropiling and Balfour Beatty Ground Engineering for sponsoring this research.

I would also like to thank the technical staff and David Haldane who helped with the laboratory testing reported in this thesis. In particular I wish to thank Alistair Macfarlane and Tom Scott who assisted in the setup of the testing equipment.

The research would not have been possible without the generous donation of testing materials. In particular, I would like to thank the following:

- Penning Vibropiling for the supply of cementacious materials and large aggregates.
- Castle Cement for the supply of the Protomix and experimental materials. Also the long term loan of the high shear mixer was appreciated.
- Scotash for the supply of the pulverized fly ash and similar products.
- Fife silica sands for the supply of gravel
- Pavement Technology Limited (PTL) for the donation of sieves

I would like to thank my family for their emotional and financial support during this research. My immediate family has sacrificed so much family time in order for me to complete this work.

ACADEMIC REGISTRY

Research Thesis Submission

Name*:*	Stuart Law		
School/PGI:	School of the Built Environment		
Version: *(i.e. First, Resubmission, Final)*	Final	Degree Sought (Award **and** Subject area)	Doctor of Philosophy Civil Engineering

Declaration

In accordance with the appropriate regulations I hereby submit my thesis and I declare that:

1) the thesis embodies the results of my own work and has been composed by myself
2) where appropriate, I have made acknowledgement of the work of others and have made reference to work carried out in collaboration with other persons
3) the thesis is the correct version of the thesis for submission and is the same version as any electronic versions submitted*.
4) my thesis for the award referred to, deposited in the Heriot-Watt University Library, should be made available for loan or photocopying and be available via the Institutional Repository, subject to such conditions as the Librarian may require
5) I understand that as a student of the University I am required to abide by the Regulations of the University and to conform to its discipline.

* *Please note that it is the responsibility of the candidate to ensure that the correct version of the thesis is submitted.*

Signature of Candidate*:*		Date:	

Submission

Submitted By *(name in capitals):*	
Signature of Individual Submitting:	
Date Submitted:	

For Completion in the Student Service Centre (SSC)

Received in the SSC by *(name in capitals):*			
Method of Submission *(Handed in to SSC; posted through internal/external mail):*			
E-thesis Submitted (***mandatory for final theses)***			
Signature:		Date:	

Table of Contents

Chapter Five

List of Figures

List of Tables

Nomenclature

The following abbreviations and symbols are used in this thesis. Where practical the symbols have been standardised from specific publications to those below.

Abbreviation

ASTM	American society for testing and materials
BS	British standard
CMC	Constant modulus columns
CPT	Cone penetration test
CSC	Composite stone columns
DR	Drained analysis
FEA	Finite element analysis
FEM	Finite element method

HS	Hardening soil model
LOI	Loss on ignition
MC	Mohr-Coulomb perfect plasticity model
OCR	Over-consolidation ratio
PI	Plasticity Index
PFA	Pulverised fuel ash
SC	Stone columns
UC	Undrained-consolidation analysis
UCS	Unconfined compressive strength
vf	Very fine mesh
2D	Two dimensions
3D	Three dimensions

Symbols

a	Unit cell radius
a/d_s	Distance from column axis
A	Area of the soil per column in a large grid (also known as area of the foundation in unit cell or rectangular grid spacing)
A_c	Cross sectional area of the stone column
A/A_c	Area ratio
A_c/A	Area replacement ratio (after Priebe, 1995)
A_s	Area replacement ratio (after Barksdale and Bachus 1983)
A_o	Original sample cross sectional area
A'	Effective sample cross sectional area
b	Unit cell radius
α	Gradient of the slope of the line for each L/H ratio
α_c	Ratio of stress in clay to average stress over a tributary area
B	Breadth of the foundation
c	Cohesion

c'	Effective cohesion
c_u	Undrained cohesion
c_i	Cohesion of the interface
c_{avg}	Average cohesion
C_c	Compression index
C_s	Swelling index
C_k	Permeability change index
d_e	Diameter of the unit cell
d/D	depth to diameter ratio
d	Diameter of the column
d_e/d	Ratio of the diameter of the unit cell to the diameter of the column
D	Diameter of a circular footing
D_c	Density of the column
D_s	Density of the soil
e_0	Initial void ratio
E	Young's modulus (also referred to as the stiffness)
E_{chord}	Chord modulus of elasticity (in psi)
E_{col}	Young's modulus of the column
E_{soil}	Young's modulus of the soil
$E_m/E_{m,initial}$	Ménard moduli
E_P	Young's modulus of a pile
E_{50}	Secant Young's modulus at 50% deviatoric stress
E_{50}^{ref}	Reference Young's modulus for primary loading
E_{oed}	Young's modulus from oedometer
$E_{oed,i}$	Young's modulus oedometric modulus for the interface
E_{oed}^{ref}	Reference Young's modulus from oedometer
E_{ur}	Young's modulus for unload-reload

E_{ur}^{ref}	Reference Young's modulus for unloading-reloading
E_{col}/E_{soil}	Modular ratio of column to soil Young's modulus (or stiffness ratio)
E_c/E_s	Modular ratio of column to soil Young's modulus (or stiffness ratio)
f_d	Depth factor (after Priebe, 1995)
g	Grain size
G	Shear modulus
G_i	Shear moduli of the interface
H	Thickness of the soil deposit
h	Depth of the soil layer
I_L	Liquidity index
I_P	Plasticity index
k	Permeability
K_o or K_{oc}	Coefficient of lateral earth pressure at rest
$K_{o,initial}$	Initial coefficient of lateral earth pressure at rest
K_A	Coefficient of active earth pressure
K_P	Coefficient of passive earth pressure
$K_{measured}$	Measured coefficient of earth pressure
K_s	Modulus of the sub-grade reaction
K_{ho}/K_{vo}	Anisotropy ratio of horizontal to vertical K_o
L	Length
L_0	Initial sample length
ΔL	Change in sample length
L/H	Ratio of column length to thickness of the soil deposit
L/d	Normalised column length (or length to diameter ratio)
L_1	Layer 1
L_2	Layer 2
L_3	Layer 3

L_4	Layer 4
L_5	Layer 5
m_v	Coefficient of compressibility
m_c	Slope of critical state line in compression
m_e	Slope of the critical state line in extension
n	Stress concentration ratio
n_{col}	Stress concentration in the column
n_{soil}	Stress concentration in the soil
n_{max}	Maximum ground improvement factor (after Priebe, 1995)
n_0	Basic improvement factor (after Priebe, 1995)
n_1	Improvement factor (after Priebe, 1995)
n_2	Final improvement factor (after Priebe, 1995)
n_{pred}	Predicted stress concentration ratio
n_{meas}	Measured stress concentration ratio
N_c	Bearing capacity factor a granular column
P_r	Punching ratio
P_{ref}	Reference pressure
P_c	Pressure in the column
P_s	Pressure in the soil
p	Total stress
p'	Mean effective stress
q	Deviatoric stress
q_c	Uncorrected tip resistance
R_f	Failure ratio
R_{inter}	Interface strength reduction factor
s	Spacing of columns
S	Consolidation settlement unimproved

S'	Consolidation settlement improved
S_c	Settlement of the column
S_s	Settlement of the soil
S_{uc}	Settlement of the unit cell
S/S_{uc} or S/S_∞	Settlement ratio
q_{ult}	Ultimate load
q_f	Ultimate deviatoric stress at failure
q_a	Asymptotic value of deviator stress
t	Curing time
u	Pore water pressure
U_y	Vertical displacement from Plaxis 3D Foundation
U_{col}	Vertical displacement from Plaxis 3D Foundation at the column base
U_{soil}	Average Vertical displacement of the soil around the base of the columns from Plaxis 3D Foundation
$U_{footing}$	Surface Vertical displacement from Plaxis 3D Foundation for footing
σ	average stress over the tributary area
σ_c	Stress in the clay
σ_s	Stress in the soil
σ_h	Horizontal stress
σ_v	Vertical stress
σ_1	Ultimate vertical stress
σ_3	Ultimate cavity pressure or lateral resistance of the soil
σ_a	Axial stress
σ_r	Radial stress
σ_{ro}	Total *insitu* lateral stress
σ_{rl}	Ultimate lateral stress
σ_n	Normal stress
τ	Shear stress

ε_1	Principal stress direction
ε_v	Volumetric strain
ε_h	Horizontal strain
ε_z	Vertical strain
ε_a	Axial strain
ε_r	Radial strain
φ	Friction angle
φ'	Effective friction angle
φ_i	Column friction angle of the interface
φ_c	Column friction angle
φ_s	Soil friction angle
φ_c	Friction angle in compression
φ_e	Friction angle in extension
ν	Poisson's ratio
ν_i	Poisson's ratio of the interface
γ_s	Unit weight of the soil
λ	Gradient of the normal compression line
κ	Slope of the swelling line
Δ	Change in a parameter or quantity

Units

cm	Centimetres
kg/m^3	Kilogram's per metre cubed
kN/m^2	Kilo Newton per metres squared
kPa	Kilo Pascal's
kPa/m	Kilo Pascal's per metre
mD	*Milidarcy*
D	*Darcy*
mm	Millimetres

mm/min	Millimetres per minute
mm/hr	Millimetres per hour
m	Metres
MPa	Mega Pascal's
ppm	Parts per million
psi	Pounds per square inch
™	Trademark

Terminology - Clarification

In this research topic two terms are commonly referred to as the area ratio and area replacement ratio. These terms are defined as:

- Area ratio: calculated by dividing the area of the foundation per column, *A*, by the area of the column, A_c.
- Area replacement ratio: calculated by dividing the area of the column, A_c, by the area of the foundation, *A*.

Area of Column, Ac (m)	Area of Foundation, A (m)	Area Ratio A/Ac	Area Replacement Ratio, Ac/A (Decimal)	Area Replacement Ratio, Ac/A (%)
0.2826	1.00	3.5	0.28	28%
0.2826	1.56	5.5	0.18	18%
0.2826	2.25	8.0	0.13	13%
0.2826	3.06	10.8	0.09	9%
0.2826	4.00	14.2	0.07	7%

Chapter 1

Introduction and aims of this research

1.1 Introduction

Granular or stone columns are a form of ground improvement which alters the *in situ* properties of the soil by the inclusion of circular columns composed of granular material which acts to reinforce and stiffen the soil. The increase in stiffness of this composite ground acts to reduce the settlement of foundations installed on the improved ground. The presence of the granular material in the soil offers unsaturated pore spaces between the grains into which pore water from the soil can drain which aids consolidation and reduces the time taken to reach equilibrium. Unlike piling or Vibrated Concrete Columns (VCC) where the load is carried by the pile, granular columns work in combination with the soil in what is referred to as a composite action. The composite action refers to a phenomena observed by Hughes & Withers (1974) in which this action is referred to as 'Stress-share' this describes a process by which the column and soil take a proportion of the applied load by the foundation. This degree of stress-share is primarily controlled by the stiffness ratio of the column to soil, the cohesion of the soil and the internal friction angle of the column components. The composite action of columns and soil working together is sometimes referred to as a "composite system".

The use of granular columns is common beneath raft and strip footings in the United Kingdom. Increasingly the availability of suitable land for construction is reducing due to green belt restrictions on construction. Developers are increasingly considering marginal soils sites such as brownfield or soft soils which traditionally would have been avoided due to high cost associated with development such as remediation and ground improvement. For domestic land use, such as housing, the use of piling techniques is not always economical due to their high cost. The use of Stone columns while offering a cost effective advantage, also provide direct physical benefits to the soil in terms of drainage and are usually within reach of tight construction budgets.

1.2 Application of granular columns to soft soils

Although columns are a great advantage in ground improvement in terms of cost, installation times and consolidation time reduction, they are limited in terms of their application by the soils on site. In soft soils their application is presently limited due to issues of column integrity. Piles have the genuine advantage in that they act

independently of the soil at shallow depths and they are able to bypass any soft or weak soil layers and transfer stress to depth by end bearing or skin friction.

Granular columns rely on the *in-situ* soil working in composite action or 'stress-share' to offer settlement control but if soft or weak layers are present the column may fail by one of four recognised mechanisms. The four mechanisms were defined by McKelvey *et al.* (2004) as bending; lateral bulging (horizontal); end bearing (or punching); and shear failure (shear plane). Of the four mechanisms described by McKelvey *et al.* (2004) three of them can generally be solved by design methods such as larger diameter or founding on firm layers. However, bulging failure remains a definite problem as the only solution would be very large diameters and area ratios which would increase costs significantly.

When granular columns are installed in soft soils 'stress-share' is not as efficient as with soils with higher shear strengths. In order for the composite system to function efficiently and reduce bulging failure potential the soil must restrain the column and in the process absorb a proportion of the stress. With soft soils the shear strength and stiffness of the surrounding soil is unable to restrain the column to the same degree. The stiffness ratio between column and soil will be higher for soft soils and stress share lesser between the two components. The soft soil will tend to deform increasing settlement. Generally granular or stone columns are not recommended for installation into soils with shear strengths less than 15kN/m² for this reason.

1.3 Purpose of this research

In soft soils the geometric configuration of granular columns installed at site is somewhat limited by the material properties of the *in-situ* soil. Soft soils typically soft clays have low shear strengths (less than 15kN/m²) and foundations installed tend to suffer from very large settlements. In such circumstances the design engineer must fully consider the suitability of such sites for construction of different foundation types. Large raft foundations with high loads should only be installed with piles beneath them since the performance of granular columns in such circumstances cannot be guaranteed because the soil is too weak to 'stress-share' between column and soil. It is also likely excessive settlements would occur at the edge of the raft as the outer columns would not benefit from group restraint.

The use of strip foundations underlain with granular columns has been investigated by Watts and Serridge (2000) and it is clear from load tests on soft clays at RSPB Bothkennar, formerly known as Science and Engineering Research Council (SERC) test bed Bothkennar, that strip footings in such clays suffer large settlements when loaded to 125kN/m². Granular columns in such instances do not benefit from mutual support of surrounding columns and their performance is dependent largely upon column and soil properties. It is clear from Watts and Serridge (2000) that high loads cannot be supported in such configurations in soft clays since performance requirements for foundations generally specify no greater than 25mm total settlement. Tomlinson (2001) considers that for strips of 1m width founded to a depth of 1m, on normally consolidated soils with shear strength in the range of 20-40kN/m², the maximum specified load should be no more than 50-100kN/m². It is clear that for soft soils the maximum unimproved upper load is likely to be closer to 50kN/m² which would be typical of lightly loaded foundations used for accommodation or low bearing commercial or industrial buildings.

This research shall consider the performance of single column, 1x3 column strip, and 3x3 column raft foundations installed in soft clays. This research proposes an approach to limiting the problem of bulging of granular columns and so extending their use to soft soils by the use of novel hybrid granular columns in the bulging zone (two to three column diameters) and over the length of a granular column.

In this research consideration is given to the addition of cementicious binder materials to granular material to overcome the limitations of application of granular columns to soft soils. The effect of this material on column performance will be examined by laboratory testing and numerical analysis where possible. The aims of this research are described as follows:

1. Examine the settlement and deformation behaviour of stone columns beneath different foundation configurations to understand the influence of key design parameters

2. Investigate a means by which the bulging or lateral failure mechanism for stone columns installed beneath a strip foundation can be minimised.

3. Examine numerically how a new improved stone column will behave in terms of settlement and deformational behaviour. Crucially determine if the new improved stone column still behaves the same as a stone column with enhanced settlement control.

1.4 Structure of this Thesis

The scope of this thesis covers the development of a numerical model to represent the behaviour of the Bothkennar clay and stone columns installed beneath small pad, raft and strip foundations. The use of a binder material to reduce the settlement of stone columns is studied in the laboratory and the results used to numerically model the behaviour of new novel composite stone columns. The thesis is divided into eight chapters.

Chapter 1 is a general introduction to this study. It describes stone columns and their general use.

Chapter 2 reviews the published literature concerning the laboratory, field and numerical modelling in the context of the behaviour of stone columns. Current design methods for stone columns are reviewed.

Chapter 3 examines the geological and geotechnical properties of the Bothkennar soil reported in the literature to create a soil profile for use in the Hardening Soil model of Plaxis 3D Foundation.

Chapter 4 reports calibration checks performed to assess the effect of mesh coarseness, column interfaces and boundaries on the numerical solution. Two field trials of a pad and strip foundation carried out at Bothkennar are modelled in Plaxis 3D Foundation to validate the soil profile. A comparison is made of the performance of Plaxis 3D Foundation versus analytical methods for a unit cell configuration.

Chapter 5 reports a sensitivity analysis carried out for a unit cell, pad, strip and raft foundation using Plaxis 3D Foundation. The effect of foundation configuration, column strength and stiffness, crust thickness and column installation effects are examined. The settlement behaviour, deformation ratios and shear stress are compared for different foundation configurations.

Chapter 6 reports the results of laboratory testing in the shear box of granular material and the selection and testing of the binder material for composite stone columns.

Chapter 7 predicts the behaviour of proposed novel composite stone columns for strip and raft configurations. The results are compared to the stone column modelling of Chapter 5 in terms of settlement behaviour, deformation ratios and shear stress.

Chapter 8 reviews the results of this thesis in the context of the published literature and proposes a new simplified design method to allow settlements calculated using unit cell methods, to be adjusted for smaller groups of columns.

Chapter 9 presents the conclusions of this thesis and suggestions are made for further work.

Chapter 2

Review of the literature

2.1 Introduction

Ground improvement by granular or stone columns offers three key benefits to the soil in terms of increasing bearing capacity, reducing consolidation times and reducing total settlement. They can be applied to both cohesive and granular soils. Granular or stone column construction was described by Bachus and Barksdale (1984) as "The partial replacement or displacement of weak and/or compressible subsurface soils with a compacted vertical column of stone that completely penetrates the weak strata". This definition describes the columns very well since by introducing a denser material the intention is to reduce the compressibility and increase stiffness. The usage of this technique has become more prominent in recent times but the first recorded use was in 1830 in France when they were installed in soft estuarine deposits to control settlements allowing the installation of a heavy structure (Moreau and Mary, 1835).

Granular or stone columns offer key advantages in terms of construction times and cost of installation over conventional piling techniques but are limited because of the interactive nature of column and soil. The degree of improvement is controlled not only by the columns themselves but by the soil composition and geotechnical properties. Granular or stone columns, work well in granular soils, and in cohesive soils with shear strengths above 15kPa. However, in soft soils where the shear strength is lower granular columns tend to suffer a specific type of failure, known as bulging or lateral failure. This failure type is a symptom of the breakdown of the composite system in this technique, which relies on the combination of stone column and soil working together to stress-share the applied load. When the load exceeds the ultimate bearing capacity of the column the stress concentration in the column causes the column to bulge laterally.

This chapter reviews the recent developments in terms of understanding the behaviour of granular columns in field, laboratory and numerical studies, as a basis to the research carried out in this thesis. For the purposes of simplification the terms 'granular' and 'stone' columns are considered the same, as this thesis is primarily examining the stress-strain behaviour and not drainage.

2.2 Installation methods of granular columns

Installation of granular columns in Europe and the Americas by vibroflotation is a commonly used technique. It offers quick installation times and good quality control assuming the rig is operated by an experienced professional.

2.2.1 Vibroflotation equipment and column compaction

Vibroflotation equipment has been described by various authors (Greenwood and Kirsch, 1984; Baumann and Bauer, 1974; Goughnour and Bayuk, 1979:1,2). The equipment consists of a Vibroflot suspended from a crane (Figure 2.1). The Vibroflot is lowered and by its weight is able to penetrate the soil assisted usually by air or water jets present at the tip and at various points along the Vibroflot. The purpose of the Vibroflot is two-fold: Firstly the creation of the hole to allow filling with stone; Secondly it is used to compact the stone column and create a solid skeleton composed of aggregates/ gravel.

Figure 2.1 Vibro rig for installation of bottom feed stone columns (Fayat, 2013)

2.2.2 Installation techniques

Granular columns can be formed by a number of different techniques which include Vibroflotation, rotary drive and others. Consideration is now given to the main installation techniques that are presently used throughout the world. Note that the Compozer method although strictly not a granular (aggregate/gravel) column technique, is included to illustrate similar methods which can be used.

In ground engineering practice most contractors are now installing stone columns by Vibro-displacement due to the speed of installation and because the systems run on air, this means no fluid or spoil is created which requires costly disposal. The development of bottom feed systems with Tremie tube stone delivery to the tip of the Vibroflot means that columns can be formed in soft sensitive soils without the need for removal of the Vibroflot and hence the risk of borehole collapse is minimised.

Vibro-displacement and vibro-replacement

Bachus and Barksdale (1984), Baumann and Bauer (1974) and Greenwood (1970) describe the different methods of ground improvement by Vibro systems. Broadly speaking two methods are currently in use; namely Vibro-displacement and Vibro-replacement. Both techniques have the same purpose of installing stone columns which will improve stability, reduce settlements, dissipate pore pressures and accelerate consolidation times. The use of each method is dependent upon site conditions (particularly for weak soils). Each method has its benefits and drawbacks and should be chosen according to appropriate soil conditions.

Bachus and Barksdale (1984) stated that stone column construction involves the partial replacement or displacement of weak and/or compressible subsurface soils with a compacted vertical column of stone that completely penetrates the weak strata. Both construction methods create a hole in the weak strata with a Vibroflot or poker which is then infilled with stone either from the end of the Vibroflot or tipped downhole from the surface directly.

Vibro-displacement methods involve the creation of a hole in weak strata by the advancement of a Vibroflot by hydraulic means or by the eccentric weight of the Vibroflot itself (Figure 2.2). The exact method varies from contractor to contractor. Pennine Vibropiling systems incorporate the use of Vibroflot weight and/ or by hydraulic drive. The action of the Vibroflot on the weak strata causes the soil to displace laterally forming a hole or void which can then be infilled. Greenwood and Kirsch (1984) suggests this method is applicable in stable insensitive soil conditions with shear strengths of 30 to 60kN/m^2.

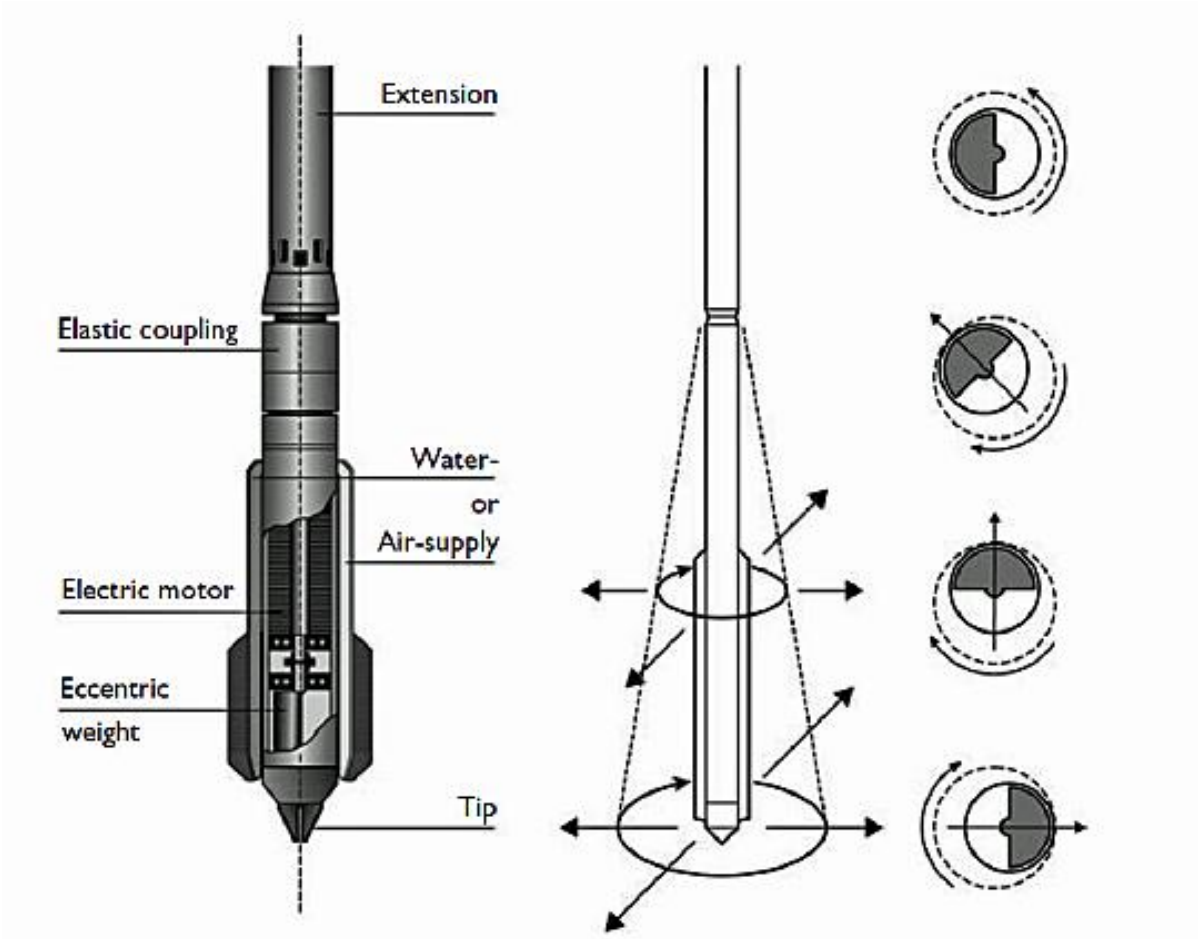

Figure 2.2 Vibroflot and principle of vibro-compaction (Sondermann and Wehr, 2004)

Vibro-replacement methods differ from displacement methods because they rely on the use of water or air jets built into the Vibroflot or poker. The eccentric weight of the Vibroflot aids the jets which push down into the soil scouring out the weak strata. Once the desired depth is reached the jetting pressure is increased in several cycles in what has become known as "surging" to clean the newly created void or hole of debris. It is vital in situations where cohesive soils are involved that no material is left in the hole or loose on the sidewall which could enter the column during construction so as to have a detrimental effect on the column friction angle. Research by McKelvey *et al.* (2004) suggests fines can reduce column strength by reducing the inter-granular friction angle. It is vital during this method that the water or air is kept flowing to maintain hole integrity particularly the sidewalls. This method has a significant drawback when used in the United Kingdom, particularly if there are contaminants nearby or *in-situ*. The water used in construction must be treated as a contaminant and disposed of according to current site regulations for spoil and waste.

Vibro-replacement has traditionally been employed where soils are incompetent or cohesive and there is a risk of borehole collapse. It is generally employed in soils with shear strengths of 15kN/m² to 50 kN/m² (Greenwood and Kirsch, 1984).

Columns formed by this technique tend to be larger than those formed by Vibro-displacement and more costly in terms of column forming material. The size of the column is very large and also the water spoil on the surface which must be disposed of carefully.

Increasingly with construction challenges machines have evolved which operate on the principles of a Vibro-displacement method with the aid of air jets which help to reduce suction during upwards retraction of the Vibroflot in instances of very weak cohesive soils. Observations of these machines in operation suggest that care must be taken to ensure that the air jetting pressures are controlled and kept to a minimum to avoid excessive disturbance to the surrounding soil. Recent discussions with contractors Pennine Vibropiling (Preece, 2007) suggest that Vibro-displacement is the most common technique in use today because of its speed and the fact that there is no (or minimal) waste disposal which is advantageous in cost control.

Bottom and top-feed vibroflotation

For Vibro-displacement and Vibro-replacement the goal of hole creation is the same. The methods may differ in the mechanics of how hole formation is achieved but they are essentially the same in terms of the fact that stone fills the hole and is compacted. In the United Kingdom the tendency has been towards Vibro-displacement. Two techniques of this method of column construction are now in common use. The use of the two techniques, Bottom and Top feed Vibroflotation systems, are dependent upon site conditions and client requirements.

Top feed systems, as the name suggests, is a method of introducing stone to a hole created by Vibro systems (Figure 2.3). In this technique the hole is created by the Vibroflot and it is retracted sufficiently or to the surface (soil shear strength permitting) at which point stone is tipped downhole. The Vibroflot is then reintroduced to compact the stone. By the force of the weight of the Vibroflot or hydraulic means the stone is displaced laterally forming a column of larger diameter than the Vibroflot. The process of introducing stone and compacting is continued until the hole is filled and the completed column reaches the surface. Typically this technique may only be used in

certain soil conditions. It is recommended for soil conditions where shear strengths are greater than 20kN/m² because below such strengths there is a risk of hole collapse. In this type of column aggregate sizes tend to be 40 to 75mm and can be angular or rounded. Top feed systems tend to be faster at installing columns than bottom feed systems but are usually not able to penetrate as deep into the strata because of the risk of borehole collapse or column contamination by the *in-situ* soil.

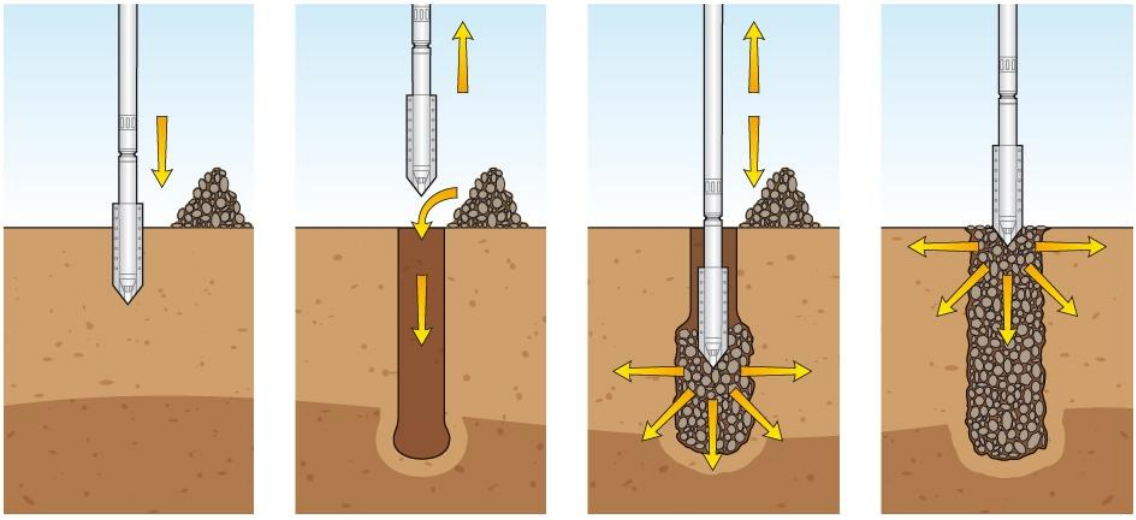

Figure 2.3 Top feed stone column installation (BBGE, 2012)

Bottom feed systems differ from top feed systems because they introduce the stone directly at the tip of the Vibroflot (Figure 2.4). Bottom feed systems can be employed as wet (water) or dry (air) jetting systems and tend to be better suited to working with soft cohesive soils because they are able to keep the hole open minimising borehole collapse and they are also able to penetrate deeper. It is recommended that this system be used for soil conditions where shear strengths are greater than 10kN/m². Bottom feed systems tend to use aggregate sizes in the range of 10 to 40mm and are usually rounded in shape to minimise the chances of Tremie tube blockage. The Vibroflot is driven into weak strata by the eccentric weight and typically with the aid of water jets in modern systems will penetrate the strata to the desired depth. It is recommended that stone columns are always constructed on firm or stiff layers to prevent end bearing failure (McKelvey *et al.*, 2004). Bachus and Barksdale (1984) suggest the Vibroflot should be retracted uphole by between 600 and 1200mm. Stone is then introduced via a delivery tube, typically called a Tremie tube, incorporated into the Vibroflot and fed from a hopper on the mast. Once a certain charge of stone has been delivered the Vibroflot is lowered and compacts the stone creating a column with a wide diameter. The Vibroflot

is raised and a further charge of stone introduced and the stone compacted again. This process continues until the column reaches the ground surface.

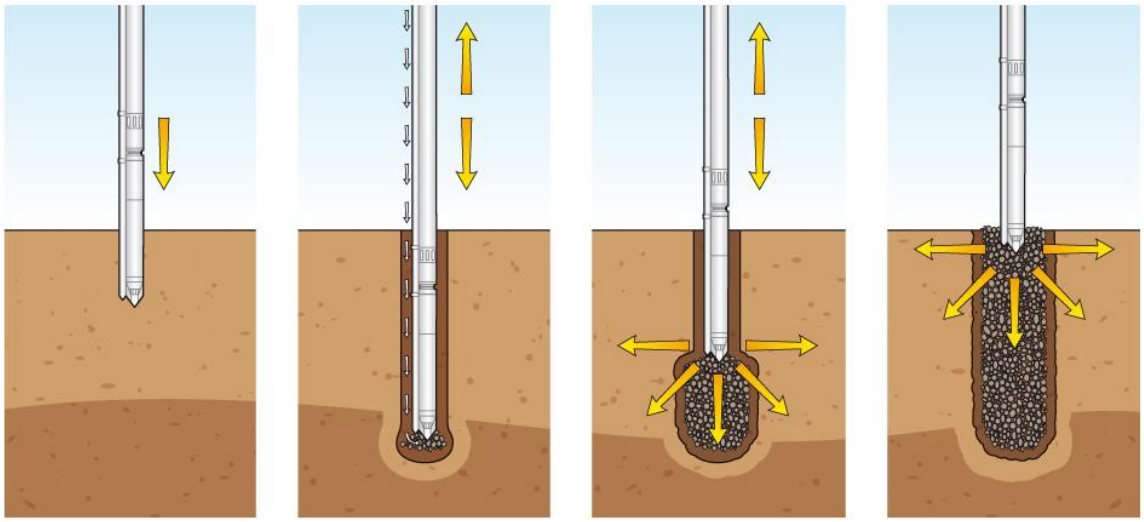

Figure 2.4 Bottom Feed stone column installation (BBGE, 2012)

Compozer method

Aboshi *et al.* (1979) described the Compozer method of Ground improvement. The method consists of the use of rows of large diameter compacted sand columns driven into soft clay subsoil. It was first tested in 1955 in a coastal district of Japan as a foundation for a structure. The process of column forming involves the use of a large diameter casing pipe which is driven into the soft subsoil by a vibrating rammer. When the pipe reaches a specific depth it is filled by a hopper at the top end of the pipe. The pipe is gradually withdrawn in stages which allow the sand to form into a column. The pipe is then re-driven to depth to compact the sand. It forms a column with a larger diameter than the pipe. The process of withdrawing and reintroducing the pipe is repeated until the column is formed. Typically sand columns vary from 60cm to 80cm in diameter, but the largest can be as big as 200cm in diameter. This method including design methodology is covered in detail by Aboshi *et al.* (1979).

Rotary installed stone columns

Goughnour (1997) described the installation of Stone Columns by the rotary method. Traditionally Stone Columns have been installed via vibratory technology but in certain soil conditions a less invasive method is preferable where clean and uncontaminated stone columns are vital. It is useful in situations where Vibroflotation would provide limited compaction and where saturated soils of low permeability cannot be compacted

with ease. The Rotocolumn™ is a system which involves the use of a rotary impeller positioned at the bottom of a 41 centimetre diameter probe. A rotary drive system allows the impeller to penetrate the ground creating a cylindrical void. The impeller consists of two symmetrically located logarithmic spiral sections (Goughnour, 1977). It sits close to the bottom of the feed pipe and is operated by a rotary drive shaft. Stone is allowed to emerge at the impeller flowing in an annulus between the inner and outer pipe. As the impeller rotates stone is forced away and expands outward. As the impeller and shaft rise a column is formed. The feed pipe is vibrated at the upper levels of the machine to avoid blockages.

2.3 Laboratory studies of granular columns

Laboratory testing and analysis of granular columns in the literature can be divided into single and group column behaviours. The single column behaviour is included to allow appreciation of the differences in use of columns and the differences in group behaviour. Current design practice and philosophy is still based on worst case isolated single column behaviour e.g. Priebe (1995).

2.3.1 Single column studies

Hughes and Withers (1974) performed a number of stress controlled laboratory tests to examine the behaviour of Leighton Buzzard sand columns placed in a one dimensionally consolidated Kaolin clay. Column diameters of 12.5mm and 38mm were used in testing. The single columns were inserted into the clay after consolidation to the desired pressure in the triaxial cell. Loading was applied to the samples from the surface in small time intervals to allow pore water pressure to dissipate. The results revealed that footings on model columns showed significant improvements in bearing capacity in comparison to footings on clay. It was noted during testing that model columns developed end bearing pressures and adhesive frictional stresses similar to those observed with concrete piles.

Observations of the column, before and after tests, revealed that the sand column expands or bulges laterally (Figure 2.5b) but that the bulging is constrained by the lateral support of the soils. It was considered that the load bearing capacity of an isolated model column is a function of the lateral support (or restraint) provided by the soil in the bulging zone. The bulging zone is considered to be between 1 and 2 column diameters. The bulging depth was found to occur to a maximum of four diameters; this

is considered as the critical column length at which punching failure would occur followed by bulging failure. The composite action of model column and clay was observed to have provided noticeable benefits in terms of the consolidation which was found to have an effect up to 1.5 diameters. The model columns increased the rate but reduced the size of settlements (Figure 2.5a). The clay within a definable cylindrical zone of two-and-a-half-times the diameter were found to have improved in strength as a result. This suggests a column could act independently if placed 2.5 diameters apart.

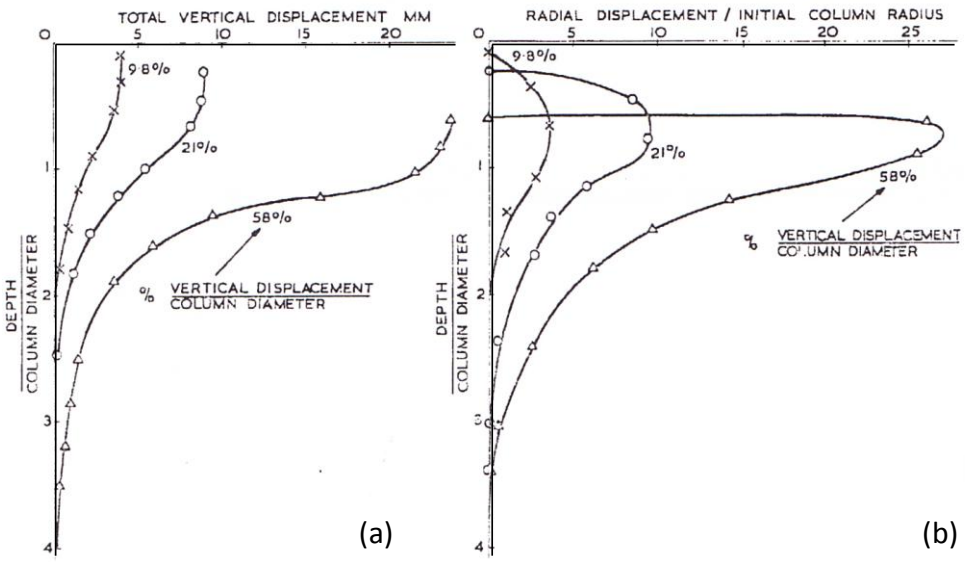

Figure 2.5 Vertical displacement within the column with depth (a) and radial displacement at the edge of the column/ initial column radius against depth (b) (Hughes and Withers, 1974)

Charles and Watts (1983) conducted a series of laboratory tests in a large triaxial cell to examine the effect of different column diameters on the vertical compressibility of model stone columns loaded through a rigid raft. The columns were full length and rested on the base of the triaxial cell to simulate end bearing stone columns. The testing revealed that by increasing the diameter and the area replacement ratio, the vertical compressibility of the clay was significantly reduced. It suggested that the column and soil work together to reduce the compressibility thereby sharing the stress load applied. It was noted that an area replacement ratio of 33% was found to significantly reduce compressibility, hence in order to achieve a reduction in compressibility, a ratio greater than this was recommended.

Narasimha Roa *et al.* (1992) performed a series of laboratory load studies on model gravel columns used to stabilise soft marine clays in a large triaxial cell. Marine clays were utilised during testing because of their low shear strength and high compressibility. Three different column diameters with different lengths were selected for testing. It was found that the ultimate load carrying capacity of the stone columns becomes asymptotic with column lengths such that beyond a column length of 5 to 8 diameters the load transfer of a column does not increase suggesting an optimum length. It was concluded that bulging occurs as a result of load transfer in stone columns. The bulging is considered more noticeable in soft clays than in stiff clays and bulging is considered to help mobilise passive resistance in support of the column.

Stewart and Fahey (1994) performed four scaled laboratory experiments in a centrifuge to examine the effect of installing Stone Columns beneath an embankment for a proposed construction. The tests were performed at a gravity level of 100 and the field dimensions scaled down by 100. Two soil layers were formed, the upper of sand and the lower of clay. The clay had an undrained shear strength of 23kPa. The embankment was formed of fine graded silica and sand. Cast iron shot was used to simulate an iron stockpile. The columns were installed into the layers by replacement. The replacement ratio of the model layer was 9%. The results of testing revealed a reduction in settlement and lateral deformation as a result of the columns presence. The columns were found to be stiffer when carrying axial load and provided axial restraint to movement when under load from the embankment. Stress concentration factors were recorded of 4.2 and 4.6. Evidence of bulging and bending were observed in connection with lateral movements. The bulging appeared to generate additional confining stress around the columns inhibiting shear failure. No shear failures were observed during testing due to insufficient loading i.e. the load level was not sufficient to cause high enough stress concentrations within the columns which could create the potential for failure.

Sivakumar *et al.* (2004) performed a series of experiments on model columns in a large triaxial cell. One series of tests was performed with normal model columns of varying lengths. In all tests performed the presence of columns, regardless of length, were found to increase the bearing capacity. When the columns were installed onto the base of the triaxial cell substantial increases in load carrying capacity were observed compared to shorter floating columns. Columns with lengths greater than five times the column diameter did not show improvement in load carrying capacity. The tests with

columns installed were found to reduce settlement compared to those performed without columns.

Andreou *et al.* (2008) examined the influence of the main controlling parameters in the design of stone columns through a series of laboratory experiments in a large triaxial cell. The effects of drainage conditions, grain size of the column material, the confining pressure of the soil and the rate of deformation was investigated. The results revealed that the drainage of the column was found to have a significant effect on the maximum load carried by the reinforced soil. The partial draining of the soil surrounding the column was found to significantly increase the resistance of the reinforced soil to the applied loading. The maximum load carried by the reinforced soil with a sand column under drained conditions was found to be twice that of the column under undrained conditions, regardless of confining pressure.

2.3.2 Group column studies

The performance of columns in a group is often assumed from the results of single column studies. The approach has been to take the performance of a single column and assume this as a 'worst case' approach for behaviour. With the development of more sophisticated laboratory techniques the behaviour of columns in large triaxial systems has been possible.

A series of displacement controlled tests on rigid strip footings installed in a soft kaolin clay test bed were performed by Hu (1995) and Muir-Wood *et al.* (2000) to examine the deformation behaviour of granular columns. The displacement rate was 0.061mm/min which was considered by the author to be slow enough to ensure drained conditions in the clay. Parametrically three variables were examined: Area replacement ratio; length of column and method of installation. The study considered the behaviour of columns and soil as a composite system. Columns were installed in a manner similar to the vibro-displacement method and included both end bearing and floating stone columns. The length to diameter ratios examined were in the range of 6 to 15. The laboratory results were verified by a numerical study by Lee & Pande (1994) which was performed parallel to this study.

It was found that column behaviour in a strip is different from single column behaviour as described by Hughes and Withers (1974), i.e. deepening of a conical wedge failure mechanism was observed visually within a five column strip. The overall stiffness of

the reinforced ground was found to increase with increasing length of the columns. It was discovered that the load bearing mechanism of the clay reinforced with several columns is significantly influenced by the size of the footing unlike a single column.

This study revealed four modes of column deformation: bulging, bending, punching and shearing. The mode of deformation was found to be dependent upon column and foundation configuration. The clay beneath the rigid foundation was found to behave elastically but as loading increased the composite ground developed irrecoverable plastic deformations. Vertical loading of the strip was also found to cause the columns to shorten in length and expand horizontally with depth which is considered evidence of bulging. The depth of bulging was found to be controlled by the lateral confinement of neighbouring columns. The columns at the edge of the strip (Figure 2.6 (a)-(c) B) were found to have a shallower bulging depth than the one at the centre of the five column strip (Figure 2.6 (a)-(c) A). The bulging was found to follow the conical slip surface. The degree of bulging was found to increase and the depth of bulging was found to decrease with increasing area ratio.

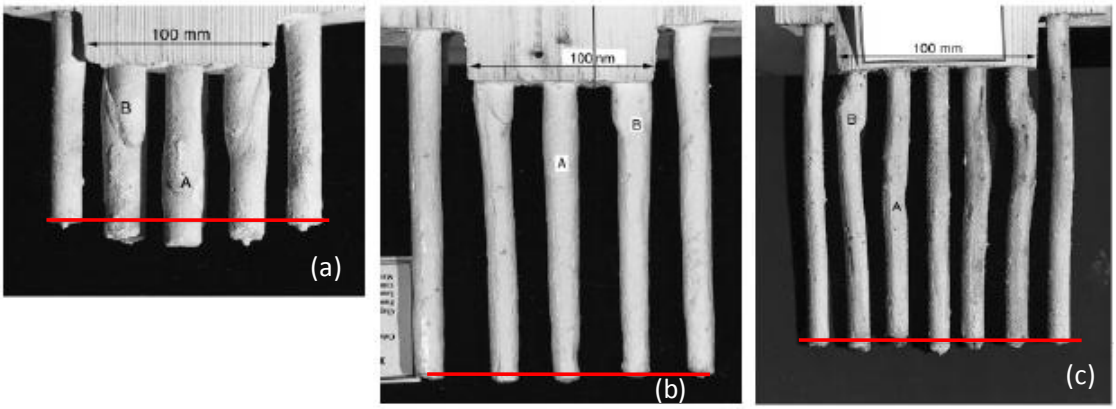

Figure 2.6 Photographs of deformed sand columns exhumed at the end of the footing penetration (red lines indicate original level of column bases) (modified from Muir-Wood *et al*. 2000)

Punching failure was observed for short columns when they were not long enough to transfer the load to depth (Figure 2.6 (a)). If the length of the column is less than or equal to the footing diameter (or breadth) the base of the columns will transfer the load to depth and develop end bearing failure simultaneously with the development of bulging failure. This is considered to be related to the level of the vertical stress distributed to the column base and is suggested that for columns which have a length of one and a half times the footing diameter the penetration phenomenon of 'punching' at

the column base is insignificant. Bending failure of columns was observed when the column was subject to lateral loads (from adjacent columns) (Figure 2.6 (c) B). Column length was found to have a direct effect on foundation performance. Columns which were long and thin suffered bending failure which is considered to occur due to the insufficient flexural rigidity of the columns. It is suggested that there is an effective length beyond which the extra length of column would no longer benefit the bearing capacity but may offer settlement reduction. The effective length is considered to be approximately one and a half to two times the footing diameter (or breadth). It is considered that the displacement method of installation produced lateral compaction of the surrounding clay and consequently generated extra stiffness. Shear failure was found to occur when insufficient lateral restraint was provided to the columns and can be observed at the edge of the foundation (Figure 2.6). It was found to occur at the edge of the foundation near the ground surface. The depth of the zone of influence for the foundation is dependent on the mobilised friction of the composite soil mass. The depth can increase at low area replacement ratios.

The presence of columns was found to contribute to accelerating the consolidation of the surrounding clay because of drainage pathways created by the columns. With consolidation a strength gain in the surrounding clay was noted. It was discovered that the larger the area replacement ratio the greater the drainage of the clay. The area replacement ratio was found to be an important parameter in controlling the overall performance of the composite foundation. Significant improvements in load bearing capacity were correlated with high area replacement ratios above 25%. Low ratios of 10% were found only to improve the load bearing capacity slightly. It was noted that in terms of the group effect, increasing the area replacement ratio enabled the composite ground to hold the loading action closer to the loaded area and transfer the load deeper. Observation of the stress-share between columns and soil was identified with the surface stress being more concentrated on the columns than in the clay in all model tests. The ratio of average contact stress in the column to soil was found to be between 0.5 and 5. The degree of consolidation was found to control the degree of stress concentration. The stress concentration ratio, n, the ratio of stress in the column to clay was found to rise when the area replacement ratio is increased from 10% to 24% (fully drained clay). Beyond 24% there is no further increase in stress concentration observed.

McKelvey *et al.* (2004) studied the performance, stress concentration ratio and failures of stone columns placed in soft soils in a large triaxial cell. Columns of various lengths were examined and are considered to be 'floating' i.e. not end bearing on the base of the triaxial. Two group arrangements of model columns, triangular and a strip footing, were tested. Two column lengths were used beneath the model foundations with a length to diameter ratio of 6 and 10. Bulging was noted in both short and long columns (Figure 2.7). In short columns with length to diameter ratio of 6 bulging occurred over the entire length of the column. In longer columns with a length to diameter ratio of 10 deformation occurred in the upper region with the lower region recording no significant deformation. Short columns were noted as punching into the soft clay beneath. It was noted that in groups the central columns were restrained more than the outer columns which deformed away from the group in the unrestrained direction. It was observed that in the shorter columns, the load bearing capacity was increased by 130% compared to soil with no column reinforcement. By installing the longer columns the bearing capacity increased to 135%. This small additional increase in bearing capacity between the two lengths suggests that beyond a certain length to diameter ratio no significant increase in load carrying capacity is observed. It is therefore suggested that an optimum column length lies between a length to diameter ratio of 6 and 10. Testing of the clay bed after column installation and loading revealed the stiffness to be four times greater than the unreinforced clay bed. It suggests that the columns are useful in settlement reduction. The stress concentration ratio, n, was also examined. The results revealed that the short columns provided less resistance to loading (as they punch into the soft clay below) compared to the longer columns which show resistance to punching.

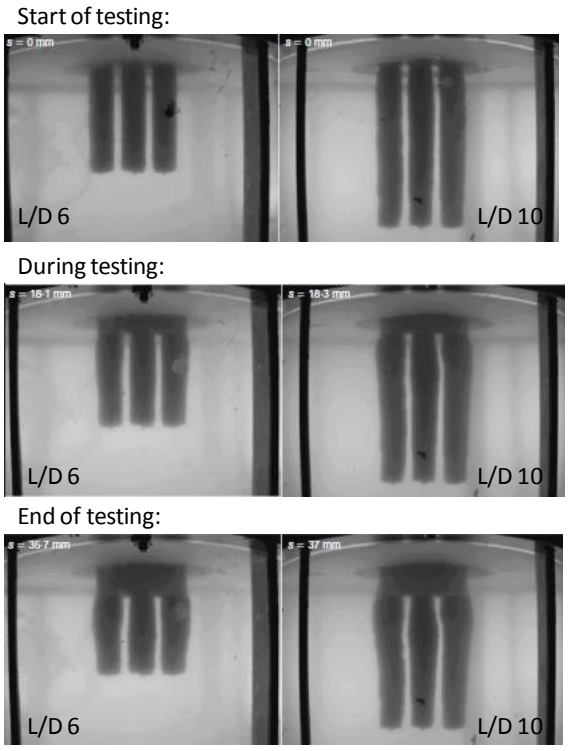

Figure 2.7 Photographs of sand columns beneath circular footing at the beginning, middle and end of foundation loading process (modified from McKelvey *et al.*, 2004)

The stress distributions between the two column lengths were found to be very different. It was found that beyond the working stress ratio it approaches a value of 3 regardless of column length. Column spacing was found to increase the confining stress field in the upper portions of the columns. It is considered that it moves friction support to greater depths where smaller settlements were observed. Beneath the rigid footings it was noted that the longer columns accepted a higher proportion of the applied load than the clay in contrast to the smaller columns where the stress concentration was smaller.

Ambily and Gandhi (2007) considered the group behaviour of model granular columns in a large diameter triaxial cell to examine the effect of clay consolidation on column performance. Three different shear strengths were achieved through consolidation of kaolin slurry. Groups of seven columns were installed into each clay bed by the replacement method and as end bearing columns. The column length to diameter ratio was 4.5. The column loading was displacement controlled. It was found during loading of the column area alone that failure occurred by bulging failure to a depth of 0.5 times the column diameter. It was noted that as the spacing of the columns increased the axial capacity of the column decreased and settlement increased by up to a spacing to diameter factor of 3 beyond which little change was observed. The stiffness

improvement factor was found to be independent of shear strength of the surrounding clay and depends mostly on spacing of the columns and the internal friction angle of the columns.

Black (2007) examined the group behaviour of large diameter single and small groups of columns, beneath a circular foundation installed in soft clay. A large triaxial cell was used to assess the effect of three area ratios (A/Ac 2.5, 3.6 and 5.8) for various column lengths. A comparison of the load-displacement results (Figure 2.8) for single and groups of columns, suggests that the groups are under-performing in comparison to the single columns. This is considered due to what has been termed 'block failure' which occurs when the columns act together to punch into the underlying soil (Figure 2.9).

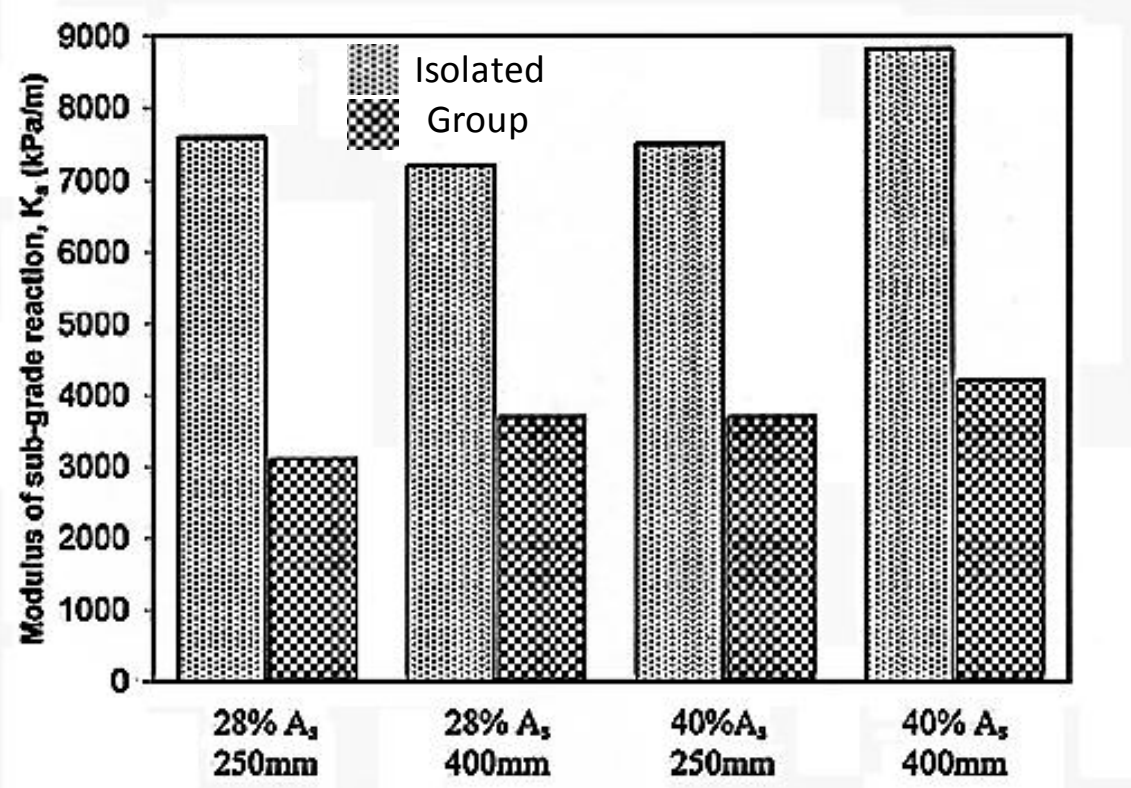

Figure 2.8 Comparison of modulus of sub-grade reaction, Ks, for isolated and group column formation (Black, 2007)

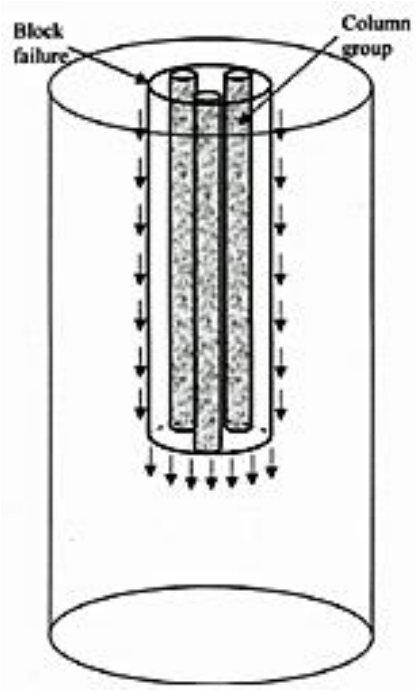

Figure 2.9 Illustration of block failure in group columns (Black, 2007)

The results suggest that the mode of deformation is dependent upon the column length and column configuration. For columns with length to diameter ratios of 3 to 5, regardless of column arrangement, punched into the underlying soil which caused end bearing failure. For columns with length to diameter ratios of 7 to 10, single columns displayed bulging failure whereas groups punched into the underlying soil. It is suggested that due to the 'block failure' behaviour with the columns acting as a single entity that the length to diameter ratio should be altered with the diameter equivalent to the foundation diameter. This gives a revised length to diameter ratio of between 4 and 6. For the end bearing columns bulging was observed. For the cases considered that the critical length to diameter ratio at which the mode of failure changes from end bearing to bulging is 8 under drained conditions.

The testing revealed similar findings to Sivakumar *et al*. (2011) for relationships between stress concentration and column length. No increase in vertical stress was observed for short columns due to their tendency towards punching failure and as such could not absorb any additional vertical stress. In contrast however, stress concentration was found to increase with column length. This is to be expected since longer columns tend to have higher ultimate bearing capacities. The pressure beneath the centre of the foundation was higher than the columns, this was considered to create a lateral force on the surrounding column which contributes to their bulging in the

unrestrained direction. This is considered to partly explain the underperformance of the group compared to single columns in this study.

Sivakumar *et al*. (2011) examined the load-share behaviour of stone columns installed in a clay bed utilising a large triaxial cell. The pressure along the column with depth was examined and it was found that a reduction in pressure with depth occurred due to the load transfer mechanism between the column and surrounding clay. The load in the column appeared to transfer to the surrounding clay as increased lateral pressures as a result of the bulging and side friction. The pressure was found to rise for columns longer than the critical length. Stone columns unlike rigid piles, rely on the *in-situ* soil to provide lateral restraint especially at shallow depths. The bulging is considered to generate enhanced lateral pressures and shear stresses in the upper region, which in turn leads to settlement of the surrounding clay. In a pile the negative skin friction will develop in instances where the settlement is less than that of the surrounding clay. The compression of the column below the critical length was found to not to be significant and the column was found to develop negative skin friction like a pile. Comparison of measured and predicted settlements utilising the method of Priebe (1995) suggest that settlement reduction predicted was higher due to the assumption of the unit cell used in the method and the fact that lateral strain is ignored in the calculation.

Black *et al.* (2011) examined the settlement behaviour of a small group of stone columns in a large triaxial system. Parameters examined in this study included column length to diameter ratio, area ratio and single/ group configurations (Figure 2.10). The results suggest that there is an optimum area replacement ratio between 30-40% for settlement performance. It was discovered that the performance of the column could be enhanced if the tendency to bulge is restricted. For columns which had moderate replacement ratios and were supported by other columns beneath the foundation, the effect of vertical loading and the tendency towards bulging behaviour could be reduced. The beneficial effect is dependent on the thickness of the annulus which is significantly reduced in the case of high area replacement ratios as the columns were unable to offer restraint as a group. In such cases the overall performance is compromised and bulging failure occurs more readily. A reduced performance of column was encountered at the edge of the footing where columns were not restrained on all sides by other columns. It was discovered that there is potentially some degree of flexibility in the design of stone columns. It is suggested that the settlement can be controlled when using larger area ratios and shorter columns (length to diameter ratios of less than 6) or long columns

(length to diameter ratios greater than 6) with relatively small area ratios. It is further suggested that such findings can be of benefit on sites with difficult site conditions to allow greater flexibility in the design. The existence of a block failure mechanism, similar to Black (2007), was noted when localised stress in the enclosed soil confined by the small group configuration proved to have a detrimental effect on settlement compared to an isolated column and punching failure occurred.

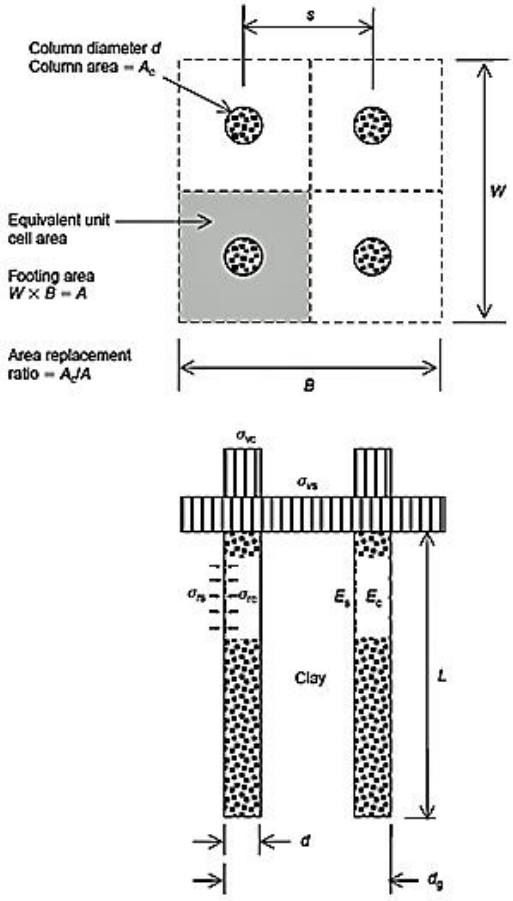

Figure 2.10 Key factors affecting granular columns performance (Black *et al.*, 2011)

Kelly (2014) conducted a series of laboratory tests on isolated single column and column strip foundations at reduced scale in transparent clay beds. The study aimed to examine internal soil displacement and detection of pre-failure strains using laser aided imaging and particle image velocimetry. This allowed for real-time displacement of the columns to be observed. Single columns were found to fail in an axisymmetric manner through a combination of compression and bulging with minimal punching at the column base which suggested a critical length of 4 times the diameter, d. Increasing column length from 4d to 6d and 8d led to moderate increases in bearing capacity of 8.5 % and 13 %. For strips of columns local shear failure, bulging, bending, punching and block failure were observed depending on the geometrical configuration. Column

length was found to have a significant effect on bearing capacity of column strip foundations. Increasing column length from 4d to 6d and 8d lead to an increase in bearing capacity of the composite foundation of 29 % and 67 %. It was suggested that in terms of optimising the bearing capacity a critical length of 8d should be adopted. Increasing the foundation size rather than column length was found to be more effective in terms of increasing load capacity.

2.3.3 Summary of laboratory studies

The laboratory studies have focussed on the behaviour of single and small groups of columns installed in soft clay. In all cases the introduction of stone columns was found to reduce the settlement and improve the bearing capacity compared to the untreated soil. The degree of reduction was found to be dependent upon area ratio, column length and spacing. From the various studies key observations have been summarised as follows:

- *Stress-share:* stone columns unlike piles rely on the stress-share between column and soil to reduce settlement. The appearance of 'stress-share' was noted by Hughes and Withers (1974), Charles and Watts (1983), Narasimha Roa *et al.* (1992), Stewart and Fahey (1994), Sivakumar *et al.* (2004), McKelvey *et al.* (2004), Sivakumar *et al.* (2011), Black (2007) and Black *et al.* (2011).
- *Bearing capacity*: their appears to be an optimum length for a stone column beyond which the bearing capacity does not increase but further settlement reduction is possible. Hughes & Withers (1974) suggest this length is 4 diameters. Narasimha Roa *et al.* (1992) suggests the optimum length is between 5 to 8 diameters, this compares well with Sivakumar *et al.* (2004) who suggests that the optimum length is 5 diameters beyond which no increase in bearing capacity is observed. McKelvey *et al*. (2004) suggests the optimum length is between 6 to 10 diameters.
- *Critical length:* Increasing column length in all cases was found to reduce the settlement and increase bearing capacity. Critical length to avoid punching failure was considered to be 4 diameters by Hughes and Withers (1974). Black (2007) suggests 3 to 5 diameters and 7 to 10 diameters to guard against end bearing and bulging failure respectively. Black (2007) also suggests that beyond a critical length of 8 diameters end bearing failure becomes bulging failure.

- *Deformation modes:* Four modes of deformation have been identified from the literature. Hughes and Withers (1974), Charles and Watts (1983), Narasimha Roa *et al.* (1992) examined column behavior and noted that bulging failure occurred. Hu (1995) and McKelvey *et al.* (2004) noted that four modes of deformation could be observed which were bending, bulging, punching and shearing. The presence of a particular mode of deformation was found to dependent mainly on area ratio, column configuration and column length.
- *Bulging deformation:* The appearance of bulging failure was found to be dependent upon column length, column configuration and lateral restraint provided by the *in-situ* soil. Hughes and Withers (1974) suggest that the bulging zone is 1-2 column diameters. McKelvey *et al.* (2004) noted that bulging failure occurred across the whole length for column to diameter ratios of 6 and in the upper section for length to diameters of greater than 10. It is recognised however that the appearance, depth and extent of bulging will be dependent upon site conditions.
- *Optimum area replacement ratio:* It has been suggested that an optimum ratio exists for stone columns which reduces settlement to an acceptable level. Charles and Watts (1983) suggest this is 33% with further settlement reductions observed for values greater than this. Hu (1995) found that area replacement ratios above 25% reduced settlements. Black *et al.* (2011) suggests that an optimum area replacement ratio of 30-40% should be utilised.
- *Column spacing:* It has been noted that column spacing affects the settlement performance of improved ground and the maximum spacing. Hughes and Withers (1974) suggest that the zone of highest improvement around the column is up to 1.5 diameters but up to 2.5 diameters offers significant improvement. Beyond this no improvement is observed. Ambily and Gandhi (2007) noted that beyond 3 diameters spacing no improvement was observed. Black (2007) and Black *et al.* (2011) noted that if columns were placed together in a small group and sufficient applied load to the foundation took place then potentially the columns could suffer block failure.
- *Stress concentration:* was found to vary with area replacement ratio and column length. Hu (1995) noted that the stress concentration increased as the area replacement ratio increased from 10% to 24%. Beyond 25% no further increase was noted. McKelvey *et al.* (2004) noted that the stress ratio was constant

regardless of length in the range of 6 to 10 diameters, however Black (2007) noted that stress concentration in the column increased with length.

2.4 Field studies of granular columns

Five case studies are described to illustrate the application of vibro granular column techniques to different ground engineering challenges and their performance. The field trial at Bothkennar, Scotland is described in detail as this site is intended for use in field testing in this research.

2.4.1 Dry bottom feed stone column installation at Bothkennar, Scotland

Watts and Serridge (2000) carried out a field installation of granular columns by bottom feed vibro-displacement at the Bothkennar soft clay test site, Scotland. The field trial examined the effect of column length, spacing and footing configuration on settlement performance. The shear strength of the *in-situ* soil varies from 20-60kN/m² from 2 m to 20 m depth. For the application of vibroflotation 20kN/m² is considered the minimum value. Due to the depth of bedrock the columns were installed as partially penetrating (floating) columns with a bulb at their base to minimise the potential for punching failure. Prior to installation the minimum length was calculated by the method of Hughes & Withers (1974). The method of Baumann and Bauer (1974) to calculate the stress distribution and factor of safety against column bearing failure was used. Composite foundation improvement factors were calculated utilising the method of Priebe (1995). Design parameters used in the design included an internal angle of friction for the column of 42.5°, undrained shear strength of 20kN/m² for the soil and initial column diameter of 0.65m.

Inspection of the columns during and post construction revealed the columns were well formed and uncontaminated by the *in-situ* soil. Shear field vane measurements suggested a small drop in peak clay strength post installation as a result of the installation process. Pressure cells present in the soil recorded increases in stress during column compaction regardless of length suggesting that stress transfer was taking place from the vibroflot to column. During column construction high earth pressures up to 80kPa were observed above pre-treatment values. Six days after column installation pore water pressure was found to return to pre-installation values due to the drainage path provided by the granular column. With longer installation times more soil disturbance occurred which led to an increase in the time taken for pore water pressure

to dissipate. Different strip configurations (Figure 2.11) were used with different lengths and depths (Table 2.1) to assess their influence on composite foundation performance. Loading of the strip foundations was in three stages with loads of 33kN/m², 70kN/m² and 107kN/m² applied by kentledge blocks. The settlement behaviour of the strips was found to vary with footing length and configuration (Figure 2.12). The settlement of the strip footings varied according to column length and spacing. Strip 1, underlain by four columns at 1.5m centres, appeared to show slightly higher settlements than Strip 2 which was underlain by three columns at 2m centres. Strip 6 was founded on the base of the crust on 5.7m columns and settled the most due to lack of support provided by the crust. The predicted values for the second load increment of 70kN/m² were higher than the measured values although settlement was still occurring at the end of the second increment. Estimates for settlement calculated using Priebe (1995) were about 50% of the untreated ground.

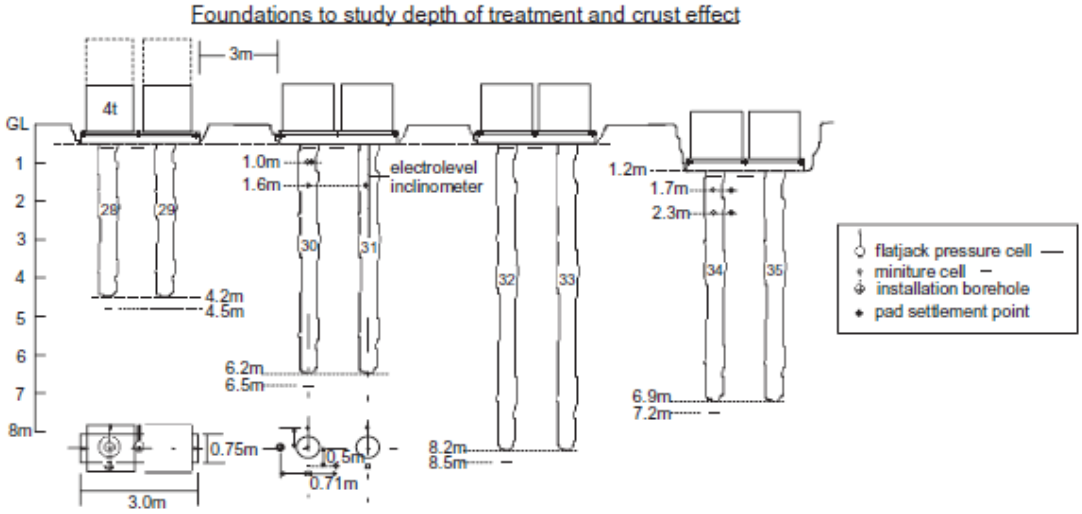

Figure 2.11 Trials foundations 3 to 6 and instrumentation (Watts and Serridge, 2000)

Foundation	Dimensions (L × B)	Founding Depth	Ground Treatment		
			Number of Columns	Columns Spacing	Column length (below foundation)
1	6.0 m × 0.75 m	0.5 m	4	1.5 m	5.7 m
2	6.0 m × 0.75 m	0.5 m	3	2.0 m	5.7 m
3	3.0 m × 0.75 m	0.5 m	2	1.5 m	3.7 m
4	3.0 m × 0.75 m	0.5 m	2	1.5 m	5.7 m
5	3.0 m × 0.75 m	0.5 m	2	1.5 m	7.7 m
6	3.0 m × 0.75 m	1.2 m	2	1.5 m	5.7 m
7	1.5 m × 1.5 m	0.5 m	2	1.2 m	5.7 m
8	3.0 m × 0.75 m	0.5 m	No treatment	–	–

Table 2.1 Ground treatment and trial foundation details (Watts and Serridge, 2000)

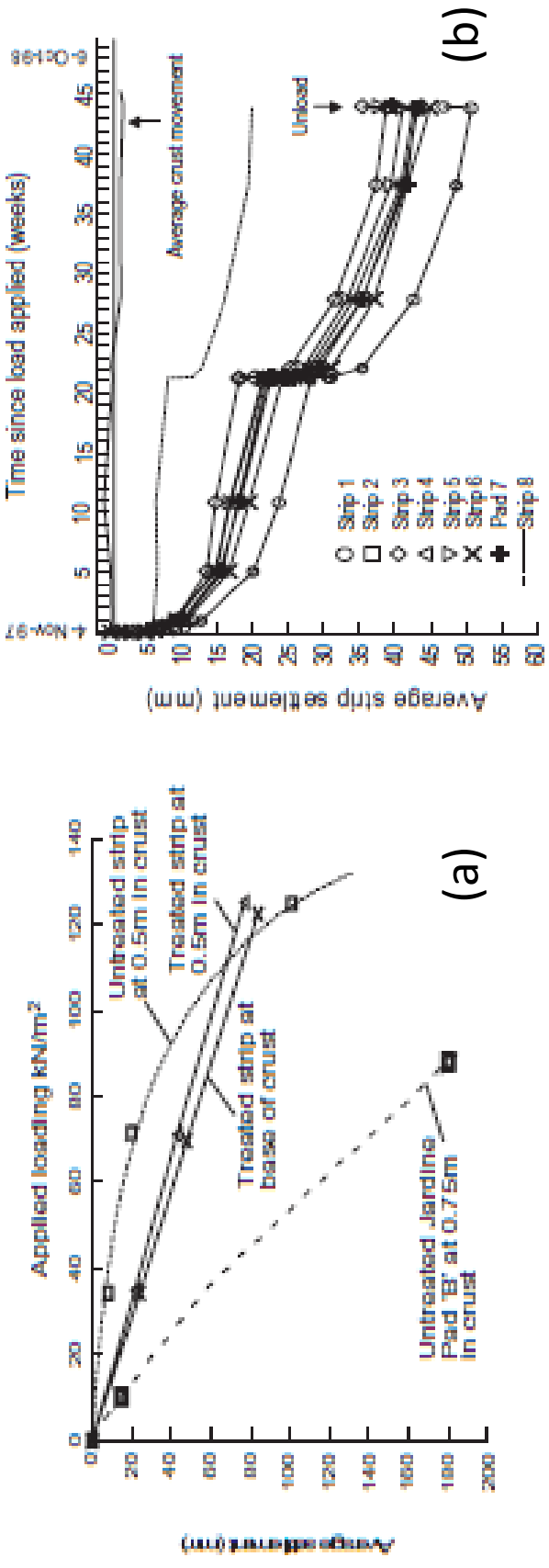

Figure 2.12 (a) Settlement with time of loaded trial foundations (b) Load/ Settlement Curves (from Watts and Serridge, 2000)

The columns are considered to have reinforced the soil below the crust reducing the overall settlement and providing a factor of safety against bearing failure. It was suggested that the stresses applied to the strips were comparable to values for low rise buildings indicating that the columns are effective. The testing programme revealed that the behaviour of the composite system is very complex. Different factors including pore pressures, soil stress ratios and stiffness all affect the performance of the system. The results indicated that the Hughes and Withers (1974) assumptions regarding minimum column lengths and stress-share were appropriate. Evidence for soil reinforcement was seen but minimal benefit was seen in terms of settlement reduction.

2.4.2 Deep stone columns in marine clay, Spectacle Island, USA

Klein and Tobin (1996) described the use of dry bottom feed and top feed stone columns to improve marine clay at Spectacle Island. The use of 19.8m columns was proposed to allow improvement of the soft clay and to enable the construction of a landfill containment dyke on the island to be built from earth and compacted till. The soil beneath the dyke is a marine clay. It was found to be very stiff from the surface to depths of 1.8m to 3.6m across the site, becoming medium stiff to stiff with depth. Beneath the thick zones of refuse onsite the clay appears to be normally consolidated. The clay has a high plasticity and is stratified with lenses and layers of silt and fine sand. The clay also was found to contain layers of coarse sand to gravel distributed randomly across the site. The stone columns were installed with a design diameter of 1.1m in a triangular arrangement to give an area ratio of 0.15. Once installed the dyke was constructed on top. With the addition of the dyke the areas where columns had been installed showed an insignificant rise in pore water pressure. However, untreated areas recorded a 77% pore water pressure surcharge which reduced after 11 months to 55%. The stone columns were found to reduce the consolidation time and reduce settlements by 22%. The low reduction in settlement maybe due to the fact that the clay was stiff to very stiff.

2.4.3 Albany airport terminal expansion, USA

Munfakh (1984) described the use of spread footings to support column loads at the building and loading bridges. Preliminary borings indicated the presence of loose to medium dense silty sands throughout the area. Clays were encountered at depths of 3.7m below the surface in two boreholes. Variability was seen in soil stiffness during site testing. Differential settlements under low loads were considered an issue due to

the variation in geology across the site area. Reduction in foundation pressure or the use of deep foundations was considered uneconomical. On this basis soil improvement by Vibroflotation was considered as it would allow higher bearing pressures which would allow for additional savings in footing concrete, reinforcement and depth of excavation. Vibroflotation beneath each individual foundation was therefore chosen.

Due to variability of soils across site 4.5m to 6.0m length of columns were chosen with a medium to coarse gravel material (13mm to 64mm). Columns were formed with diameters of 0.75m to 1.0m. By installing the columns beneath the footings and at selected locations around the footings the columns were found to reduce the settlements from 5cm to 2.5cm, approximately a 50% reduction in settlement. The stone columns are considered to have had a minimal effect on improving the soft layer of clay at depth.

2.4.4 Jourdan road terminal, USA

Munfakh (1984) described the use of stone columns in a reinforced earth-stone column system in a wharf structure by Vibro-replacement to reduce settlements. The choice of this method was based upon cost considerations compared to piling. The site was composed of 18.28m of soft clays and silty clays with interbeds of silt and fine sand. It was underlain by medium to very dense sands which were used as a primary bearing layer. The columns were installed from ground surface to the bearing layer. Two test embankments were constructed prior to installation to assess the benefit of the columns to the soil. One embankment was underlain by vibro stone columns and the other was constructed on unimproved ground. The stone columns were found to increase the load carrying capacity of the soil by 50% and reduce settlements by 40% due to the presence of columns. The column improved soil was found to reduce lateral movements and act as pore water drains which aided consolidation thereby reducing the time taken. Some lateral bulging was detected at the top of the stone columns but this did not cause failure. When the columns were installed beneath the wharf structure the recorded surface settlement reduced by 70% at the end of consolidation. High stress ratios between 5 and 6 were recorded by instrumentation at the end of the consolidation period.

2.4.5 Single column studies at Canvey Island, England

Hughes *et al.* (1975) performed a plate load test on an isolated stone column installed in soft clay at Canvey Island on the north bank of the Thames estuary. The aim of the test

was to allow an assessment of column performance and to allow an assessment of the theory devised by Hughes and Withers (1974). The columns were installed by vibro-replacement with water jetting to assist hole formation. The columns were installed to a depth of 10m into soft alluvial clays interleaved with sandy lenses. In the area of the test the clay was found to be around 9m in depth underlain by 11m of silty sand.

Beneath the silty sand at a depth of 25m Thames Gravel was encountered. A crust was detected at the surface of 1m to 2m in thickness which is similar to Bothkennar. The crust was considered to provide a form of restraint to the column and hence increase bearing capacity and reduce settlement as a result. A critical length for the column was calculated at 2.25m and columns were therefore installed to a depth greater than this. The ultimate load was calculated as 170kN on a 0.660m diameter column. After performing a short plate load test of over half an hour's duration, the column behaved stiffer than expected. When the column was excavated it was found to have a deformed shape comparable to 'bulging' as described by Hughes and Withers (1974). A field load test calculated the capacity as 220kN. The column was considered to have increased bearing capacity by 2.5 to 4 times the original value. This was considered variable depending on the value of soil cohesion interpreted from the site data.

2.4.6 Reviews of field performance of stone columns in soft soils

McCabe *et al.* (2009) reviewed a number of case studies published in the literature which reported the treatment of soft soils with vibroflotation. A settlement improvement database was assembled from over twenty case studies which consisted of a series of data points representing settlement improvement factors. The majority of data points related to wide spread loading with three case studies relating to pad and strip footings. The authors plotted the improvement factor data points against the basic improvement factor curve of Priebe (1995) with an angle of 40° internal friction angle for the column material. The authors state that this friction angle was chosen as a safe lower-bound value for actual feed performance in the absence of sufficient data from the case studies. The comparison of field data points from the case studies and the curve generated by the method of Priebe (1995) show a reasonable trend (Figure 2.13).

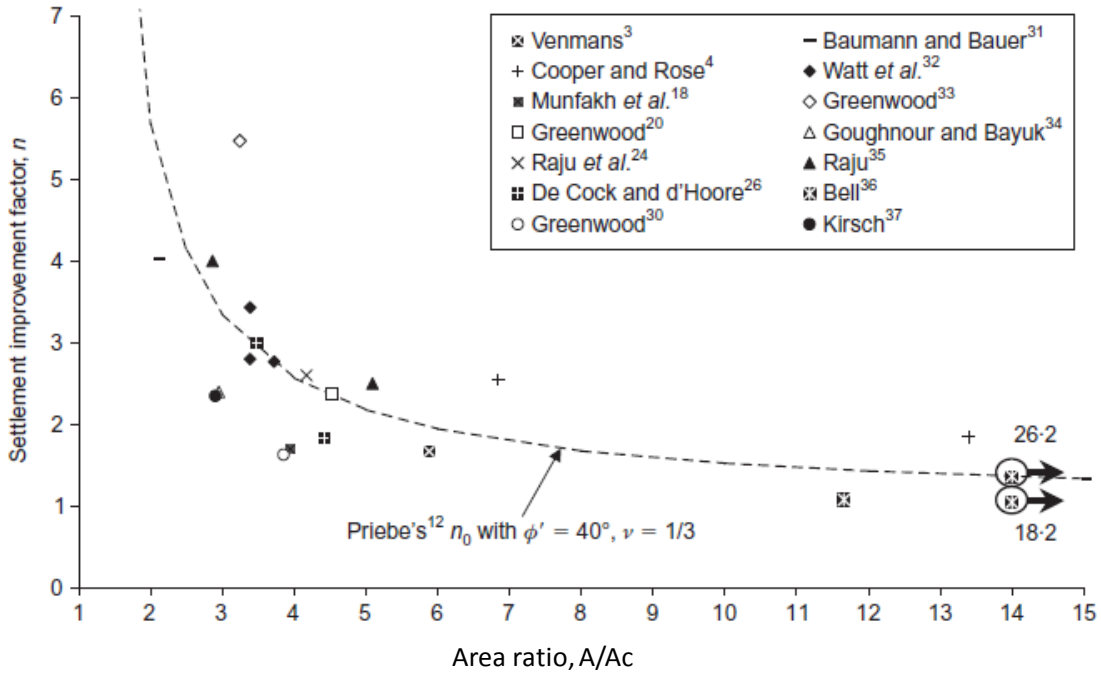

Figure 2.13 Settlement improvement factor against area ratio for sites with widespread loading (modified from McCabe *et al.*, 2009)

The effectiveness of different granular column construction techniques was examined by comparing the predicted and measured settlement improvement factors (Figure 2.14). It was suggested that the technique used to construct the granular columns had a significant influence on the settlement performance of the composite system. The data points also suggest that the bottom feed system was better at creating columns which performed closer to the design. It was suggested that the use of 40° internal friction angle may be conservative in terms of bottom feed design applications for columns. The authors examined the generation of pore pressures around columns during installation and noted that maximum values were similar in magnitude to driven piles. However, these high pressures were dissipated faster with stone columns as they act as vertical drains. The lack of adequate (and high quality) data on lateral stress effects were found to limit the analysis.

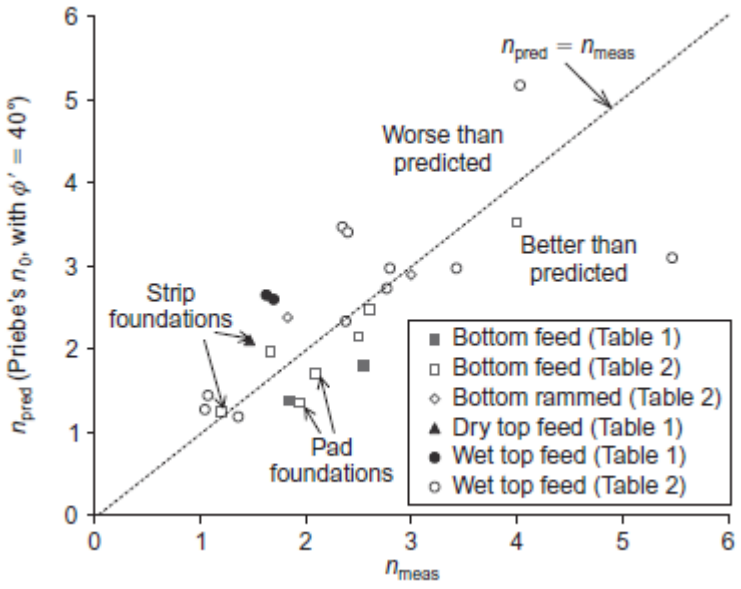

Figure 2.14 Predicted against measured settlement improvement factor for all widespread loading and footings (from McCabe *et al.* 2009)

Douglas and Schaefer (2012) reviewed a large number of field trials which used the method of Priebe (1995) and examined the accuracy of the method in predicting settlement versus the actual settlement. This followed on from the work of McCabe *et al.* (2009) and examined a much larger pool of case studies. McCabe *et al.* (2009) had earlier found that the method of column installation determined how accurate the prediction of settlement would be using Priebe (1995). The study identified the bottom feed installation method as being the closest to creating settlements close to design estimates. Douglas and Schaefer (2012) extended the approach of McCabe *et al.* (2009) by suggesting that three main reasons are responsible for the difficulties in estimating settlements: design parameter selection, installation effects and stress distribution. The design parameter selection was highly dependent on the quality and coverage of the site investigation. The installation effects controlled the method of column construction i.e. top or bottom feed systems. The stress distribution and the depth to which stress is considered to effect the untreated and treated soil zones influenced the depth of treatment. It is also noted from the work of Balaam and Poulos (1985) that flexible foundations supported by stone columns offer less reduction than that of columns beneath a rigid foundation.

The authors considered over 100 stone column studies to evaluate the accuracy of the Priebe (1995) method in predicting settlements. However, the difficulty in evaluating the available case studies was the lack of comparable data with not all cases reporting the same level of detail, site and design parameters. The authors evaluated the settlements for stone columns installed in untreated areas and plotted the results graphically (Figure 2.15). The results suggest that in six of the twelve cases the measured settlements were over-estimated or un-conservative. It was highlighted however that 12 data points lie along the expected trend line. The authors also reported on their own evaluation of estimated and measured settlements for stone columns installed in treated ground. Priebe (1995) was found to under predict the settlements in 6 of 38 cases and for the reminder over predicted the settlement (Figure 2.16). The authors acknowledge that although most of the data over predicted the settlements the lack of published case studies in cases where settlement was under predicted skews the conclusions that can be drawn.

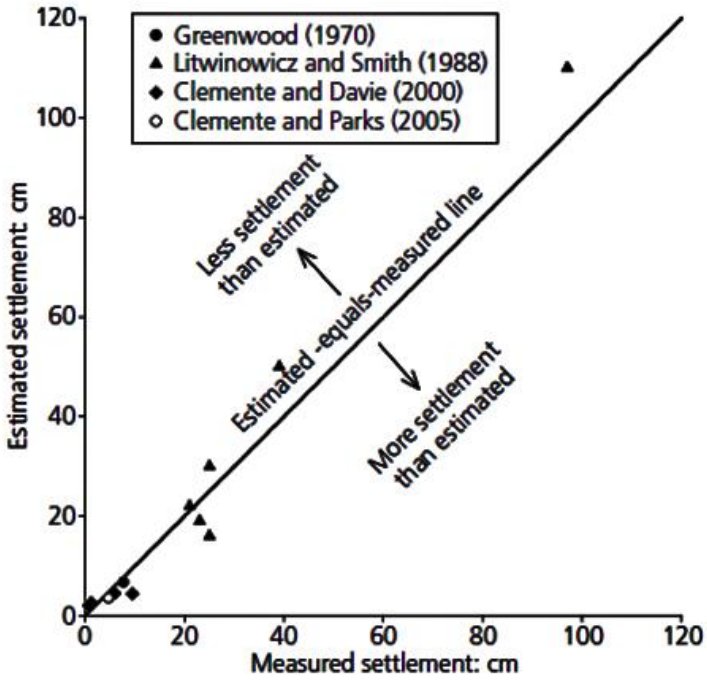

Figure 2.15 Comparison of estimated and measured settlements in untreated areas (Douglas *et al.*, 2012)

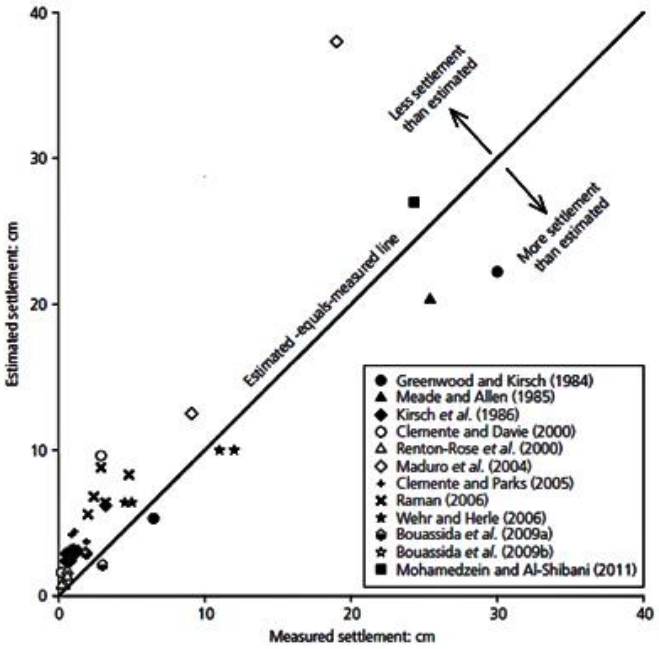

Figure 2.16 Comparison of estimated and measured settlements in treated areas using the Priebe method (Douglas *et al.*, 2012)

Douglas and Schaefer (2012) conclude that due to the variation in information provided for site conditions, soil parameters, design considerations, construction process and settlement monitoring, comparisons between the different case studies is very difficult. The quality of the design and settlement prediction on both untreated and treated ground is considered highly dependent upon the quality of the site investigation data used as the basis of that design. The authors suggest their findings confirm the earlier work of McCabe *et al.* (2009). They suggest that there is an 89% probability, based on the case studies examined where settlement is less than 8cm, that Priebe (1995) will suggest higher settlements than the actual measured settlement post installation.

2.4.7 Installation effects of stone columns

The use of vibratory technology in soft soil is considered to have an effect on the ground during and post installation of stone columns. As the poker enters the soil it displaces the soil laterally and vertically below. It has been recognised that during this installation the soil structure is altered in the near 'wellbore' area due to increased stress and elevated pore pressures. Watts and Serridge (2000) reported that the rate of penetration and time taken to construct the column affect the end performance of the column.

Kirsch (2006) and Kirsch (2008) examined the effect of stone columns installation in a sandy silt soil in terms of the *in-situ* stress regime for two large groups of columns. Each group has 25 columns and the variations in pore water pressure, effective horizontal stress and soil stiffness were analysed to determine the effect on stress state post column installation. The acquired data was compared with calculated values using the analytical method of Cunze (1985) based upon cylindrical cavity expansion theory. A reasonable correlation between the field and analytical data was observed although a degree of scatter was observed. The horizontal stress (Figure 2.17) and soil stiffness (Figure 2.18) were plotted against distance from column axis. The plots suggest that the horizontal stress and stiffness appear to have increased for a distance of one column diameter for values between of 4 and 8. The soil stiffness and horizontal stress increased as the vibroflot moved towards the measuring locations. The increase in soil stiffness and horizontal stress can be considered to be offset by the effects of remoulding and dynamic excitation for values of column diameter less than 4.

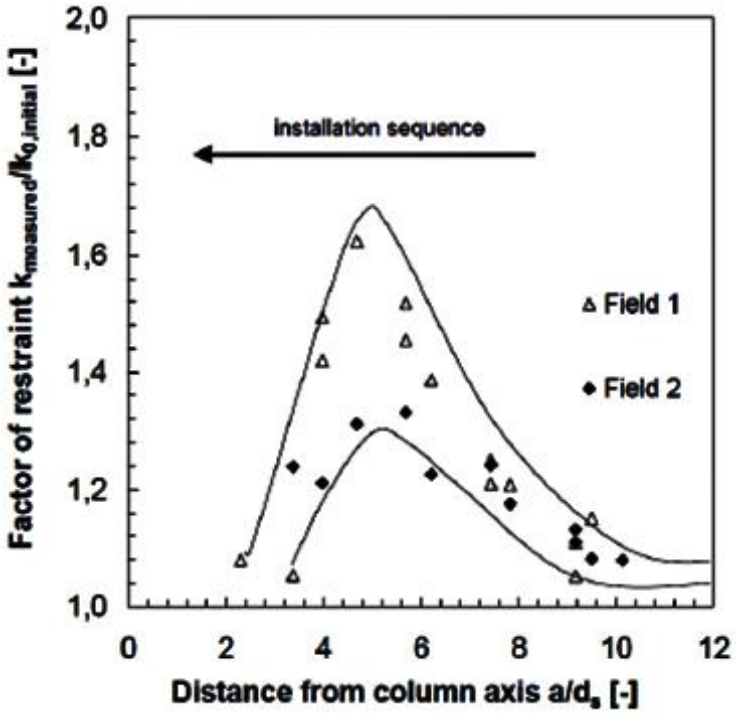

Figure 2.17 Factor of restraint measure during the installation of stone columns (Kirsch, 2006)

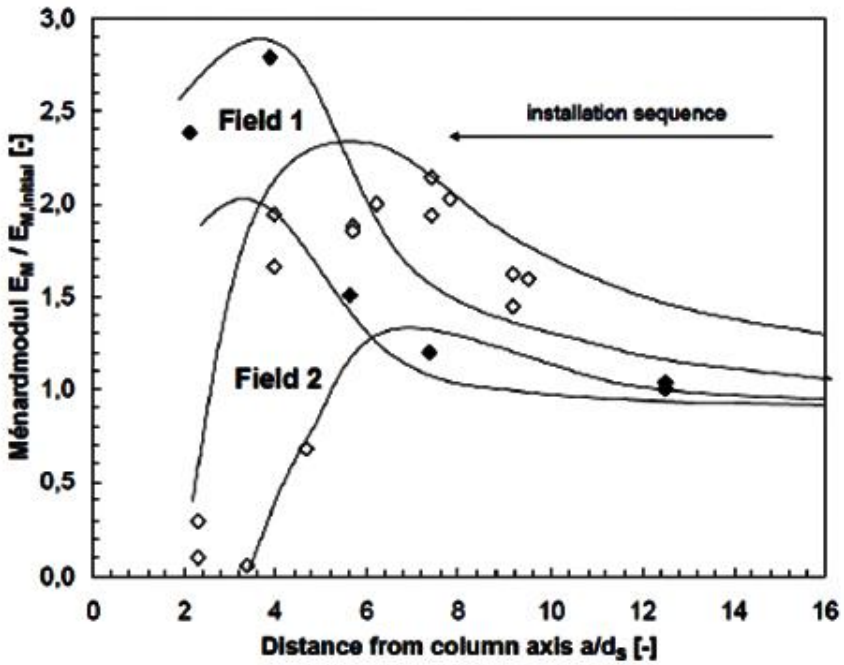

Figure 2.18 Development of ground stiffness during the installation of stone columns (Kirsch, 2006)

Castro (2007) reported the development and reduction in pore water pressure post installation for a group of seven stone columns in a normally consolidated clay. The pore water pressure was found to increase during vibroflot penetration and reached its maximum as it passed the piezometers installed in the soil. Similarly, this effect was also recorded by Watts & Serridge (2000). Significant heave was noted at the ground surface, possibly due to surging as the vibroflot entered shallow soil depths. However plain strain conditions were considered to be present and cylindrical cavity expansion theory was used to simulate column installation by the vibroflot. The increase in pore pressure recorded during the initial vibroflot soil penetration was compared with analytical values calculated using the method of Randolph (1979). It was assumed that the undrained shear strength of the surrounding soil reduced due to the increase in pore pressure (which is seen in conventional pile driving). The correlation between field and theoretical values was found to fail once additional columns were installed as the assumed boundary conditions were no longer valid. Dissipation of pore water pressure was found to occur very quickly, which was found to differ from the numerical solution by an order of magnitude of 100 times. It was suggested that this was due to fractures in the clay caused by high pressure from the vibroflot which then acted as drainage pathways into the stone column.

Egan *et al.* (2008) examined data relating to various sites where stone columns were installed. It was considered that heave may occur during the installation of stone columns when the column density was high. Heave was also considered a function of column size, spacing and construction method. The foundation arrangement was also considered to influence the amount of heave as small groups and strips of stone columns were found to produce less heave than large treated areas.

2.4.8 Summary of field studies on stone columns

The field studies have mostly considered the group behaviour of stone columns for different foundation types ranging from strip foundations to larger loaded areas e.g. embankments, rafts, etc. The *in-situ* soil in most of the cases examined has been soft clay, however a number of studies have also highlighted their use in mixed fill or silty sand. The application of stone columns was found to reduce settlements, reduce consolidation times and increase bearing capacity. In addition the columns were found to create installation effects such as increased pore water pressure and heave. From the various studies the key observations are summarised, as:

- *Bearing capacity:* Introducing stone columns into the *in-situ* soil was found to improve the soil such that an increase in bearing capacity was observed. Munkakh (1984), Hughes *et al.* (1975) and Watts and Serridge (2000) reported an increase in bearing capacity as a result of column installation. The field trials of Hughes et al. (1975) and Watts and Serridge (2000) reported that the presence of a crust aided the bearing capacity of the columns and soil.
- *Settlement performance and Priebe (1995) method:* The introduction of stone columns has been found to reduce settlements. Various authors (Klein and Tobin, 1996; Munfakh, 1984; McCabe *et al.*, 2009; Douglas and Schaefer, 2012) reported that the introduction of columns did reduce settlement. However, the magnitude of the reduction in settlement was found to be site specific.
- *Critical Length:* Prior to field installation Watts & Serridge (2000) and Hughes *et al.* 1975) calculated the critical length, and columns were subsequently installed to exceed this length. In such instances the columns did not fail by punching failure.
- *Deformation modes:* Bulging was recorded for the field trial of Watts and Serridge (2000) and Hughes *et al.* (1975). No evidence of end bearing failure

was recorded with the field examples designed against such failure by ensuring column length exceeded this critical length.

- *Column spacing:* As column spacing increased the settlement would also be expected to increase. However, Watts and Serridge (2000) record that a strip underlain by four columns settled more than an equivalent strip with three columns. It is possible that this may be evidence of block failure as described by Black (2007) and Black *et al.* (2011).
- *Pore water pressure increase and dissipation:* the effect of installing stone columns into soft soils is that, due to poor drainage, the area surrounding the column is able to dissipate pore pressure quickly and as such elevated pore pressure has been recorded by various studies (Klein and Tobin, 1996; Watts and Serridge, 2000; McCabe *et al.*, 2009; Castro, 2007). In each case the stone column was found to act as a vertical drain allowing consolidation to proceed. Watts and Serridge (2000) also reported that the length of time taken to construct the column affected the dissipation time post installation. Columns which had longer installation times were found to take longer to dissipate due, in part, to soil disturbance by the vibroflot.
- *Occurrence of surface heave:* An unwanted effect of column installation can occur if the column density is high. Egan *et al.* (2008) reported that this is considered a function of column size, spacing and construction method.

2.5 Numerical studies of granular columns

Numerical analysis of granular column performance has been performed by different researchers and historically they have adopted the unit cell axi-symmetric analysis or homogenisation methods due to computational power and time constraints. With the advent of more sophisticated computing systems and software capable of 3D modelling, its use has become more common.

2.5.1 Unit cell axisymmetric analysis

Balaam *et al.* (1977) examined the behaviour of a single stone column with an infinite array by adopting the unit cell approach. The unit cell approach considers a single column acting within a column-soil unit. The presence of columns within an array acts to increase stiffness and promote rapid consolidation. The behaviour of the unit cell applies only to columns within the array; note for those on the edges of the loaded areas of a large foundation they will not be restrained in all directions. In using this approach

the columns are arranged in a triangular pattern which considers a single unit cell to have a hexagonal zone of influence which can be approximated to a cylindrical body. The nature of the axi-symmetric analysis considers a slice taken from the centre of the column-soil to the outer diameter of the cylindrical body. By applying a basic finite element equation for elastic analysis and adopting a flow rule for elasto-plastic behaviour it is possible to approximate the system. The flow rule for elasto-plastic behaviour requires a yield criterion for increasing load and defining a stress-strain law for the material in the plastic range to permit analysis.

To predict the rate of settlement of the composite ground (column and soil) by vertical consolidation of the clay and by the dissipation of water pressure, Biot's theory was adopted. The results showed that under drained conditions soft clays reinforced with granular piles indicate a reduction in settlement. Undrained conditions were not considered by Balaam *et al.* (1977).

A comparison was made of elastic and elasto-plastic solutions which revealed a discrepancy of 6% between the results which occured at the outer boundary of the cell. The results suggested that elastic analysis was sufficient for analysis which avoids lengthy calculations of elasto-plastic analysis. It was concluded, in terms of column configuration and spacing, that when granular piles are installed in a regular pattern over a large area significant reductions in settlement can be achieved if columns are closely spaced and usually only if the columns are installed to the full length of the consolidating layer (as end bearing columns). It is reported that increasing the stiffness ratio of pile to soil, E_p/E_s, can reduce the settlement (Figure 2.19a). It is considered that consolidation is increased dramatically by the simultaneous reduction of pile spacing and increased pile penetration (Figure 2.19b).

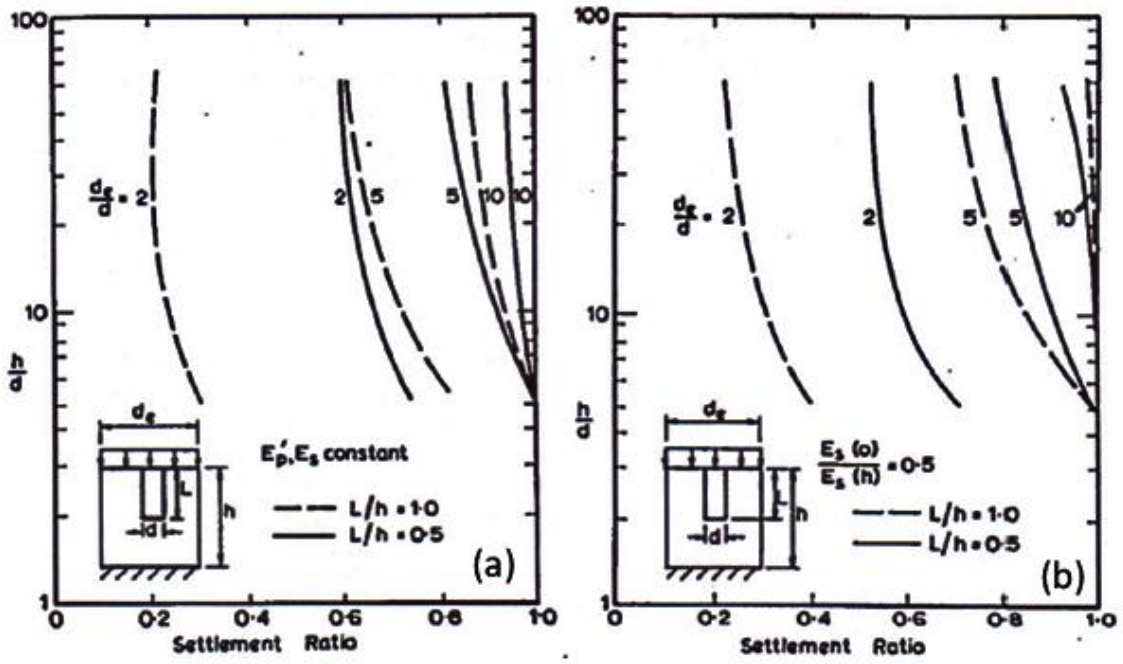

Figure 2.19 Settlement behaviour with (a) E_p/E_s ratio and (b) degree of pile penetration L/h (from Balaam *et al*, 1977)

Balaam and Booker (1981) analysed the settlement behaviour of rafts supported by stone columns installed in soft clay for three different column arrangements using the unit cell method. An examination of the effect of the ratio of column modulus to soil modulus was made. Comparison of the results of Balaam *et al.* (1977) revealed that for a perfectly flexible raft the load is shared depending on the replacement ratio. As the raft becomes more rigid the stress on the stone columns increases as more load is transferred to the stiffer columns. The vertical stress in the column is greater than the clay. During initial loading it is considered likely that the contact stress on the clay maybe greater than the columns. This is because the clay is initially undrained and incompressible. With time, as excess pore water pressure is dissipated by radial flow into the column, the relative stiffness of the clay and column change. After dissipation the clay becomes drained and the soil skeleton of the clay is less stiff than the column. The contact stress on the column preferentially concentrates on the stiffer column material. Maximum shear force was found to occur at the interface of the two materials with zero shear at the centre of the column. It was found that the magnitude of maximum shear force is determined by the diameter of the column and reaction pressure which increases with the ratio of unit cell width divided by column width. For a given diameter, increasing the spacing results in larger maximum shear forces. Shear force is considered a function of stiffness ratio of column modulus to soil modulus. Increasing

the stiffness ratio results in larger shear forces. Application of Biot's theory of consolidation showed that for a given spacing as the stiffness ratio increases, the columns take a greater proportion of the applied load, the rate of consolidation increases and the settlement decreases.

Balaam and Booker (1985) examined the behaviour of a rigid footing supported by a clay layer stabilised by a stone column in an infinite array utilising the unit cell concept and assuming the columns were arranged in a triangular pattern. By extending the research of Balaam and Booker (1981) it was possible to examine the behaviour with new computing methods to extend to elasto-plastic analysis and examine the undrained behaviour. Consideration was given to the undrained behaviour such that the clay soil will deform as an incompressible material and the column composed of highly permeable material would deform under drained conditions. Initial results indicated that the undrained settlement was insignificant and so was not explored further. The results of drained analysis revealed that the spacing ratio and angle of internal friction of the column directly govern column performance. Loss of stiffness is lower for columns with higher friction angles. Loss of stiffness of clay deposits is less severe for higher spacing ratios. This was found to occur for a given modular ratio as the proportion of vertical load carried by the column is less for higher spacing ratios and the potential for yielding is lower. The analysis also revealed that the settlement reduction due to stiffness is negligible when columns are widely spaced (d_e/d = 5) but the columns can still aid consolidation by drainage.

Wehr (2004) compared the behaviour of single and groups of stone columns numerically using plane strain finite element analysis. The model employed an elasto-plastic constitutive law in a Cosserat continuum. The analysis showed that for the case of a single stone column, a wedge of undeforming stone displaced in both the radial and vertical directions. A secondary failure mechanism in the form of a shear plane which develops along the column-soil interface can also be observed. The results of the group behaviour of stone columns highlighted similar results to Hu (1995). The central column (Figure 2.20a, left most edge of both meshes) highlights that the deformation occurs at a much deeper depth than the columns at the edge of the foundation regardless of column length. The columns appear to bulge at the shallowest depths closest to the edge with the long columns (Figure 2.20b) highlighting the development of shear planes. It is suggested that the shear planes between the internal and external columns may combine if the spacing of the columns is reduced and lateral deformation limited.

Such a combining of columns would also be dependent upon the relative movement of column and soil. The thickness of the shear planes increases with column depth. The short columns (Figure 2.20a) appear to show punching into the soil below whereas the longer columns show bulging (Figure 2.20b). Both observations are consistent with Hu (1995).

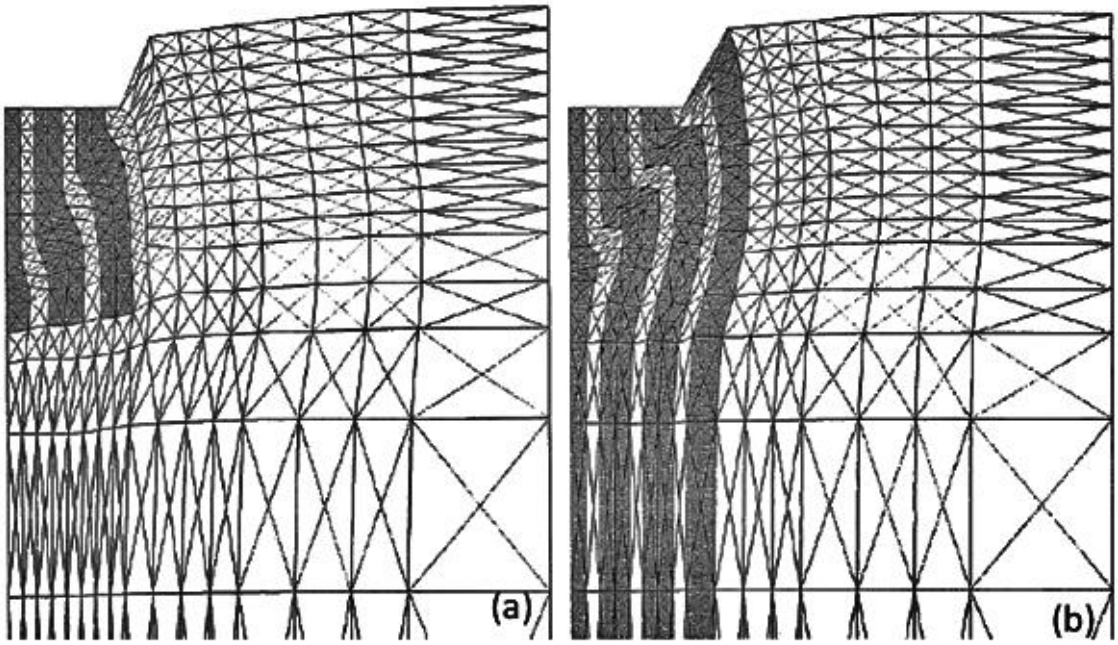

Figure 2.20 Deformed group of (a) short columns and (b) long columns with columns present outside the footing area. Clay is shown in white and columns are grey. (Modified from Wehr, 2004)

Andreou and Papadopoulos (2006) examined the influence of the applied load, area ratio, angle of internal friction and undrained shear strength on the deformation behaviour of a stone column utilising axisymmetric finite element analysis. The columns are considered to be subject to wide area loading from a rigid foundation and as such are modelled in a similar manner to Balaam *et al.* (1977) using the unit cell concept. The column and soil in the study are modelled using the Mohr-Coulomb model. The column is specified as end bearing with a diameter of 0.8m and length of 20 m, which suggests a length to diameter ratio, L/D, of 25. When the column was loaded, increasing the load from 10 kPa to 120 kPa was found to increase the depth of the zone of plasticity and the settlement improvement factor decreased from 3.1 to 1.9. Decreasing the area ratio from 14.2 to 5.1 and increasing the angle of friction from 38° to 44° was found to reduce the extent of the formation of a plastic zone in the column which was found to reduce settlement. The effect of increasing the undrained shear

strength on bulging behaviour was examined for values in the range of 10 kPa to 60 kPa and it was found that due to the incompressible nature of the soil that it had no effect.

Wehr (2006) reviewed the earlier work of Wehr (2004) and extended it to examine the effect of a flexible foundation. In contrast to the earlier work a wedge shaped zone of undeforming soil was not observed and the columns were found to bulge rather than bend. At the edge of the footing a wide vertical shear zone occurred with a number of wedge shaped and parallel shear zones visible. The number of shear zones was found to have increased compared to the rigid footing type. The author also suggests that the shear zones extend to a limit depth and is like the rigid cases dependent on the relative movement of column and soil. It is suggested that the flexible foundation has a better load carrying capacity than the rigid footing due to the larger shear zone near the edge of the footing edge and increased shear zones between the columns in the soil.

Ambily and Gandhi (2007) performed axi-symmetric finite element analysis in Plaxis 2D to numerically model the results of laboratory tests of model granular columns in soft clay. The unit cell approach was adopted in all modelling. A parametric study was also performed. The software was validated in Plaxis 2D by modelling the tests of Narasimha Roa *et al.* (1992) for a single column adopting the Mohr-Coulomb criterion for both column and clay. It was noted that a good approximation between laboratory and numerical analysis over most of the applied range was observed. Numerical analysis was then performed on the experimental laboratory tests of Ambily and Gandhi (2007). The soft clay and granular materials were modelled using the Mohr-Coulomb criterion. All materials were assumed to be drained. For the column within the loaded area it was found that as the spacing to column diameter ratio increases, the limiting axial stress of the column decreases. The ratio of limiting axial stress to shear strength was found to be constant for a given ratio of spacing to diameter and internal column friction angle.

The settlement improvement factor, defined as the stiffness of treated ground divided by the stiffness of the untreated ground, was found to be independent of shear strength of the surrounding clay soil and to depend mainly on column spacing and the column internal angle of friction. It was also noted that as the shear strength of the clay decreases, there is more of a stress concentration on the column. It was found that when the column itself was loaded bulging failure occurred at 0.5x column diameter. When the column and soil are loaded together, and the spacing increased, the axial capacity of

the column decreases and settlement was found to increase up to a spacing to diameter ratio of 3, beyond which no significant change was noticed.

Domingues *et al.* (2007a) and Domingues *et al.* (2007b) examined the influence of column spacing and compressibility on the performance of an infinite grid of stone columns supporting a 2m high embankment. The study adopted axisymmetric finite element analysis in both studies. The use of axisymmetric analysis was chosen to model the column-soil interaction as the embankment represented a wide area loading i.e. infinite array and each column could be considered to be acting within a 'unit cell'. The p-q-φ critical state model was adopted by the authors to simulate the behaviour of column and soil. The p-q-φ is an extension of the Modified Cam Clay model for modelling stress in three dimensions using the Mohr-Coulomb failure criteria. The end-bearing columns were assigned a diameter of 1.0m and fully penetrated the normally consolidated clay to a depth of 5.5m. The coefficient of lateral earth pressure was increased to account for the effect of column installation ($K_0 = 0.7$); with an intermediate value between $K_0 = 1 - \sin\varphi'$ (Jaky, 1944) and $K_0 = 1$ (Priebe, 1995).

The study considered the effect of column spacing over a range of area ratios, A/A_c, between 3 and 10. It was observed that settlement reduced the most for lower A/A_c which gave improvement factors between 1.2 and 2.0. No difference in differential settlement was recorded. It is suggested that columns act as vertical drains due to their high permeability which is considered to explain why the rate of consolidation increased at lower A/A_c. Horizontal displacement at the column-soil interface was found to be smallest at low A/A_c, which in part may be due to the restraining effect of neighbouring columns. The influence of column compressibility was investigated in a similar manner to Balaam and Booker (1985) by varying the modular ratio of column, E_c, to soil, E_s, from 10 to 100 for an area ratio of A/A_c of 5.3. It was found that both settlement improvement factor and differential settlement increase with increasing column stiffness. It was noted that the time taken to consolidate was shorter for higher column stiffness, for example 16 weeks for E_c/E_s = 20 and 10 weeks for E_c/E_s = 100. The stress concentration was also found to increase linearly by Domingues *et al.* (2007b) from 3.9 to 14.0 with increasing modular ratio.

Elshazly *et al.* (2008) investigated the applicability of settlement calculation methods based on the unit cell concept by analytical and numerical methods. Numerical analysis was performed by use of the axisymmetric finite element analysis technique. It is

suggested that although most design methods use the unit cell concept its application beyond that of an infinite grid array of columns is somewhat problematic to apply to column groups. In the case of groups of columns beneath foundations, columns on the outer edge will not be restrained in outer facing directions and the distribution of vertical stress decreases with depth below small foundations.

In order to relate the settlement of finite groups to that of infinite groups the authors developed modification factors. Two soil profiles consisted of a layered estuarine deposit (from Mitchell and Huber, 1985) and typical parameters from a soft soil deposit. The stiffness ratio, E_c/E_s, was varied between 1.3 to 2.6 for the estuarine deposit and a value of 8.5 was chosen for the soft soil deposit. Stone column installation effects were accounted for by increasing the coefficient of lateral earth pressure of the soil in the immediate area surrounding the columns to 1.5 and 1.2 for the estuarine and soft soil deposits respectively. The area ratio ($A/A_c = 3.4$) and column lengths were held constant, with the number of columns beneath the foundation varied to produce footing widths from 0.5 to 4.7. Loading of the foundation was modelled through a stone distribution blanket. Long term settlements were calculated using axisymmetric finite element analysis.

Two counteracting effects were noted by the authors in regard of the footings and wide loaded areas in regard of the unit cell. Firstly, when a column is present beneath a small footing the outer columns are unrestrained in the exterior direction and may be subject to bulging which increases the settlement. However, beneath a wide load area a column is considered part of an infinite array, with each column restrained by neighbouring columns as conceptualised in the unit cell. This leads to enhanced lateral restraint and reduced settlement. Secondly, distribution of stress beneath a foundation is considered to be different for a small footing and a wide loaded area. Vertical stress beneath a footing generated from an applied load is known to reduce rapidly with depth and is negligible beyond a depth equivalent to twice the footing breadth. Whereas for the case of a wide loaded area and unit cell stresses are considered to act to the full depth of the foundation and as such settlement can cover the entire length.

The results of the analysis suggest that for the case of a layered deposit the settlement of the small footing (B/L<2) was less than that of the unit cell (Figure 2.21a). This implies that the stress reduction with depth is more beneficial and that the loss of lateral confinement becomes less significant. However, as the footing breadth increases

(B/L>2) the settlement of the small footing becomes greater than the settlement of the unit cell. This is due to the increased vertical stress in the soil as a result of increasing the foundation width. For the remaining case of two layers of thick soft clay (Figure 2.21b and c) the settlement of the small groups is more than that of the unit cell. The increased settlement can be attributed to the lack of lateral restraint provided to the columns by the soft soil.

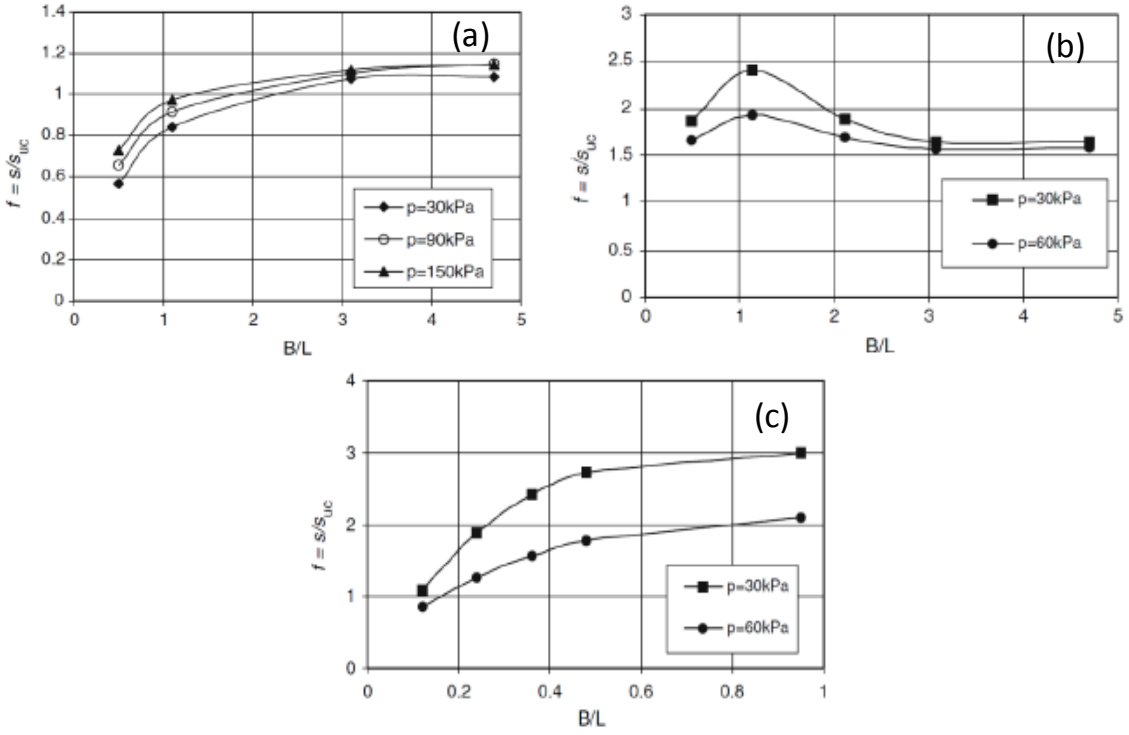

Figure 2.21 Settlement correction factor versus size ratio (a) layered deposit (b) 10.8m thick soft clay layer and (c) 30m thick soft clay layer (from Elshazly *et al.* 2008)

2.5.2 Homogenisation method

The unit cell method is restricted in that it can only be used where boundary conditions can be neglected and where loads are applied only in the vertical direction. The homogenisation method has no such restrictions. The homogenisation technique as applied to axi-symmetric finite element analysis assumes that the distribution pattern of granular columns is uniform and as such the columns are scattered homogeneously and isotropically within the area of analysis. It is also assumed that perfect bonding between column and soil exists. In this method of analysis the column and soil are treated as a composite material. The stress-strain response and response of the composite foundation is subjected to arbitrary loading and boundary conditions analysed.

Pande *et al.* (1994) used the homogenisation technique for elasto-plastic analysis of granular columns and soil. The column material behaviour was modelled using a Mohr-Coulomb criterion (with non-associated flow rule to permit dilation during shearing). The soil material behaviour was modelled using a critical state model. The column and soil as constituent materials were considered to be undergoing elastic or elasto-plastic deformation states depending on loading level. The columns were assumed to be installed by the displacement method with an area replacement of 15%. A square foundation underlain by columns in a five by five grid was modelled. The results revealed that the homogenisation method of modelling granular-column reinforced foundations, through the use of compatibility and equilibrium conditions through elastic and elasto-plastic analysis, was successful by the use of a sub-iteration scheme.

Lee and Pande (1994) used the homogenisation technique to analyse granular-column reinforced soil by treating the combination of column and soil as a composite through axi-symmetric finite element analysis. The columns were assumed to be homogeneously and uniformly distributed throughout the homogeneous zone for analysis. Both materials were assumed to be elasto-plastic materials with each material assigned separate yield functions. The soil was represented by the modified cam clay model and the columns by the Mohr-Coulomb criterion with a non-associated flow rule. The dilation of granular columns on shearing was represented by adjusting the dilatancy angle. A sub iteration scheme was applied to satisfy compatibility and equilibrium conditions. The numerical study was performed to compare with the results of Stewart and Hu (1993) and Hu (1995). The foundation geometry and material properties for the experimental laboratory and numerical analysis were similar for both studies and were considered acceptable by the authors.

The experimental setup of a circular steel footing resting on a granular-column reinforced foundation assumed a replacement method of installation having 30% area replacement ratio which represented an equivalent volume replacement of 30%. The results for the numerical analysis were compared with the experimental data in Figure 2.22 (reproduced from Hu (1995)) which illustrates the difference in behaviour between the two datasets. The results of both analysis show good agreement in terms of the ultimate loads. However, the numerical results of Lee and Pande (1994) appear to over-predict the initial stiffness as illustrated by the initially high vertical stress and elastic response of the curve before the onset of plastic behaviour. It was suggested by the authors that the softening behaviour is a result of the generation of tensile stress beneath

the edge of the stiff footing this reaches the dry side of the critical state model and its effect, combined with the non-associated flow rule of the Mohr-Coulomb yield criterion, influences the overall behaviour of the composite foundation. The numerical results suggested a settlement of 28mm compared to the experimental results of 27mm which suggests the numerical simulation was representative of the model columns.

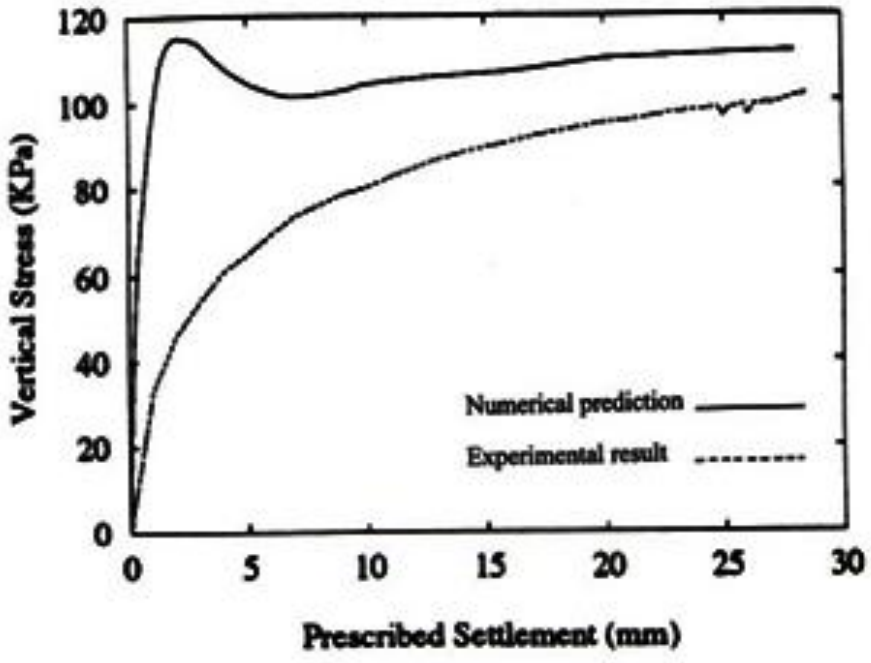

Figure 2.22 Comparison of the Numerical solution (from Lee *et al.* (1994)) and experimental results (from Hu (1993). (reproduced from Hu (1995))

2.5.3 Three dimensional analysis

The three dimensional analysis of stone columns is still evolving. In recent years the development of software capable of performing the analysis (rather than simply extending two dimensional cases) has seen challenges in representing the columns and soil in terms of developing appropriate material models and adequate geometrical representations.

Sathishbalamurugan and Muhunthan (2008) modelled the deformation characteristics of an embankment on weak clay which was improved by stone columns. The analysis was carried out in FLAC 3D which uses the finite difference method. The weak clay was represented by adopting the modified Cam-Clay model. The sand, fill and column material was represented by use of the Mohr-Coulomb model. The columns were represented by cylindrical meshes. The column and soil mesh were formed using triangular elements. It was found that beneath the embankment, the improvement

effectiveness was governed by the layout and extent of the stone columns. It was recorded that very little displacement improvement was observed beyond an improved area replacement ratio of 40%.

Killeen (2012) examined the behaviour of stone columns numerically using Plaxis 3D Foundation in three dimensions. The behaviour of small groups of stone columns supporting small area footings (pad and raft) at working loads was examined numerically for a soft clay based on the Bothkennar geotechnical test bed. The advanced elasto-plastic hardening soil model was utilised to model the behaviour of both in-situ soil and stone column backfill. Parameters for the column were selected rather than determined by back modelling field trials at Bothkennar (in this thesis column parameters are determined in this manner). The influence of key design parameters such as area ratio, column length, stiffness, strength and the effect of column installation on settlement performance was examined for small raft foundations. Deformational behaviour of the column and soil was also examined.

The results suggested that area ratio and column length have a significant effect on the settlement performance. At low area ratios, the column length was found to have a greater effect. Increasing the number of columns and hence confinement was found to reduce settlements. It is suggested that effect of key design parameters is dependent upon the mode of deformation. Compression and punching ratios were defined to describe three distinct mechanisms: punching, block failure and bulging. The punching ratio allows for an assessment to be made of the degree of punching which occurs by comparing the displacement of the base of the column relative to that of the surrounding soil and foundation. The compression ratio describes the proportion of surface settlement transferred to the column base and was used to identify bulging i.e. the higher the compression ratio towards unity the less bulging is likely to occur. The presence of these mechanisms was identified by analysing the distribution of shear strain within columns and soil. Additionally the distribution of stress and strain along the column length was also examined. It was discovered that area ratio and column length control the load transfer mechanism for small groups of stone columns rather than the density of stone columns.

Examination of the deformational behaviour revealed that a combination of bulging and punching occur simultaneously. One of the mechanisms will be more dominant depending upon the area ratio and column length. It is suggested that a unique critical

length for columns in a small group does not exist. The presence of a stiff crust in most soft clays, which is absent in laboratory studies, is considered to have a significant effect on the deformational behaviour of stone columns. As such the observation of critical length in the laboratory studies of homogenous clay beds is considered in part due to the absence of a stiff crust as columns are more likely to bulge in the upper regions of the column and cannot transfer their load to the base of the column.

Stress concentration ratios were examined at the ground surface and found to relate to the mode of deformation. It was noted that stress concentration ratios were dependent on column position and were found not to uniquely reflect the settlement behaviour of columns. It was found that stress concentration ratios were constant with depth in the sections of the column which had yielded and decreased towards unity to the base of the floating column.

2.5.4 Summary of numerical studies on stone columns

The numerical simulation of stone columns has been studied by a number of different researchers using three main methods: axisymmetric, homogenisation and three dimensional analysis.

Axisymmetric analysis uses the unit cell concept for analysis. The unit cell assumes a single column to be acting within a column-soil unit. The unit cell is considered to be present within an infinite array of stone columns across a wide loaded area. However, it has been shown to be of limited use in predicting the settlement of columns at the edge of loaded areas as the assumption of column restraint in all directions, which is a key unit cell assumption, is not valid in outward facing directions. The homogenisation approach considers the column and soil to be treated as a composite material. As such values have to calculated for each composite layer before calculating settlement. Three dimensional analysis allows for the modelling of both small and large groups of stone columns without the need for the methods of the axisymmetric and homogenisation approaches. Essentially allowing the stone columns to be modelled according the geometry and actual column/ soil properties i.e. 'as is' without the need for assumptions and modifications.

The numerical studies have focused on the behaviour of stone columns in soft clay. For the three methods the introduction of stone columns was found to reduce settlement and improve bearing capacity compared to the untreated cases. The degree of reduction was

found to be dependent upon area replacement ratio, area ratio, column length and spacing. From the various studies key observations have been summarised as follows:

- *Consolidation of the in-situ soil:* By reducing the pile spacing and increasing the depth of penetration the consolidation time can be reduce (Balaam *et al.* 1977; Domingues *et al.* 2007a). The columns act as vertical drains allowing for the dissipation of pore water.
- *Stress concentration in columns and soil:*

  - *Area replacement ratio* controls the load share and therefore stress distribution between the column and soil (Balaam and Booker, 1981; Mitchell and Huber, 1985; Pande *et al.* 1994; Domingues *et al.* 2007a).

  - *Column diameter* and *spacing* directly influences the stress concentration within the column (Balaam and Booker, 1981; Ambily and Gandhi, 2007).

  - *Foundation rigidity* influences the stress distribution between the column and soil. As the foundation rigidity increases the stress on the column increases as more load is transferred to stiff columns (Balaam *et al.* 1977; Balaam and Booker, 1981).

  - *Shear force* is considered to be highest at the edge of the column and zero at the column centre (Balaam and Booker, 1981). Increasing column spacing is considered to increase shear force and reaction pressure (Balaam and Booker, 1981).
- *Settlement performance*: The spacing ratio and column internal friction angle control the magnitude of column settlement (Balaam and Booker, 1981; Ambily and Gandhi, 2007). Increasing the friction angle was found to reduce the settlement (Balaam *et al.* 1981; Andreou and Papadopoulos, 2006). As spacing increases the settlement increases. Ambily and Ghandi (2007) note that beyond a spacing to diameter ratio of 3 no settlement reduction occurs, Balaam and Booker (1981) similarly suggest that beyond a ratio of d_e/d of 5 no settlement reduction occurs although consolidation may still occur. Balaam and Booker (1981) suggest that as the column spacing increases the lateral support and stiffness will therefore decrease which can be observed as a loss of clay stiffness at high spacing ratios. Increasing the modular ratio i.e. column stiffness to soil stiffness was found to reduce settlement and lead to higher stress concentrations in the column (Balaam and Booker, 1985; Domingues *et al.* 2007).

- *Deformational and Settlement Behavior of small groups of stone columns:* Studies by Wehr (2004) showed the development of a bulging zone for the case of single stone column. Analysis of small group behaviour of stone columns revealed similar results to Hu (1995). For columns arranged along a rigid strip a shear plane was visible. The central column was found to have the deepest shear plane depth with the shallowest plane occurring at the end of the foundation regardless of short or long column configuration. Short columns developed punching failure with long columns found to develop bulging failure. Wehr (2006) extended the earlier work to flexible foundations and discovered that large shear zones developed at the edge of footings which is considered to improve bearing capacity.
- *Simulation of stone columns:* Elshazly *et al.* (2008) prescribes caution when using axisymmetric analysis based on the unit cell concept for small groups of columns since column behavior at the outer edges will not be restrained as is the case for columns within a wide loaded area/ infinite array of columns.

2.6 Design theory and column performance

2.6.1 Design philosophy

The use of stone or granular columns in soils, regardless of type, seeks to improve the *in-situ* soil so that construction of low to medium-rise buildings can take place. As the column and soil work together to control the settlement, there are working loads which must be defined at the design stage so as to ensure that the columns are capable of supporting the stress applied without suffering failure. The main purposes of using this composite system can be defined as follows:

- *Reduction of the total and differential settlement of the foundation installed due to the application of load.* This is the primary function of the system and the ability of the columns to achieve this depends on ensuring the design is fit for purpose and the applied loads are not excessive so as to cause failure.
- *Reduce the time required for consolidation settlement to take place*. This is achieved by the columns acting as pore-water drainage pathways. Spacing should be close enough to allow radial drainage to take place. With drainage the soil stiffness increases.
- *Increase the bearing capacity of the foundation by increasing stiffness and transferring stress to depth by the columns*. This transfer is achieved by the

stress-share between the columns and soil, with the columns taking a greater share of the load as the stiffer element.

- *Reduction in potential for the development of shear failure beneath the foundation*. This is achieved by stress transfer to depth by the stiffer columns and reduction of stress in the upper soil depths.

In designing the composite system good practice should allow a configuration such that the failure mechanisms described by Hughes and Withers (1974), Hu (1995), Muir-Wood *et al.* (2000), McKelvey *et al.* (2004) and Kelly (2014) do not occur. The following four failure mechanisms are described and recommendations in regards of design made to prevent failure:

- *Bending failure:* occurs when the column is of insufficient diameter so as to cause the column to buckle and bend laterally. To avoid this a sufficient diameter should be designed particularly in soft cohesive soils where lateral support is limited.
- *Punching failure:* occurs when the column is not founded on sufficiently stiff material. When a load is applied the column will sink or punch into the layer below. This can be limited in field application by increasing column length and forcing the vibroflot downhole until a sufficiently stiff layer is identified. The use of site investigation borehole data should be used at the design stage.
- *Lateral or 'bulging' failure:* occurs when the column deforms laterally into the surrounding soil by barreling. This causes excessive settlements and is common in soft cohesive soils. To avoid this the column spacing can be reduced, the column diameter or length increased, or by excavation bypass the soft layers. All four options present an increase in cost and time.
- *Shear failure:* occurs when shear planes form. This can be due to an insufficient diameter of the column or excessive load applied to the composite foundation, particularly at the outer edge where the columns cannot provide optimum restraint to each other.

The four failure mechanisms present significant difficulty and cost increases to designers, which is normally passed on to the client. In all designs the specified allowable load on the columns needs to be accurate to ensure that the columns are not overloaded, which would cause one or more of the failure mechanisms described above to occur.

Key design recommendations in terms of column designs are:

- *Founding of columns on stiff or rigid layers to avoid punching failure*. In practice the vibroflot can be forced downward until refusal to ensure a firm base is identified. McKelvey *et al.* (2004) identified this as a key factor in improving performance.
- *Minimum length of columns to avoid bulging or lateral failure*. Columns should be of sufficient length so as to avoid stress concentration in short columns. Hughes and Withers (1974) and Hughes *et al.* (1975) suggests that bulging occurs to a maximum of four column diameters below the foundation level. Hu (1995) noted that for columns beneath strip footings that if the length of column was less than or equal to the footing breadth then the columns will develop punching simultaneously with bulging failure. McKelvey *et al.* (2004) noted that length had a significant effect on the development of bulging failure. Columns with a length to diameter ratio of 6 were found to develop bulging along the entire length. Beyond this ratio bulging was confined to the upper regions of the column. Minimum length should therefore be greater than a length to diameter ratio of 6 and if a strip foundation is built greater than the breadth.
- *Sufficient length of column to ensure bearing capacity sufficient for design*. With increasing length of column the material costs increase. Columns should therefore be designed such that they meet client criteria in terms of bearing capacity without excessive cost. Two laboratory studies examined the behavior in soft clays. Narasimha Roa *et al.* (1992) suggested an optimum length of 5 to 8 diameters. McKelvey *et al.* (2004) suggests that optimum length lies between 6 and 10 diameters. It is hereby suggested that a minimum of 6 diameters be used in terms of bearing capacity. Note: beyond this little benefit may be seen for increases in bearing capacity.
- *Optimum length for Settlement Control*. As noted previously the increasing length of columns increases material cost and demands on installation plant. The use of columns longer than 6 diameters may however lead to a benefit in terms of settlement reduction. Longer columns can be used in marginal or soft clays to meet settlement requirements in the absence of a stiff layer (cost permitting).

- *Minimum diameter of column and bearing capacity*. During the design process a minimum design diameter should be specified to avoid the development of shear planes or bending failure. In soft soils larger diameters are recommended as they also increase bearing capacity. Hughes *et al.* (1975) and Charles and Watts (1983) found that as the diameter increased bearing capacity also increased.
- *Column spacing and consolidation*. Each granular column installed into a soil will have an effective radial drainage area. In cohesive soils they will be smaller than granular soil due to the lower permabilities of the clay. The closer the spacing the greater the increase in bearing capacity and settlement reduction. Hughes *et al.* (1975) notes that columns were effective in consolidating the clay within two and a half diameters. It is recommend that this be adopted as the maximum spacing equivalent to a field column (e.g. a spacing of 1.5m with a 0.6m diameter). The greater the drainage and consolidation the greater the increase in stiffness which in turn will reduce settlement.

2.6.2 Stress concentrations in granular columns and soil

When load is applied to a foundation the stress is transferred to the soil beneath. As a consequence if the stress exceeds the bearing capacity of the soil failure will occur. When granular columns are installed beneath the foundation they stiffen the soil and stress-share with the soil altering the *in-situ* stress state. The contrast in stiffness between the soil modulus and column modulus (which is stiffer) leads to a preferential concentration of stress in the columns. In the stress-share system the stiffer the column the greater the proportion of the load it will attract. The Stress Concentration ratio, n, the ratio of average vertical stresses in the column and soil can be calculated as follows:

$$Stress\ concentration\ ratio, n\ = \frac{\sigma_s}{\sigma_c} \qquad [2.1]$$

where σ_s is the vertical stress in the soil and σ_c is the vertical stress in the column due to the applied load. Bachus and Barksdale (1983) described the relationships of the vertical stresses to the improvement factor, n, based on the unit cell concept:

$$\sigma_s = \sigma_V * \frac{n}{[1+(n-1)a_s]} = n_{soil} \ * \ \sigma_V \qquad [2.2]$$

$$\sigma_c = \sigma_V * \frac{1}{[1+(n-1)a_s]} = n_{col} \ * \ \sigma_V \qquad [2.3]$$

where σ_V is the average applied vertical stress and n_{col} and n_{soil} are the ratios of stress concentration ratios in the stone column and soil respectively. The column is limited in its ability to attract stress by its internal angle of friction, the restraint provided by the soil and geometry of the column. The evidence for this 'stress-share' phenomena has been well established by various researchers: Hughes and Withers (1974); Balaam and Booker (1981); Charles and Watts (1983); Barksdale and Bachus (1983); Bell *et al.* (1986) ; Narasimha Roa *et al.* (1992); Hu (1995); McKelvey *et al.* (2004) and Ambily and Ghandi (2007). The 'stress-share' behaviour and stress concentrations in the composite system (column and soil) is governed by two main parameters: Modular ratio and geometry.

Modular ratio, *Ec/Es*, describes the ratio of column stiffness, *Ec*, to soil stiffness, *Es*. Balaam and Booker (1981), Balaam and Booker (1985) and Ambily and Ghandi (2007) found parametrically that as column stiffness increases there will be a greater degree of stress concentration observed within the column. As the modular ratio increases, the columns take a greater proportion of the applied load.

Geometry of the columns has been identified as a controlling factor in stress distribution within the composite system of column and soil. Hughes and Withers (1974) examined the distribution of stress in a single column and found that it developed end bearing and adhesive stresses similar to piles. This suggests that columns transfer stress to depth as a function of column length. Charles and Watts (1983) found that column diameter controlled stress concentration. Small diameter columns were found to be in a state of failure and more prone to dilatancy. Increasing the diameter was found to reduce the stress concentration. McKelvey *et al.* (2004) suggests that stress concentration in the column increases the confining stress field in the upper regions of the column. Longer columns are considered to move friction support to greater depths and produce smaller settlements. It is suggested that beneath a rigid footing supported on long columns, the columns accepts a higher proportion of the load. The working stress ratio was found to approach a constant value of 3 regardless of length. Barksdale and Bachus (1983) found values for stress concentration between 2.5 and 5. Bell *et al.* (1986) found ratios to lie between 1.24 to 3. Hu (1995) noted that for a strip foundation stress concentrations were between 0.5 and 5. The degree of consolidation was found to control the degree of stress concentration.

In summary, it is clear that modular ratio and geometry have a significant effect on the stress distribution and the ability of the system to perform 'stress-share' for a rigid foundation. The modular ratio appears to permit stress-share until such time as the contrast between column and soil is so great that the stress is transmitted mostly through the columns (it becomes a pile). The geometry of the columns appears to have a significant effect on the limiting potential for ultimate bearing capacity failure. Failure is more easily achieved in smaller diameter columns. Increasing column length transfers stress deeper but beyond a certain length it may provide little benefit in terms of bearing capacity and settlement control. Spacing controls the degree to which columns work together. In close spacing the columns stiffen the ground and allow better settlement control.

If the columns are placed further apart they can have a reduced ability to permit 'stress-share' if the soil is weak. Balaam and Booker (1981) suggests that increasing the spacing results in maximum shear forces in the columns, whereas closely spaced columns show reductions as the columns work together to create a stiffened composite zone. Thus closely spaced columns should offer the highest bearing capacities and settlement reductions.

The stress distribution within a system is not constant and varies during and post installation as a soil deposit moves from undrained to drained conditions. When a load is applied to the foundation, soft clay is assumed to be near full saturation and as such is incompressible. The stress would therefore be shared with the clay and columns, as such the stress concentration would be lower. With the onset of drainage of pore-water into the column and laterally (consolidation) this relationship would change. The applied load would then transfer down through the foundation and be preferentially concentrated within the stiffer column material. This would increase the stress concentration within the columns. As the deposit becomes fully consolidated it is possible that the soil will stiffen slightly, bulging to some degree will occur in the column and the soil could potentially take an increase in stress. This would potentially decrease the stress distribution.

2.6.3 Unit cell concept

Stone columns, when used in a large array to support wide loaded areas, will typically be installed in one of three geometric grid patterns (Figure 2.23). The choice of grid configuration between triangular, square and hexagonal patterns is dependent upon the

design requirements of the project. The grid configuration influences the zone of influence of the column, however each configuration will give slightly different results. Within the large array (excluding columns on edge of the loaded area) each column can be considered to be identical in terms of symmetry. The unit cell concept considers that each column acts as a single pile-soil unit (Figure 2.24) and that the boundary conditions are rigid such that the sides of the unit cell are free from radial displacements and shear stresses. The unit cell is in effect an approximation as different grid configurations have different zones of influence which are approximated to an equivalent circular zone of influence (Figure 2.23). The unit cell assumptions do not apply to columns on the edges of wide load areas or beneath small foundation configurations such as pad or strips as the columns are not constrained laterally by other columns in all directions. Many of the current design methods are however based on the concept of the 'unit cell'.

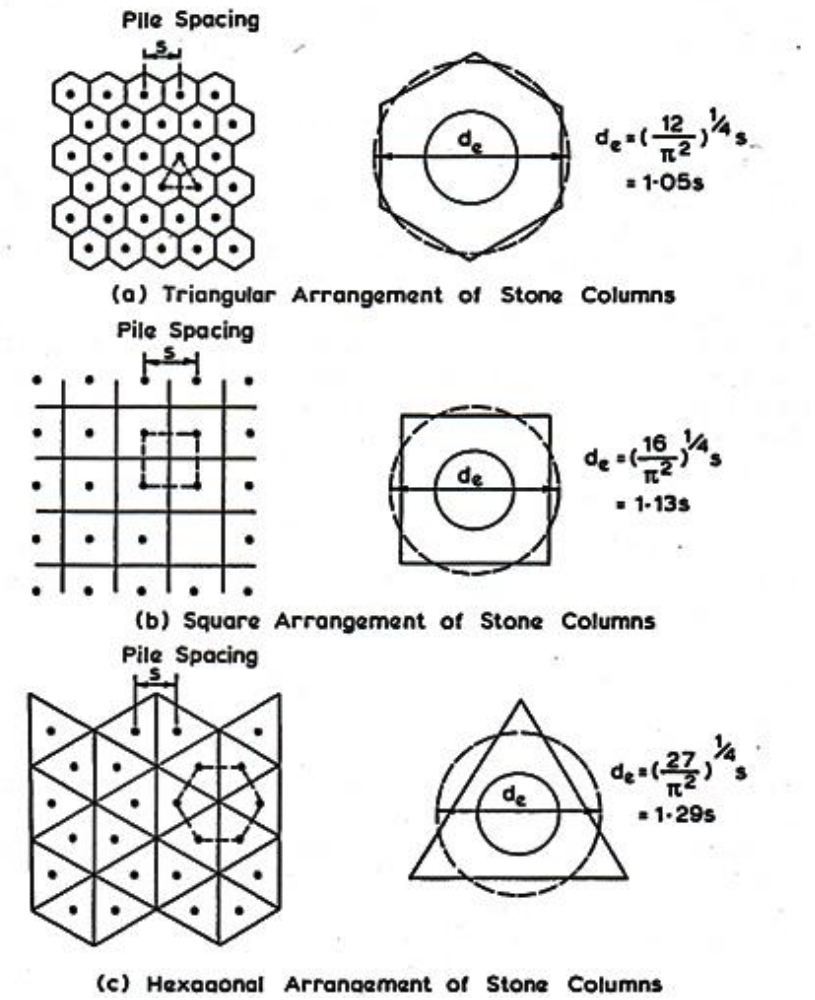

Figure 2.23 Various arrangements showing the domain of influence of each column (a) triangular arrangement of stone columns; (b) square arrangement of stone columns; (c) hexagonal arrangement of stone columns (Balaam and Booker, 1981)

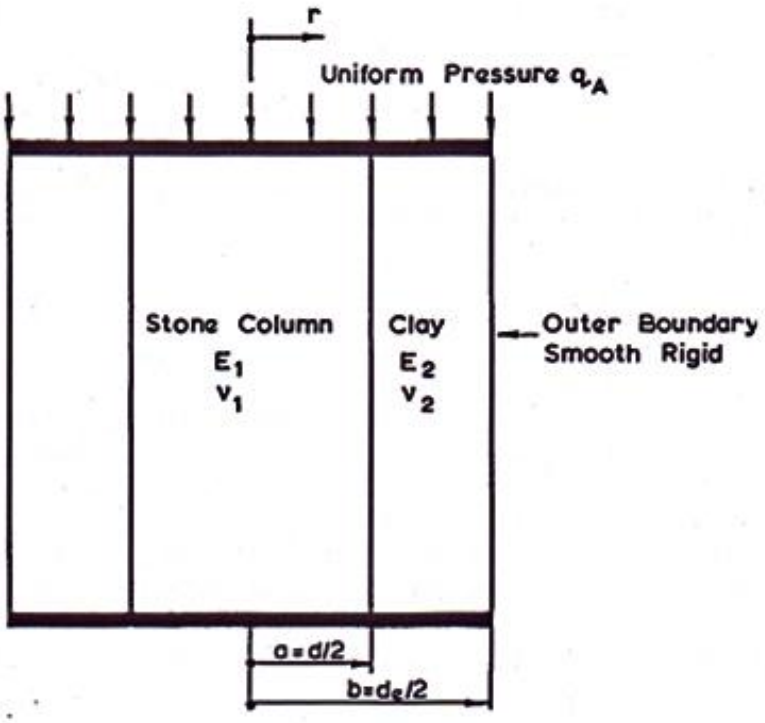

Figure 2.24 Schematic of a unit cell (modified from Balaam and Booker, 1981)

2.6.4 Bearing capacity

Bearing capacity of columns has been examined by various workers and the accepted methods are summarised here.

Thorburn and MacVicar

Research based on a single column assumes a column to be in a triaxial state of stress and that the surrounding soil supports this state. When a composite foundation fails it is assumed that both the column and soil are in a state of failure. Thorburn and MacVicar (1968) suggested an empirical relationship between allowable working load and the undrained shear strength of a soil based upon the behaviour of a single column (Figure 2.25). It is based on the researcher's experience of the performance of granular columns in a field application as applied beneath strip foundations for low-rise buildings in the Glasgow area during the 1960s.

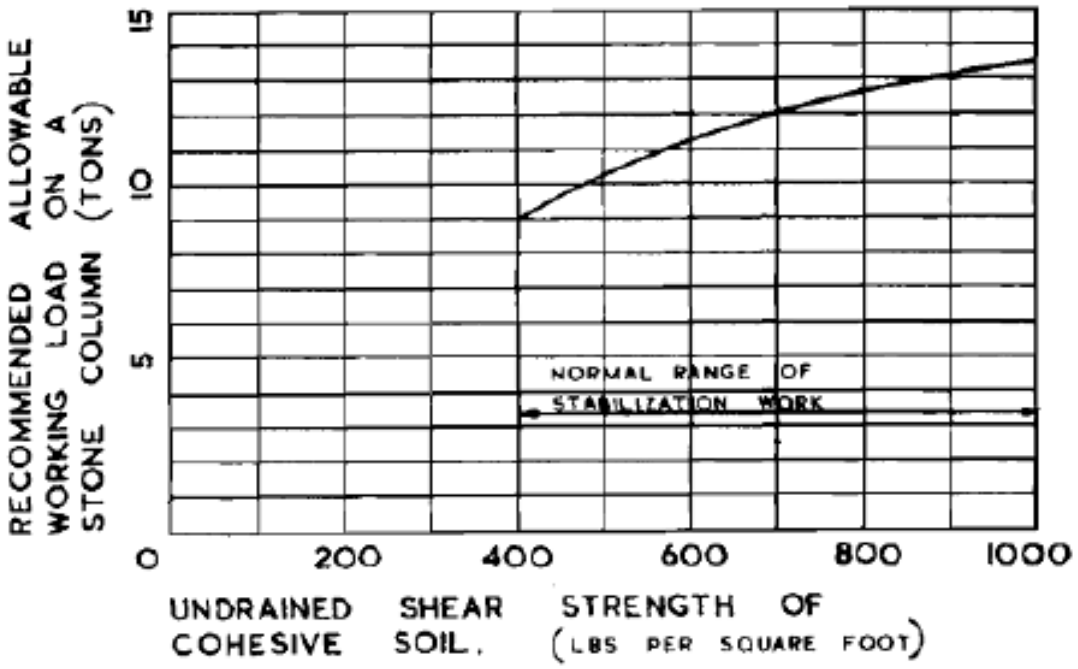

Figure 2.25 Relationship between allowable vertical stress on stone column and undrained shear strength (Thorburn and MacVicar, 1968)

Hughes and Withers

Hughes and Withers (1974) examined the behaviour of a single column in a triaxial system. The column is considered to be cylindrical and any subsequent lateral movement or bulging resembles a pressure meter test in which a cylinder expands against the side of the borehole. Analysis of pressure meter tests suggest that as the column expands the radial resistance provided by the soil achieves a limiting value at which indefinite expansion occurs. Based on the theory of Gibson and Anderson (1961) the limiting stress equation can be used to derive a relationship for the lateral ultimate stress by adopting elasto-plastic theory to give the following expression:

$$\sigma_{rL} = \sigma_{ro} + c_u \left[1 + log_e \frac{E}{2c_u(1+\nu)}\right] \qquad [2.4]$$

where σ_{ro} is the total *in-situ* lateral stress, E is the elastic modulus, ν is Poisson's ratio, and c_u is the undrained cohesion. The stone column can be considered to be confined in a triaxial type system where the cell (or lateral) pressure is limited. As the cell pressure is limited the column has an ultimate load beyond which failure can occur. The authors suggest, from a review of field records of quick expansion pressure meter tests, that the above relationship can be simplified:

$$\sigma_{rL} = \sigma'_{ro} + 4c_u + u \qquad [2.5]$$

where u is the pore pressure. The ultimate vertical stress a column can carry as it reaches its critical state (onset of bulging or lateral failure) is:

$$q_{ult} = K_P(\sigma_{ro} + 4c_u - u) \qquad [2.6]$$

Where K_P is the passive earth pressure. In a design situation the long term bearing capacity will occur in drained conditions so u = 0 would be a reasonable assumption.

Vesic's cavity expansion theory

Vesic (1972) proposed a cavity theory which derived an equation for estimating the ultimate cavity pressure, σ_3. This equation is:

$$\sigma_3 = c'F_c + qF_q \qquad [2.7]$$

Where *c*' is the cohesion of the soil and q is the stress occurring at the average depth of the bulge. The author describes F_c and F_q as dimensionless spherical cavity factors which can be obtained from Figure 2.26.

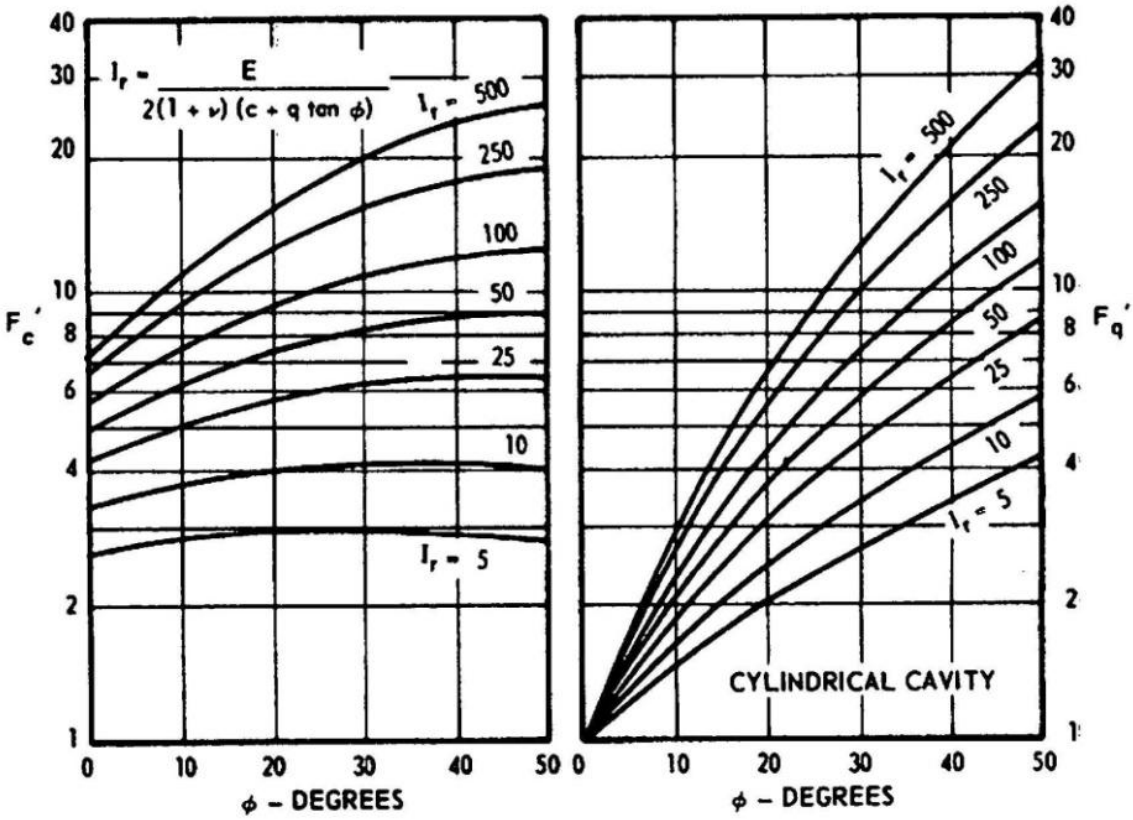

Figure 2.26 Cylindrical Cavity Expansion Factors (from Vesic, 1972)

Barksdale and Bachus (1983) and McKelvey *et al.* (2004) suggest that a granular column is assumed to be in a state of failure when bulging failure occurs. The ultimate

vertical stress that a granular column can carry, σ_1, is equal to the effective confining pressure multiplied by the coefficient of passive pressure, K_p. The passive earth pressure can be calculated from:

$$K_P = \frac{1+sin\varphi'}{1-sin\varphi'} \quad [2.8]$$

Where φ' represents the internal friction angle of the column material. The authors suggest that the ultimate vertical stress, σ_1, is equivalent to the ultimate load, q_{ult}. Thus the relationship from Equation 2.7 becomes:

$$q_{ult} = (c' F_c + q F_q)\, K_p \quad [2.9]$$

Barksdale and Bachus

Barksdale and Bachus (1983) examined the field performance of columns and concluded that a combination of 'past experience and good engineering judgement' should be used along with current design theory when determining the ultimate load of a granular column. The authors suggest that the bearing capacity of a single granular column can be determined using the following equation:

$$q_{ult} = c_u N_c \quad [2.10]$$

Where q_{ult} is the ultimate bearing capacity of the granular column, c_u is the undrained shear strength of the *in-situ* soil and N_c is a bearing capacity factor for the granular column. The authors suggest that N_c can be affected by stress levels in the soil and that when estimating from field data the stress concentration ratio should be considered. The authors suggest that the ultimate bearing capacity be taken as $5c_u$ with an upper limit of $\alpha_c \sigma$ where α_c is the ratio of stress in the clay, σ_c, to the average stress over the tributary area, σ. It is clear from the single column design theory that the performance of the column is heavily influenced by the soils ability to restrain the column and the stress concentration ratio in column and soil. The stress concentration ratio is a product of modular ratio.

The behaviour of a group of granular columns was found to differ from a single column underneath a rigid pad or strip foundation. The authors suggest that the ultimate bearing capacity of a group of columns may be considered to depend on lateral resistance, σ_3, of the soil beneath the foundation and the shear resistance provided by the composite of column and soil along the inclined shear surface. It is assumed that the foundation fails

on a shear surface and the strength of column and soil are fully mobilised. The equation derived by the authors can be described in three parts: the cohesion of the composite foundation, c_{avg}; the slope of the failure plane, β; and the lateral resistance of the soil block, σ_3, can be determined using the following equations:

$$c_{avg} = (1 - A_s)c_u \quad [2.11]$$

$$\beta = 45° + \frac{\varphi'_{avg}}{2} \quad [2.12]$$

$$\sigma_3 = \frac{\gamma_s B \tan\beta}{2} + 2c_u \quad [2.13]$$

Where c_u is the undrained shear strength of the *in-situ* soil; A_s is the area replacement ratio; φ'_{avg} is the composite angle of friction; γ_s is the unit weight of soil and *B* is the width of the footing. If σ_1, the ultimate vertical stress (q_{ult}) and radial stress, σ_3, are the stresses then for equilibrium of the soil block beneath the foundation, the following equation was derived:

$$q_{ult} = \sigma_1 = \sigma_3 tan^2\beta + 2c_{avg} tan\beta \quad [2.14]$$

This method considers only the geometry of the foundation and the material properties of the column and soil. The authors state that failure mechanisms such as bulging are not taken into account by this method. It is further suggested that application is limited to soils with undrained shear strength greater than 30kPa. The authors suggest that for groups of columns in softer soils the ultimate bearing capacity should be predicted by multiplying the q_{ult} for a single column (Equation 2.10) by the number of columns in the group.

2.6.5 Settlement control and consolidation

The settlement of foundations underlain by columns has been examined by various researchers and the accepted methods are summarised here.

Greenwood's method

Greenwood (1970) described the behaviour of stone columns in cohesive soils and suggested a series of curves for estimating the consolidation settlements of widespread foundations on soft clays with stone columns installed by vibroflotation. Figure 2.27 illustrates the curves for estimating consolidation settlements (long-term) of soft clays which are strengthened by stone columns. The curves provide for spacing of stone

columns between 2 and 3.25m in soft clays and their related settlements for clay strengths between 20 and 40kN/m² founded on firm or hard ground. The curves should be used with caution and treated as an approximation as they do not account for immediate or shear displacements.

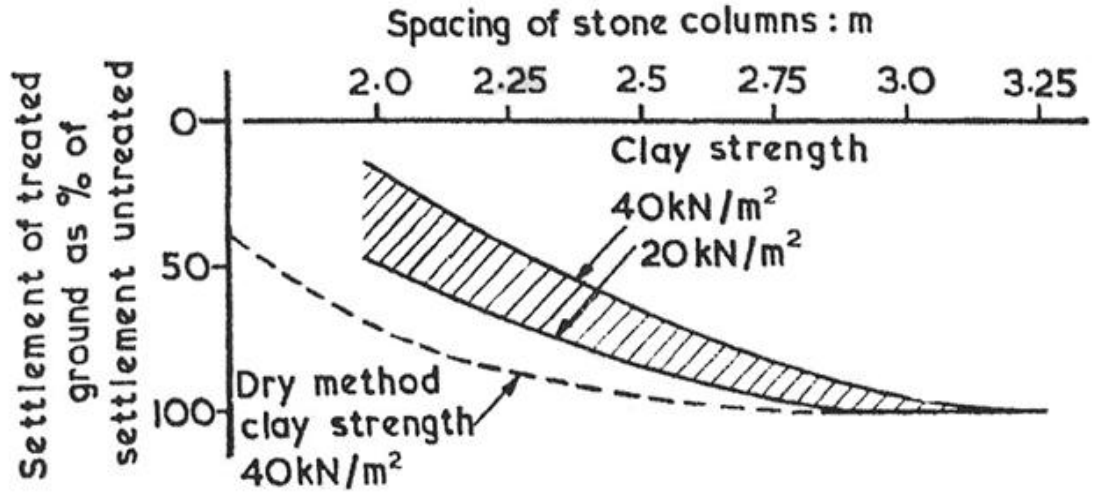

Figure 2.27 Settlement diagram for stone columns in uniform soft clay (from Greenwood. 1970)

Priebe's Settlement method: Ground Improvement factors

Priebe (1995) updated and advanced the work of Priebe (1991) by describing the design of vibro replacement from a theoretical perspective. The paper describes the installation of stone columns by vibro-replacement in cohesive soil. The degree of improvement can be estimated by the calculation of the ground improvement factors. The degree of ground improvement specifies the approximate reduction in settlement that will be seen as a result of the application of stone columns. Three factors are calculated: the basic improvement, compressibility of the column and overburden. The 'Unit Cell' concept is applied to consider the degree of improvement seen. It considers a single column within an infinite grid. The unit cell is defined for an area *A* with a single stone column with cross sectional area A_c and surrounding soil. The column is assumed to be founded on a firm layer which implies that it does not suffer end bearing failure. Any bulging of the column is assumed to occur over its entire length.

The basic Ground Improvement factor, n_0, suggests the degree of improvement of the *in-situ* soil which will be seen by the introduction of stone columns. The column is assumed to be composed of incompressible material with the bulk densities of column and soil neglected.

An assumption is made that the column behaves by plastic shear from the onset of loading and that the soil reacts elastically. It is assumed that the coefficient of earth pressure, K_o, is equal to 1. The basic improvement factor, n_0, is defined as follows (for Poisson's ratio of 1/3):

$$n_0 = 1 + \frac{Ac}{A}\left[\frac{5 - Ac/A}{4 * K_o * (1 - \frac{Ac}{A})} - 1\right] \qquad [2.15]$$

The basic improvement factor, n_0, neglects column compressibility. Any loads which are applied to the foundation, which are not connected with bulging, will cause settlement. Design curves for the basic improvement factor, n_0,, are shown in Figure 2.28. The improvement factor n_1 seeks to account for the column compressibility by a reduced improvement factor by increasing the reciprocal area ratio *A/Ac* to *Δ(A/Ac)*.

$$n_1 = 1 + \frac{\overline{Ac}}{A}\left[\frac{1/2 + f(\nu, \overline{Ac/A})}{K_0 * f(\nu, \overline{Ac/A})} - 1\right] \qquad [2.16]$$

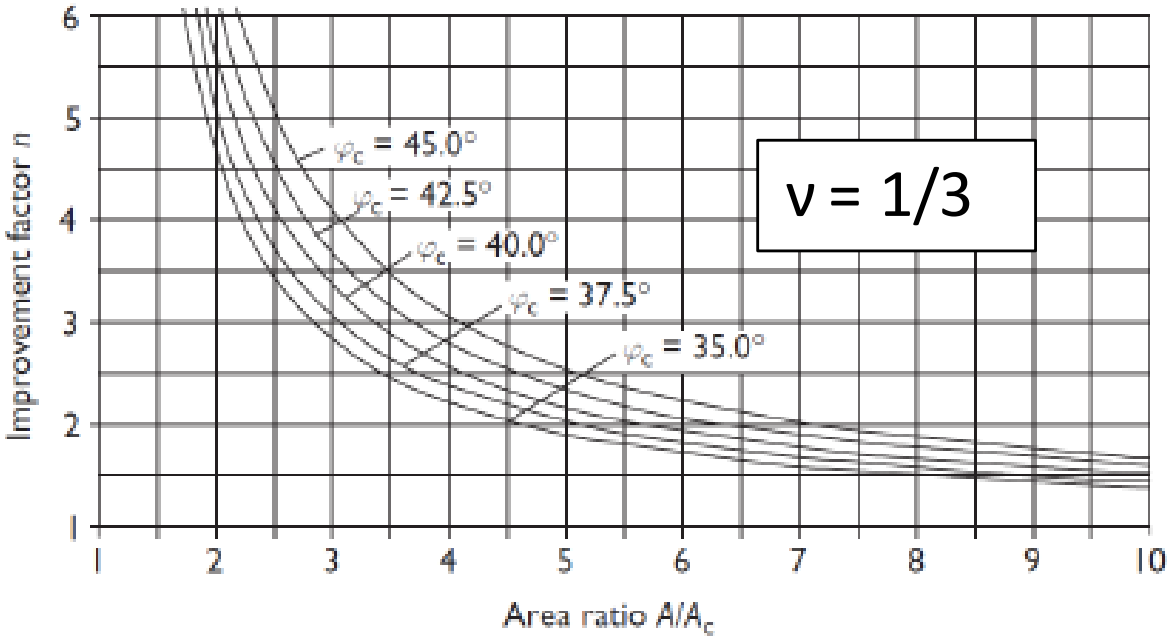

Figure 2.28 Design curves for basic settlement improvement factor n_0 with Poisson's ratio ν = 1/3 (Priebe, 1995)

By neglecting the bulk densities of the column and soil the initial pressure difference between soil and column is neglected. This pressure causes bulging of the column so without accounting for it, the equations cannot determine the true approximate behaviour of the column. Bulging behaviour depends solely on the distribution of the

load on the foundation (column and soil) and is constant over the entire length (for the purposes of this research). The weight due to column and soil may exceed the external loads and as such must be accounted for. With increasing overburden it is recognised that the columns are better supported laterally and provide a greater bearing capacity. The initial pressure difference, and the one depending on depth, can be expressed as a Depth factor, f_d. It generally increases the improvement factor n_1. The depth factor and ground improvement factor n_2 are defined by Equation 2.17 and 2.18 respectively. K_o is the earth pressure at rest, γ_s is soil unit weight; Δd is change of depth and p_c is the pressure on the column.

$$f_d = \frac{1}{1+\frac{Ko-1}{Ko}*\frac{\Sigma(\gamma_S*\Delta d)}{p_c}} \quad [2.17]$$

$$n_2 = f_d * n_1 \quad [2.18]$$

In order to ensure that the column behaviour is not over or under estimated, Priebe (1995) considered how the column and soil would behave with changing or maximum depth factors. Two compatibility controls are applied with the intention of ensuring that the column and the soil are not excessively overloaded (causing large settlements).

The first compatibility control is applied to dense or stiff soils to ensure that the settlement of the column does not exceed the settlement of the composite column and soil system. This can be summarised by Equation 2.19 where f_d is the depth factor; the densities of the column and soil are *Dc* and *Ds* respectively. The pressure on the column and soil are represented by *Pc* and *Ps* respectively. A depth factor of less than one can be considered unrealistic even if a result of the calculation is:

$$f_d \leq \frac{Dc/Ds}{Pc/Ps} \quad [2.19]$$

The second compatibility control relates to the maximum value of the improvement factor. It allows a check to be made to ensure that settlement of the columns do not exceed the settlement of the composite system of columns and soil beneath a foundation. This second control applies when the existing soils are unconsolidated or have low soil stiffness.

$$n_{max} = 1 + \frac{Ac}{A} * \left(\frac{Dc}{Ds} - 1\right) \quad [2.20]$$

Priebe (1995) presented a design chart (Figure 2.29) which relates the settlement of a group of columns beneath pad footings to the settlement of stone columns beneath an infinite area (s_∞). The curves are considered to account for the stress distribution beneath footings but consider a reduced bearing capacity for columns on the edge. He states that the footing area must be calculated from the area ratio, A/A_c, to compensate for footing size since larger footing areas have higher A/A_c ratios which give lower improvement factors for settlement. The curves are considered to be valid for area ratios up to 10.

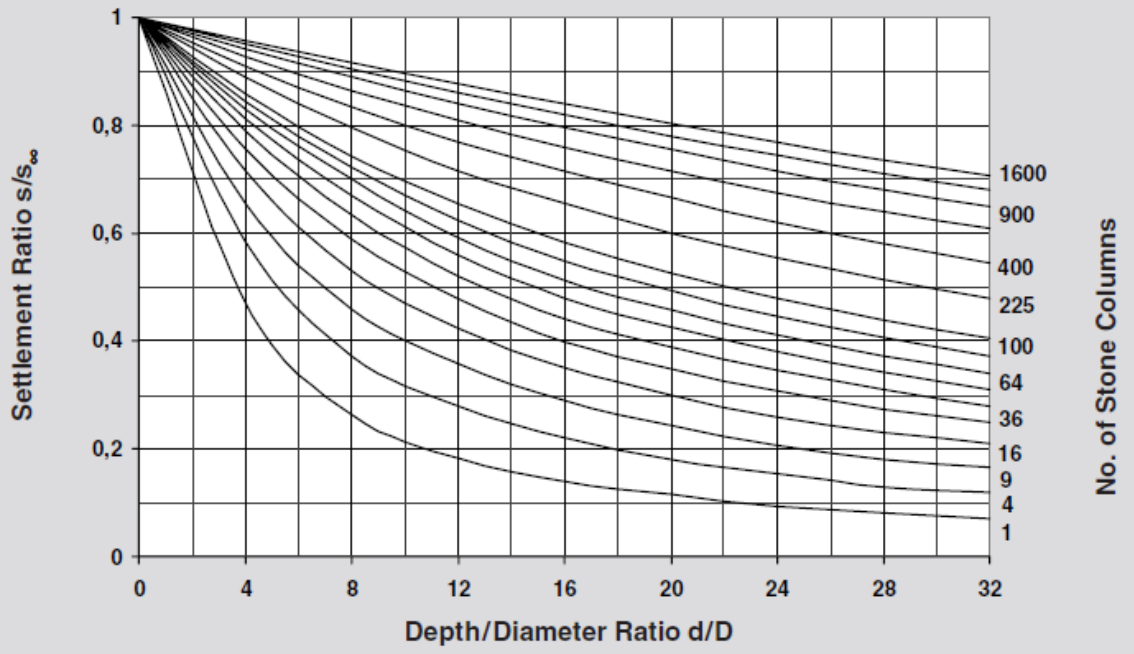

Figure 2.29 Settlement of single footings on groups of columns (Priebe, 1995)

Priebe (1995) states that the settlement curves are valid only for homogeneous soil conditions. The curves (Figure 2.29) indicate that settlement ratio reduces rapidly with increasing depth. This decrease is particularly rapid for small groups of columns between 1 and 9 columns. It is suggested that this is due to the reduction in vertical stress beneath the footing which implies that the influence of the depth factor is reduced for footings. In order to overcome this limitation he suggests calculating the settlement by sub-division of the soil into layers and calculating the settlement of each layer individually to avoid the potential for settlement over-calculation. This settlement is calculated by the use of the following formula from Priebe (1995):

$$\Delta s = \frac{p}{D_s n_2} \left[(s/s_\infty)_L \, d_L - (s/s_\infty)_U \, d_U \right] \qquad [2.21]$$

Equilibrium Method

Aboshi *et al.* (1979) suggested a method for the calculation of settlement beneath a foundation reinforced with large diameter sand compaction piles under a flexible raft. The method can also be applied to stone column design as described by Bachus and Barksdale (1984). By adapting a 'unit cell' assumption, the method estimates settlement reduction due to stone column installation by using one dimensional consolidation theory. The settlement is considered only in the vertical direction. A settlement reduction ratio, n, can be calculated which is the ratio of improved to unimproved soil from the following equations:

$$S = m_v * \sigma * H \quad [2.22]$$

$$S' = m_v * \sigma_c * H = m_v * n * \sigma * \mathrm{H} \quad [2.23]$$

$$\frac{S}{S'} = n = \frac{1}{1+(n-1)A_s} \quad [2.24]$$

Where S and S' are the consolidation settlements of the unimproved and improved soil respectively, m_v is the coefficient of compressibility of the unimproved ground and H is the thickness of the soil layer. n represents the stress concentration factor and A_s is the area replacement ratio.

Bachus and Barksdale (1984) urges caution on the use of this method as an upper bound approach since accurate measurement of stress concentration using existing field methods can be difficult. As long as the stress concentration ratio is between 3 and 5 this method is considered adequate for settlement estimation.

Incremental Method

Goughnour *et al.* (1979:1) developed a method based on the unit cell concept to consider a single column and its surrounding clay. The method assumes that the stone column and soil behave elastically from the onset of applied vertical loading of the foundation and consolidation after plastic strains occur in the column; after which column and soil are considered to be in a state of equilibrium.

The method requires that the confining pressure with depth is accounted for using an analysis of the horizontal slices of the unit cell model. The vertical strain in each slice or element is calculated under two states. Firstly, the column material is treated as rigid-plastic and incompressible. Secondly, the column material is treated as linearly

elastic. The vertical strains are then compared and the larger of the two selected. The reliance of the method on high quality data on soil properties can make the calculations complicated. Goughnour (1983) described the approach in further detail and presented design charts to simplify the process. A comparison of this method was made with a field study in Goughnour and Bayuk (1979:2). The research revealed a good comparison between the predicted and actual settlements under the centre of the loaded area. However, at the corner of the foundation the settlement appears to be overestimated. The predicted stress ratios indicated good agreement with the actual field test.

Balaam & Booker

Balaam and Booker (1981) examined the settlement of an infinite array of end bearing stone columns using axisymmetric finite element analysis (FEA). From the analysis the authors suggest an analytical method which can be used to calculate the settlement based upon the Constant Cavity Expansion Theory (CCET) and unit cell concepts. The stone column and in-situ soil are considered to be elastic materials which are defined by the parameters Young's modulus, *E*, and Poisson's ratio, *v*. The analysis is performed by considering the compression of a cylindrical body (unit cell) between a smooth raft and rough substratum layer. The lateral confinement is provided by a laterally restrained smooth rigid wall. Initial FEA revealed that a triaxial state of stress exists which acts on the column, shear stresses develop along the sub stratum are generally small and values of field quantities remote from the substratum were insensitive regardless of assumption of perfectly smooth or perfectly rough. Thus a smooth substratum was assumed to allow for an exact analytical solution to be calculated.

The first approximation (solution A) assumes a pile-soil unit (Figure 2.30) in a state of confined compression. The authors report a discontinuity in the horizontal stress at the pile-soil interface due to the contrast in column-soil stiffness, which can be considered as representing column bulging in a real situation. The stiffer column will absorb more stress than the surrounding soil and generate a higher radial stress than the *in-situ* soil. In order to account for the bulging a second solution B was developed and added by the authors corresponding to the zero movement of the plate with an applied radial stress equal in magnitude but opposite in sign to the discontinuity found in solution A at the column-soil interface. The final solution, C, was found by super-imposition of solutions A and B (Table 2.2).

Lame's parameters $\lambda = \frac{\nu E}{(1-2\nu)(1+\nu)}$, $G = \frac{E}{2(1+\nu)}$

and where $F = \frac{(\lambda_1-\lambda_2)(b^2-a^2)}{2a^2(\lambda_2+G_2-\lambda_1-G_1)+b^2(\lambda_1+G_1+G_2)}$, [2.25]

a is the stone column radius and *b* radius of the unit cell

The relationship between the average applied stress and strain is resolved by integrating the vertical stresses across the soil surface:

$$q_A\, b^2 = [(\lambda_1 + 2G_1)a^2 + (\lambda_2 + 2G_2)(b^2 - a^2) - 2a^2(\lambda_1 - \lambda_2)F]\varepsilon \quad [2.26]$$

	Region 1 Stone column	Region 2 Clay
ε_z	ε	ε
u_r	$Fr\varepsilon$	$\left[F\frac{a^2}{r}\frac{(b^2-r^2)}{b^2-a^2}\right]\varepsilon$
σ_r	$[\lambda_1-2(\lambda_1+G_1)F]\varepsilon$	$\left[\lambda_2+\frac{2a^2F}{b^2-a^2}\left(\lambda_2+G_2+G_2\frac{b^2}{r^2}\right)\right]\varepsilon$
σ_θ	$[\lambda_1-2(\lambda_1+G_1)F]\varepsilon$	$\left[\lambda_2+\frac{2a^2F}{b^2-a^2}\left(\lambda_2+G_2-G_2\frac{b^2}{r^2}\right)\right]\varepsilon$
σ_z	$[\lambda_1+2G_1-2\lambda_1F]\varepsilon$	$\left[\lambda_2+2G_2+2\lambda_2\frac{Fa^2}{b^2-a^2}\right]\varepsilon$

Table 2.2 Solution C (Balaam and Booker, 1981)

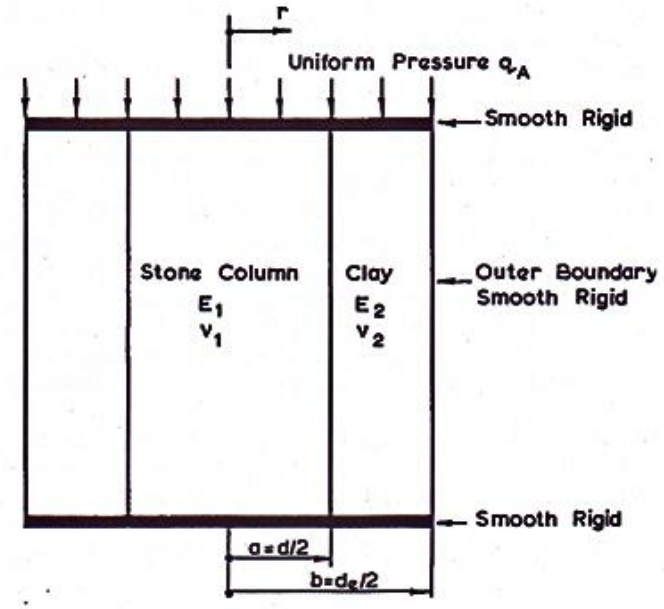

Figure 2.30 Definition of terms for analysis of equivalent cylindrical unit (from Balaam and Booker, 1981)

Balaam and Booker (1985) revised the original analysis method (Balaam and Booker, 1981) which was focused on elastic behaviour to include yielding. The previous method had been shown to over-estimate the effectiveness of stone columns in reducing settlements. They performed an interaction analysis with simplifying assumptions to account for the yielding with FEA to confirm its validity. The original analysis had assumed that the major principal stress acted close to the vertical plane with significant yielding in the column but minimal deformation in the soil. The column and soil material is treated as dilatant materials and modelled as idealised elasto-plastic material satisfying the Mohr-Coulomb yield criterion with a non-associated flow rule. In order to make the analysis more realistic the authors made the following assumptions:

- Stone columns in the pile-soil unit are held in a triaxial stress state
- Yielding can occur in the stone columns but not in the soil
- No shear stress will develop along the stone-soil interface

The settlement calculation methodology requires that the one dimensional settlement, *S*, be calculated for the clay without stabilisation. The settlement is calculated from multiplying the vertical strain, ε_z, by the depth or length of column, h. The vertical strain is calculated by multiplying the coefficient of compressibility, m_v, by the change in vertical stress, $\Delta\sigma_z$.

$$S = \varepsilon_z h \qquad [2.27]$$

$$\varepsilon_z = m_v \Delta\sigma_z \qquad [2.28]$$

$$m_v = \frac{(1+\nu)(1-2\nu)}{E_s(1-\nu)} \qquad [2.29]$$

Once the settlement without stabilisation has been calculated the settlement of the tank founded on stabilised clay by stone columns can be calculated. The stone columns and clay soil are assumed to be elastic. The elastic parameters of column and soil stiffness, E_s, and Poisson's ratio, ν, can be used to calculate values for Lames parameters. Once known the values are inserted into Equation 2.25 to obtain a value for the constant F. Utilising the Lame parameters for column and soil and the constant F in Equation 2.26 a value for the elastic settlement is obtained. In order to account for yielding in the column the authors use correction factors which are extensively presented for various geometric configurations similar to Figure 2.33 for the specific case of a column with d_e/d = 2, φ = 40°, ψ = 0 and ν = 0.3. The elastic settlement obtained by calculation is

then divided by the correction factor from the chart to give the corrected settlement which accounts for yielding of the column.

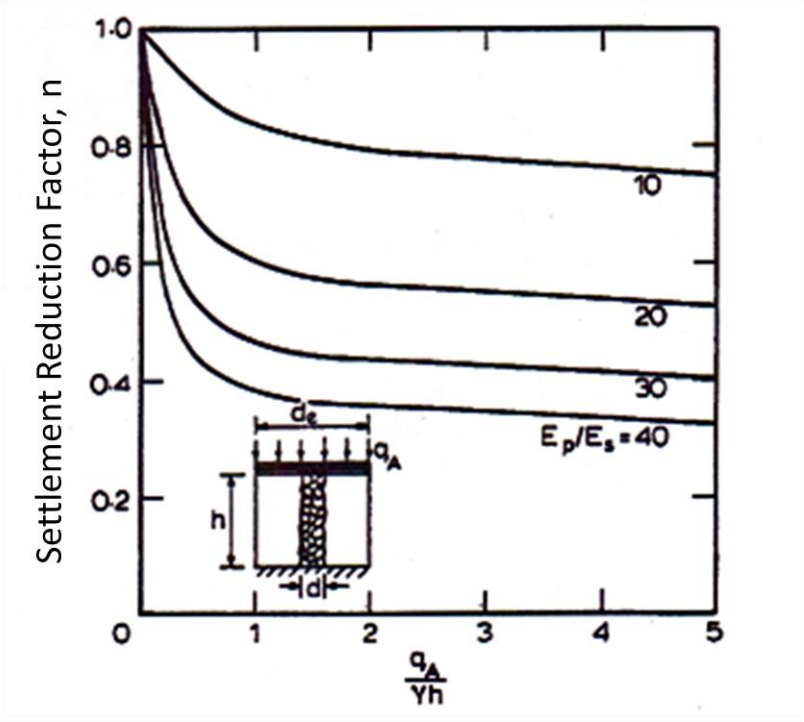

Figure 2.31 Elastic settlement correction factors; d_e/d = 2, φ = 40°, ψ = 0 and ν = 0.3 (from Balaam and Booker, 1985)

Pulko and Majes

Pulko and Majes (2005) propose a method which extends the elastic analysis method described by Balaam and Booker (1981) to include column yielding which is accounted for by dilatancy theory. The soil is assumed to be elastic while the column is assumed to behave as an elastic material to the yield point beyond which it behaves according to the Mohr-Coulomb perfect plasticity criteria. It is designed similarly to Priebe (1995) to account for applied stress levels and *in-situ* overburden stress. Column yielding will occur once the elastic limit is reached. The elastic and plastic strains are integrated along the length of column to determine settlement improvement factors.

2.7 Conclusion

Increasingly soft cohesive soils are being considered for use as buildable land to support low to medium bearing buildings. Difficulties arise from the fact that soft cohesive soils are generally composed of clay which will often suffer from large magnitudes of settlement over time unless improved. Stone or granular columns offer the economical

improvement of the soils and allow building of low to medium bearing structures without the need for expensive, potentially uneconomical piling.

Good application and configuration of the stone column installation will provide reductions in settlement and the time taken for the soil to consolidate as the granular nature allows for their use as drains to dissipate the excess pore water pressure during loading. An improvement may also be seen in bearing capacity if the column configuration is able to sufficiently stiffen the soil deposit. It should be noted that for medium to high loads stone columns would not be suitable due to the potential for excessive settlement.

The analysis of laboratory, field and numerical analysis of stone columns has been reviewed in this Chapter. The research suggests that the two main controls on settlement in group behaviour appear to be the area ratio and modular ratio of the column and soil. Consideration will be given to both during the research presented in this thesis. It is clear from the current research that there is still uncertainty in terms of the application of the design methods for predicting column and soil behaviour in cohesive soils. The design methods tend to focus on either a unit cell approach, where columns are assumed to benefit from surrounding columns, or the case of a single column and hence this area on a worst case basis. It is the opinion of the Author that it is the upper areas of the column that will suffer the highest settlements (visible as bulging) and hence that needs to be considered further. This thesis will therefore examine the behaviour of granular columns in soft soils and consider how these excessive settlements may be prevented.

Chapter 3

Modelling approach and development of the Bothkennar soil profile

3.1 Introduction

The Finite Element Method has been widely used to analyse complex engineering problems numerically. The method approximates the real behaviour by using the principle of virtual work to simulate the distribution of stress and strain throughout a continuum. In this research the Plaxis 3D Foundation software is adopted to simulate the behaviour of stone columns both in large arrays and small groups. The behaviour of the foundation, stone columns and soil are simulated through the use of constitutive models.

RSPB Bothkennar, formerly known as Science and Engineering Research Council (SERC) test bed at Bothkennar, is located near to Grangemouth, close to the Kincardine Bridge on the south bank of the Forth estuary, Scotland. The site has been used for testing various foundation configurations and a field trial examining the settlement performance of stone columns has been carried out at this site (Watts and Serridge, 2000). In this chapter the properties for a Bothkennar soil model are selected from the literature. The soil model is then examined and validated before an analysis of the settlement and deformation (Chapter 5) of stone columns beneath small raft and strip foundations is performed.

3.2 Modelling approach

3.2.1 Model setup and use of Plaxis 3D Foundation

The setup and use of Plaxis 3D Foundation is extensively described in Brinkgreve (2007). Further information is available on specific aspects such as the setup of boundary conditions, mesh generation and setup of material models.

3.2.2 Material modelling

Representing the behaviour of real soil is highly complex. Soil is composed of organic and inorganic components that have been deposited over geological time which will vary depending on the original source of the material resulting in a heterogeneous deposit. When soil is deposited it will be exposed to many different processes particular to a specific site. Such processes can include erosion, weathering and flooding amongst others which can cause variations in the soil e.g. erosional/ weathered layers, layering

and as a result effect the geotechnical properties. The behaviour of real soil can be considered highly non-linear as a result of its geological history, with soil strength and stiffness dependent upon the stress and strain level (Potts and Zdravkovic, 1999). Capturing all aspects of soil behaviour is very difficult. While some very advanced soil models such as S-CLAY1 and S-CLAY1S (Castro and Karstunen, 2010) allow for the study of specific aspects of soil behaviour e.g. creep behaviour, no one model is presently able to capture all the effects. The use of the linear-elastic, Mohr-Coulomb, and hardening soil models used in this thesis are discussed below. The models have proven applications in the modelling of stone columns including large arrays of columns (Gäb *et al.* 2008).

3.2.2.1 Linear elastic model

The model considers a material as an idealised linear-elastic material which excludes any plastic deformation, preventing the development of irreversible strains during loading and unloading. The model requires two parameters to be specified in order to simulate behaviour, Young's elastic modulus, E, and Poisson's ratio, ν. The model is considered too simplistic to capture the stress-strain behaviour of soil and is instead apllied to model the foundation behaviour in this research.

3.2.2.2 Elastic perfectly plastic mohr-coulomb model

The elastic perfectly plastic Mohr-Coulomb (MC) model considers the soil as a linear-elastic, perfectly plastic material. It is considered a first approximation model of soil behaviour (Brinkgreve, 2007). It assumes a constant Young's modulus, E, before failure and as a result cannot model stress level dependency, i.e. increasing stiffness with increasing confining pressure. The behaviour of the soil in the elastic domain is modelled by Hooke's law of elasticity, once a material yields, the failure is modelled using the Mohr-Coulomb failure criteria. The failure of the soil is defined by the internal friction angle, Φ, and cohesion, c, of the material. The soil will initially behave as a linear-elastic material until the shear strength has been mobilised and the yield criterion has been met. At which point all further load increments will lead to plastic strains. The elastic deformations are a function of Hooke's law which relate stress to strain through:

$$Young's\ modulus = \frac{stress\ ,\sigma}{strain\ ,\mathcal{E}} \qquad [3.1]$$

In order to evaluate if strains will be elastic or plastic, a yield criterion is applied which is a function of stress, cohesion and friction angle. The model adopts the Mohr-Coulomb failure criterion to model the plastic shear response of the soil to stress. The criterion is defined as:

$$\tau = c' + \sigma'_n \tan\varphi' \qquad [3.2]$$

where: τ = shear stress failure envelope

σ'_n = normal stress at the interface

c' = cohesion

φ' = friction angle

The stress present in the soil is related to the difference between the major and minor principal stresses, σ_1 and σ_3. The Mohr-Coulomb failure envelope (see Figure 3.1) indicates that stress points under the line are in an elastic state. When the stress circles touch the failure line (as defined by $\tau = c' + \sigma'_n \tan\varphi'$), failure will occur i.e. the soil passes from an elastic state to a plastic state. The representation of the Mohr-Coulomb failure surface in three dimensions resembles a cone with its point at the origin and hexagonal base (see Figure 3.2). Inside of the cone elastic deformations will develop which are controlled by Young's modulus and the Poisson's ratio. When an element within the numerical model reaches the stress surface the deformations become plastic. The model will not generate irreversible strains below the yield surfaces (Mar, 2002). Irreversible plastic strains caused by shearing are modelled by a non-associated flow rule, which is defined by the angle of dilation, ψ.

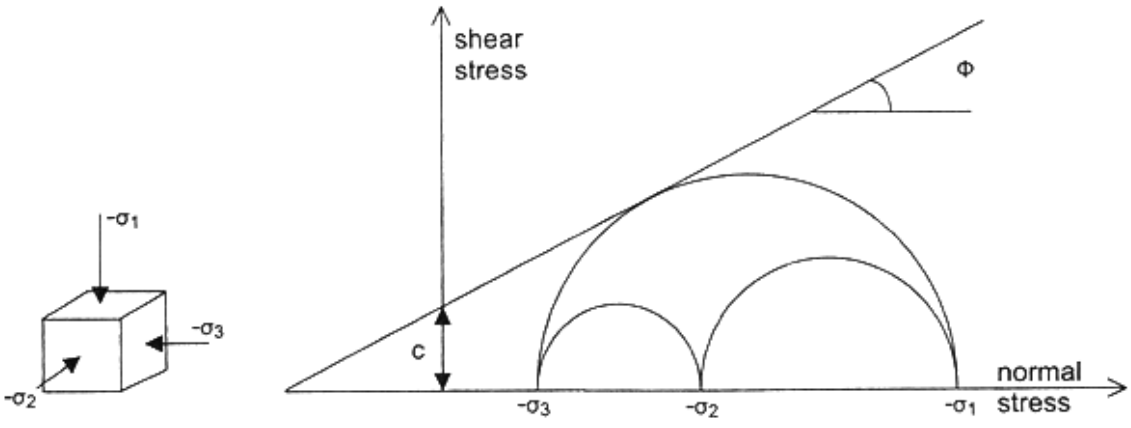

Figure 3.1 Mohr Coulomb failure criteria in two-dimensions (Brinkgreve, 2007)

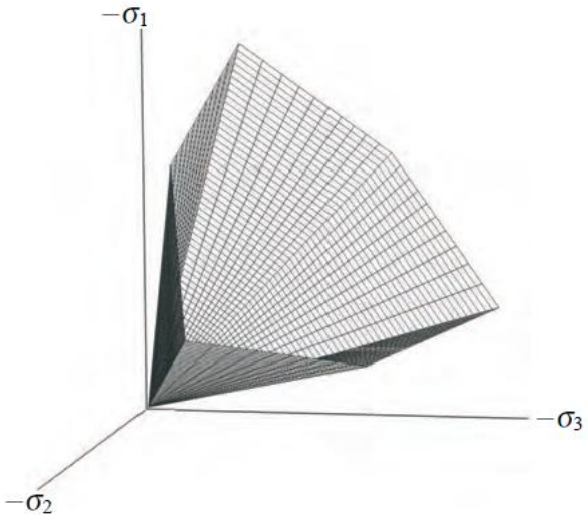

Figure 3.2 Failure surface for Mohr-Coulomb model in three dimensions (Brinkgreve, 2007)

3.2.2.3 Hardening soil model

First order models such as the elastic perfectly plastic Mohr-Coulomb are convenient and readily useable with field and laboratory data. However, some details of soil behaviour are not accurately represented. To obtain accurate results for certain types of problems an advanced constitutive model is more appropriate. The hardening soil (HS) model is an advanced constitutive model which has a proven ability to represent both soft and stiff soils (Schanz, 1998). This advanced model has a number of key advantages over the elastic perfectly plastic Mohr-Coulomb (MC) model:

- The MC model assumes that soil behaviour is linearly elastic prior to failure. However, soils such as over consolidated clays have been shown to exhibit stiffness reduction at stress levels that are well below those typically expected to cause failure (Figure 3.3). The HS model can model this gradual loss of stiffness which occurs as failure is approached.
- In the MC model, within the elastic range, the stiffness of soil during loading and unloading is the same. From triaxial testing it is known than soil responds with some stiffening on unloading compared to primary loading (Figure 3.4). This behaviour can be modelled in the HS model.
- The MC model is limited in that it cannot represent the development of plastic strains when the soil is unloaded in shear. The HS model can model the development of plastic strains under compressive loading.

- The MC model is simplistic in the sense that stiffness parameters are independent of the stress level. The HS model is able to relate the stiffness to the stress level.

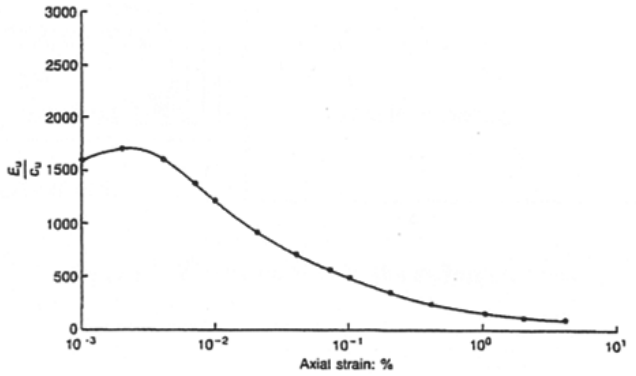

Figure 3.3 Secant Young's Modulus from undrained tests on London Clay showing small strain non-linear behaviour (Jardine *et al.* 1985)

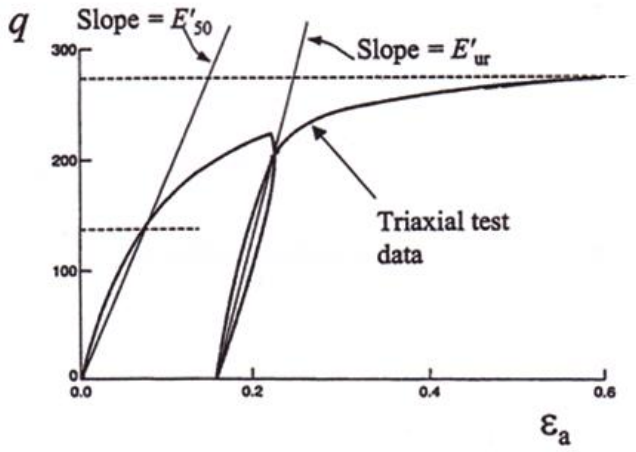

Figure 3.4 Triaxial test data showing stiffness in primary loading and unloading (data from Clayton and Khatrush, 1986)

The Hardening soil model is an extension of the hyperbolic model developed by Duncan and Chang (1970). The hyperbolic model was based on the theory of elasticity. Non-linear elasticity can be used to represent a non-linear loading path, but is not adequate in modelling the soil response since it returns along the loading path (Figure 3.5). The HS model is based on the theory of plasticity with soil dilatancy and a yield cap behaviour modelled. It can be considered a work hardening plasticity model, with the non-linearity in the stress-strain response which is a consequence of the development of plastic irrecoverable strains as the load level is increased (Burd, 2005). When the soil is unloaded it will return along a path which is stiffer than the loading

path (Figure 3.5). The model is able to account for both shear and volumetric hardening, which allows for the behaviour of irreversible strains generated by deviatoric or compressive loading to be captured.

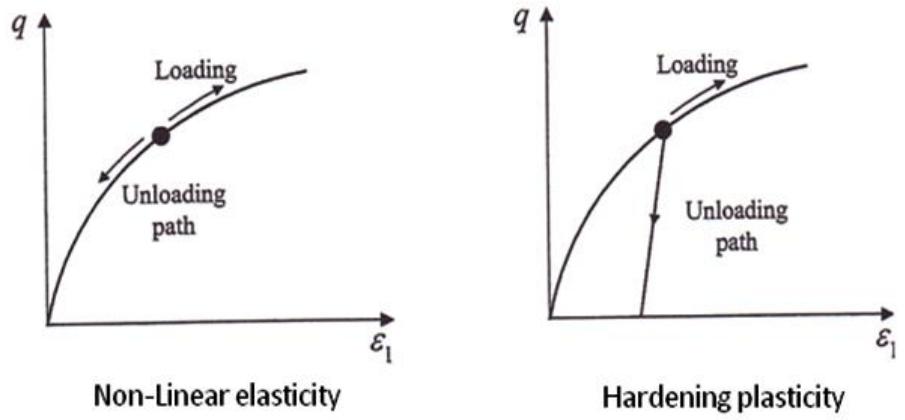

Figure 3.5 Modelling approaches for non-linear soil behaviour (Burd, 2005)

In order to represent soil loading in shear, the hardening soil model uses a work-hardening plasticity approach. The inner yield surface expands as the plastic shear strain increases (Figure 3.6). The inner yield surface will expand to meet an outer Mohr-Coulomb failure surface.

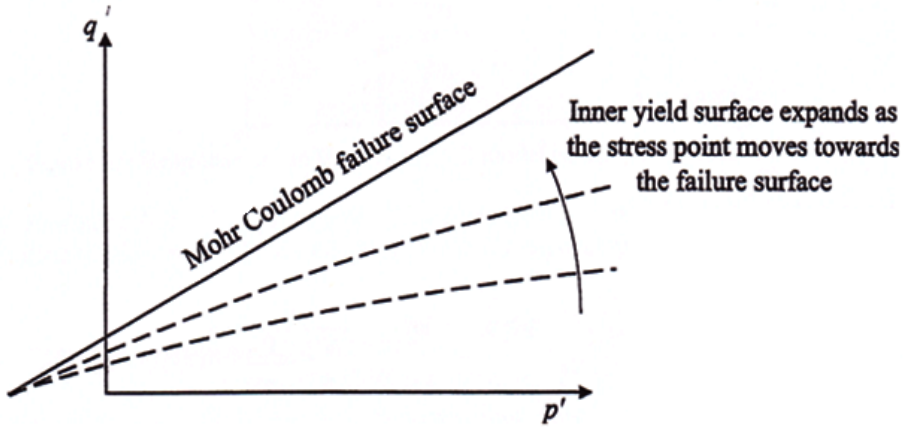

Figure 3.6 Expansion of the inner yield surface (Burd, 2005)

The hardening soil model was constructed to simulate the behaviour of soil in a drained triaxial test (Figure 3.7). It relates the deviatoric stress, q, to the vertical strain, ε_1 for primary loading and is approximated by a hyperbola defined by Equation 3.3.

$$q = \frac{\varepsilon_1}{\frac{1}{2E_{50}} + \frac{\varepsilon_1}{q_a}} \quad for\ q \leq q_f \qquad [3.3]$$

where q_a is an asymptotic value of deviator stress, E_{50} is the secant Young's modulus, q_f is the ultimate deviatoric stress.

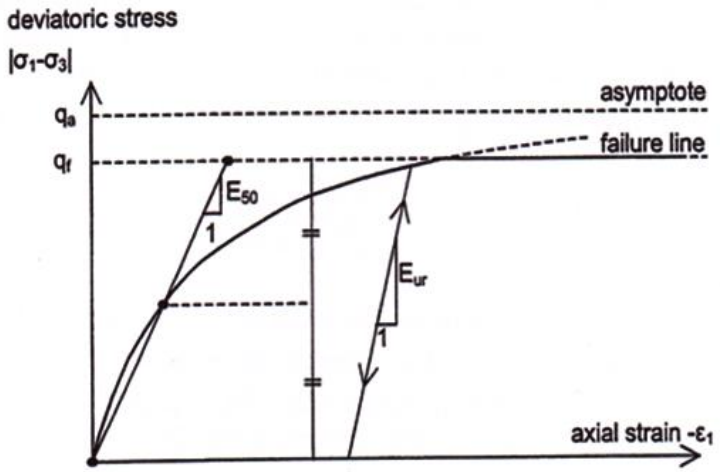

Figure 3.7 Response of the Hardening soil model in a drained triaxial compression test (Burd, 2005)

The ultimate deviatoric stress is derived from the Mohr-Coulomb criterion and can be related to the asymptotic shear strength (Equation 3.4).

$$q_f = \frac{6\sin\varphi}{3-sin\varphi}(p + c.cot\varphi) \qquad [3.4]$$

where φ is the angle of friction, c is the cohesion and p is the mean total stress. Once the ultimate deviatoric stress is reached during loading and the Mohr-Coulomb criteria met, perfect plasticity yielding occurs. The HS model is able to capture plastic shear strains which occur from decreasing stiffness. It also captures the effect of volumetric strains due to dilatancy. Plastic volumetric strains are modelled using the stress-dilatancy theory developed by Rowe (1962). A yield cap surface accounts for volumetric strains resulting from isotropic loading. The yield surface for the HS model in principal stress space (Figure 3.8) contains a yield cap surface compared to the Mohr-Coulomb yield surface (Figure 3.2).

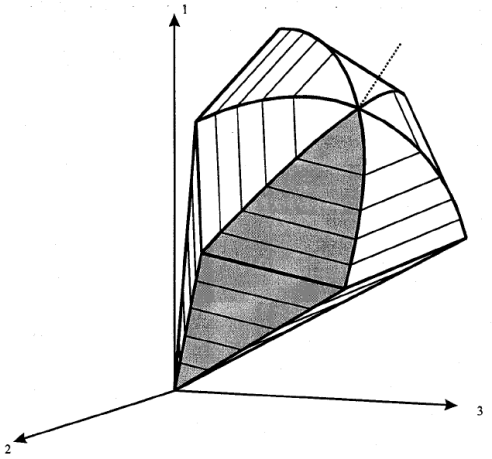

Figure 3.8 Hardening soil yield surface in principal stress space (Brinkgreve, 2007)

The key input parameters for the hardening soil model are as follows:

- *Deviator stress at failure, q_f:* Failure in the HS model occurs by the same criteria as for the MC model. The deviator stress at failure is dependent on two parameters: effective cohesion, *c'*, and effective angle of internal friction, φ'.

- *Failure ratio, R_f:* The asymptotic shear strength, q_a, is calculated using the failure ratio. The asymptotic shear strength is calculated by dividing the deviator stress at failure by the failure ratio.

- *Reference Young's modulus for primary loading, E_{50}^{ref} :* The drained stiffness of the soil (when normally consolidated) in primary loading is determined by this parameter. It is the drained secant Young's modulus when $q = q_f/2$. The relationship between E_{50} and the current stress level is defined by Equation 3.5.

$$E_{50} = E_{50}^{ref} \left\{ \frac{c\ cot\varphi' - \sigma'_3}{c\ cot\varphi' + p^{ref}} \right\}^m \qquad [3.5]$$

where p_{ref} is the reference pressure, σ'_3 is the current value of minor principal stress and *m* is an input parameter. The stress dependency determined by, m, ranges from 0.5 for Norwegian sands and silts (Janbu, 1963) to 1.0 for soft clays (Brinkgreve and Broere, 2006). The stiffness of the soil increases with increasing stress level. For soils which are stiffer than normal consolidation

values the model automatically adopts a stiffness that is larger than Equation 3.5.

- *Reference Young's modulus for unloading,* E_{ur}^{ref} *:* is used to define the unloading which takes place under elastic conditions with the drained Young's modulus, E_{ur}, and Poisson's ratio, ν. The Poisson's ratio for unloading is independent of stress level. The Young's modulus for unloading is defined by equation 3.6.

$$E_{ur} = E_{ur}^{ref} \left\{ \frac{c\ cot\varphi - \sigma'_3}{c\ cot\varphi + p^{ref}} \right\}^m \quad [3.6]$$

where E_{ur}^{ref} is the reference value of the Young's unloading modulus.

The HS model, although more advanced than the elastic perfectly plastic MC model, it does not capture all aspects of soil behaviour. It does not include modelling of anisotropic strength and stiffness or time dependent behaviour of soil. The model requires more material parameters than the elastic perfectly plastic MC model making its use problematic if only field testing has been carried out without triaxial analysis.

3.3 Development of the Bothkennar soil profile and parameter selection

RSPB Bothkennar, formerly known as the Science and Engineering Research Council (SERC) test bed at Bothkennar, is located near to Grangemouth, close to the Kincardine Bridge on the south bank of the Forth estuary, Scotland. The site is located on reclaimed tidal flats of the River Forth downstream from the Kincardine Bridge. Figure 3.9 illustrates the location of the site in Scotland and the location of the site relative to the Powfoulis Manor hotel. The geological and geotechnical properties have been extensively researched (Allman and Atkinson (1992); Barras (2000); Hight *et al.* (1992); Leroueil *et al.* (1992); Nash *et al.* (1992a,b); Paul *et al.* (1992)) and covered in Géotechnique 42 (1992). These studies are used as the basis for the development of the Bothkennar soil model used for stone column simulation.

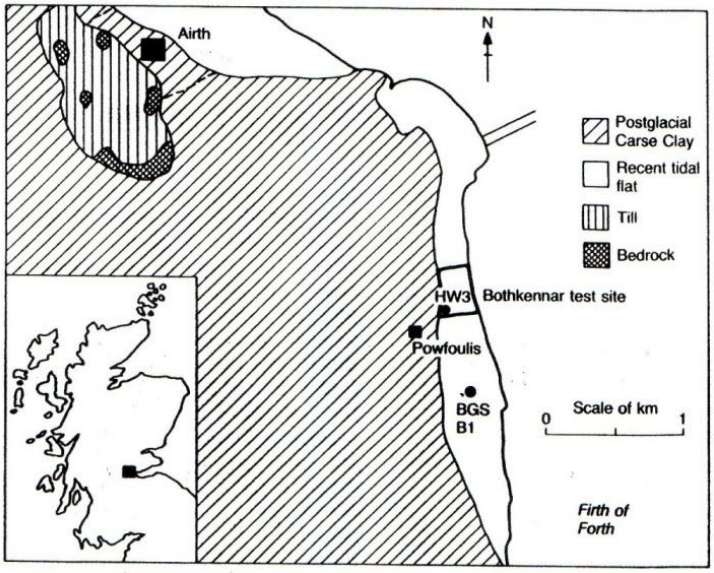

Figure 3.9 Location of RSPB Bothkennar/ test site in Scotland (from Paul *et al.* 1992)

3.3.1 Site geology

The engineering geology of RSPB Bothkennar was extensively studied by Paul *et al.* (1992) and the main geological units have been identified to a depth of 20 metres. The stratigraphic facies sequence suggests a modern tidal flat deposit from the surface to a depth of 1.5 metres which is composed of weathered facies with a shell bed at its base marking the boundary with the bed below. The claret beds exist from 1.5 m to around 18.5 m, the succession consists of weathered facies underlain by mottled facies interbedded with bedded facies down to depth of approximately 10m below which bedded facies predominate interbedded with mottled facies. The facies were deposited in a stable marine environment. Below 18.5 m to approximately 20 m the Letham beds are composed of silty clay. Below 20 m the Bothkennar gravel is present. Paul *et al.* (1992) divided the geological succession into distinct lithological units by facies types as shown in Figure 3.10.

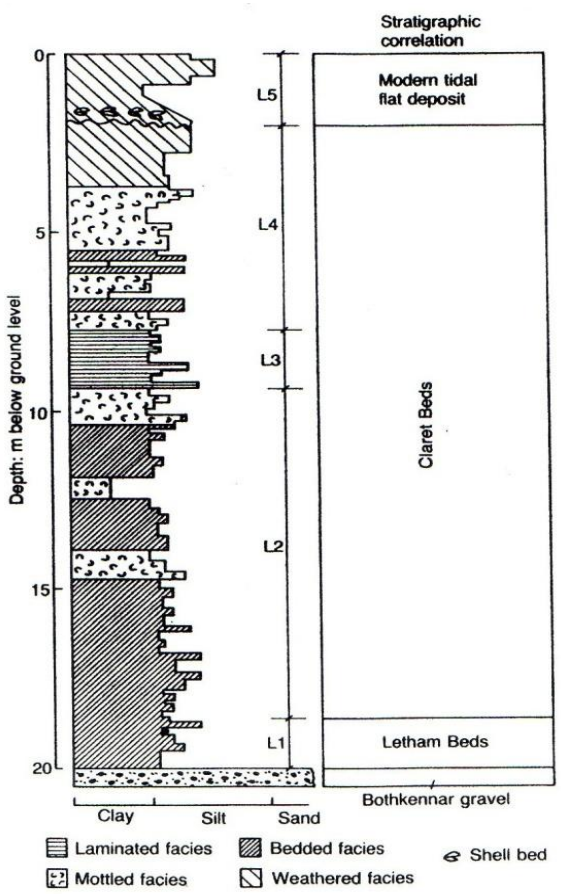

Figure 3.10 Geological succession and facies type at RSPB Bothkennar (from Paul *et al.* 1992)

3.3.2 Sub division of soil layers for model

The work of Paul *et al.* (1992) describes the soil profile as four distinct soil units: Modern tidal flat deposit, Claret beds, Letham beds and the Bothkennar gravel. Properties are assigned to each soil unit. The initial sub division of the layers will be based upon the top three layers with the gravel regarded as a firm stratum. The presence of the 'stiff crust' necessitates the need for layer A to be designated from ground surface to 1.5m. The Claret and Letham beds are commonly referred to as Carse clay in the literature (Hight *et al.* 1992; Paul *et al.* 1992; Barras *et al.* 1999) as such the layers are subdivided into lower and upper Carse clay to take account of changes in the geotechnical properties. Layer B will be designated from 1.5m to 2.5m and is termed the Upper Carse clay. Layer C will be designated from 2.5m to 15m and is termed the Lower Carse clay. Layer D is designated from 15m to 18.5m and is referred to as the Bothkennar gravel in this thesis but is not modelled in Plaxis 3D. Barras and Paul (1999) identified that that layer thicknesses exist across the Bothkennar site and as such the Bothkennar gravel is considered to start at 15 m in this thesis. To save

computational time the base of layer C is modelled as a hard substrate to simulate the gravel.

3.3.3 Soil description

The soil units at Bothkennar were extensively tested by Nash *et al.* (1992) in a series of *in-situ* and laboratory tests. The results of the index tests are presented in Figure 3.11. The moisture content of the soil increases from 30% at the surface to 75% at 8 m before decreasing to 40% at the top of the Bothkennar gravel unit. The Atterberg limit test results when plotted on the plasticity chart suggests an inorganic clay with high plasticity. However, Paul *et al.* (1992) reported that the clay fraction of the soil varies between 35%-50% and as such the soil can be considered silty clay. The bulk density of the soil was found to vary between 1600kg/m³-1800kg/m³. For the purposes of the soil model the values are adopted according to average values (Figure 3.11). It is clear that there are three distinct clay layers which range from 0.0m-2.5m, 2.5m to 15.0m and 15.0m to 18.5m based on unit weights. The organic content loss on ignition at 425°C was found to be between 2%-8%.

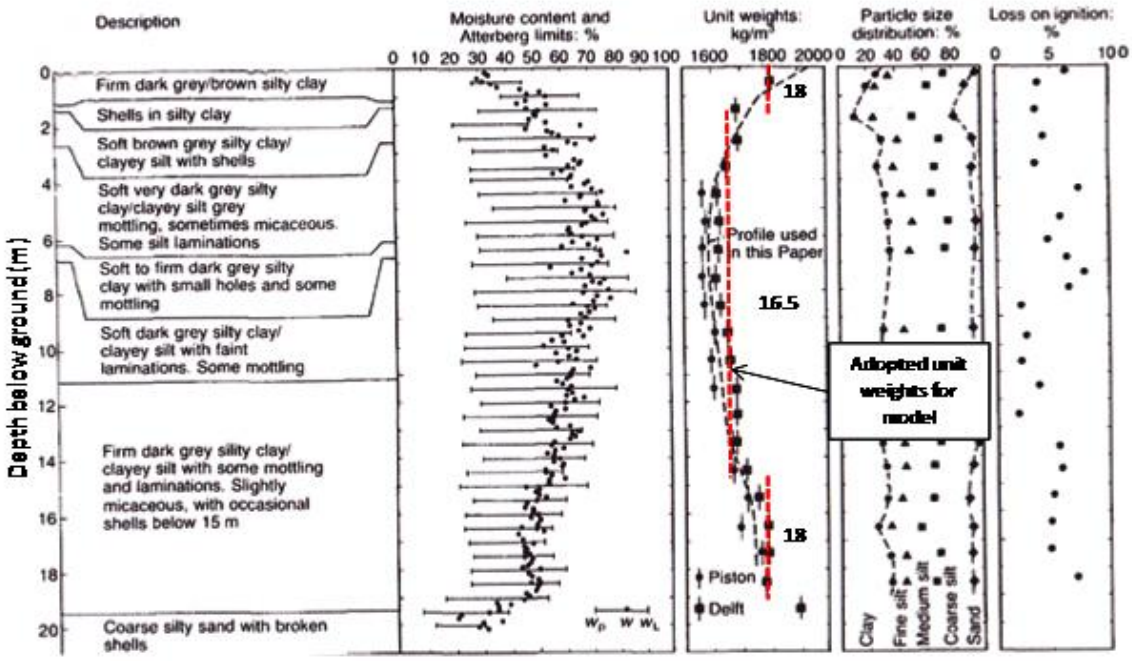

Figure 3.11 Geotechnical profile for soft clay in and around borehole D1 (modified from Nash *et al.* 1992)

3.3.4 Initial soil stress state parameters

The initial stress state of a soil reflects its geological history and its exposure to earth processes such as erosion, flooding or weathering. Barras (2000) reported that

examination of the yield stress and yield stress ratio suggested that between a depth of 3m and the base of the shell bed the yield stress ratio can be as high as 2.5. Below 3m it was found to be constant around 1.6, which suggested that the deposit is lightly overconsolidated. Below 4m depth to 20m the undrained shear strength was found to increase from approximately 18kPa to 50kPa; above 4m until the level of the water table is reached the values were found not to vary greatly which is considered to be consistent with lightly overconsolidated clay. In the crust the strength was found to increase up to 100kPa at the surface, likely due to the result of increased effective stress due to partial saturation. Hight *et al.* (1992) suggested that post depositional processes such as erosion, groundwater and tidal effects, have affected the clay at Bothkennar. The geological history of the Bothkennar clay indicates that a maximum unloading due to erosion of approximately 15kPa took place. The authors suggest that this would be observed as a reduction in OCR from 5m to 15m of 1.25 to 1.15 respectively, where OCR is equivalent to the yield stress ratio. Nash *et al.* (1992a) compared the extrapolated stress history and data from incremental load tests (Figure 3.12). The profile compares favourably with the observations of Barras (2000) although for values of yield stress ratio below 4m the yield stress ratio appears to decrease. This may be due to effects associated with inherent variability present in the clay. The authors recommend a value of 1.55 for the soft clay between depths of 4m and 16m which is similar to the value recommended by Barras (2000) of 1.6 for the yield stress ratio. A value of 1.55 is selected for the OCR in the soil model in Plaxis 3D foundation for the interval 2.5m-16m based on the yield stress ratio in Figure 3.12 after initial simulation modelling suggested a value of 1.55 gave the best history match.

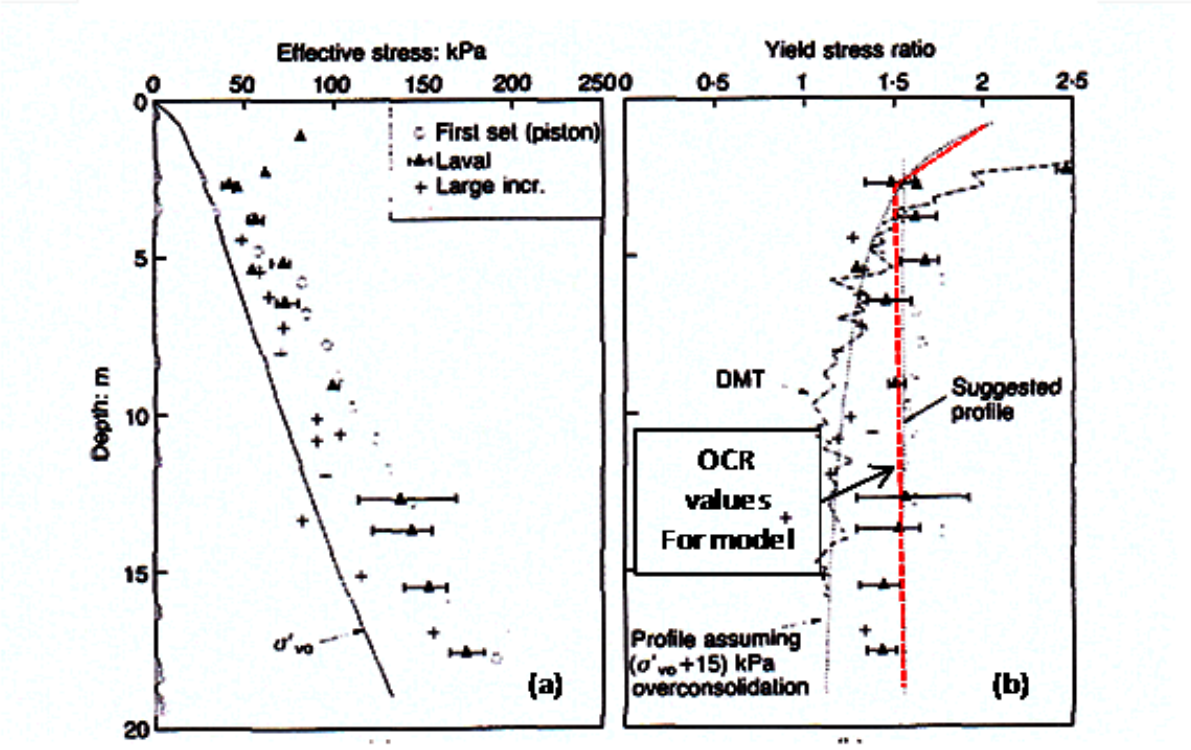

Figure 3.12 (a) Yield stress and (b) yield stress ratio from incremental load consolidation tests (modified from Nash *et al.* 1992a)

The hardening soil model in Plaxis 3D requires the specification of the coefficient of lateral earth pressure, K_0. Nash *et al.* (1992a) produced a plot of *in-situ* lateral total stress and coefficient of lateral earth pressure with depth (Figure 3.13). Hight *et al.* (1992) suggests that the coefficient of lateral earth pressure is highest in the upper layers due to recent groundwater fluctuations. The values of K_0 adopted for the soil model are illustrated in Figure 3.13.

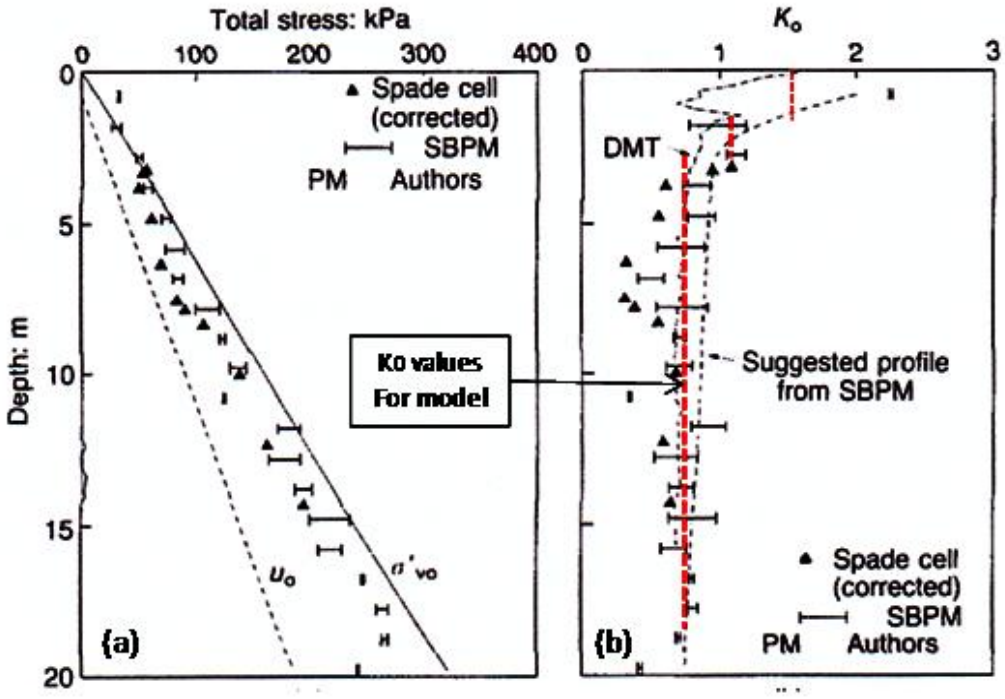

Figure 3.13 Variation of (a) lateral total stress measured in-situ and (b) K_0 with depth from self-boring pressuremeter, spade cell and dilatometer tests (modified from Nash *et al.* 1992a)

3.3.5 Clay strength parameters

The strength parameters required for the Bothkennar soil model consist of a friction angle and cohesion values. These parameters then determine the failure surface in the Mohr-Coulomb criterion.

3.3.5.1 Friction angle

Three potential sources of friction angle were identified in the literature: triaxial cell in Allman and Atkinson (1992); cone penetration test (CPT) in Hight *et al.* (1992); and plasticity index in Hight *et al.* (1992).

Allman and Atkinson (1992) examined the strength characteristics of the reconstituted Bothkennar clay sampled from depths of 3.5 m - 6.5 m. The samples were reconstituted in the laboratory and a clay slurry created at 1.25 times the liquid limit. The slurry was then consolidated one dimensionally to yield a clay sample which was transferred to the triaxial cell for testing. The samples were then subjected to further one dimensional compression or swelling to obtain a normally-consolidated or slightly over-consolidated state before subjecting it to shearing. Most samples reached well defined constant stress ratios indicated by the stress-dilatancy and stress strain curves at shear strains above 15

%. The critical state stress ratios were corrected to a zero rate of dilation for compression and extension which gave values of $M_c = 1.38$ and $M_e = -1.00$ respectively. M_c and M_e correspond to friction angles of φ_c = 34° and φ_e = 37° for compression and extension respectively. The authors report that the friction angles are higher than those normally associated with a high plasticity clay and are close to values normally associated with granular silts, sands and gravels.

Cone penetration test (CPT) data were sourced from Hight *et al.* (1992) (Figure 3.14) and interpreted by the method of Durgunoglu and Mitchell (1975) (Figure 3.15) which relates the cone penetration resistance and effective overburden pressure to give an approximation for the friction angle at a specific depth (in this case values were chosen at layer mid-points). The CPT data does not provide for values of effective cohesion.

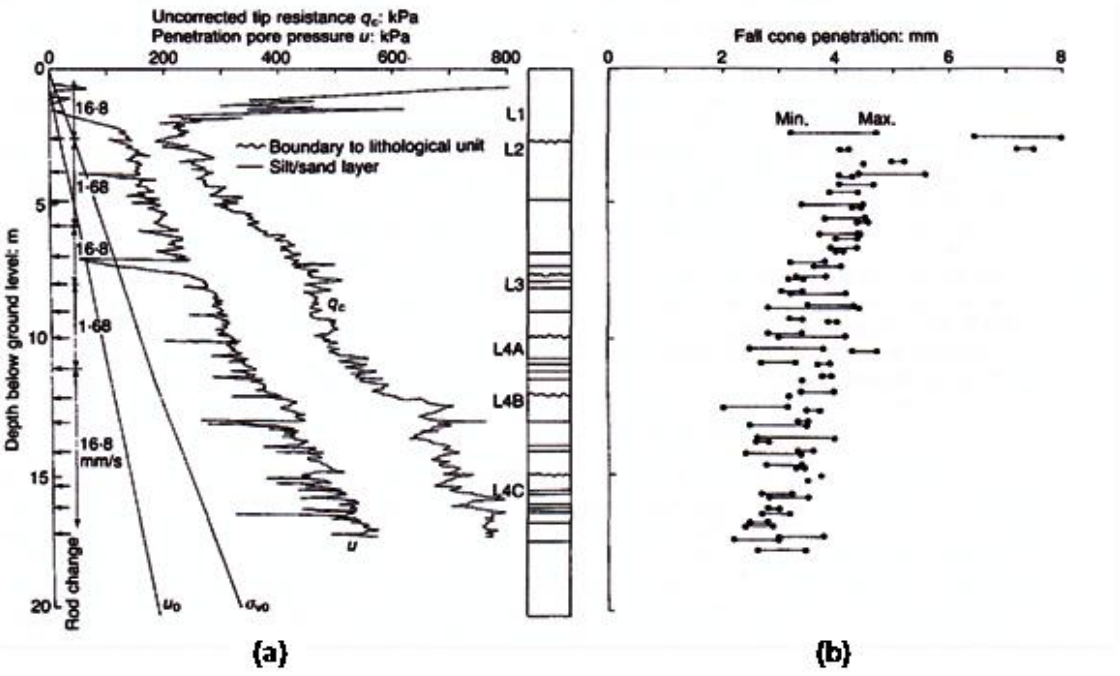

Figure 3.14 Cone Penetration data for Bothkennar sourced from Hight *et al.* (1992)

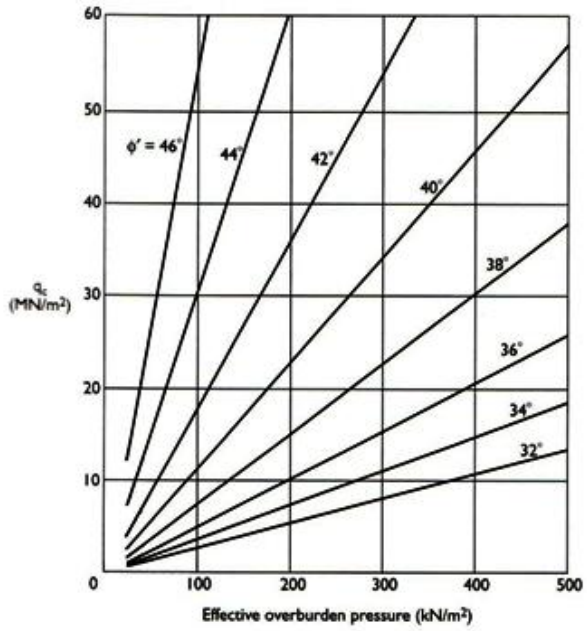

Figure 3.15 Correlation between effective friction angle, cone penetration resistance and effective overburden pressure (Durgunoglu and Mitchell, 1975)

The Plasticity index data (Figure 3.16) was sourced from Hight *et al.* (1992). Utilising the method of Kennedy (1959) the plasticity index (PI) can be related to Sin φ of the soil. By plotting the plasticity index for a known mid-layer depth on the graph and extrapolating the intersection of the point with the line annotated BS8002 the Sin φ' value for the soil layer can then be converted to get the Friction angle, φ', for the layer. Figure 3.17 illustrates the graph from Kennedy (1959) illustrated for use in this research. The samples of Bothkennar soils were not taken at exact regular intervals, the plasticity index (PI) values and the interpreted friction angles do not give adequate coverage.

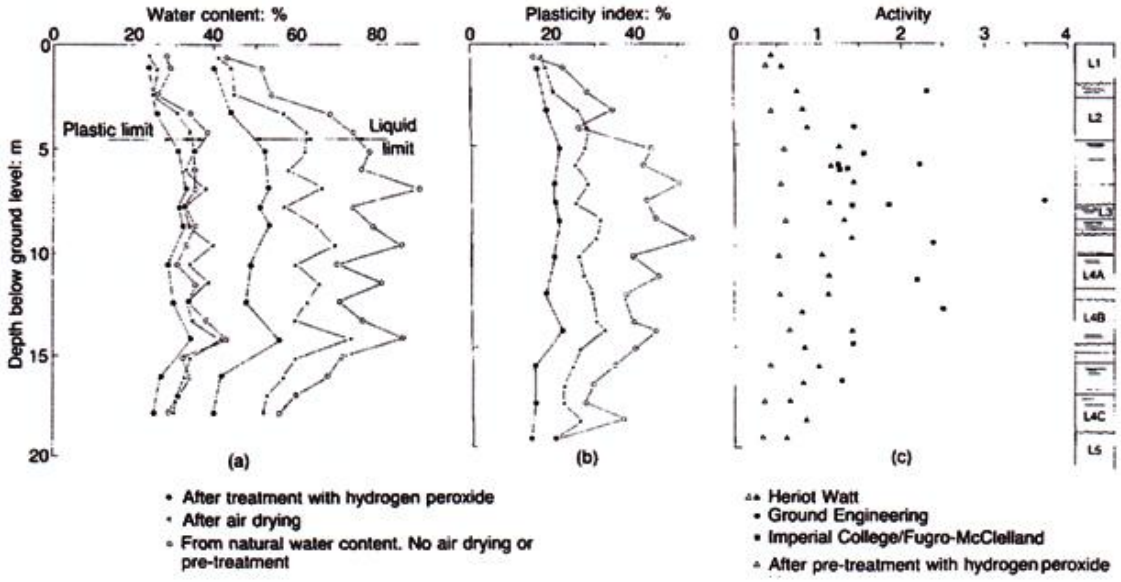

Figure 3.16 Atterberg limits and activity before and after removal of organics (a) liquid and plastic limits; (b) plasticity index; (c) activity (from Hight *et al.* 1992)

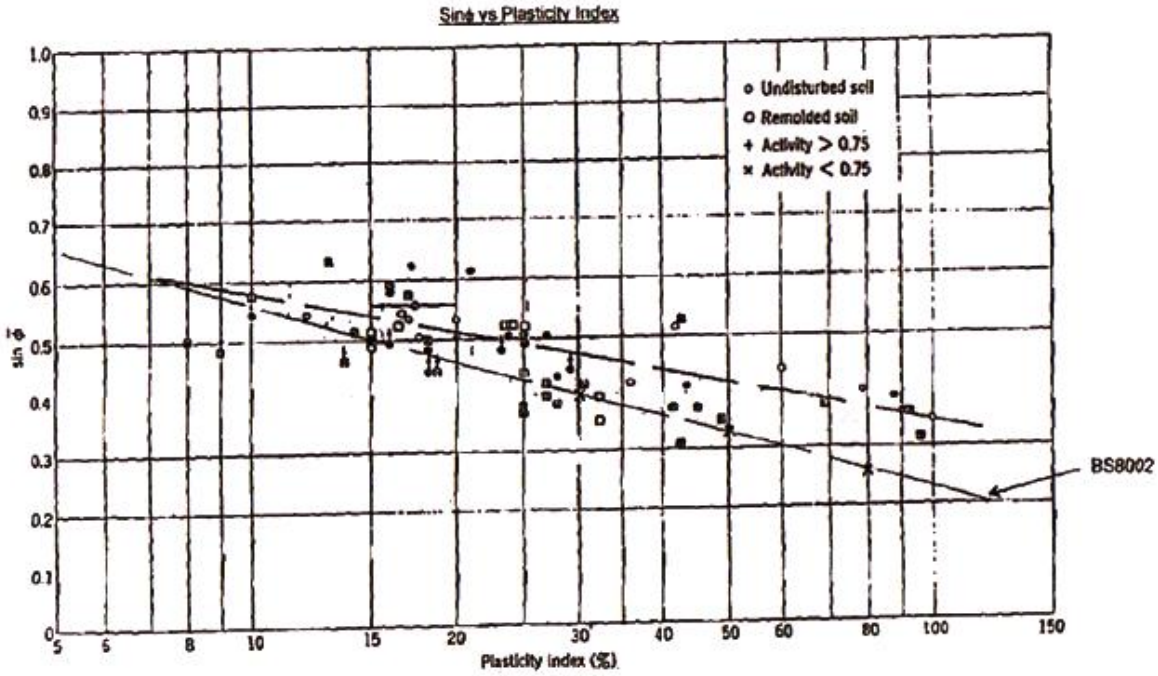

Figure 3.17 Plasticity index (PI) angle related to Sinφ (Kennedy, 1959)

The friction angle results for the triaxial cell, cone penetration test and plasticity index are plotted in Figure 3.18. The initial sub division of the layers will be based upon three layers defined in Section 3.2.2 and summarised in Table 3.1.

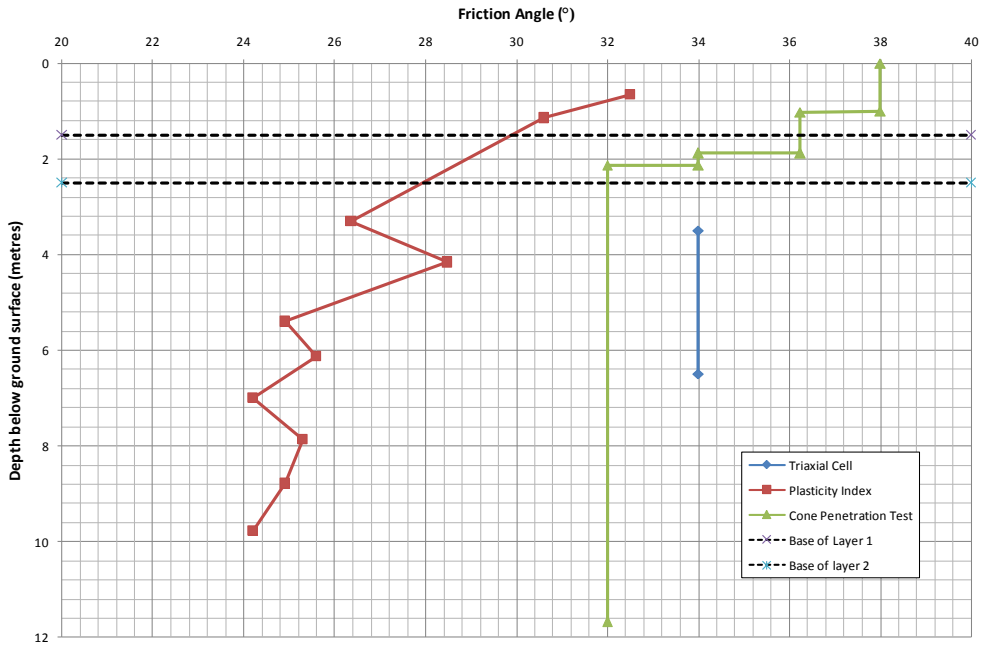

Figure 3.18 Comparison of friction angles obtained from triaxial, CPT and plasticity index

3.3.5.2 Cohesion

No effective cohesion was recorded during the drained triaxial tests on Bothkennar soil. As a result small values of cohesion are adopted to ensure numerical stability. Brinkgreve (2007) recommends a value of 1kPa or greater be adopted. A value of 2kPa is initially assigned to layer 1 ('Stiff crust') to reflect its higher stiffness and due to the fact that overburden stresses are lowest in this layer which leads to a stress state closer to the yield surface. A value of 1kPa is assigned to layers 2 to 3.

3.3.6 Stiffness parameters

The Bothkennar site contains a stiff crust which has been described extensively by Paul *et al.* (1992), Barras *et al.* (1999) and in Géotechnique (1992). In the laboratory studies described in Chapter 2 the effect of a stiff crust on stone column performance has not been considered. However, for the purposes of this study the effects of the crust are accounted for in the choice of soil parameters for the model. Watts and Serridge (2000) noted that the crust was considered to limit the deformation in the upper region of the column. The stiff crust will be able to absorb a greater degree of applied stress from the foundation than would be expected of a normally consolidated soil and as such will minimise the effect of elevated stress levels at the edges of rigid foundations.

The Bothkennar soil profile requires values of stiffness to be calculated for input into the hardening model. An initial approach was to obtain the stiffness from interpreting the oedometer stiffness from the m_v values supplied by Serridge (2006) from unpublished sources. However, initial indications suggest that the stiffness values were too low and had to be increased significantly when using the Mohr-Coulomb perfect plasticity model. Consideration was then given to using the compression index,c_c and initial void ratio, e_0 from Nash *et al.* (1992b). This study examined the behaviour of Carse clay in terms of one dimensional stiffness with samples taken across a large depth interval of 0m to less than 18m. The samples were tested using a fixed ring oedometer cell by incremental loading in most cases. This allowed for the void ratio, e, and coefficient of compressibility, c_c, to be established for different depths between ground the surface and down to approximately 18 m. This offered reasonable coverage with depth (Figure 3.19) for both compression index and the initial void ratio. The selected values for the Bothkennar soil model are highlighted in red for each layer.

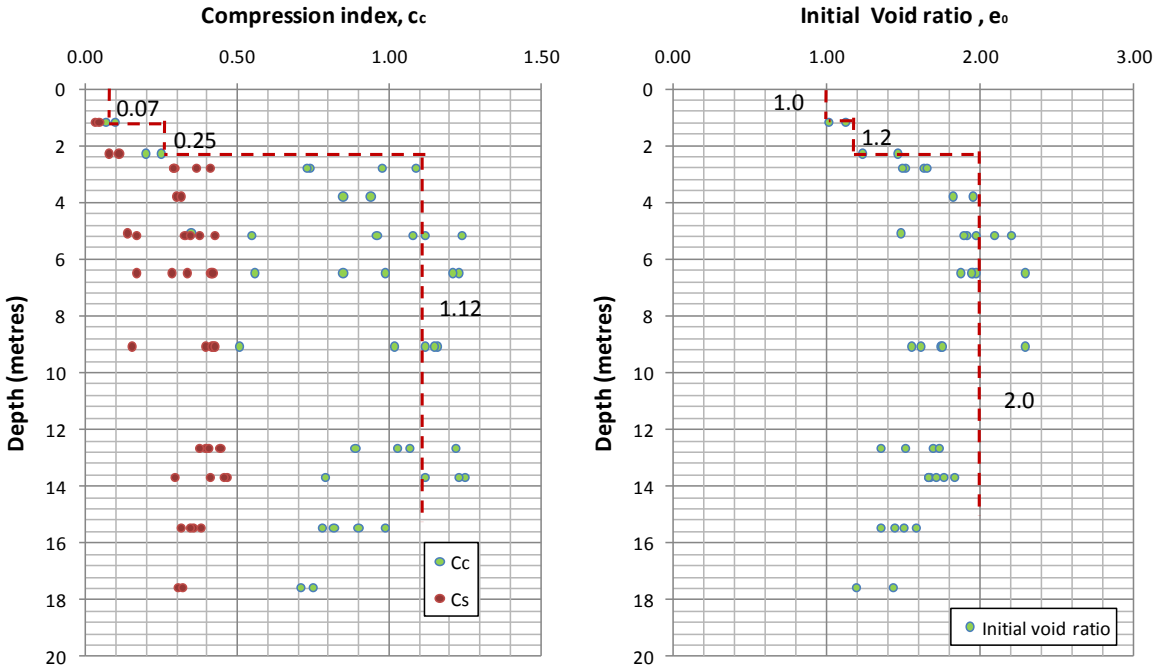

Figure 3.19 Plot of Compression Index and Initial Void Ratio with Depth

In order to calculate suitable reference values for Young's unloading modulus, E_{ur}, and tangent stiffness modulus for primary oedometer loading, E_{oed}^{ref}, Equations 3.7 and 3.8 from Brinkgreve (2007) are used respectively.

$$E_{oed}^{ref} = \frac{2.3(1+e_0)p^{ref}}{c_c} \qquad [3.7]$$

$$E_{ur}^{ref} = \frac{2.3(1+e_0)(1+\nu)(1-2\nu)p^{ref}}{c_s(1-\nu)} \quad [3.8]$$

Where p_{ref} is the reference pressure. These equations allow for the conversion of the one dimensional stiffness parameters (compression index, c_c; initial void ratio, e_0 and the coefficient of swelling, C_s) to three dimensional parameters E_{ur} and E_{oed}^{ref}. Nash *et al.* (1992b) did not record the behaviour of samples prior to yielding which makes the calculation of C_s difficult for the data in Figure 3.19. However, Allman and Atkinson (1992) carried out an examination of stiffness behaviour for reconstituted samples from Bothkennar. Values were obtained for the slopes of the normal compression line, λ, and swelling line, κ, of 0.181 and 0.025 respectively. They used the ratio of λ/κ = 7.2 to calculate values for C_s based on the relationship λ/κ = C_s/C_c= 7.2.

3.3.7 Permeability and consolidation parameters

In order to simulate consolidation behaviour values for permeability and consolidation need to be assigned. Leroueil *et al.* (1992) analysed the hydraulic conductivity characteristics utilising laboratory and *in-situ* testing. Hight *et al.* (1992) compared the data from the various methods and suggests that the data from the self boring permeameter gives the most realistic profiles with depth. The hydraulic conductivity, k_{h0}, was found to increase from $1.17x10^{-9}$m/s at 2.97m, to $1.43x10^{-9}$m/s at 5.95m, $1.17x10^{-9}$m/s at 8.88m, $1.93x10^{-10}$m/s at 12.02m and then increases to $1.08x10^{-9}$m/s at 15m. The last value of hydraulic conductivity at 15m is close to the interface with the Bothkennar gravel and explains the rise. The vertical hydraulic conductivity, k_{v0}, was observed from laboratory tests and was found to be lower than the horizontal values. An anisotropy ratio, k_{h0}/k_{v0} of 1.5-2.0 was recorded. Leroueil *et al.* (1992) reported that the permeability change index, C_k, can be described by the relationship $C_k = \Delta e/\Delta \log k$. It was found that for natural clays it can be defined by $C_k = 0.5e_0$. The coverage of permeability data is considered somewhat limited to one borehole.

3.4 Hardening soil model: determination of Bothkennar soil parameters

The soil parameters discussed in Sections 3.3.4 to 3.3.7 are used to determine the properties for entry into the hardening soil model. Layer division is based upon the layers described in Section 3.3.2. Values for the Bothkennar gravel are not included at this stage due to the depth being 15 m or greater and to reduce computing time. Unlike

the Mohr-Coulomb model which adopts a constant value of Young's modulus to define the stiffness response, the HS model simulates the stress path and stress level dependency experienced by the soil. Determination of suitable values for Young's moduli is crucial in ensuring that the soil model is able to accurately capture the stress path and stress level dependency.

The HS model accounts for stress path dependency by the use of two stiffness moduli: E_{50}, a secant modulus at 50% strength and E_{ur}, an unload-reload modulus. Typically, the E_{50} secant modulus is used for primary loading of the soil while the unload-reload modulus is used for tunnelling or excavation analysis. Soils display stress level dependency when exposed to increasing confining pressure which is observed as increased stiffness. Equation 3.6 relates the increased stiffness as a result of the confining pressure to the Reference Young's modulus for primary loading, E_{50}^{ref}. The parameter 'm' for the Bothkennar soil profile can be determined from Nash *et al.* (1992b). One dimensional oedometric moduli, E_{oed}, are converted into oedometric moduli using Equation 3.7. The major confining pressure is considered to be the major principal stress as testing was conducted using oedometric conditions. The oedometric moduli are converted to depth using the effective overburden stress at the depth at which the samples were taken from the soil. The calculated values are plotted in Figure 3.20 and it can be observed that for the lower Carse clay that the ratio of E_{oed}/σ_v is constant with increasing vertical stress, σ_v. This suggests a value of m = 5 which was initially utilised in the Plaxis modelling. However, after initially trialling this value a poor history match was achieved in simulation. After reviewing modelling approaches details in Brinkgreve (2007) a value of m = 1 is assumed for the lower Carse clay. This assumption is consistent with Brinkgreve and Broere (2006) and Brinkgreve (2007) recommend a value of m = 1 for soft clays. For the upper Carse clay and stiff crust insufficient data is available due to limited sampling coverage. A value of m =1 is selected for the upper Carse clay and stiff crust which is consistent with the recommendation by Brinkgreve (2007). Calculated and assumed values for entry into the HS model are summarised in Table 3.1. Validation of the Bothkennar soil profile is examined and discussed in Chapter 4.

Hardening Soil Model Parameter	Stiff Crust Layer A	Upper Carse Clay Layer B	Lower Carse Clay Layer C
Depth Interval	0.0m to 1.0m	1.0m to 2.0m	2.0m to 15.0m
Bulk unit weight, γ (kN/m³)	18	16.5	16.5
Over consolidation ratio, OCR	1.75	1.75	1.5
Pre-overburden stress (kPa)	15	15	
Coefficient of lateral earth pressure, k_0	1.5	1.1	0.75
Effective cohesion, c' (kPa)	2	1	1
Angle of internal friction, ø (°)	34	34	34
Initial voids ratio, e_0	1.00	1.19	1.98
Compression Index, C_c	0.07	0.25	1.12
Swelling index, C_s	0.02	0.06	0.28
Reference pressure, p_{ref} (kPa)	13.50	30.94	37.13
Vertical coeff. of permeability, k_{vert} (m/day)	6.77E-05	5.08E-05	5.08E-05
Horiz. coeff. of permeability, k_{horiz} (m/day)	1.02E-04	1.02E-04	1.02E-04
Stiffness (E_{oed}) at reference pressure (100kPa)	6571	2024	616

Table 3.1 Initial soil parameters used for calculation of parameters for hardening soil model

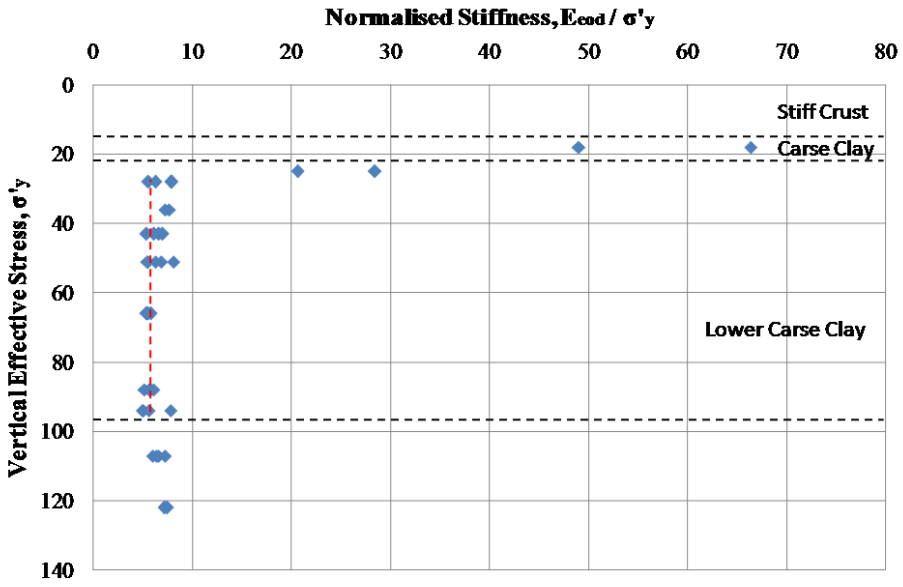

Figure 3.20 E_{oed} / vertical stress vs depth

Chapter 4

Simulation Modelling: Mesh Calibration and Bothkennar field trials

4.1 Modelling checks

The following checks were carried out to ensure that the modelling approach was acceptable and to optimise the simulation methodology in terms of time efficiency.

4.1.1 Localised mesh refinement

The Plaxis 3D foundation introductory tutorials showed the need for careful consideration of the mesh refinement locally around areas of interest. Initial simulations showed that for coarse to very fine simulations the use of localised refinement in the area of the foundation reduced the potential for discontinuities at intra-element boundaries. Therefore for all subsequent analysis in this thesis a local refinement of one step is applied to reduce the mesh size, unless otherwise stated, to the foundation area after the global mesh is generated.

4.1.2 Mesh sensitivity

The use of finite element analysis for geotechnical analysis requires consideration of the material model, mesh configuration and boundary conditions. In Plaxis 3D the mesh is automatically generated depending on the configuration of the foundation, soil layers and work planes. The software uses 15 noded wedge elements. The number of elements in a mesh is dependent upon the degree of mesh coarseness selected which can be varied from very coarse to very fine. Mesh sensitivity analysis was conducted for pad and strip foundations with configurations of length and breadth dimensions the same as those used in this research. The Bothkennar soil model is used to assess the effect of coarse to very fine meshes on the vertical displacement, U_y, and mean effective stress, p' at selected points beneath the foundation. The field test of Jardine *et al.* (1995) recorded a failure load of 138kN/m² for a pad foundation of dimensions 2.2m by 2.2m. The working load, a factor of safety between 2.5 and 3, would give a maximum value in the range of 55.2kN/m² to 46kN/m². For settlement analysis in this thesis the typical working load selected is 50kN/m². For the mesh sensitivity analysis a working load of 25kN/m² is selected based upon the typical working load on a stone column foundation being in the range of 25kN/m² to 50kN/m², thus to save on computational time the lower load limit is selected. The foundation depth is 0.8m below ground level. Selected points

are 0.8m, 1.8, and 2.8m representing points 0m (A), 1m (B) and 2m (C) below foundation level for pad and strip foundations (Figures 4.1 and 4.2). Vertical displacement below the foundation is of key interest in this research as the settlement of stone columns is of primary concern and the accuracy of the mesh will influence the settlement prediction. The accuracy of the mesh is examined by calculation of the normalised error for both vertical settlement, U_y, and mean effective stress, p' for coarse, medium and fine meshes relative to the very fine (*vf*) mesh:

Normalised error for vertical displacements, $U_y = \left(\frac{U_{y,vf} - U_y}{U_{y,vf}}\right)$ x 100 [4.1]

Normalised error for mean effective stress, $p' = \left(\frac{P_{y,vf} - p'}{p'_{vf}}\right)$ x 100 [4.2]

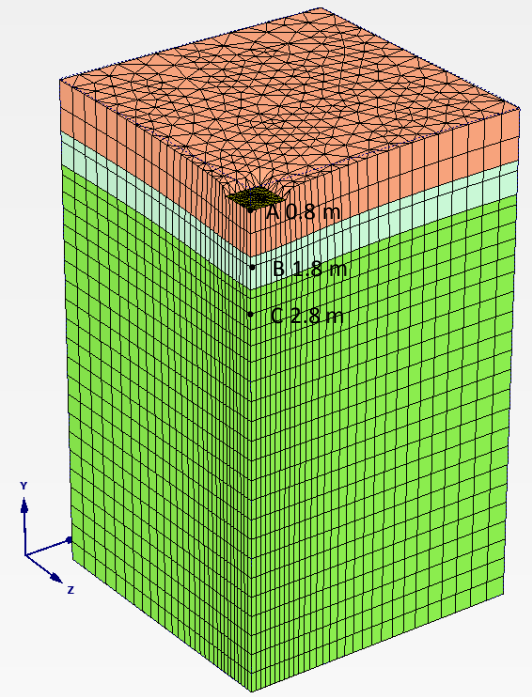

Figure 4.1 Vertical displacement and mean effective stress at points A, B and C below pad foundation

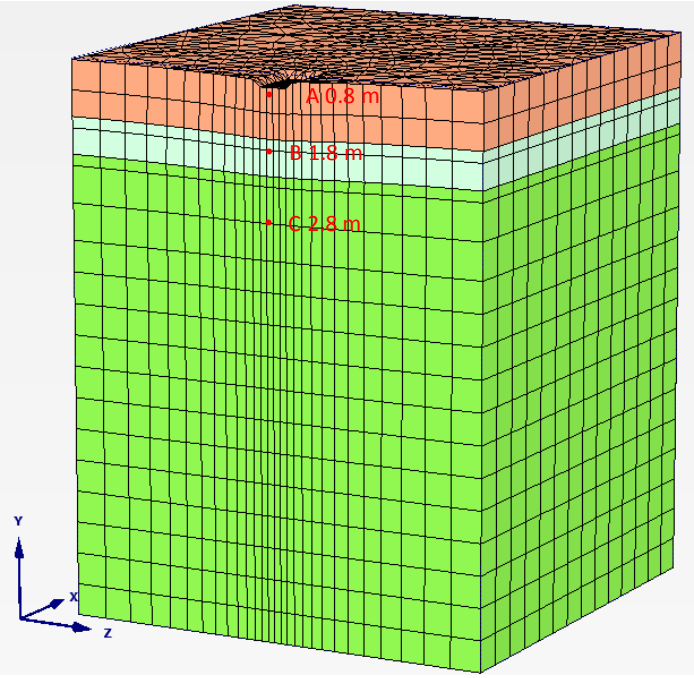

Figure 4.2 Vertical displacement and mean effective stress at points A, B and C below strip foundation

The results of the finite element analysis are summarised in Table 4.1. The number of elements, settlement and mean effective stress is reported. The normalised error was found to reduce with each refinement of the mesh. The values suggest that for both pad and strip foundations the meshes are converging towards the very fine mesh. The normalised error between the fine and very fine meshes for settlement was found to be low (maximum normalised error is less than 3.81% and 1.38% for pad and strip foundations respectively). The normalised error was found to be small for the mean effective stress (maximum normalised error was less than 4% and 1% for pad and strip foundations respectively). The results suggest that to reduce computational time the fine mesh can be used for analysis in this research with acceptable accuracy.

Pad Breadth (m)	Mesh	No. of Elements in 3D mesh	Vertical Settlement, Uy (mm)			Normalised Error (%)			Mean Effective Stress, p' (kPa)			Normalised Error (%)		
			A	B	C	A	B	C	A	B	C	A	B	C
2	Coarse	1888	24.31	21.19	16.31	6.39	3.06	2.16	19.13	24.03	26.49	0.82	4.21	0.41
	Medium	4160	24.14	21.03	16.19	7.05	3.80	2.88	19.11	23.59	26.43	0.92	5.96	0.65
	Fine	12636	24.98	21.33	16.35	3.81	2.42	1.92	19.24	24.08	26.59	0.25	4.00	0.02
	Very fine	29748	25.97	21.86	16.67				19.28	25.08	26.60			
3	Coarse	1534	41.38	40.42	32.53	8.37	1.25	1.00	19.99	27.16	27.99	6.19	0.76	3.17
	Medium	3120	41.38	40.42	32.53	8.37	1.25	1.00	19.99	27.16	27.99	6.18	0.76	3.17
	Fine	9842	45.11	40.90	32.81	0.11	0.07	0.15	21.31	27.37	28.91	0.00	0.00	0.00
	Very fine	20774	45.16	40.93	32.86				21.31	27.37	28.91			
4	Coarse	1416	60.75	58.63	48.09	5.70	3.74	3.01	22.51	24.74	27.01	1.00	4.98	3.88
	Medium	2704	62.69	60.52	49.30	2.69	0.64	0.56	22.66	25.68	27.24	0.32	1.11	2.94
	Fine	7488	63.99	60.58	49.42	0.67	0.54	0.32	22.71	25.58	28.04	0.13	1.48	0.07
	Very fine	15980	64.42	60.91	49.58				22.74	25.97	28.06			
5	Coarse	1298	76.39	73.62	64.51	9.20	9.38	3.89	23.45	25.67	28.74	2.25	0.78	1.23
	Medium	2496	83.99	80.89	67.00	0.17	0.43	0.18	23.97	24.66	28.41	0.10	4.65	2.34
	Fine	7252	84.02	81.20	67.05	0.13	0.05	0.10	23.97	25.71	28.59	0.10	0.60	1.72
	Very fine	13583	84.13	81.24	67.12				23.99	25.87	29.09			
6	Coarse	1180	85.43	89.84	78.18	14.04	6.93	4.60	23.50	24.54	28.94	4.13	1.29	0.01
	Medium	2288	87.22	92.80	80.24	12.24	3.86	2.09	23.50	24.45	28.94	4.13	1.66	0.01
	Fine	6734	98.51	95.79	81.34	0.88	0.77	0.74	23.56	24.83	28.86	3.87	0.16	0.29
	Very fine	11985	99.38	96.53	81.95				24.51	24.87	28.94			

Strip Length (m)	Mesh	No. of Elements in 3D mesh	Vertical Settlement, Uy (mm)			Normalised Error (%)			Mean Effective Stress, p' (kPa)			Normalised Error (%)		
			A	B	C	A	B	C	A	B	C	A	B	C
2	Medium	12987	12.72	10.60	8.41	5.15	2.12	1.18	17.214	18.189	25.236	5.16	0.45	1.78
	Fine	13764	13.33	10.80	8.49	0.60	0.28	0.24	17.993	18.199	25.648	0.87	0.40	0.18
	Very fine	37797	13.41	10.83	8.51				18.151	18.272	25.693			
3	Medium	4712	17.31	14.86	12.04	3.73	2.04	1.31	17.50	18.20	25.02	6.45	4.78	2.41
	Fine	11882	17.83	14.96	12.08	0.83	1.38	0.98	17.88	18.67	25.08	4.41	2.30	2.22
	Very fine	31968	17.98	15.17	12.20				18.70	19.11	25.64			
6	Medium	4050	26.67	23.73	20.17	0.15	1.74	1.47	17.92	19.84	26.62	7.41	1.24	0.48
	Fine	9823	26.71	24.15	20.47	0.00	0.00	0.00	19.35	20.09	26.75	0.00	0.00	0.00
	Very fine	26182	26.71	24.15	20.47				19.35	20.09	26.75			

Table 4.1 Mesh sensitivity analysis: vertical displacement and mean effective stress at points A, B and C below pad foundations

4.1.3 Boundary effects

The use of finite elements requires a domain to be defined around the foundation. This domain or boundary is normally composed of the soil with the outer boundary specified with sufficient width such that it does not affect the numerical solution. A sensitivity analysis is conducted for a square pad foundation of 2.2m and a strip foundation of 0.75m by 3m. The distance from the centre of the pad or strip foundation was examined for a value of four times the largest length to 14 times the length. For the square pad this is the breadth and for the strip the length is utilised. The foundations were loaded to 25kN/m² as previously in Section 4.1.2 to save on computational time. The vertical displacement and mean effective stress at points A, B and C for the different boundaries are reported in Table 4.2. It can be observed that positioning the boundary at less than eight times the centre to outer boundary length causes more settlement beneath the foundation for both the pad and strip foundation. The distance to boundary is selected for further analysis for a ratio of eight times the largest foundation dimension. Azizi (2000) suggested that the minimum distance to boundary should be five times the greater foundation dimension (width of pad or length of strip). Killeen (2012) suggested that a foundation width of eight times the breadth for a foundation of 3m negated the influence of the outer boundary. This suggests the results obtained are valid.

Pad foundation

Distance to boundary	Vertical Settlement, Uy (mm)			Normalised Error (%)			Mean Effective Stress, p' (kPa)			Normalised Error (%)		
	A	B	C	A	B	C	A	B	C	A	B	C
4B	36.70	32.23	25.77	23.40	24.25	28.72	19.76	27.91	28.62	-1.51	8.48	-5.28
6B	31.87	27.62	21.26	7.16	6.48	6.19	19.72	27.58	28.22	-1.72	7.22	-3.80
8B	30.69	26.54	20.35	3.19	2.31	1.65	19.67	27.43	27.63	-1.96	6.62	-1.62
10B	30.48	26.41	20.26	2.49	1.81	1.20	20.13	26.99	27.39	0.32	4.91	0.77
12B	30.12	26.20	20.16	1.28	1.00	0.70	20.10	26.40	27.30	0.16	2.62	0.42
14B	29.74	25.94	20.02	0.00	0.00	0.00	20.07	25.72	27.18	0.00	0.00	0.00

Strip foundation

Distance to boundary	Vertical Settlement, Uy (mm)			Normalised Error (%)			Mean Effective Stress, p' (kPa)			Normalised Error (%)		
	A	B	C	A	B	C	A	B	C	A	B	C
4B	18.81	15.99	12.91	32.09	33.36	41.40	18.72	19.35	25.67	0.02	0.02	0.01
6B	15.68	13.06	10.06	10.11	8.92	10.19	18.56	19.28	26.02	0.03	0.03	0.00
8B	14.80	12.41	9.44	3.93	3.50	3.40	19.06	19.62	25.90	0.00	0.01	0.00
10B	14.59	12.13	9.22	2.46	1.17	0.99	19.05	19.80	25.90	0.00	0.00	0.00
12B	14.22	11.96	9.11	0.14	0.25	0.22	19.03	19.62	25.87	0.00	0.01	0.00
14B	14.24	11.99	9.13	0.00	0.00	0.00	19.04	19.79	25.89	0.00	0.00	0.00

Table 4.2 Outer boundary sensitivity analysis: vertical displacement and mean effective stress at points A, B and C below pad and strip foundations

4.1.4 Modelling of long-term settlement for stone columns

Representing the long term settlement behaviour of soft cohesive soils can be modelled by two different methods in PLAXIS 3D Foundation: Undrained-Consolidation Analysis (UC) and Drained Analysis (DR). Undrained-Consolidation analysis requires information regarding the soil permeability which may not be routinely measured during field investigations or trials. If the data are accurate and the area of interest has good coverage i.e. multiple boreholes across the site then this method can offer a closer simulation of reality. Unfortunately for Bothkennar the data obtained by Leroueil *et al.* (1992) is somewhat limited and does not give full site coverage. Any model will therefore contain some degree of uncertainty. In this type of analysis the soil is treated as undrained initially during foundation loading. This gives undrained settlements obtained instantaneously after which consolidation analysis is run for a set period of time, usually a period of days. The soil parameters can be inputted either as total or effective stress parameters. The total stress approach is limited as the HS model cannot capture the soil stiffness dependency. The increase in soil strength parameters cannot be captured during consolidation analysis. For this thesis inputs are effective parameters to the soil model. PLAXIS models the undrained response by adding a bulk modulus to the pore water stiffness matrix, this makes the pore water incompressible and ensures that the stresses created from the applied load to the foundation are borne by the pore water. During consolidation analysis the extra bulk modulus is removed and stresses present in the pore water are then transferred to the soil matrix. This leads to primary consolidation from which the settlements are computed. Drained analysis uses effective strength parameters but unlike UC analysis does not separate the undrained and consolidation settlement rather it estimates the total settlement.

An analysis was performed using the Bothkennar soil profile (Section 3.3) to compare the settlement improvement factors from UC and DR analysis. The results are shown in Figure 4.3 for two 1x3 column strip and two 3x3 column rafts with area ratio of 3.5. It can be seen that both methods have comparable results for a 3x3 column raft but that DR analysis predicts a slightly higher improvement factor than UC. For a strip footing the use of UC gives a higher improvement than DR analysis. As both methods predict a similar trend of settlement improvement factor with column length for all configurations of columns (within a normalised maximum error of 6%) the results are considered reasonable. In order to permit timely analysis in this research drained analysis is

adopted to reduce computational time and to allow for a greater number of sensitivity analyse to be run (Chapters 4 and 6).

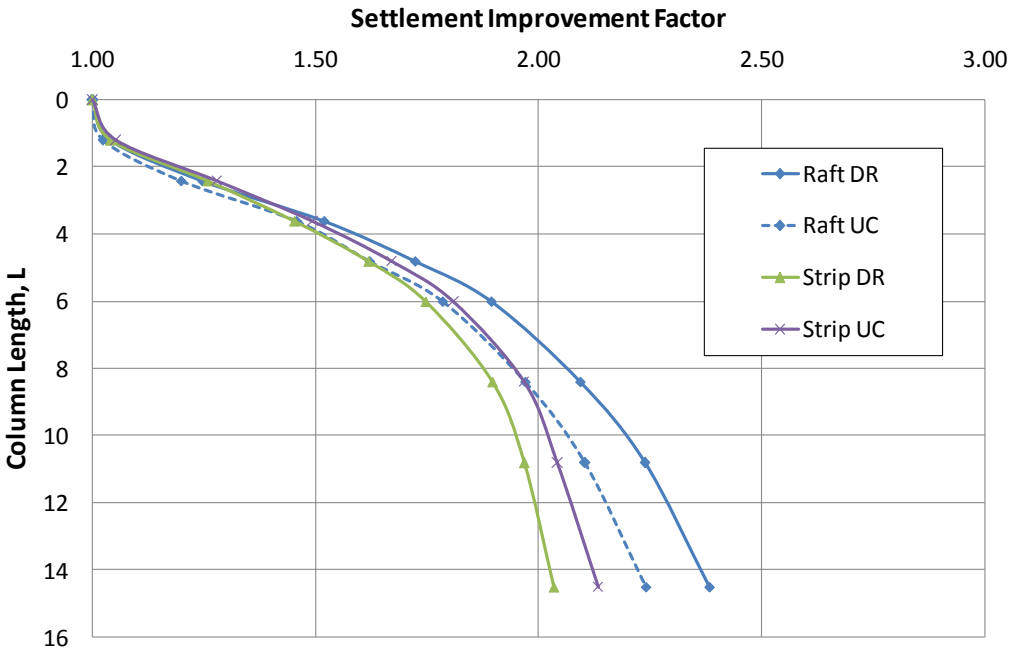

Figure 4.3 Drained vs consolidated settlement

4.1.5 Modelling of the column-soil interface

The modelling of stone columns requires consideration of how they will behave when installed in the soil and subjected to an applied load from the foundation. The PLAXIS 3D Foundation program allows for the modelling of smooth and rough surfaces. Typically, when modelling piles there is the potential for slip associated with pile loading due to the uniform and smooth nature of the surface. Stone columns however are installed in such a manner that they have a rough surface which is dependent upon the material comprising the column and compaction by the Vibroflot. This installation method for stone columns tends to lead to a mixed transition zone between column and soil. This leads to the soil moving as one body. PLAXIS can represent gap and slip displacements which occur normal and parallel to the interface.

PLAXIS models the behaviour of the interface elements using the Mohr-Coulomb perfect plasticity model. The 16 node interface elements consist of 8 pairs of nodes, one set located on the soil wall and the other on the column wall. Brinkgreve (2007) describes how to represent loss of strength at the interface using strength reduction factor (R_{inter}), which describes the relationship between interface and soil strength through the use of the friction angle, Φ, and cohesion, c:

$$c_i = R_{inter} * c_{soil} \quad [4.3]$$

$$tan\theta_i = R_{inter} * tan\Phi_{soil} \leq tan\Phi_{soil} \quad [4.4]$$

Brinkgreve (2007) suggests that elements are assigned a virtual thickness to allow for an element stiffness to be assigned. Gap and slip displacements are calculated from the oedometric, $E_{oed,i}$ and shear modulus, G_i, respectively. The two moduli are related by the Equation 4.5 for a value $v_i = 0.45$:

$$E_{oed,i} = 2G_i \frac{1-v_i}{1-2v_i} \quad [4.5]$$

The use of interface elements was first examined by Balaam *et al.* (1985) who concluded that it was not required for modelling of granular columns as the most significant yielding will occur within the column and little in the surrounding clay. It is assumed that no shear stress occurs at the interface and the column is considered to be in a triaxial state. Later studies by Gäb *et al.* (2008), Elshazly *et al.* (2008), Domingues *et al.* (2007) and Killeen (2012) assumed a perfect bond between the column and soil which did not require elements. Guetif *et al.* (2007) used rigid elements on the basis that stone columns were formed of tightly compacted granular material and was tightly bound to the surrounding soil. This assumed a perfect bond between column and soil.

The influence of the presence of elements upon the settlement performance for three configurations of column is shown (Figure 4.4). Utilising the method of Brinkgreve (2007) to include elements around the stone columns acts to reduce the settlement improvement seen by the introduction of stone columns. The interface elements cause the simulation to over predict the settlement of stone columns. It is therefore considered appropriate to omit the use of interfaces in modelling stone columns and to keep parity with the modelling approach adopted by previous researchers.

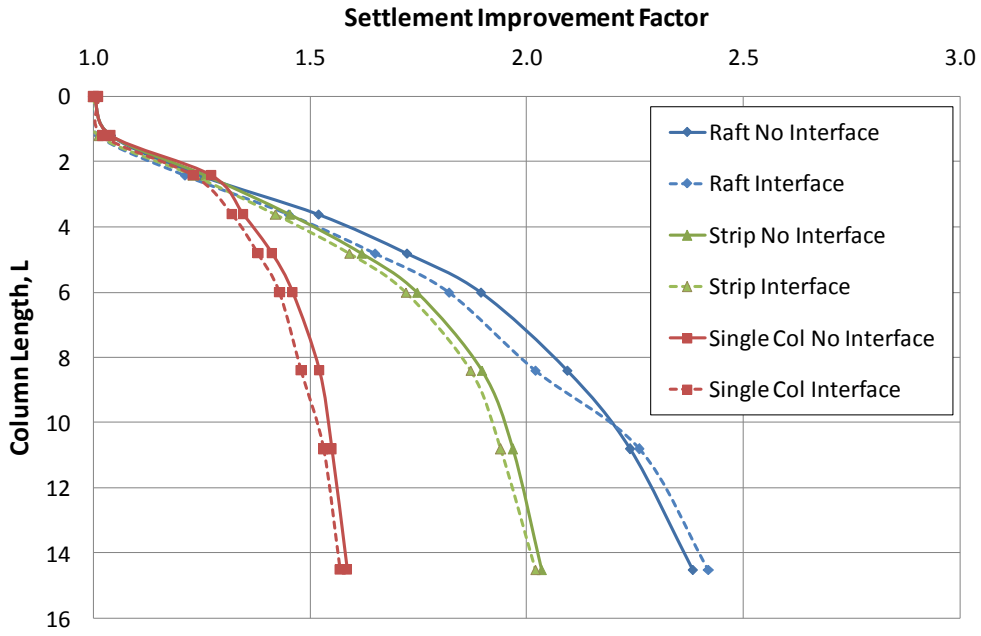

Figure 4.4 interface vs no interface settlement

4.2 Validation of the Bothkennar soil profile

The Bothkennar soil profile is validated utilising the field tests of Jardine *et al.* (1995) and Watts and Serridge (2000). Further analysis is then made using the infinite grid (unit cell) concept to compare the stone column behaviour to analytical design methods.

4.2.1 Field test of pad foundations at Bothkennar

Jardine *et al.* (1995) investigated the bearing capacity and stress-displacement behaviour of two rigid strip foundations at the Bothkennar test site. The pads were installed at 0.8m below ground level with Pads A and B widths of 2.2 m and 2.4 m respectively. The field test was carried out under fully instrumented conditions with pneumatic piezometers, spade cells, inclinometers and magnetic extensometers. The bearing capacity was investigated by loading the first footing, Pad A, to failure to obtain the ultimate bearing capacity of the soil. The second footing, Pad B, was loaded to 67 % of the failure load. The loading rate and duration of the test was different for each rigid footing, with Pad A being loaded to failure in a short period of time, while the field test of Pad B with 67% of the applied failure load continued for two years. The loading rate was applied using Kentledge blocks directly to the pad foundations. Loading of the foundation was halted whenever the settlement rate exceeded 8 mm/hr (and overnight), as a result the applied pressure and time plot indicates a stepped profile. The settlement was measured within an accuracy of 0.1 mm.

The field test of Pad A was conducted under a short time duration of less than 100 hours and can be considered to be an undrained loading test. Lloyd (1989) recorded water levels that were within 0.5 - 1.0 m of the ground surface. The upper layer (ground surface to 1.5 m depth) is referred to as modern flat deposits and is heavily weathered. The lower part of the upper layer also contains a shelly layer which artificially increases the stiffness at the base of this layer. The upper layer consisting of the upper heavily weathered modern flat deposits and shelly layer are referred to as the 'crust'. This layer was modelled as a drained layer, as the field test of Jardine *et al.* (1995) reported a water table approximately 0.9 metres below ground level.

The load-displacement behaviour of Pad A was modelled in Plaxis 3D Foundation (Figure 4.5) and compared with the field data from Jardine *et al.* (1995) (Figure 4.6). Pad A was deemed to have an ultimate bearing capacity of 138 kPa with a settlement at failure of approximately 160 mm. The friction angle for the soil profile was selected from three different sources: cone penetration test (CPT), plasticity index (PI), and triaxial as described earlier in Section 3.3.5.1. An initial run using the Bothkennar soil profile properties and the friction angle from the triaxial test was run (Figure 4.6). The initial run suggested that the chosen stiffness properties for the stiff crust were too stiff. The crust thickness was initially 1.5 m. Barras and Paul (1999) identified a variation in thickness of the stiff crust of between 0.8 m and 1.0 m across the Bothkennar site through examining borehole records. The shell bed which is considered in this research as part of the stiff crust was found to vary between 0.2 m and 1.00 m. It is conceivable that given the depositional environment, i.e. modern tidal flat deposits, that depositional thickness will vary due to the change in down slope thickness between the high tide limits and the base of seaward slope. The borehole cross section covers the southern edge of the site and it is possible that the layers may be thicker or thinner in the central and northern areas of the site. As a result it is considered probable that the field trial may have taken place at a different place in the site from the site testing.

The effect of stiff crust thickness on the load-displacement history match was assessed. In order to determine the approximate thickness of the stiff crust a sensitivity analysis was run (Figure 3.26). By sensitivity analysis a crustal thickness of 0.935m was found to offer the best match to the field trial (Figure 3.26) and is within the limits of the layer thickness described by Barras and Paul (1999). The effect of friction angle on the determined crustal thickness was assessed using data from CPT and PI sources for different crustal thickness. A comparison of the best matches from each of the three

friction angle sources (Figure 3.18): CPT , PI and triaxial is shown in Figure 3.27. The friction angle from the triaxial is constant while CPT and PI friction angles vary. It is observed that the Triaxial gives the best match to the field trial of Jardine *et al.* (1995). As a result for the Bothkennar profile in this thesis this source of friction angle is chosen to complete the profile.

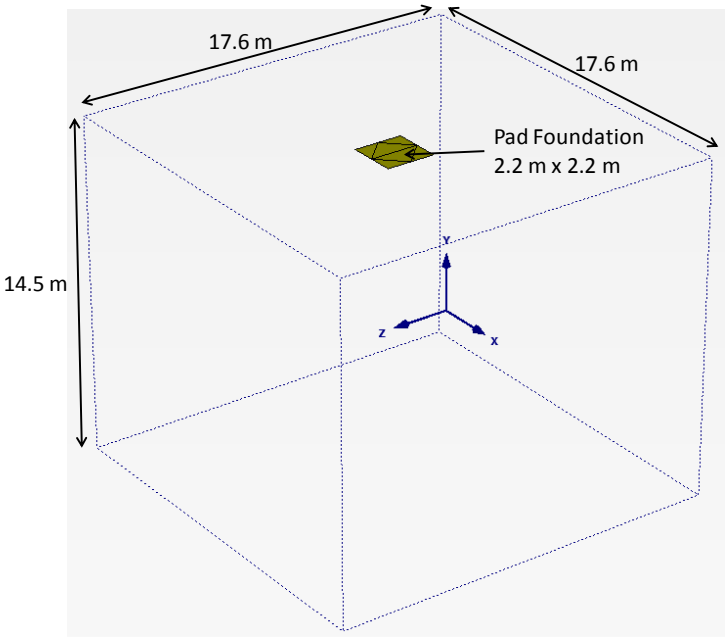

Figure 4.5 Geometry of the Pad foundation and boundaries in Plaxis 3D for Jardine *et al.* (1995)

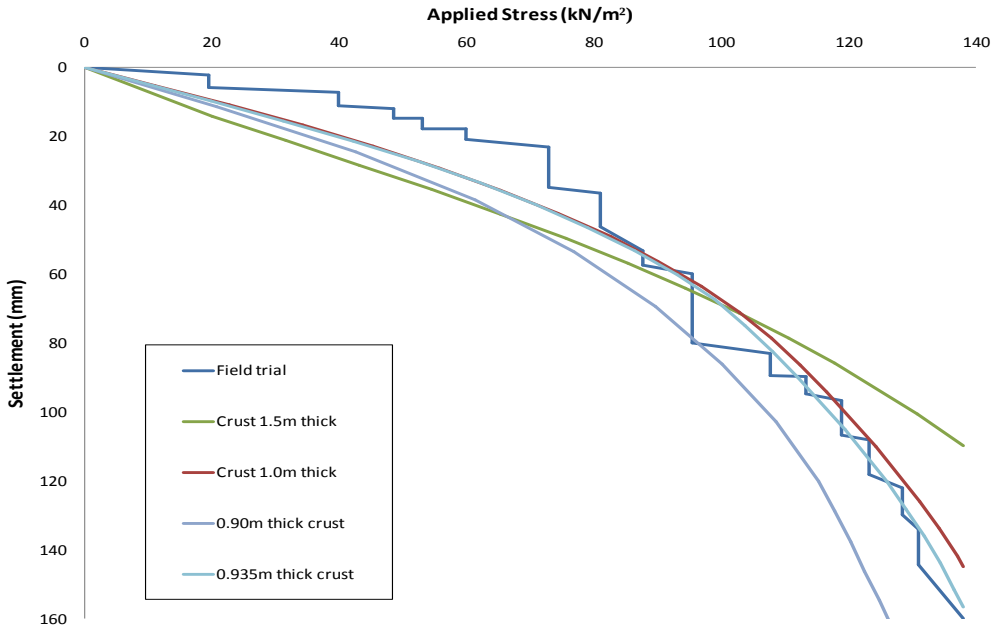

Figure 4.6 Load-displacement behaviour of the Jardine *et al.* (1995) field trial and Plaxis simulations

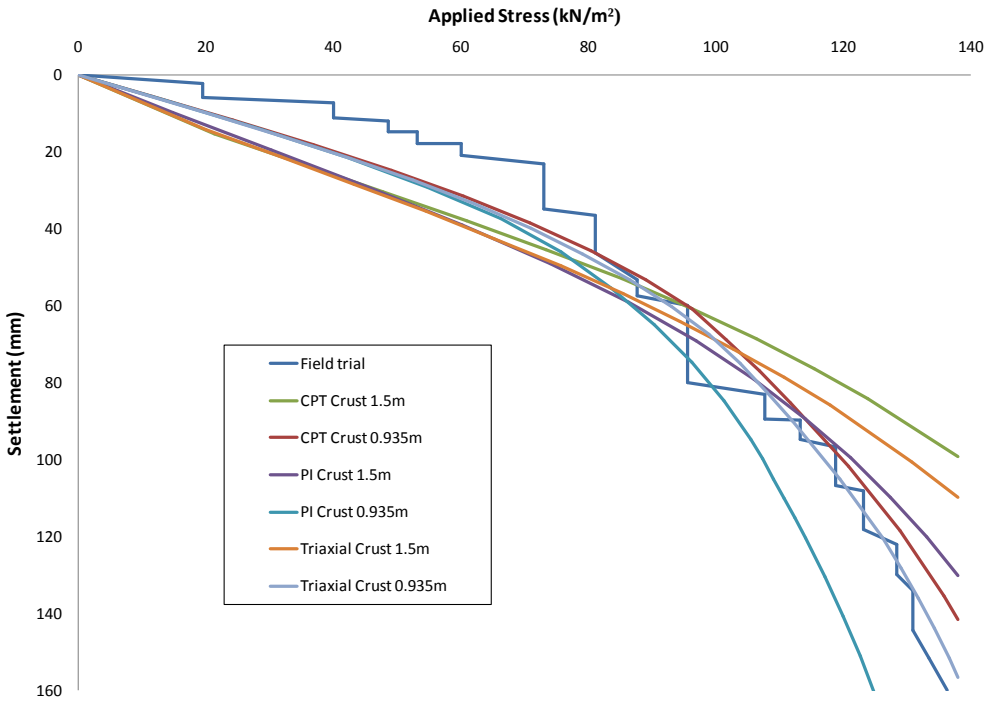

Figure 4.7 Comparison of the effect of stiff crust and friction angle data on load-displacement

The long term response of Pad B was not modelled due to the limitations of the Plaxis 3D Foundation software. The load test contained an unload-reload loop and the recorded displacement includes both primary and secondary settlement. Creep settlement forming part of the secondary settlement is not modelled since primary settlement of the long term response of stone columns and composite columns is the focus of this research.

4.2.2 Field trial of stone columns at Bothkennar

A field trial of stone columns in soft clay beneath strip foundations was undertaken at Bothkennar by Watts and Serridge (2000). The field trial was carried out under fully instrumented conditions to assess the performance of vibro stone columns installed in soft clay using the bottom feed method. The study showed that the effect of the installation process at low loads was to create settlements which were greater than untreated ground but at higher loads the columns were found to significantly reduce the rate and magnitude of settlements. Two strip configurations were modelled in Plaxis 3D Foundation, all founded to a depth of 0.5m. A strip with dimensions 3 m by 0.75 m was modelled to represent the unimproved settlement (Figure 4.8). An improved strip foundation with dimensions 3 m by 0.75 m was modelled with two columns present founded at 0.5 m below ground level. In the improved strip case the columns were

spaced at 1.5 m centre to centre, with a diameter of 0.60 m and column length of 5.7 m below foundation level.

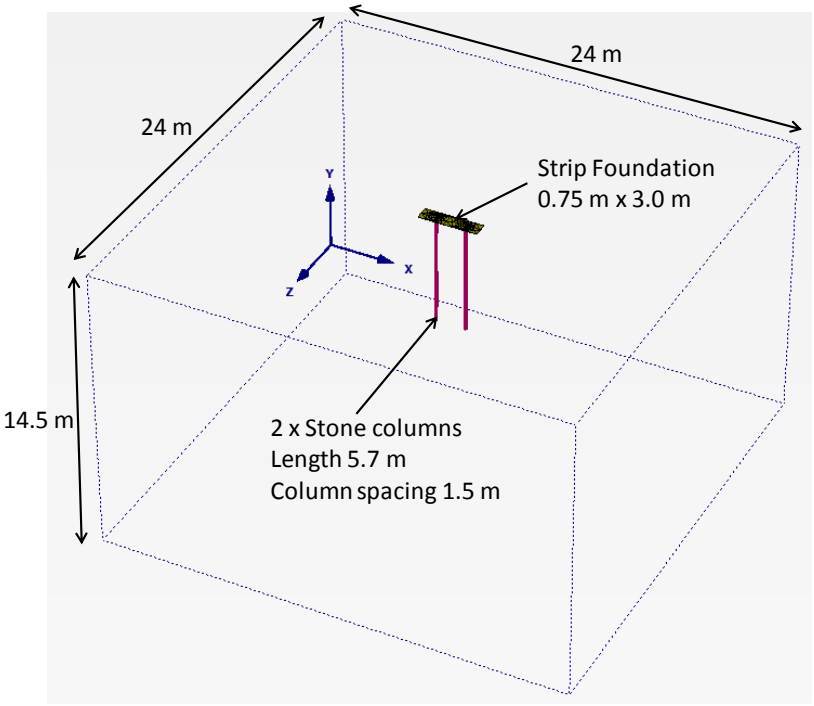

Figure 4.8 Geometry of the Strip foundation, columns and boundaries in Plaxis 3D for Watts and Serridge (2000)

Initially the stiff clay was assumed to have a thickness of 1.5m (Section 3.3.2). The stiff clay thickness is variable across the Bothkennar site (Barras and Paul, 1999) and the position of the field trial relative to the investigation boreholes is unknown as no site plan is provided by Watts and Serridge (2000). The thickness of the layer was incrementally reduced until a match with the field trial was achieved (Figure 4.9). A stiff clay thickness of 0.6 m was found to approximate field behaviour. The normalised error between the field trial and numerical model was found to be 2.5%. This suggests that the numerical model is within an acceptable level of accuracy.

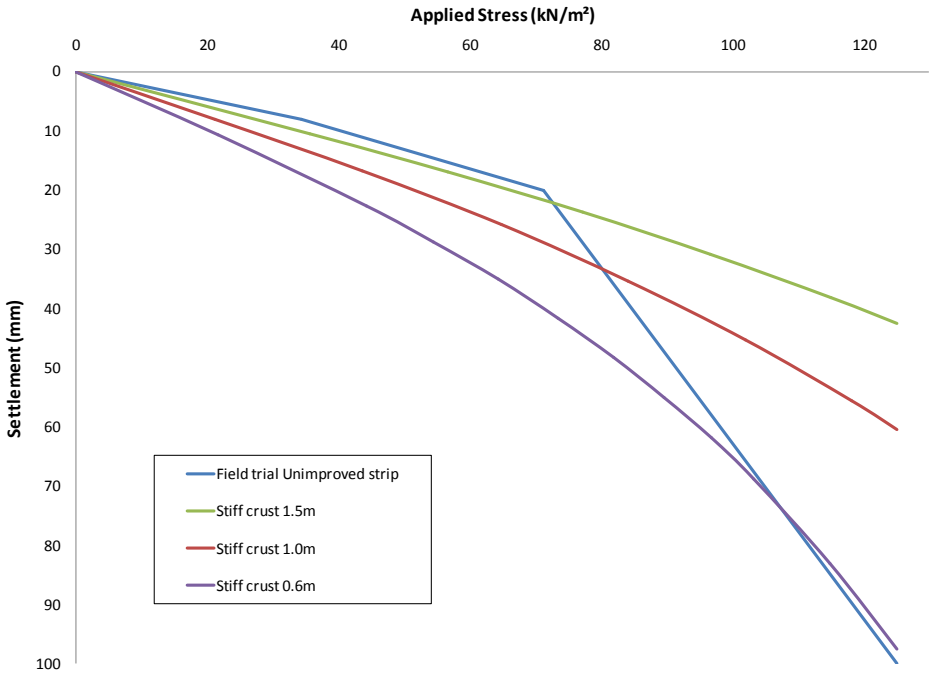

Figure 4.9 Load-displacement behaviour of the Watts and Serridge (2000) field trial and Plaxis simulation for an unimproved strip foundation

The unimproved strip load-displacement behaviour was modelled in Plaxis 3D and compared to the field trial data (Figure 4.10). Watts and Serridge (2000) give limited information in terms of the column material properties, however it is stated that the preliminary design friction angle of the material is 42.5°. The dilation angle was selected from the empirical relationship suggested by Bolton (1986): Dilation angle, ψ = friction angle, φ - 30°. The unit weight, γ, of the stone backfill selected was 18 kN/m³ based upon guidelines in Pennine (2001). Ambily and Gandhi (2007) used unit weights of 15-17.3kN/m³ and Choobbasti *et al*. (2011) used values of 19 kN/m³ so the values in the design manual are deemed reasonable. Values for the stiffness of the column material are not stated or in the later paper by Serridge and Sarsby (2008). Barksdale and Bacchus (1983) stated that the stiffness of columns are generally in the range of 30 - 58 MPa for top feed stone columns. However, McCabe *et al.* (2009) suggests that column stiffness can be as high as 70 MPa for bottom feed stone columns. A brief sensitivity analysis for column stiffness in the range of 30-80 MPa in 10 MPa increments suggested that a stiffness of 40 MPa was suitable for stone columns based upon the history matched settlement in Figure 4.9 and 4.10.

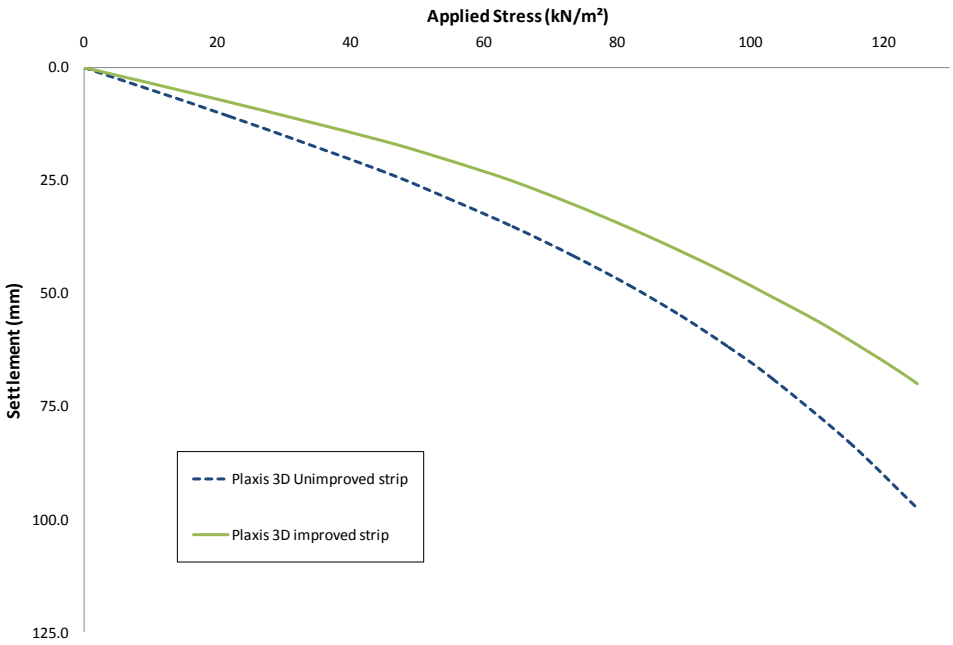

Figure 4.10 Load-displacement behaviour of the Watts and Serridge (2000) field trial in PLAXIS 3D for an improved strip foundation with two stone columns

In order to determine the most appropriate stiffness for the column a sensitivity analysis was run using the design friction angle of 42.5°. It was noted that by increasing the stiffness of the column material from 30 MPa to 70 MPa in 10 MPa increments that the settlement reduced. Values of stiffness greater than 40MPa were found to offer too high a reduction in settlement. In Watts and Serridge (2000) the authors comment that the settlement reduction was lower than expected but did provide an increased factor of safety against bearing failure. A further sensitivity analysis was then run using stiffness values of 30 MPa and 40 MPa which had shown settlement behaviour close to the field trial settlement with column friction angles in the range 38° - 42.5° in half degree increments. It was noted that a column friction angle of 38°, dilation angle 8°, and Stiffness of 40 MPa achieved the best match. The normalised error between field and numerical model was 3.65%. The improvement factor which is defined as the unimproved settlement of the foundation divided by the improved settlement was 1.38 and 1.39 for the field trial at maximum load and numerical model respectively which suggests a 2% difference. The Bothkennar soil profile material properties for the stiff clay, upper Carse clay and lower Carse clay are therefore considered valid for use in further modelling. The settlement response modelled for the Watts and Serridge (2000) field trial is considered to validate the soil profile and is numerically representative of the behaviour of stone columns at Bothkennar. Thus, the material properties from the

literature and determined by sensitivity analysis are used for further analysis in this research.

Hardening Soil Model Parameter	Stiff Crust Layer A	Upper Carse Clay Layer B	Lower Carse Clay Layer C
Depth Interval	0.0m to 1.0m	1.0m to 2.0m	2.0m to 15.0m
Bulk unit weight, γ (kN/m³)	18	16.5	16.5
Over consolidation ratio, OCR	1.75	1.75	1.5
Pre-overburden stress (kPa)	15	15	
Coefficient of lateral earth pressure, k_0	1.5	1.1	0.75
Effective cohesion, c' (kPa)	2	1	1
Angle of internal friction, ø (°)	34	34	34
Initial voids ratio, e_0	1.00	1.19	1.98
Compression Index, C_c	0.07	0.25	1.12
Swelling index, C_s	0.02	0.06	0.28
Reference pressure, p_{ref} (kPa)	13.50	30.94	37.13
Vertical coeff. of permeability, k_{vert} (m/day)	6.77E-05	5.08E-05	5.08E-05
Horiz. coeff. of permeability, k_{horiz} (m/day)	1.02E-04	1.02E-04	1.02E-04
E Ref Eod (kPa) at Pref 100kPa	6571	2024	616

Table 4.3 Soil material properties adopted for Bothkennar layers

4.2.3 Unit cell: Infinite array of stone columns at Bothkennar

An analysis is undertaken to valid the Bothkennar soil profile and PLAXIS 3D Foundation for the modelling of an infinite array of stone columns. An infinite array is simplified using the Unit Cell concept described in Chapter 2. The unit cell is assumed to be representative of the infinite array at any point.

The unit cell is modelled in PLAXIS and settlement behaviour compared to analytical theory for evaluation purposes for the following cases:

(i) PLAXIS unit cell foundation settlement behaviour without a column present is compared to one-dimensional compression theory

(ii) PLAXIS unit cell foundation settlement performance with a stone column present is compared to the analytical design methods of Balaam and Booker (1981), Priebe (1995) and Pulko and Majes (2005).

(i) Unimproved Strip Settlement

For the unimproved scenario the Bothkennar profile defined in Section 3.3 is used for one dimensional stiffness and stress-state parameters. The soil is divided into nine layers for this specific example and the settlement calculated in terms of vertical stress at the centre of each layer (Table 4.4).

		One Dimensional Compression Theory				FEM Plaxis 3D
Layer Identifier	Layer Thickness (m)	Effective Stress (kPa)	Effective Stress Max. (kPa)	Total Stress (kPa)	Settlement (mm)	Settlement (mm)
1	0.5	7	100	60	4	4
2	0.5	15	90	68	3	6
3	1	19	76	72	16	13
4	1.5	27	48	80	118	111
5	1.5	36	60	89	103	139
6	2	46	75	99	118	124
7	2	58	92	111	108	105
8	3	73	113	126	146	107
9	3	91	138	144	137	93
				Total	753	702

Table 4.4 Comparison of the settlement calculated by one dimensional compression theory and output from PLAXIS 3D

The settlement is calculated using Equations 3.14 or 3.15 from one dimensional compression theory:

If *in-situ* vertical effective stress, $\sigma'_{y,0}$, plus change in vertical effective stress (due to foundation load and unit weight), $\Delta\sigma'_y$, is less than the maximum effective vertical stress, $\sigma'_{y,max}$ then:

$$s_{uc} = H\left[\frac{C_s}{1+e_0} log\left(\frac{\sigma'_{y,0}+\Delta\sigma'_y}{\sigma'_{y,0}}\right)\right] \quad [4.6]$$

If *in-situ* vertical effective stress, $\sigma'_{y,0}$, plus change in vertical effective stress (due to foundation load and unit weight), $\Delta\sigma'_y$, is more than the maximum effective vertical stress, $\sigma'_{y,max}$ then:

$$s_{uc} = H\left[\frac{C_C}{1+e_0} log\left(\frac{\Delta\sigma'_{y.max}}{\sigma'_{y,0}}\right) + \frac{C_s}{1+e_0} log\left(\frac{\sigma'_{y,0}+\Delta\sigma'_y}{\sigma'_{y,max}}\right)\right] \quad [4.7]$$

The settlement for each layer and the variation of settlement with depth is reported in Table 4.4. It can be seen that PLAXIS predicts 11% lower total settlement than the analytical solution. Both use the same soil parameters and the settlement of the soil is comparable. Layers 5 and 6 in the PLAXIS model suggest a higher settlement. The analytical solution over predicts the settlement for the lower Carse clay significantly which includes layers 5 and 6. The difference is considered a result of the hardening soil model to capture increased stiffness of the soil with loading and so predicts lower settlement. One dimensional compression theory assumes constant soil stiffness.

(ii) PLAXIS unit cell foundation settlement performance with a stone column present

The settlement performance on an infinite array of stone columns from PLAXIS 3D Foundation is compared to analytical design methods. The analytical design methods which are chosen for comparison are Balaam and Booker (1981), Priebe (1995) and Pulko and Majes (2005). The design methodologies simplify the design of the infinite

array by use of the unit cell concept. The PLAXIS simulation is setup as a unit cell (Figure 4.11) with both the numerical model and analytical methods assuming the same boundary conditions i.e. at the outer boundary the unit cell is restrained by other unit cells within the infinite array.

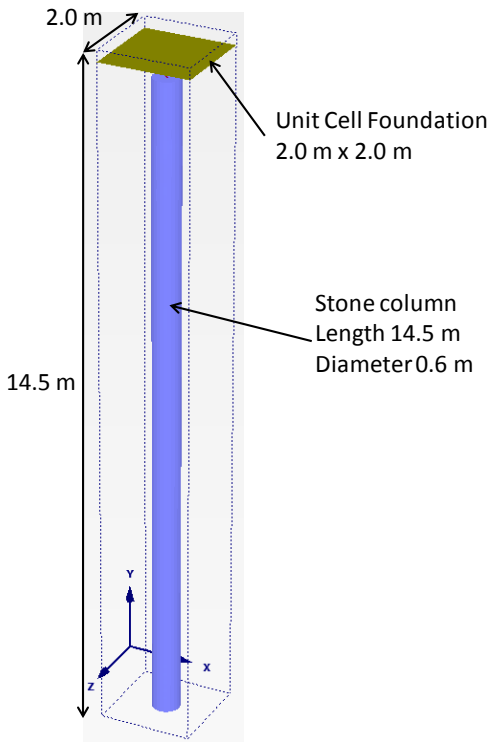

Figure 4.11 Setup geometry of a 2m unit cell with stone column present

The parameters used in the design methods contain simplified assumptions. The numerical model uses the hardening soil model which allows the dependency of variables to change with increasing applied load. Assumptions surrounding initial soil stress state and column and soil stiffness are now discussed.

The initial soil stress state is known to influence the settlement performance of stone columns and is accounted for in two of the methods: Priebe (1995) and Pulko and Majes (2005). Priebe (1995) suggests a minimum coefficient of lateral earth pressure, k_o, equal to 1 to account for column installation effects. The $k_0$values for the Bothkennar soil profile are however greater than 1 for the stiff crust and upper Carse clay. Pennine (2001) and Killeen (2012) suggest adjustment of the earth pressure can be made to account for the pressure difference cause by bulging using Equation 4.8 at the column-soil interface:

$$k_{o,adjusted} = \left(K_{o,col} * \sigma_{col}\right) - \left(K_{o,soil} * \sigma_{soil}\right) \quad [4.8]$$

The k_0 values adopted for the method of Pulko and Majes (2005) do not require a minimum value and the derived values for the soil profile specified in Table 3.1 are used by default. The k_0 values and material properties of the columns as used for the analytical design methods are shown in Table 4.5. The stiffness of the column and soil need careful consideration when using analytical design methods. In PLAXIS 3D the stone columns are modelled by Mohr-Coulomb perfect plasticity (MC) and the soil using the hardening Soil model (HS). The MC model assumes constant stiffness values regardless of stress level. The HS model uses two stiffness values to account for the stress path dependency of the soil (see Section 3.2.2.3). The HS model simulates the increase in stiffness observed with increasing confining pressure whereas the analytical solutions assume constant stiffness.

Layer	Depth Interval (m)	Density of soil (kg/m³)	Ko	Density of stone (kg/m³)	Friction Angle (°)	Dilation Angle (°)
A	0.5 - 1.0	18	1.5	19	45	15
B	1.0 - 2.0	16.5	1.1	19	45	15
C	2.0 - 15.0	16.5	0.75	19	45	15

Table 4.5 Design values for analytical methods

The settlement performance of an infinite array predicted by PLAXIS is compared to the analytical solutions in Figure 4.12. It appears that PLAXIS produces similar results to the analytical solutions suggesting the use of FEM produces reasonable results. The design methods offer different results from the simulation which is to be expected since they assume simplifications in soil behaviour. Balaam and Booker (1981) overestimates the settlement improvement factor, n, of the columns due to the assumption that stone column material behaves with linear elasticity which fails to account for yielding and plasticity within the column. Castro and Sagaseta (2009) found this also to be the case in similar stone column FEM analysis. Pulko and Majes (2005) suggests a better match with the simulation results for high area ratios above 5. The method attempts to account for column yielding which gives more realistic n values for A/Ac of 8 to 15. Below A/Ac value of 8 the method tends to over predict the benefit of stone columns to settlement control. PLAXIS models the column behaviour using elasto-plastic behaviour compared to the assumption of rigid plastic behaviour assumed by the authors. The method assumes that because behaviour is rigid-plastic in the analytical solution that no elastic strains develop when the columns are in a plastic state. As a result it under predicts the settlement and higher n values than the HS model in PLAXIS. The plasticity within columns is highest at low A/Ac ratios of the infinite

array due to the highest levels of confinement and they carry a higher proportion of the applied load. This leads to the largest differences between the method and PLAXIS solution observed at low A/Ac.

The method of Priebe (1995) was used to produce two settlement improvement factors, basic improvement factor, n_0, and the final improvement factor, n_2 in Figure 4.12. The factor n_0 appears to significantly underestimate the settlement performance which is to be expected since the factor does not account for column compressibility and the effect of overburden stress. The factor n_2 shows reasonable agreement with the PLAXIS results for A/Ac ratios between 8 and 14.2. It is clear that the analytical solutions approximate numerical behaviour and as such validate the use of PLAXIS 3D Foundation to model stone column and soil behaviour.

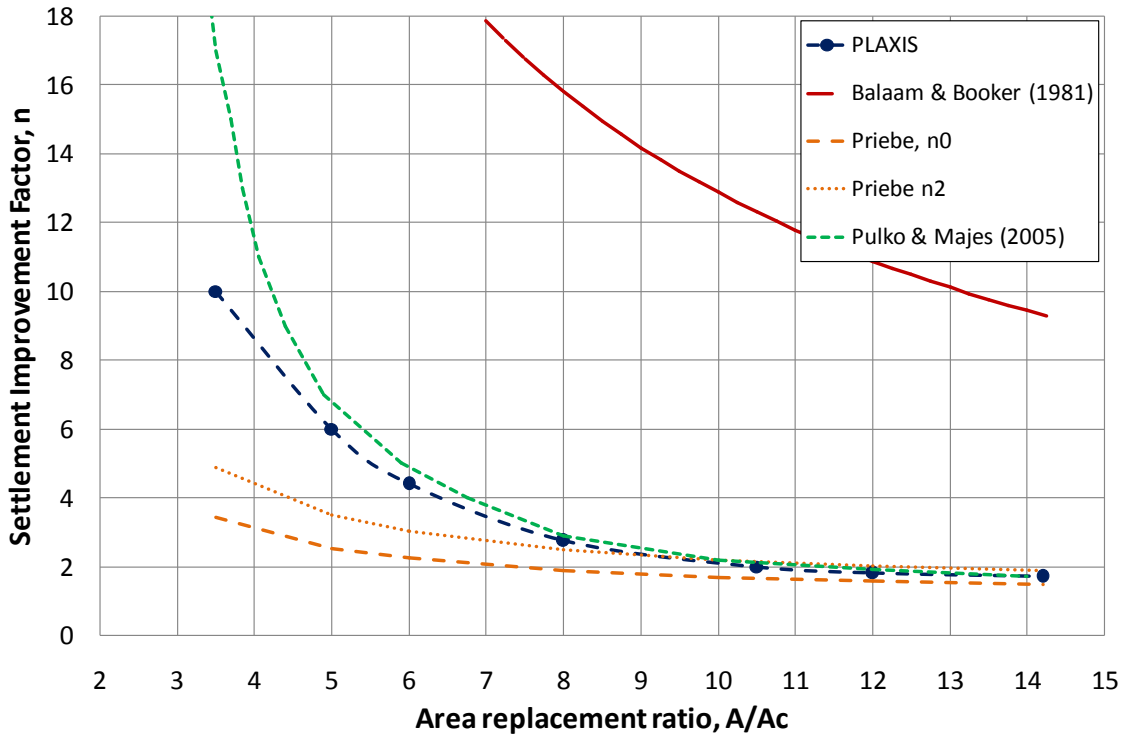

Figure 4.12 Comparison of the improvement factors for a unit cell for different area ratios with published research

4.3 Summary

4.3.1 Modelling approach

The use of PLAXIS 3D Foundation was examined in this Chapter to assess the effects of mesh refinement, boundaries, the use of drained and undrained-consolation analysis and the effect of interfaces on the numerical simulation. The findings were then used to

model field trials and one dimensional compression theory to validate the Bothkennar soil profile. The modelling approach can be summarised as follows:

- The effects of mesh coarseness were examined to assess how the grid size impacted the accuracy of the fine element solution relative to the very fine mesh. PLAXIS uses five mesh settings which are applied automatically. The use of the very fine mesh was found to take too long for drained analysis. The use of the fine mesh gave an acceptable numerical accuracy and running time to make the sensitivities in this research feasible.
- The effect of the minimum distance to boundary on the numerical solution had previously been examined by Azizi (2000) and Killeen (2012) who suggested the minimum distance to boundary should be five times the greatest foundation dimension and eight times the breadth of the foundation respectively. The results of the analysis suggest that a minimum distance to boundary should be eight times the foundation breadth or breadth and length depending on the foundation configuration of pad or strip.
- The method of simulating the foundation performance was examined for drained and undrained-consolidated analysis. It was concluded that the drained solution was close to the undrained-consolidated analysis in terms of results and had vastly reduced running times. As such drained analysis was used. Balaam *et al.* (1977), Balaam *et al.* (1985), and Killeen (2012) also used drained analysis in preference due to undrained-consolidation. It is also noted that the data from Bothkennar is limited to a single source and no across site distribution of the porosity and permeability has been quantified to date making representative modelling difficult.
- The effect of interface elements between the stone column and soil was also examined for a 1x3 column strip and 3x3 column rafts. It was concluded that the use of interfaces caused the over prediction of settlement and therefore an interface free approach was adopted. It is also noted that Balaam *et al.* (1985) and Killeen (2012) examined the effect of interfaces and found similar results.

4.3.2 Development and validation of the Bothkennar soil profile

The Bothkennar soil profile was constructed from data available in the literature. The site has been the subject of extensive characterisation studies which were used to identify three layers for inclusion in the profile: stiff crust, upper Carse clay and lower

Carse clay. The presence of stiff crust is similar to clay sites located throughout the United Kingdom. The Bothkennar soil profile was validated using two field trials which took place at the site and one dimensional compression analysis:

- Plaxis was able to capture the field trial settlement behavior of Jardine *et al.* (1985) and Watts and Serridge (2000) for a pad foundation and a strip improved by stone columns respectively for the Bothkennar soil profile. The Bothkennar soil profile was therefore considered validated for further use in stone column and composite stone column modelling in Plaxis 3D.
- Plaxis was able to model the behavior of a stone column installed in a unit cell. The settlement behavior was found to be comparable to one dimensional consolidation theory.

Chapter 5

Behaviour of stone columns in soft soils for small raft and strip foundations

5.1 Introduction

This research examines the behaviour of small groups of stone columns installed beneath small pad, raft and strip foundations in soft soils. A sensitivity analysis was conducted to examine the effect of design parameters and the soft soil profile on stone column settlement performance and deformational behaviour. The areas of key interest are summarised as follows:

- Area ratio (A/Ac)
- Column confinement
- Column Length (L)
- Column compressibility
- Column strength
- Column installation effects
- Thickness of the stiff crust

The application of stone columns to soft soil is becoming increasingly important due to shortage of buildable land in the United Kingdom. The Bothkennar test site has been the subject of considerable study due to the soft soil nature of the deposit and the influence of the crust. The introduction of stone columns into soft soil tends to increase the shearing resistance and as a result reduce the potential for bearing capacity failure beneath the foundation. The design of foundations for Bothkennar type soft soils tend to consider the settlement performance rather than bearing capacity due to the excessive settlements usually encountered. The application of stone columns is generally only considered for low to medium working loads and is generally much less than the bearing capacity. The settlement performance of stone columns is normally controlled by the friction angle of the material and the restraint provided by the surrounding columns and soil. The lateral restraint or support offered by soft soil is generally limited. The degree of settlement reduction is heavily controlled by the area ratio which is a function of column diameter and spacing. The confinement offered by neighbouring columns is dependent upon the column and foundation configuration. This is investigated by comparing the effect of area ratio for strip and small raft configurations with settlement reduction from infinite arrays of columns and single

columns. The influence of column length on foundation performance is investigated for end bearing and floating (partially penetrating) stone columns. The relationship between column length, area ratio and confinement is examined. The effect of column stiffness and strength is examined by adjusting the column Young's modulus and friction angle respectively.

The deformation behaviour of stone columns beneath different foundation configurations is examined for columns under normal working loads. Typically in stone column applications the design aims to minimise the degree to which settlement occurs and the effect of deformation under such loads allows for a greater understanding of the limitations of current designs. This is particularly relevant in the context of composite columns (Chapter 7). An important parameter which is linked to the applied load and deformation of the columns is the stress concentration ratio. The ratios under normal working load are examined to gain an understanding of how it varies with key design parameters such as ratio and column length. The stress concentration ratio is normally used in analytical design methods and understanding how this varies with column parameters and modes of deformation is key to understanding optimum configurations and how composite columns may overcome limitations.

5.2 Overview of the sensitivity analysis

The sensitivity analysis uses different foundation designs in order to understand the settlement performance of stone columns in soft soils. In the previous chapter the validity of the Bothkennar soil profile was tested using two field trials and unit cell theory. In this chapter this profile is used for all further analysis in this research. The foundations are 0.5 m thick and founded 0.5m below ground level unless otherwise stated. The foundation configurations and 3D plan view are shown in Figures 5.1 and 5.2 respectively. The installed column diameter is fixed at 0.6 m which was observed during the field trial of Watts and Serridge (2000) using a bottom feed stone column system. The field trial design friction angle of 42.5° was compared to the FEA in the previous chapter which suggested a 38° friction angle. The settlement was higher than the design anticipated; the Vibroflot should not remain in the ground for longer than is necessary and air jetting pressure should be kept to a minimum to avoid soil disturbance. In this subsequent FEA the design friction angle of 45° is adopted under the assumption that the above suggestions regarding installation are adopted. For each of the sensitivity groups the column length is increased from zero (i.e. no columns) to

14.5m. In the immediate bulging zone (to a depth of 2 m), length is increased in 0.5 m increments, with increments of 1m from 2 m onwards to 15 m.

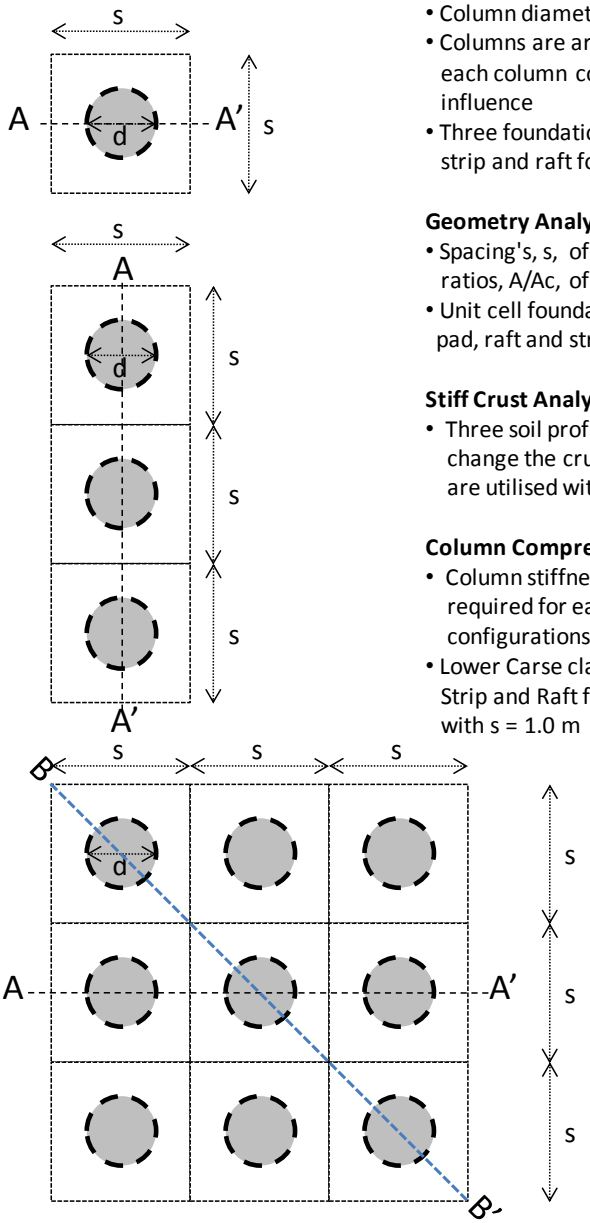

General for all sensitivities

- Column diameter, d, 0.6m
- Columns are arranged in a square grid configuration with each column considered to have a designated zone of influence
- Three foundation configurations examined are pad, strip and raft foundations

Geometry Analysis

- Spacing's, s, of 1.0 m, 1.5 m and 2.0 m allow for area ratios, A/Ac, of 3.5, 8.0 and 14.0
- Unit cell foundation also examined to benchmark pad, raft and strip foundation behaviour

Stiff Crust Analysis

- Three soil profiles are utilised (see Figure 4.3) which change the crust thickness all foundation configurations are utilised with s = 1.0 m

Column Compressibility, Strength and K_0 Analysis

- Column stiffness and friction angle are adjusted as required for each analysis. Pad, Strip and Raft foundation configurations are utilised with s = 1.0 m
- Lower Carse clay K0 values are altered for the analysis. Pad, Strip and Raft foundation configurations are utilised with s = 1.0 m

Line of Section

- Figures assume a line of section through the foundation and columns marked by A-A'. For rafts an additional line of section from corner to corner is included defined by B-B'.
- The unit cell line of section is the width of the foundation.
- For the cases of a single column the width of section extends to the outer boundary
- For the case of a 3 column strip the line of section extends 5 m out from the centre of the foundation to A and A'
- For the case of a 9 column raft the line of section extends 6 m out from the centre of the foundation to A and A'

Figure 5.1 Foundation configurations for sensitivity analysis

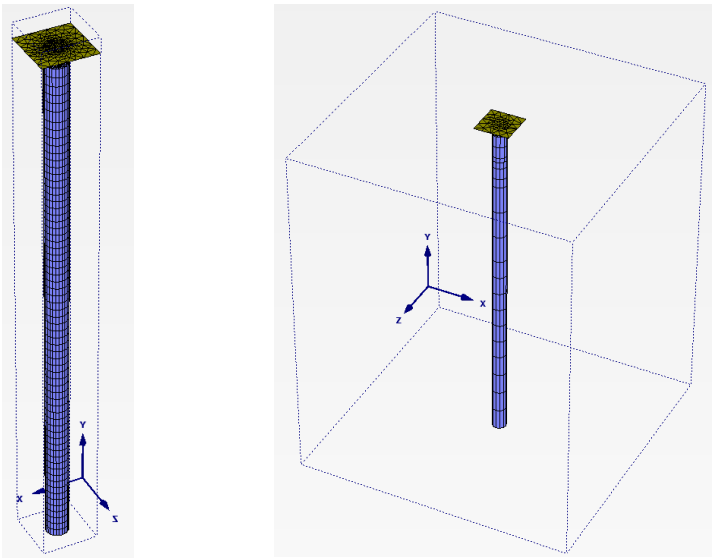

Unit Cell Single Column

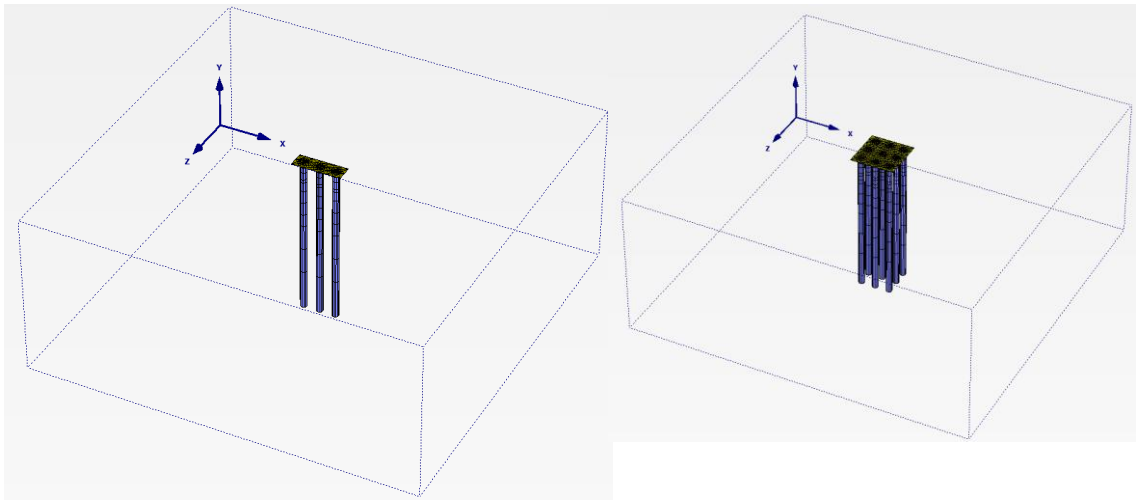

Three Column Strip Nine Column Raft

Figure 5.2 Three-dimensional view of column configuration

Area ratio and column confinement

The lower the area ratio the larger the increase in stiffness of the soil and so the greater the magnitude of settlement reduction. In such a setting each unit cell is restrained at its outer edge by another unit cell or column/ soil unit. The influence of the area ratio and column confinement is examined for a line of three columns beneath a strip foundation, a small raft of nine columns and a unit cell which is compared to the behaviour of a single column. All foundation types assume a square grid configuration with all columns located at equidistant positions relative to each other and spaced at 1.0, 1.5 and

2.0 m (Figure 5.1). The variation in the configurations will provide reference settlements for a single column, which is likely to offer the lowest confinement and settlement improvement, to a unit cell which due to the lateral confinement within the array, is likely to offer the highest confinement and highest reduction in settlement.

Column compressibility and strength

The influence of column stiffness and strength is examined for a single column, a row of three columns beneath a strip and a group of nine columns beneath a small raft foundation (Figures 5.1 and 5.2). The properties of column friction angle and stiffness derived from the Watts and Serridge (2000) field test are used for the base case with sensitivities run as follows:

- The influence of the column friction angle is assessed for values in the range of 38° - 50° with the dilation angle adjusted accordingly using the relationship derived by Bolton (1986) where dilation angle, Ψ, = φ -15°.
- The influence of column stiffness, E_c, is examined for value between 30 - 70 MPa based upon the range suggested by Barksdale and Bachus (1983).

Column installation effects

The installation of stone columns into soft clay is known to alter the coefficient of lateral pressure in the soil. The stiff crust and upper Carse clay layers are stiff i.e. K_0 greater than 1 as such the values are not altered. However, the lower Carse clay in the base case has a K_0 value of 0.75. Initial simulation studies suggested that the column installation was found to affect the lower Carse Clay more than the upper layers. A sensitivity is carried out on the lower Carse clay with K_0 values adjusted in the range of 0.75 to 1.25 to examine the impact on column performance.

Thickness of the stiff crust

The history matching of the load-displacement behaviour of the field trials of Jardine *et al.* (1995) and Watts and Serridge (2000) showed the importance of the *modern* tidal flat or stiff crust deposit in settlement behaviour. The material properties for the Bothkennar soil profile were developed from the extensive literature however the thickness of the stiff crust was found to be variable across the site. Sensitivities are run using a single column, a row of columns beneath a strip and a small nine column raft to

assess how the crust impacts stone column reinforced foundations for crust thicknesses of 0.5 m, 1.0 m and 1.5 m (Figure 5.3).

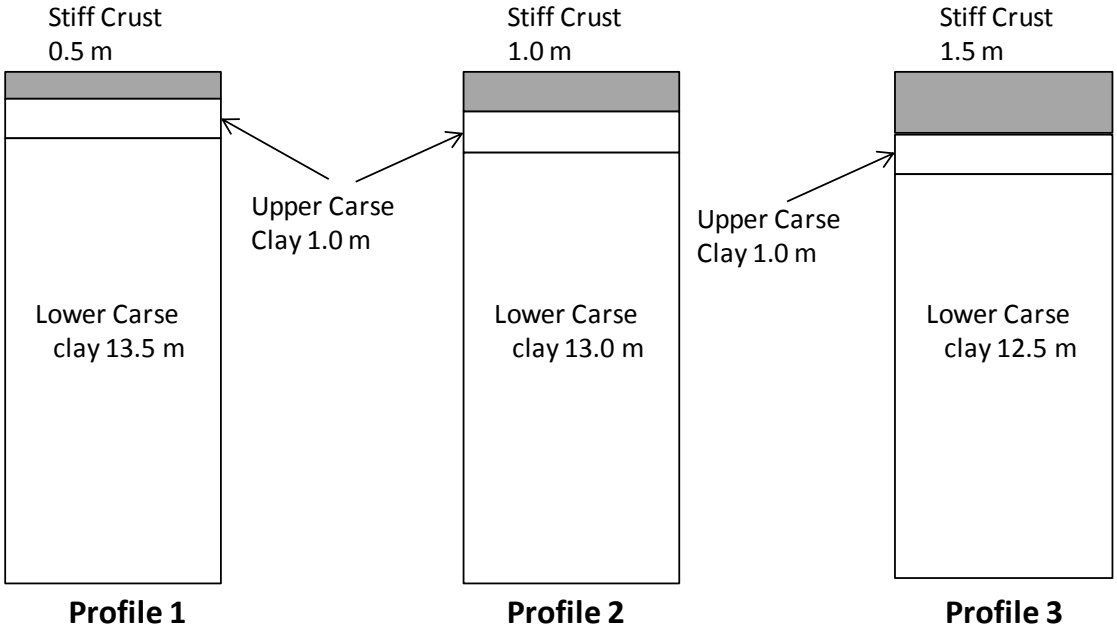

Figure 5.3 Soil Layer configuration Schematic for crust thickness sensitivity

5.3 Settlement performance of stone columns

The use of stone columns is predominately for settlement control and any increases in shear resistance and bearing capacity are a secondary consideration. Typical working loads for stone columns are in the range of 25 - 50 kN/m² and for this analysis a working load of 50 kN/m² is adopted for foundations using the Bothkennar soil profile (see Section 3.6.2). The settlement behaviour for the four types of foundation (infinite array, single column, small raft, and strip) is defined by the basic settlement improvement factor:

$$\text{basic settlement improvement factor, } n = \frac{settlement\ \ of\ untreated\ \ foundation}{settlement\ \ of\ treated\ foundation} \qquad [4.1]$$

5.3.1 Settlement performance of infinite arrays of stone columns

The unit cell method was used to represent the infinite array of stone columns and the influence of column length on settlement performance examined for different area ratios (Figure 4.4). For stone columns less than 2.4 m in length a negligible reduction is observed by a settlement improvement factor, *n*, of 1.1. This can be attributed to the presence of the stiff crust and the upper Carse clay which, due to their stiff nature, are marginally improved by the stone column. As the column length extends below this

competent layer it can be observed that the settlement improvement factor increases with increasing column length. For column lengths of 14.5 m which represent end bearing stone columns they are able to transfer stress to the underlying stratum. The highest settlement improvement factors are achieved for the closest spacing of 1.0 m. This represents the lowest area ratio of 3.5. The columns appear most effective when placed close together and least effective at a spacing of 2.0 m and area ratio of 14.2. Note from 15 m depth the Bothkennar gravel is considered to exist and therefore the base of the model is considered a hard substrate.

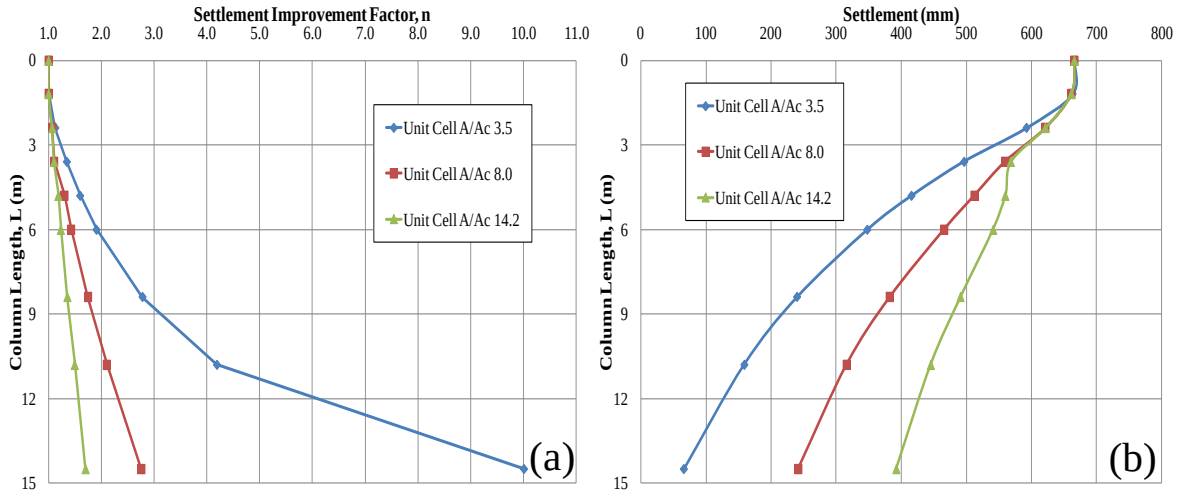

Figure 5.4 Influence of area replacement ratio on settlement and settlement improvement factors for an infinite array of stone columns

5.3.2 Settlement performance of single column, small raft and strip foundations

In conventional column design the unit cell concept is used when designing foundations. However, the assumption that all columns act within a group to restrain each other and in so doing reduce settlements is now tested for different foundation configurations. An assessment is made of the effect of column confinement using a single column, three column strip and a nine column raft adopting standard square column placement (Figure 5.1). The influence of column length and confinement on the settlement improvement factor is shown in Figure 5.5. As observed with the infinite array of columns no significant decrease in settlement is observed for column length less than 2.4 m due to the competent nature of the stiff crust and upper Carse Clay.

Settlement improvement factors are highest for columns with the lowest area ratios (Figure 5.5). This is seen in the variation of settlement improvement factors for area ratios of 3.5, 8.0 and 14.2. For all foundation configurations increasing the column length increases the improvement factor. However, the rate of settlement reduces for

column lengths greater than 4.8 m for area ratios of 8.0 and 14.2. This suggests that beyond a length to diameter ratio of 8, that settlement reduction is minimal due to the wide spacing of columns which are not transferring stress to depth. By comparison the columns with an area ratio of 3.5 indicate an increase in improvement factor with increasing length with the largest increase observed for end bearing stone columns of length 14.5 m.

It can be clearly seen in Figure 5.5 that column configuration has an impact on the settlement improvement factors. The single column does not benefit from lateral confinement from other columns and has the lowest improvement factor (Figure 5.5(b)). Strip foundations are partially confined in the inward facing directions which leads to higher settlement improvement factors. The raft foundation appears to offer higher improvement ratios due to the higher degree of confinement offered by surrounding columns. The increase in improvement factor appears to be controlled by area ratio since the highest settlement reductions occur for the closest spaced columns. For the case of the Bothkennar soil profile the highest reductions in all cases are achieved with area ratios of 3.5 with increasing column length. For area ratios the degree of improvement with column length reduces beyond a column length of 4.8 m.

An assessment of the influence of footing width, B, on settlement improvement factor is shown on Figure 5.5(b) to assess how the area ratio governs the variation of settlement improvement factor with length of column. It would be expected from Boussinesq (1885) theory that below a depth of L/B = 2 that the effect of an applied load on the foundation would not be observed in the soil settlement. So installing stone columns to improve the settlement performance below this depth should not have an effect. It appears from the plots of settlement improvement factor and normalised column length (L/B) that this significant depth does not influence settlement improvement factors as an increase in the settlement improvement factor is observed below this depth.

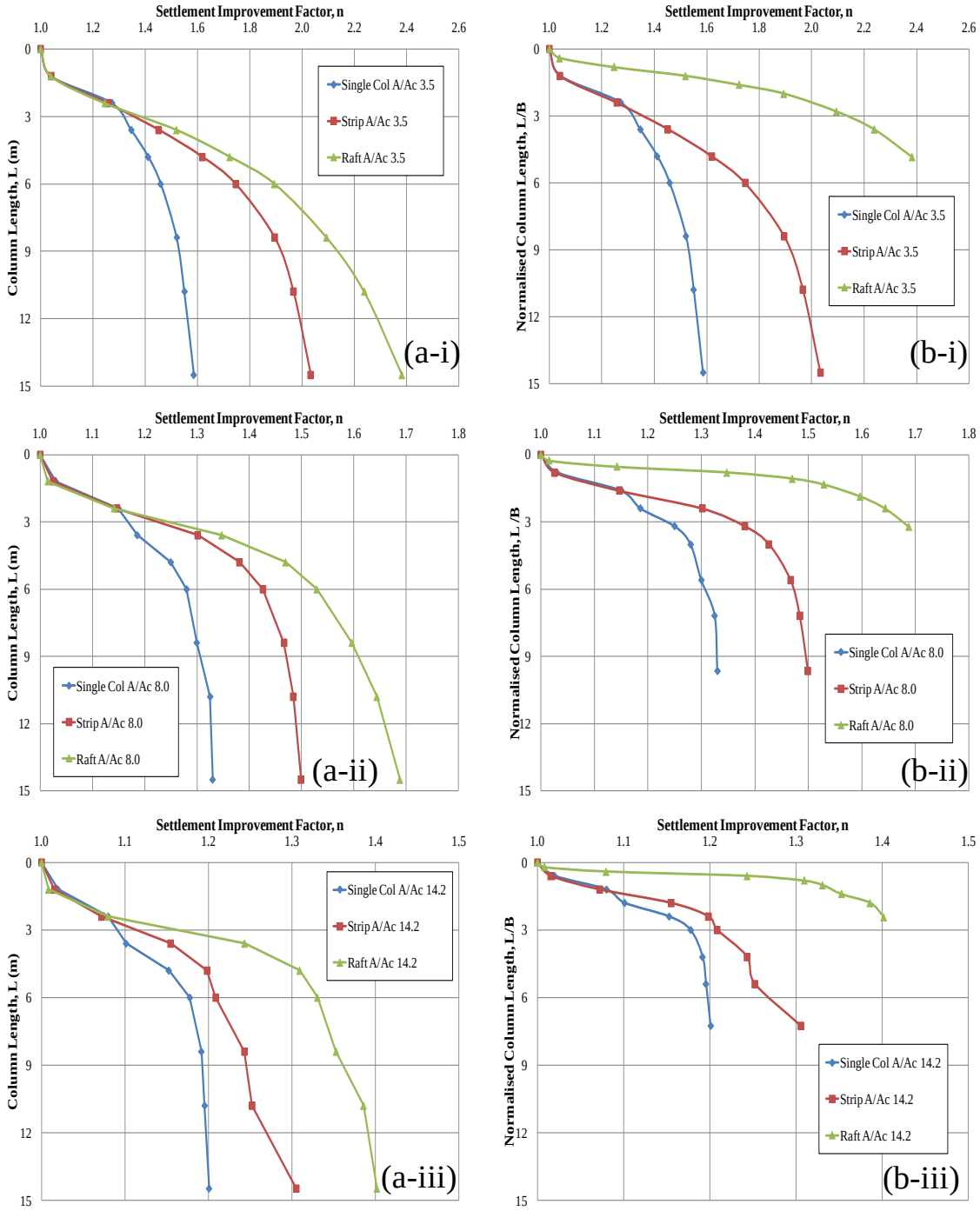

Figure 5.5 Influence of area replacement ratio on settlement improvement factors and Length to breadth ratio (L/B) for a single column, three column strip and nine column raft

The influence of the area ratio and column confinement for the different foundation types is compared in Figure 5.6 for end bearing columns of length 14.5 m. The area ratio can be clearly shown to have an influence on the settlement performance. As the area ratio increases the improvement factor reduces. The confinement offered by different group configurations for a small raft and strip foundation offers a larger decrease in settlement which is observed as an increase in settlement improvement

factor. The highest benefit due to confinement is observed for low area ratios (Figure 5.6).

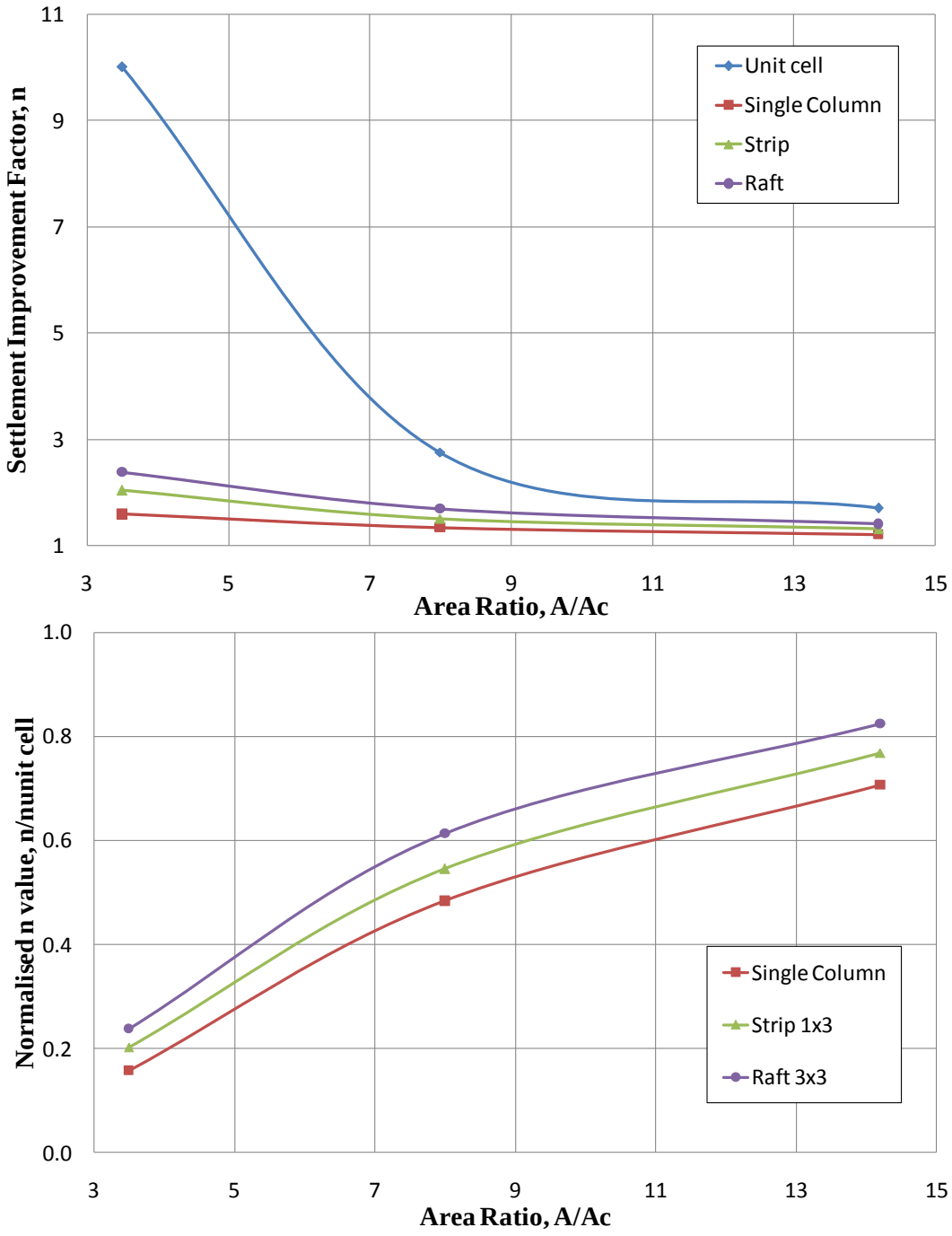

Figure 5.6 Influence of area ratio and column confinement on end bearing stone columns for (a) settlement improvement factor, n, and (b) normalised n values

5.3.3 Influence of column strength

Stone columns are composed of granular material which is compacted *in-situ* by the Vibroflot with the friction angle providing the shearing resistance. The influence of the friction angle on column strength is assessed for a single column, three column strip and nine column raft for friction angles (FA) in the range of 38° to 50° (Figure 5.7). Increasing the column length regardless of foundation configuration and friction angle has the effect of reducing the settlement. The influence of the friction angle on foundation performance was found to be less significant for a single column with an end bearing improvement factor of 1.59 for column friction angles of 44° and 50°. This is because the column is limited by the lack of restraint provided by the soil or another column. The settlement reduces and the settlement improvement factor increases with increasing friction angle for the raft and strip. Above a depth of 3.6 m, which is equivalent to a length to diameter ratio of 6, the effect of friction angle is not apparent. Beyond a column length of 3.6 m the reduction in settlement becomes significant for both raft and strip with the largest reductions in settlement observed for the raft foundation. The columns within the nine column raft foundation benefit from mutual restraint in the inward facing directions compared to the strip which is only partially restrained by other columns. The highest improvement factors are observed for end-bearing columns due to the transfer of stress to depth and are summarised in Table 5.1. It can be seen that an increase in column friction angle has the largest effect on the nine column raft as the columns benefit from mutual restraint.

Column Friction Angle (°)	Settlement Improvement Factor			Settlement % reduction		
	Single Column	3 Column Strip	9 Column Raft	Single Column	3 Column Strip	9 Column Raft
38°	1.57	1.68	1.77	-	-	-
44°	1.59	2.03	2.38	1.3	20.8	34.5
50°	1.59	2.08	3.20	1.3	23.8	80.8

Table 5.1 Influence of friction angle on end-bearing settlement improvement factors

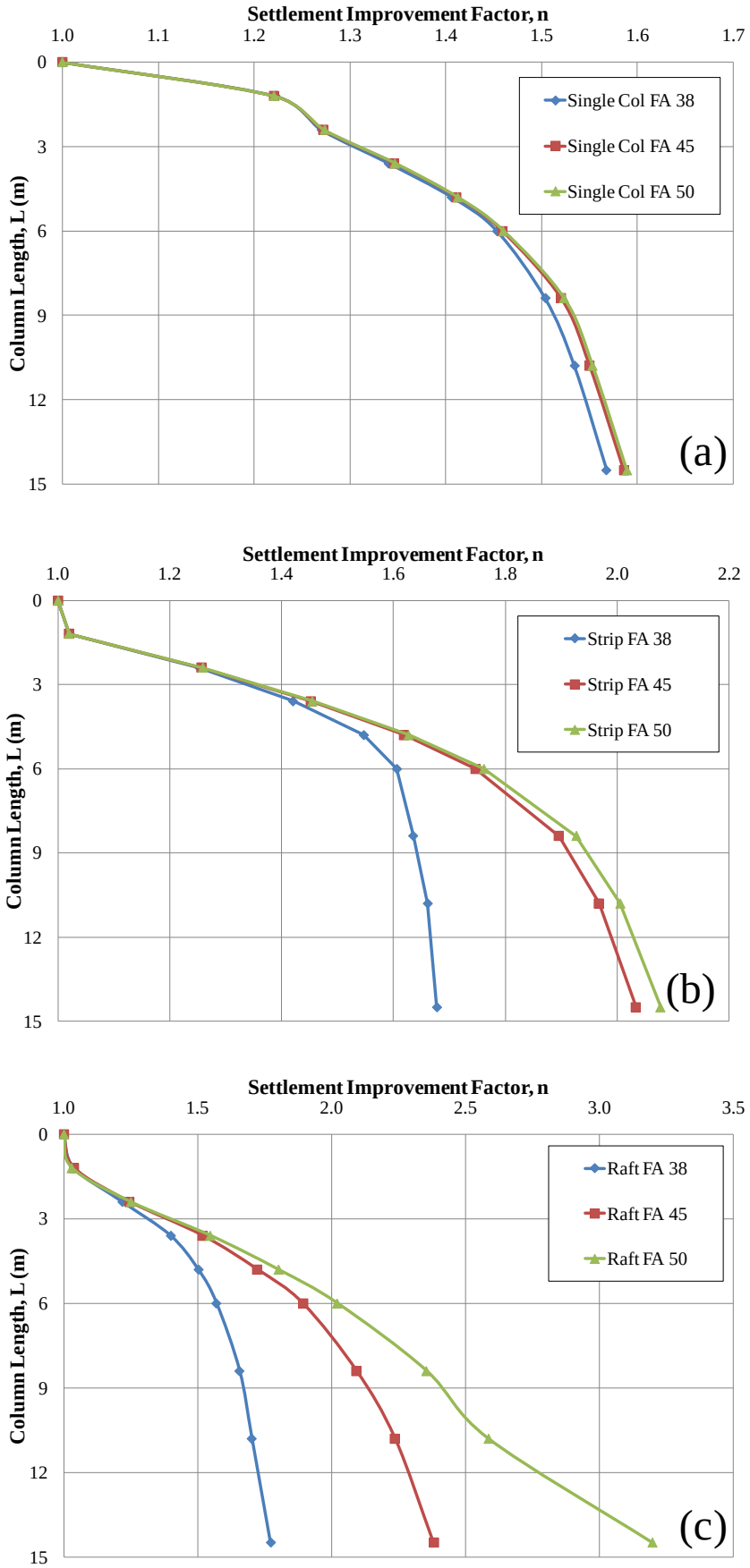

Figure 5.7 Influence of column strength on settlement improvement factor

5.3.4 Influence of column compressibility

The influence of column compressibility on settlement was assessed using column stiffness values between 30 - 70 MPa for three foundation types (Figure 5.8). The settlement improvement factor increased as the stiffness increased for all three foundation types. The largest increases in improvement factor were observed for a single column foundation and the lowest for the nine column raft. The increase in column stiffness allows a higher proportion of the stress to be carried by the columns rather than the soil. The distribution of plastic points is shown in cross section for strip and raft foundations (Figure 5.9). The Mohr-Coulomb plastic points represent elements in a plastic stress state i.e. those points which lie on the Mohr-Coulomb failure line. The extent to which columns develop plastic points reduces for the increasing number of columns. This is because the more restraint a column receives the more load it is able to absorb. The increase in settlement improvement factor with increasing column stiffness for end-bearing stone columns is summarised in Table 5.2 which suggests that the largest reductions are observed for single column foundations.

Column Stiffness (MPa)	Settlement Improvement Factor			Settlement % reduction		
	Single Column	3 Column Strip	9 Column Raft	Single Column	3 Column Strip	9 Column Raft
30	1.29	1.63	1.91	-	-	-
50	1.45	1.81	2.21	12.4	11.0	15.7
70	1.59	2.03	2.38	23.3	24.5	24.6

Table 5.2 Influence of column stiffness on end-bearing settlement improvement factors

5.3.5 Influence of stiff crust thickness

The influence of the stiff crust on settlement performance is examined for a single column, three column strip and a 3x3 nine column raft configuration. Three defined soil profiles (Figure 5.3) were examined. Profile 1 represents a stiff crust of 0.5 m thickness which allows for a foundation to be founded on the Upper Carse clay thereby bypassing the stiff crust. Profile 2 represents a stiff crust of 1.0 m thickness which is the standard profile used in this research. Profile 3 represents a stiff crust of 1.5 m thickness. The underlying Carse clay in all three profiles is 1 m thick and the lower Carse clay varies between 13.5 m, 13.0 m and 12.5 m for profiles 1 to 3 respectively.

The influence of the stiff crust on the settlement improvement factor of a single column, strip and pad foundation for various column lengths is shown in Figure 5.10(a). The settlement of the foundation is highest for the thinnest crust of 0.5 m cases. For the 0.5

m crust cases the greatest effect in reducing settlement for raft and strips is for column lengths of 1.2 m or greater. For 1.0 m and 1.5 m stiff crust stone columns are effective beyond column lengths of 1.2 m and 2.4 m respectively. This is because the stiff crust and upper Carse clay underlying the foundation is already competent and is only marginally improved by stone columns. Interestingly, the settlement reduction response with increasing column length appears to significantly reduce with increasing length beyond 6 m which is equivalent to a length to diameter ratio of 10. McKelvey *et al.* (2004) suggested that between a column length of 6 m to 10 m increasing column length reduces the settlement but beyond this length settlement reduction was minimal. Although the laboratory studies tested homogeneous soil samples it is considered that the same findings apply regardless of the presence of a stiff crust or not.

The settlement improvement factors indicate that the stiff crust thickness has a significant effect on the ability of stone columns to reduce settlement (Figure 5.10b). Below a depth of 2.4 m there appears to the largest increase in improvement factor for raft and strip foundations for crust thickness of 0.5 m. This is because more of the soil is improved to a higher degree by stone columns than for crust thicknesses of 1.0 m and 1.5 m which show a lower increase in improvement factor above 2.4 m because the stiff crust is competent and as such columns have a marginal effect on settlement reduction. The slowing rate of increase in improvement factor for column lengths beyond 6 m for a stiff crust of 0.5m thickness suggests that a critical length may exist for this case. The single columns cases also indicate a reduction in rate below 6.0 m. It is clear however that due to the different crustal thicknesses, its definition is difficult.

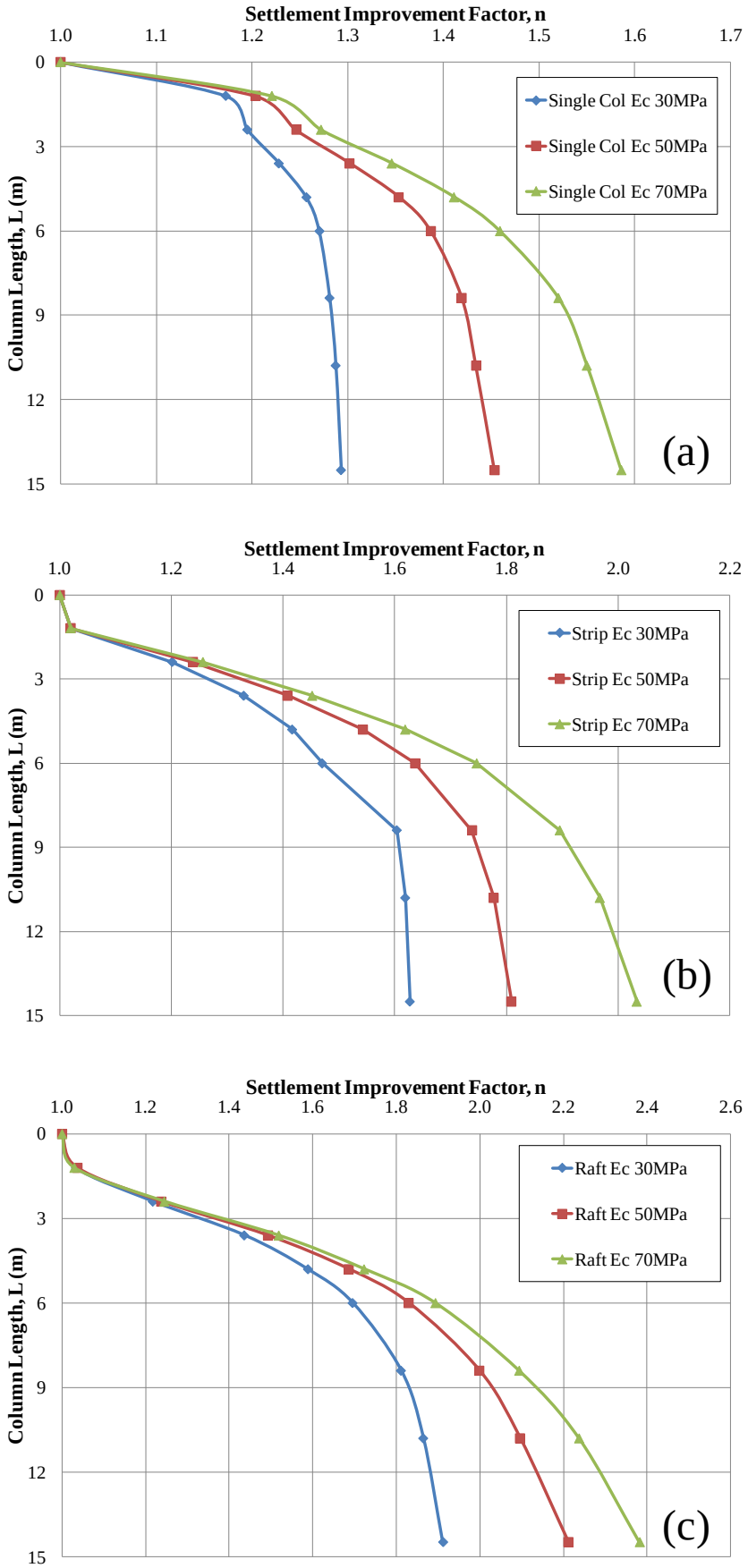

Figure 5.8 Influence of column compressibility on settlement improvement factor

5.3.6 Influence of column installation effects

The installation of stone columns alters the *in-situ* state of the soil such that the coefficient of lateral earth pressure, K_0, increases. The stiff crust and upper Carse clay are much stiffer than the lower Carse clay which appears to benefit the most from the installation of stone columns (Section 5.3.5). The influence of K_0 on the settlement performance was investigated for the lower Carse clay for a single column, three column strip and nine column raft by increasing from 0.75 to 1.00 and 1.25 (Figure 5.11). Increasing the K_0 value enhances the settlement reduction for all foundation configurations. The smallest increase in settlement reduction was observed for a single column with K_0 values of 1.00 and 1.25. The largest increase in settlement reduction was seen for the 9 column raft configuration. The increased coefficient of lateral earth pressure appears to increase the restraint provided by the soil and reduces the bulging potential. Given the raft configuration offers the most restraint to neighbouring columns it would be expected that the columns in such a configuration would benefit most from increased K_0 values. The increase in settlement improvement factors with increasing column stiffness for end-bearing stone columns is summarised in Table 5.3 and suggests that the largest reductions are observed for the nine column raft.

Lateral Earth Pressure	Settlement Improvement Factor			Settlement % reduction		
	Single Column	3 Column Strip	9 Column Raft	Single Column	3 Column Strip	9 Column Raft
0.75	1.59	2.03	2.38	-	-	-
1.00	1.70	2.02	2.72	6.9	-0.5	34.0
1.25	1.70	1.99	2.69	6.9	-2.0	32.5

Table 5.3 Influence of the coefficient of lateral earth pressure on end bearing settlement improvement factors

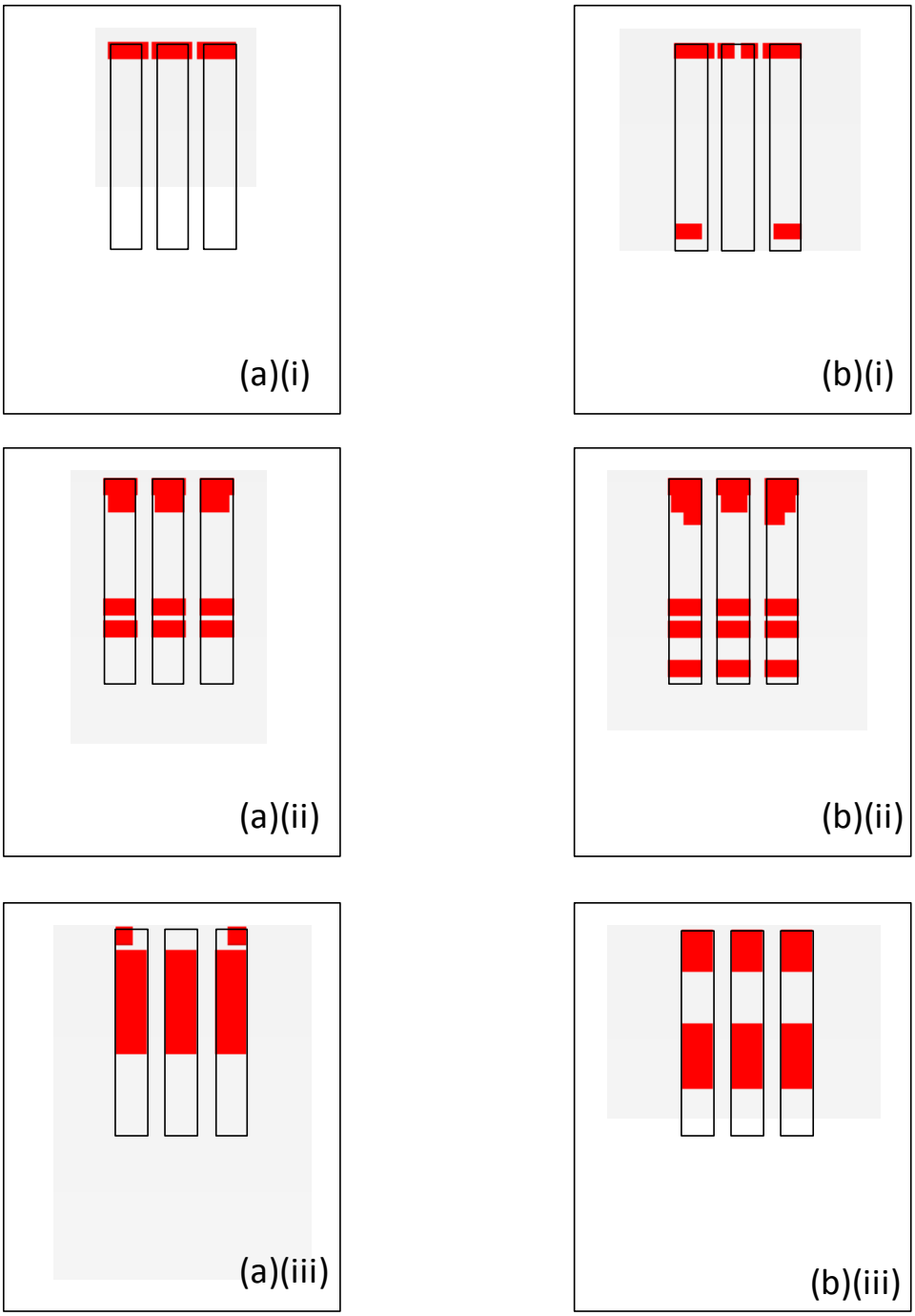

Figure 5.9 Distribution of plastic points for a (a) three column strip and (b) nine column raft with area replacement ratio (i) 3.5, (ii) 8.0 and (iii) 14.5 for column length 6 m and stiffness Ec 70 Mpa

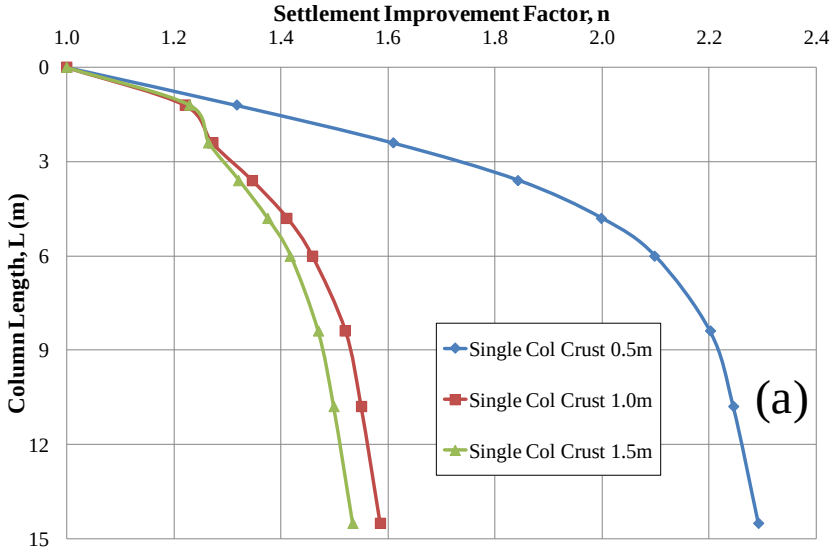

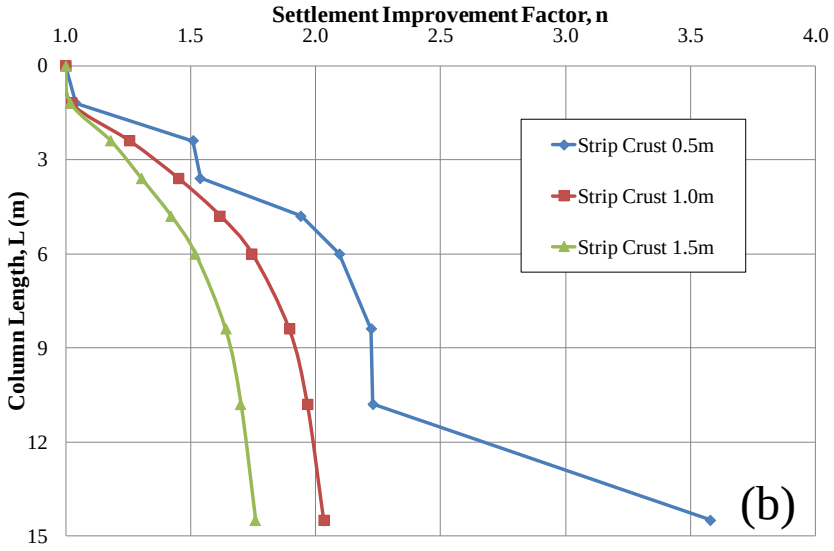

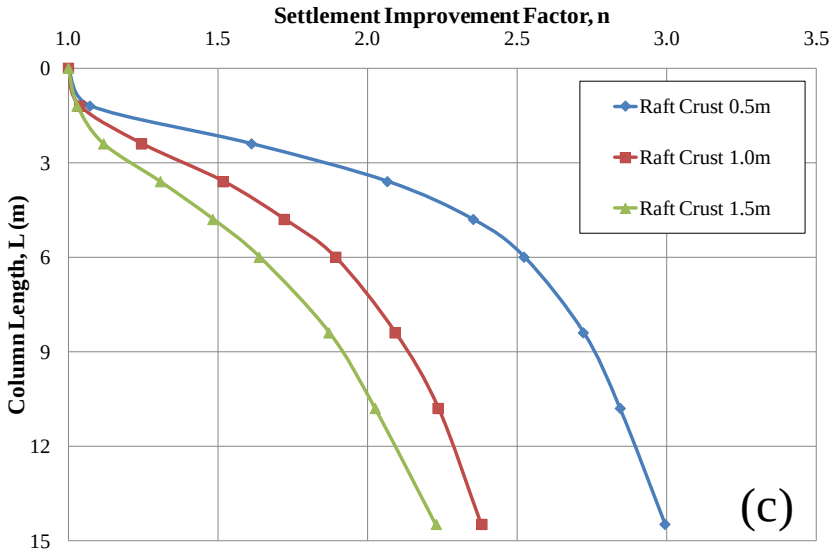

Figure 5.10 Influence of stiff crust on settlement improvement factor

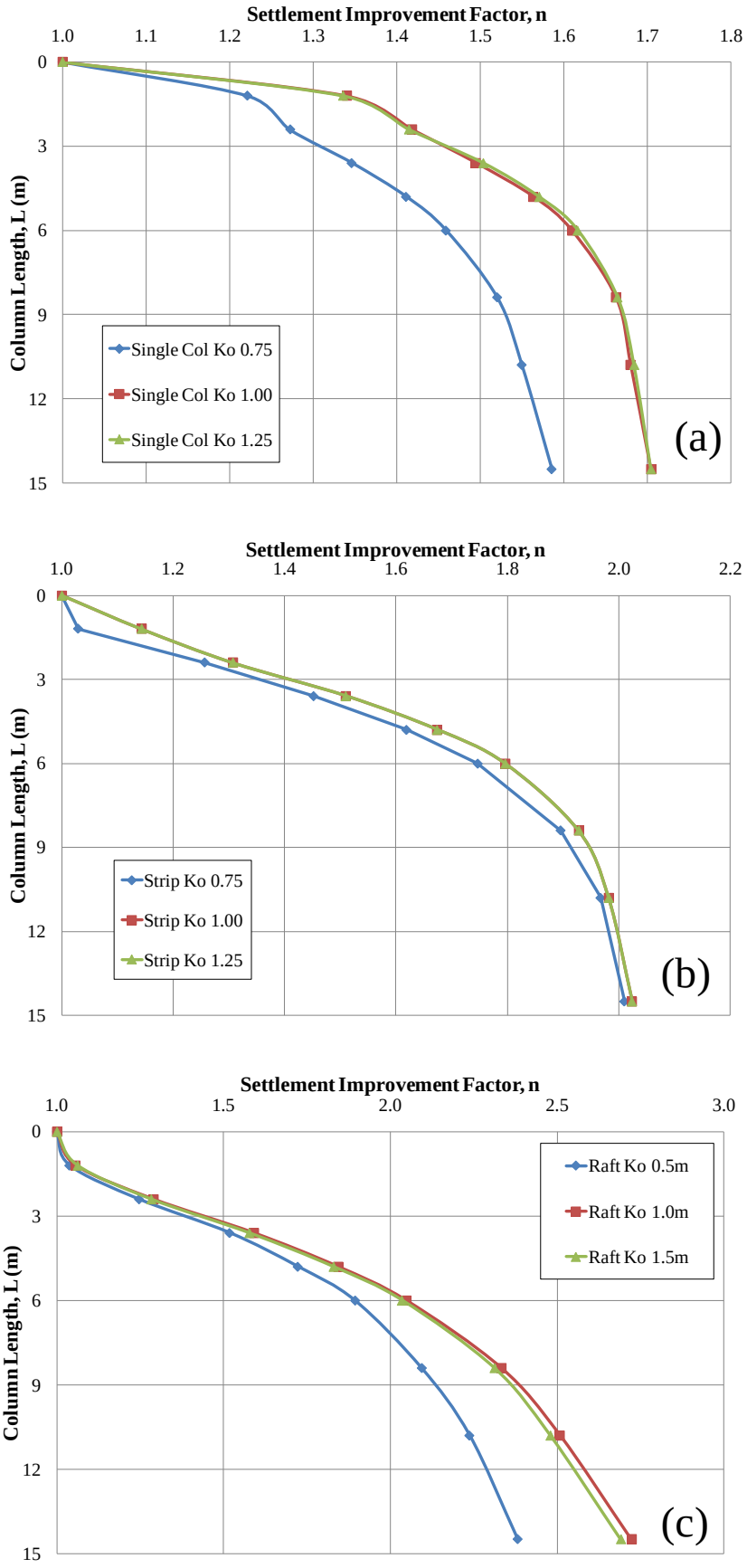

Figure 5.11 Influence of column installation effects on settlement improvement factor

5.4 Settlement inferred deformation ratios

This research focuses on the deformational behaviour of stone columns installed in soft clay. Muir-Wood *et al.* (2000) and McKelvey *et al.* (2004) identified four main modes of deformation which are considered to cause excessive settlements. These four main modes of deformation include bending, bulging, punching and shearing. Black (2007) suggested that columns can suffer from excessive settlements known as 'block failure' which occurs when the columns and soil excessively settle together. This block failure is a type of punching failure. Killeen (2012) suggested a methodology using the settlement of the columns, soil and foundation to calculate a punching and compression ratio for small groups of stone columns. In this thesis an assessment is made of the effect of column confinement using pad, strip and small rafts to assess what impact different configurations and column confinement have on column deformation. The methodology of Killeen (2012) is therefore applied in this section.

Definition of the punching ratio

The length of stone column has been shown by Hu (1995), Muir-Wood *et al.* (2000) and McKelvey *et al.* (2004) to influence the mode of deformation which occurs during foundation loading. An assessment is made of the tendency of a column to experience punching as a result of loading using the method of Killeen (2012):

$$Punching\ ratio,\ P_r = \frac{U_{col} - U_{soil}}{U_{footing}} \tag{5.1}$$

where U_{col} = displacement at the base of columns

U_{soil} = average displacement of soil surrounding the base of columns

$U_{footing}$ = displacement of surface footings

The method allows for an assessment to be made of the degree of punching which occurs by comparing the displacement of the base of the column relative to that of the surrounding soil and foundation. In order to calculate the average displacement of the soil surrounding the columns, a 1m diameter zone is defined around the column. Four points within the zone at equal spacing around the column are selected and averaged.

Definition of the compression ratio

The ability of a column to absorb stress during foundation loading is often described as 'stress-share' during which most of the stress is concentrated in the stone column. A columns ability to absorb the stress and transfer it to depth is often associated with its length. The compression ratio, as defined by Killeen (2012), describes the proportion of surface settlement transferred to the column base. The ratio (as proposed) does not discriminate between axial and radial deformation. Radial deformation due to bulging can be observed as a rapid increase in compression ratio. Axial deformation by contrast can be identified by a steady increase in compression ratio.

$$Compression\ ratio,\ C_r = \frac{U_{footing} - U_{col}}{U_{footing}} \tag{5.2}$$

where U_{col} = displacement at the base of columns

$U_{footing}$ = displacement of surface footings

5.4.1 Deformation ratios of an infinite array of stone columns

The influence of area ratio and column length on the punching ratio is shown in Figure 5.12(a). The punching ratio was found to increase with increasing area ratio. It can be observed that for column lengths of less than 2.4 m the punching ratio is negligible regardless of area ratio. This is due to the presence of the stiff crust and upper Carse clay which resists punching due to their competent nature. For a column length of 2.4 m the highest value of punching ratio for all area ratios is observed just below the base of the upper Carse clay with the column base founded in the lower Carse clay. The stiff clay and upper Carse clay are 2 m thick with the underlying lower Carse clay being less competent and able to resist punching from the column. It can be observed from Figure 5.12 (b) that the low compression ratios for columns of length 2.4 m or less coincides with the increase in punching ratio which suggests that short columns are not deforming along their length and that punching is the dominant mode of deformation.

The columns with the lowest area ratio of 3.5 were found to have the lowest punching ratios. The plots of shear strain for an infinite array shown later in Figure 5.19 suggest that the columns and soil "punch" as a single body into the underlying soil in what Black (2007) terms 'block' failure. It occurs when columns are closely spaced and is characterised by low values for both punching and compression ratios. The column and soil deform together when closely spaced hence the low values of punching ratio. The

results are comparable to Black (2007) who used area ratios of 2.5 and 3.6. As the area ratio increases the amount of load carried by the soil reduces and is transferred to the column which acts more independently and can be observed in higher punching ratios. It is suggested that at low area ratios of 3.5, columns do not deform along their length, rather block failure occurs and is the dominant mode of failure. The punching ratio is consistent for columns of length 4.8 m or longer which coincides with an increase in compression ratio. For longer columns this represents a change in mode of deformation to deformation-along-length which occurs as bulging failure in the upper regions of the column. Bulging leads to a loss of stress transfer to the base of the column which is expressed as a punching ratio of zero for end bearing columns.

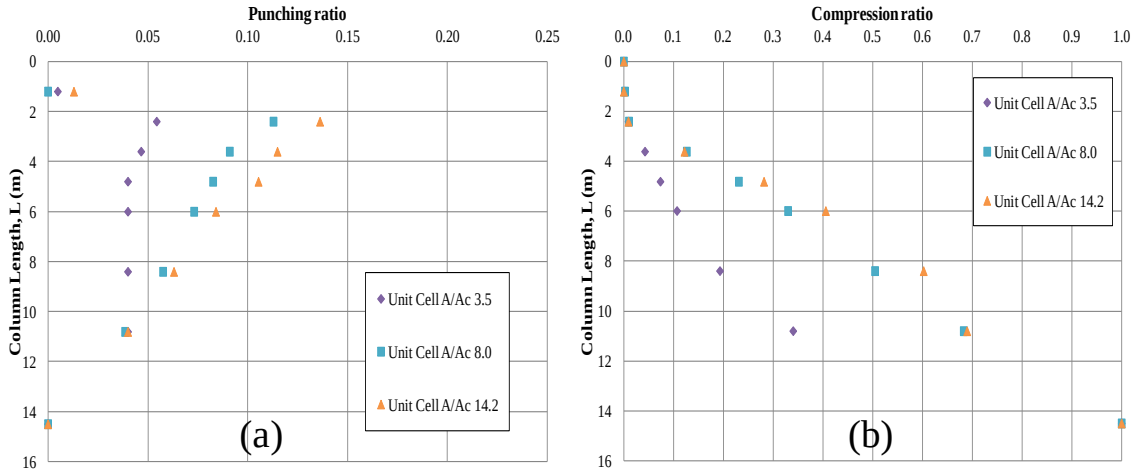

Figure 5.12 Punching and compressibility ratios for a unit cell for area ratios of 3.5, 8 and 14.2

5.4.2 Deformation ratios of a single stone column

The influence of area ratio and column length on the punching ratio for a single column is shown in Figure 5.13(a)(i). It can be seen that punching ratios increase with column length up to a maximum at a column length of 3.6m. In contrast the unit cell maximum punching ratio is observed at 2.4m. The area ratio influences the degree of punching ratio which appears to be at its highest for area ratios of 14.2 and lowest for area ratios of 3.5 for columns with length greater than of 3.6 m. For columns with a length less than 3.6 m, there does not appear to be a clear relationship. The reduced punching ratios are due to the effects of the stiff crust which resists punching. The increase observed in punching ratio is coupled with a low compressibility ratio as shown in Figure 5.13(b)(i). It appears that punching is the dominant mode of deformation for short stone columns which would be expected to develop shear stress and end bearing pressures at the base and along column length. Increased area ratio leads to a wider

width of pad foundation which will increase the applied stress from the foundation. This increased stress will be preferentially adsorbed by the column leading to a higher degree of punching and shear stress for higher area ratios. For single columns which are longer than 3.6 m the punching ratio reduces (Figure 5.13(a)(i)) as the compression ratio increases (Figure 5.13(b)(ii)). It suggests that columns are deforming along their length and that bulging is the dominant mode of deformation. The punching ratio reduces and compression ratio increases with increasing area ratio which was also observed for the unit cell cases. It is suggested that column bulging becomes more dominant with increasing area ratio.

5.4.3 Deformation ratios of stone columns beneath a strip foundation

The variation in punching ratio for the central column with column length for a 1x3 group of stone columns beneath a strip foundation is shown in Figure 5.13(a-ii). Punching ratios increase with length up to a maximum of 3.6 m which is similar to the results for a single column and raft. In a strip configuration the centre column is bounded by the two corner columns. It is suggested that for an area replacement ratio of 3.5 (Figure 5.14(a-i)) that the confinement pushes the highest punching ratio to a depth of 3.6m. The increase in punching ratios is coupled with low compression ratios, as shown in Figures 5.13(a-iii) and Figures 5.13(b-iii). This suggests that that columns do not deform along their length but rather they are transferring their load to depth down to the column base. This would imply that punching failure is the dominant mode of deformation for short columns. The increase in punching ratios associated with increasing area ratios is due to the loss in lateral confinement and the increase in applied stress from the foundation carried by the column due to increased column spacing. For columns with a low area ratio of 3.5 it is suggested that the columns are acting as a block with the surrounding soil with increasing column length up to 3.6m length. Beyond this length at higher area ratios of 8.0 and 14.2 columns deform significantly. A reduction in punching ratios and an increase in compression ratios suggest that columns are deforming along their length and are not able to transfer stress to depth leading to bulging failure. The strip foundation appears to have higher punching and lower compression ratios than the raft foundation (Figure 5.13(a-iii)) which is attributed to the higher confinement offered by the 3x3 group of columns compared to the 1x3 arrangement of the strip. The columns beneath the strip foundation are more reliant on the soil for lateral restraint than larger column group.

The variation in punching ratios for individual columns within the 1x3 group is shown in Figure 5.14. For all column lengths and area ratios punching ratios are highest for the centre columns and lowest for the corner columns. The lowest punching ratios occur for the lowest area ratio (Figure 5.14(a-i)) and the highest for the highest area ratios of 14.2 (Figure 5.14(a-iii)). The low punching ratios and associated low compression ratios (Figure 5.14(b)(i)) are considered consistent with 'block failure' which is seen in the shear stress plots in Figures 5.21(a)(i) and 5.21(a)(i) as uniform shear stress within the soil and columns which punch as a block. Columns which are punching transfer shear stress to the surrounding soil which tends to drag the columns downwards. A reduction in punching ratios below 2.4 m and increase in compression ratio is considered evidence for column deformation along length and do not transfer load to the column base observed as shear stress in the upper column for the shear strain plots (Figure 5.21(c)(i)).

5.4.4 Deformation ratios of stone columns beneath a raft foundation

The difference in punching ratio for the central column with length for a 3x3 group of stone columns is shown in Figure 5.13(a-iii). Punching ratios increase with length to a maximum of 3.6 m which was also observed for single columns and strip. This suggests that for the Bothkennar soil profile that punching beyond this depth reduces as column length increases. In a similar manner to the single column and strip sensitivities the increase in punching ratios is coupled with low compression ratios, as shown in Figures 5.13(a-iii) and Figures 5.13(b-iii) which is suggestive of load transfer to the base of the column. This suggests punching failure is dominant deformation mode for short columns.

Increasing area ratios increase the punching ratio due to the loss of lateral confinement and increased applied stress carried by the column due to the increased column spacing. Columns with low area ratios of 3.5 act as a block with the surrounding soil for columns lengths of up to 2.4m. Beyond this length with higher area ratios of 8.0 and 14.2 columns deform independently. A reduction in punching ratio coupled with an increase in compression is suggestive that columns are deforming along their length, unable to transfer stress to depth leading to bulging failure.

Within a 3x3 column group punching ratios for individual columns was found to vary as shown in Figure 5.14. For all column lengths and area ratios the highest punching ratios was observed for the central, followed by the edge and corner columns. This is expected

since the central column benefits from the highest restraint on all sides in comparison to the corner column which is only restrained partly in the inward facing direction.

Columns which had the lowest area ratios (Figure 5.14(a-i)) displayed the lowest punching ratios. By contrast the columns with the highest area ratios (Figure 5.14(a-iii)) suggested the highest punching ratios. The lowest punching ratios coupled with the lowest compression ratios ((Figure 5.14(b)(i)) are considered consistent with 'block failure' which is seen in the shear stress plots in Figures 5.22(a)(i) and 5.22(a)(i) as uniform shear stress within the soil and columns which punch as a block. Punching allows the columns to transfer shear stress to the surrounding soil which tend to drag the columns downwards. Reducing punching ratios and increasing compression ratios below 2.4m is considered evidence for column deformation occurring along length and lack of transfer to the column base observed as shear stress in the upper column for the shear strain plots (Figure 5.22(c)(i)). The change in deformation behaviour from punching to bulging with increasing length and bending outwards of the edge columns has been observed by McKelvey *et al.* (2004) and Black (2007). This behaviour is similarly seen for 1x3 strip configuration.

5.4.5 Influence of column strength on punching and compression ratios

The influence of column strength upon the deformational ratios of punching and compression for a single column, three column strip and nine column raft (see Figure 5.1) is shown in Figure 5.15. It can be seen that for a single column (Figures 5.15(a)(i) and 5.14(b)(i)) that the effect of friction angle is negligible on the compression and punching ratios. For the case of a strip foundation it appears that increasing friction angle reduces the compression ratio for column lengths of 4.8 m or greater. For columns of length less than 4.8 m the effect is minimal for friction angles of 45° and 50°. For a 9 column raft configuration (see Figure 5.14(a)(iii) and 5.14(b)(iii)) the effect of friction angle appears to be significant for columns of 2.4 m or greater with the greatest reduction observed for a friction angle of 50° and the lowest reduction for a friction angle of 38°. The punching ratios for a strip and raft foundation show an increase in compression ratio with increasing friction angle. The highest magnitude of punching ratio is observed for column lengths of 2.4 m with increasing friction angle having the effect of increasing the degree of punching. This suggests that with increased friction angle the column is able to take a greater proportion of the applied load and as such punches to a greater depth.

5.4.6 Influence of column compressibility on punching and compression ratios

The influence of column compressibility upon the deformational ratios of punching and compression for a single column, three column strip and nine column raft (see Figure 5.1) is shown in Figure 5.16. It can be seen that increasing the column stiffness results in an increase in punching ratios and a decrease in compression ratios. It can be seen in Figures 5.16(a)(ii) and 5.16(a)(iii) that the punching ratios for a raft and strip foundation are similar for a stiffness value of 30 MPa, however for stiffness values of 50 MPa and 70 MPa the punching ratios are higher for a strip foundation. This is due to the increased stiffness of the column taking a greater share of the applied stress and transferring the stress to the base of the column causing punching. In a raft configuration the central and edge columns have a greater restraint and as such show a lesser tendency towards punching. The compression ratios for a single column and 3 column strip configuration are relatively similar, however the ratios for a 9 column raft show a greater decrease. This is due to the restraint provided by neighbouring columns which allows the columns to behave in an elastic state and as such show the greatest improvement in terms of compression ratio and settlement factor.

5.4.7 Influence of stiff crust thickness on punching and compression ratios

The punching ratios can be seen to increase with column length up to a maximum length of 2.4 m for a crust thickness of 0.5 m and 2.4 m for a single column (Figure 5.17 (a)(i)), strip (Figure 5.17(a)(ii)) and nine column raft (Figure 5.17(a)(iii)). Punching ratios are lowest for a crust thickness of 1.5m for the case of a single stone column and highest for a crust thickness of 0.5m (Figure 5.16(a)(i)). It is suggested that the thicker the crust the larger the magnitude of punching ratio. It is noted that for the case of the strips the maximum punching ratios occur at a deeper depth of 3.6 m than the single column and raft cases.

The variation in compression ratios with column length is shown in Figure 5.17(b). Above a depth of 2.4 m for the single columns and 3.6 m the influence of crust on the compression ratio is negligible. Below these depths the effect of crust becomes more pronounced. The ratios are lowest for the case of 1.5 m thick crust and highest for a 0.5 m crust for all foundation types.

5.4.8 Influence of column installation effects on punching and compression ratios

The influence of the coefficient of lateral earth pressure upon the deformational ratios of punching and compression for a single column, three column strip and nine column raft (see Figure 5.1) is shown in Figure 5.18. The results suggest that lateral earth pressure has a minimal effect on the compression and punching ratios. For compression ratios an initial increase in compression ratio is observed by increasing the lateral earth pressure from 0.75 to 1.00 for the cases of a single column and strip foundation. The results for values of lateral earth pressure of 1.00 and 1.25 are the same. However, for the case of a raft foundation the effect of lateral earth pressure is negligible for compression ratios. The punching ratios suggest an initial reduction is observed by increasing the lateral earth pressure from 0.75 to 1.00 for the cases of a single column and strip foundation. The results for values of lateral earth pressure of 1.00 and 1.25 are the same. Kirsch (2006) observed that for a group of columns in FEA that column installation effects did not influence the deformational behaviour. This agrees with the cases examined in this research the compression and punching ratios for a nine column raft. The highest values of punching ratio are observed in all cases at 2.4 m which is near to the top of the lower Carse clay which is less competent than the stiff crust and upper Carse clay.

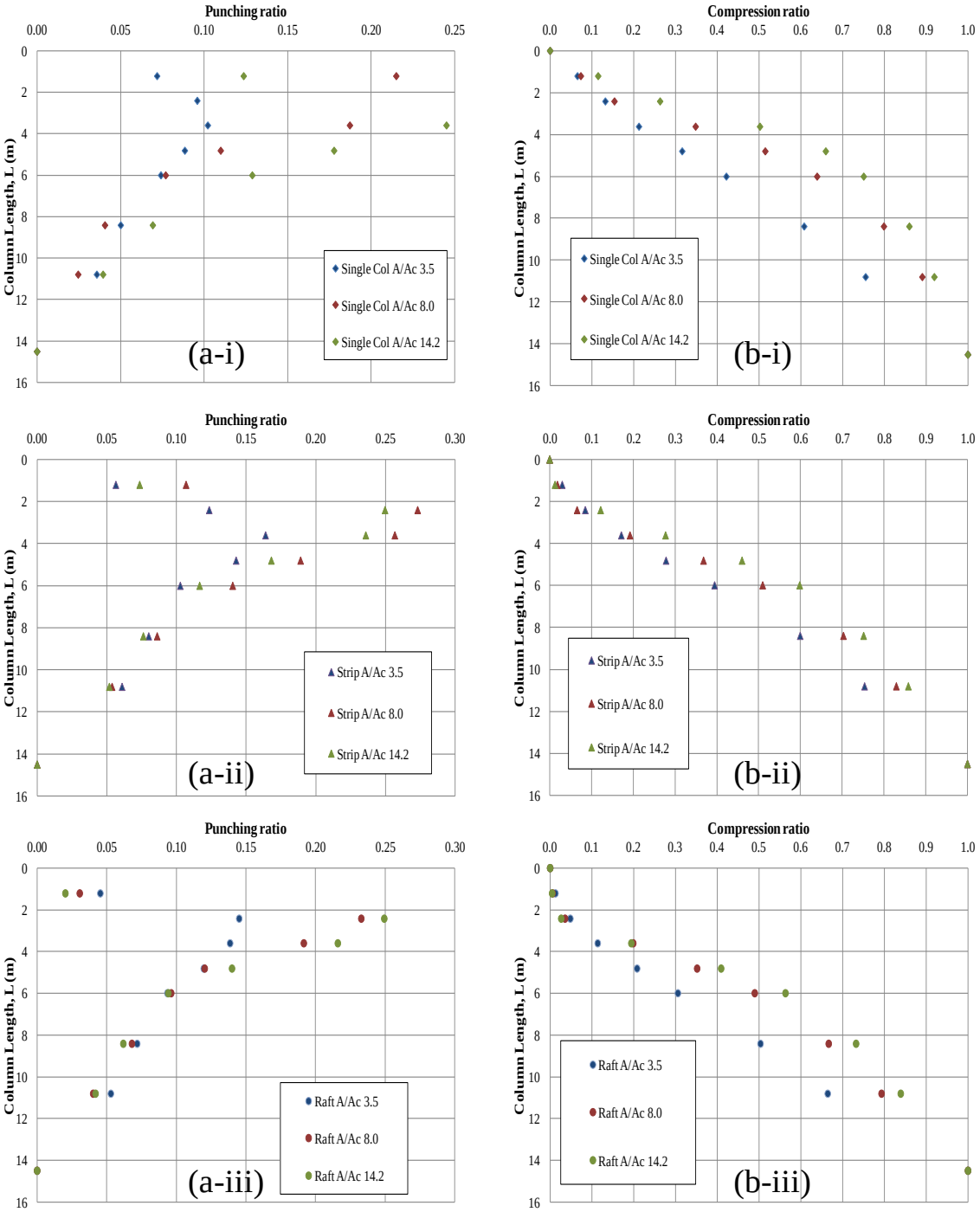

Figure 5.13 Punching (a) and compressibility (b) ratios for single column, 3 column strip and nine column raft for area ratios of (i) 3.5, (ii) 8 and (iii) 14.2

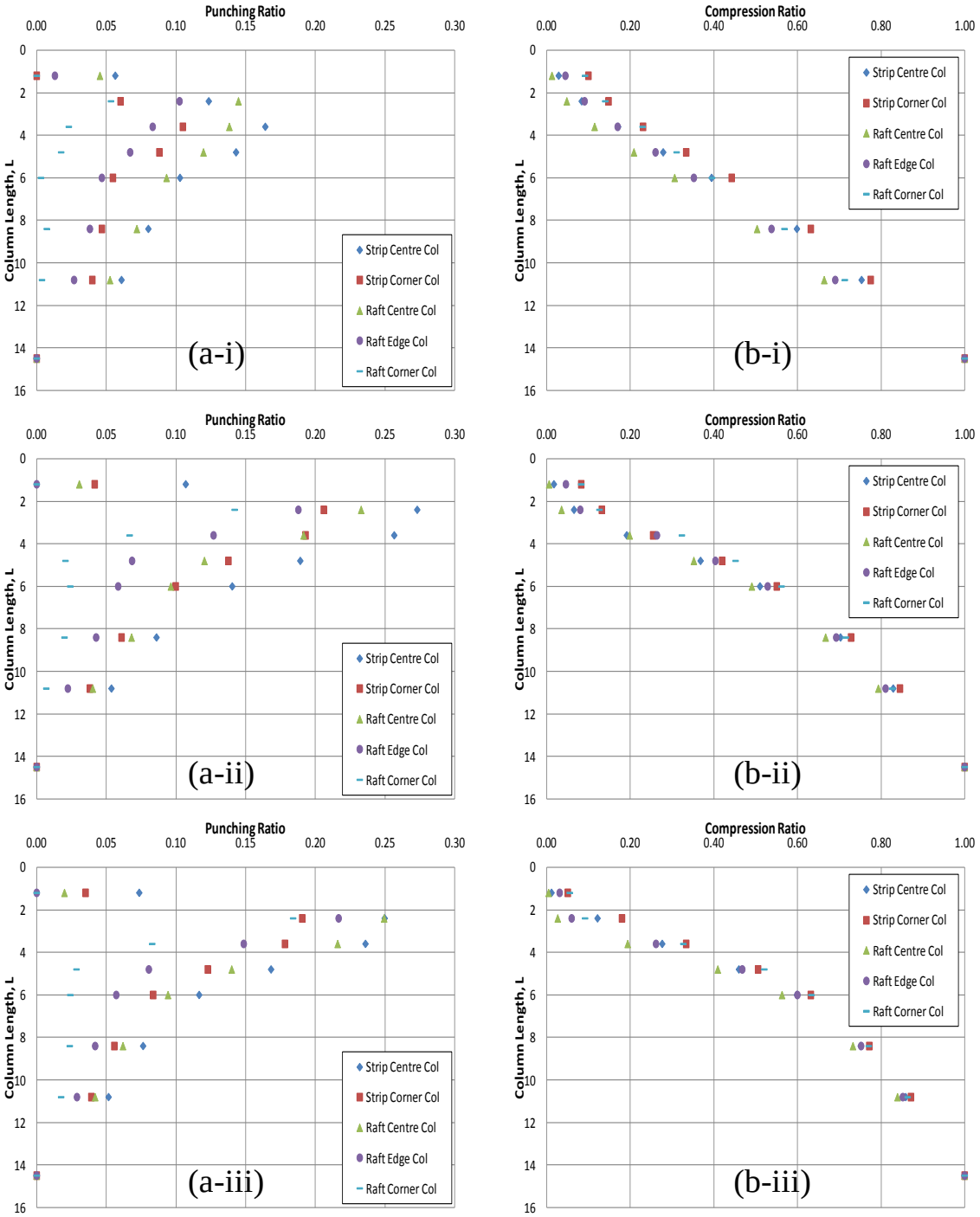

Figure 5.14 Punching (a) and compressibility (b) ratios for a three column strip and nine column raft for central, edge and corner columns area ratios of (i) 3.5, (ii) 8 and (iii) 14.2

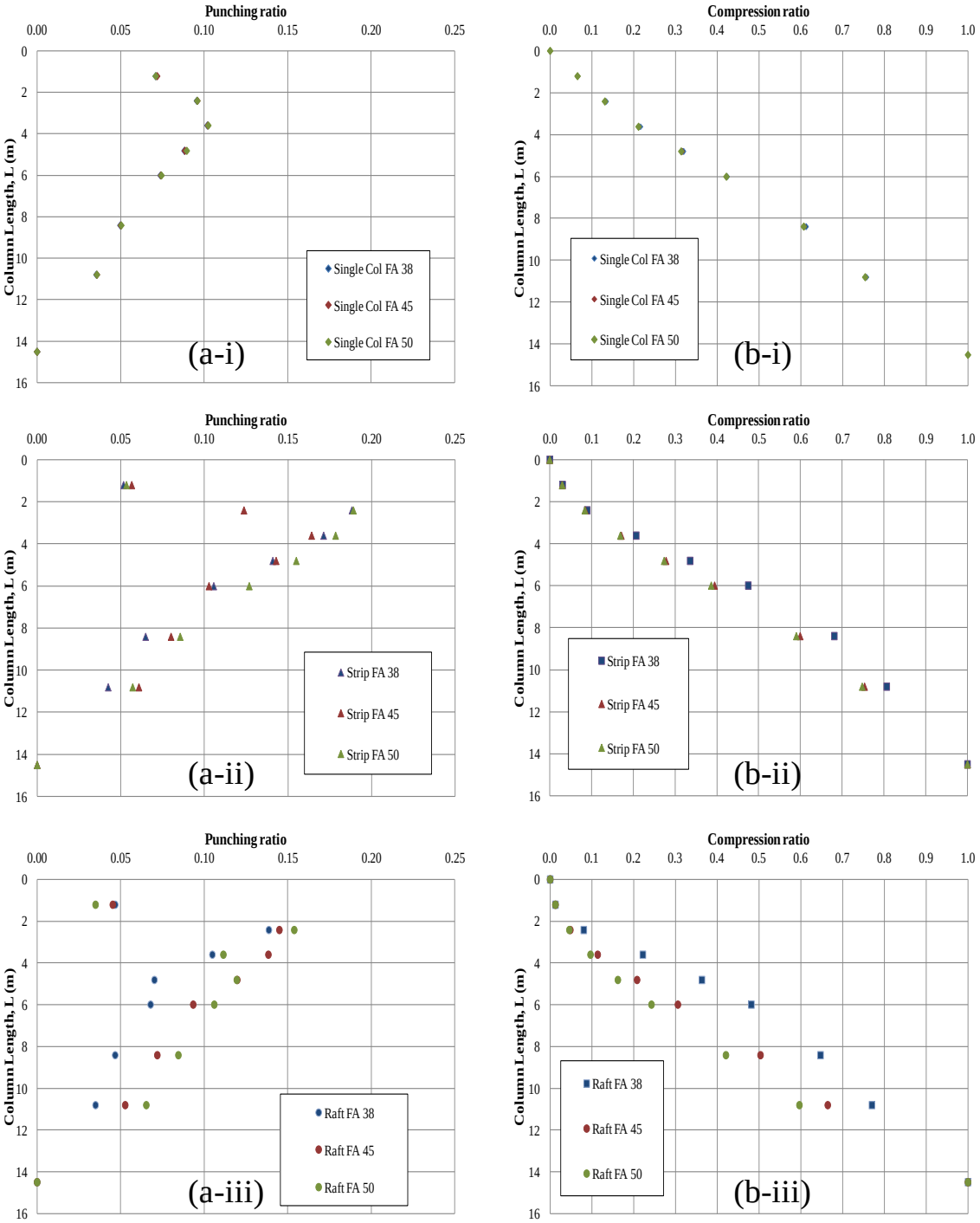

Figure 5.15 Influence of column strength (friction angle) on punching (a) and compressibility (b) ratios for (i) single column, (ii) 3 column strip and (iii) nine column raft

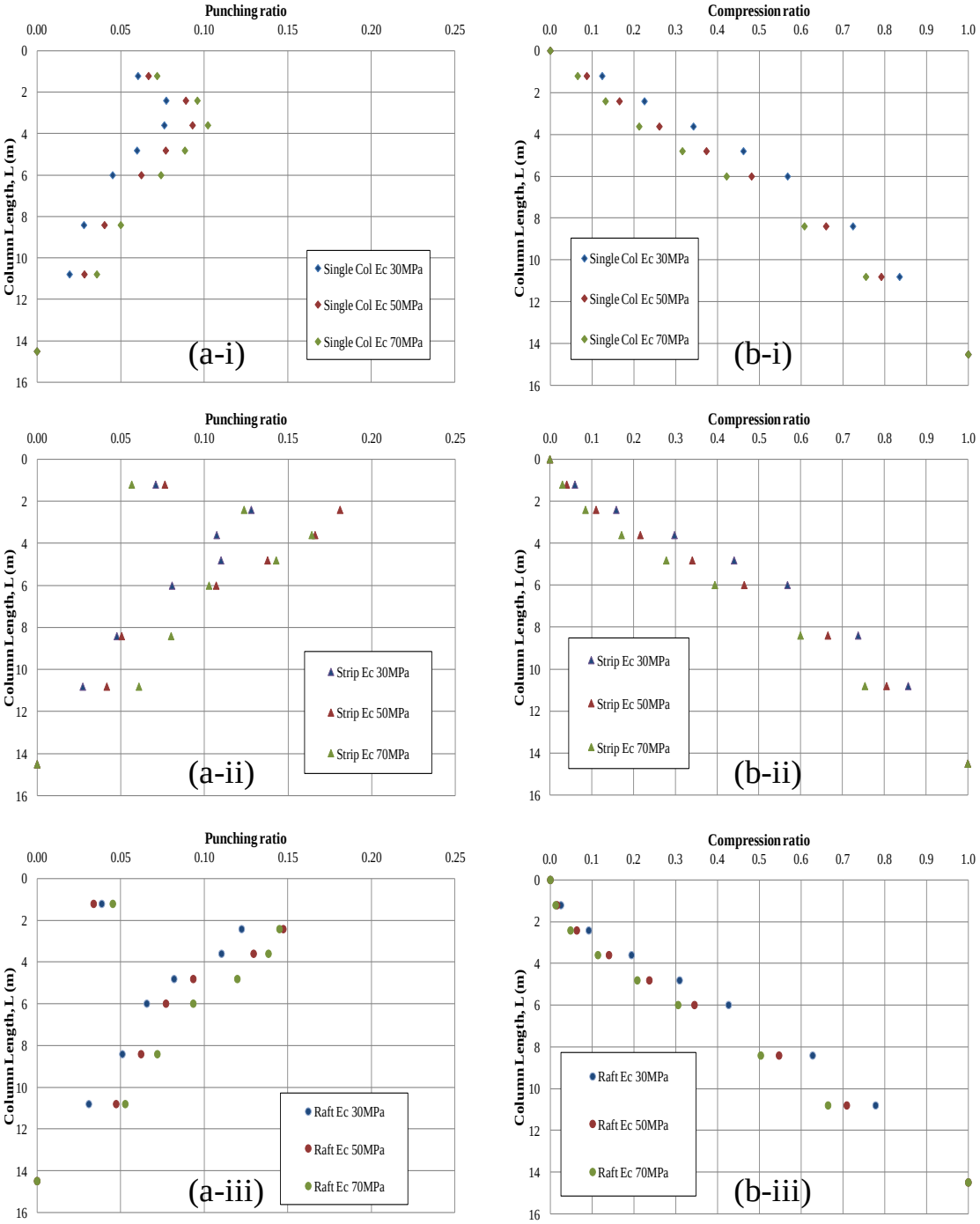

Figure 5.16 Influence of column compressibility on punching (a) and compressibility (b) ratios for (i) single column, (ii) 3 column strip and (iii) nine column raft

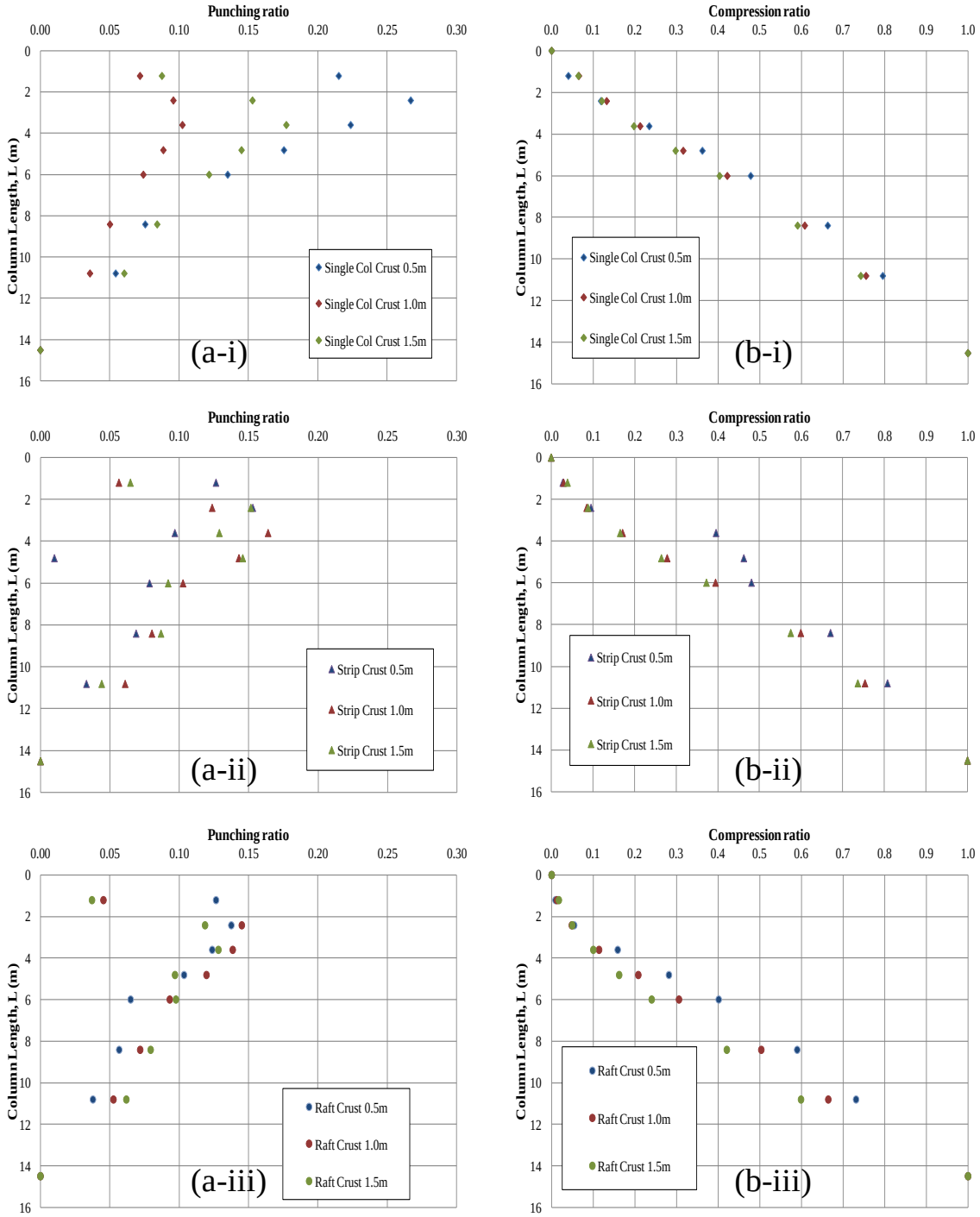

Figure 5.17 Influence of stiff crust thickness on punching (a) and compressibility (b) ratios for (i) single column, (ii) 3 column strip and (iii) nine column raft

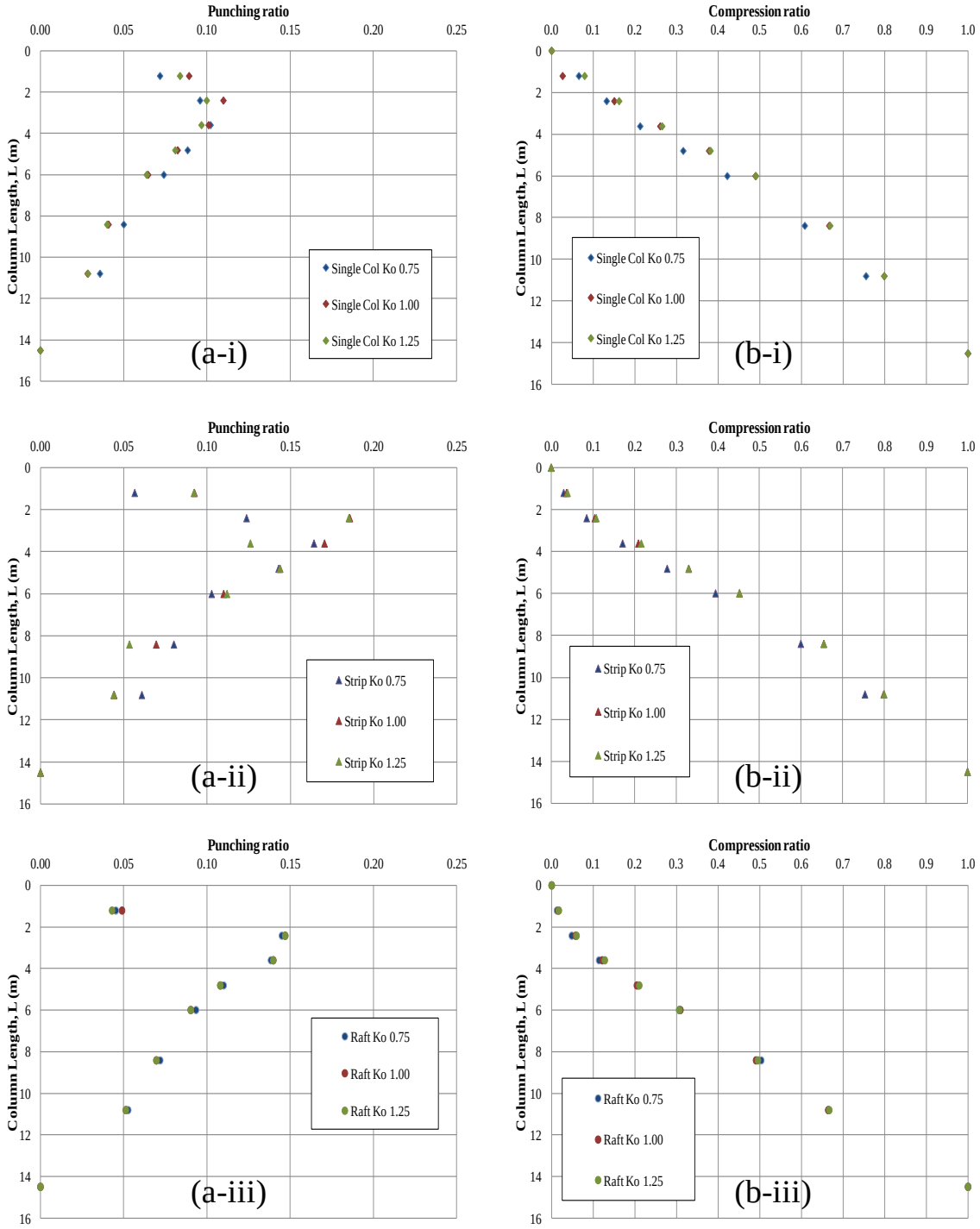

Figure 5.18 Influence of column installation effects on punching (a) and compressibility (b) ratios for (i) single column, (ii) 3 column strip and (iii) nine column raft

5.5 Distribution of shear strains

Three column lengths are selected based upon the findings of the settlement inferred deformation ratios (see Section 5.4) to examine specific modes of deformation and the associated distribution of shear strains: 2.4 m long columns are chosen to investigate punching; 6 m long columns are chosen to investigate the combined failure modes of punching and bulging; and 14.5 m end bearing columns are chosen to investigate bulging failure and since punching does not occur, due to the base of the column being founded on a rigid stratum.

The manner in which stress-share between the column and surrounding soil occurs varies according to the mode of deformation. Bulging columns tend to stress-share by bulging so impart radial stress to the soil. Punching columns tend to stress-share by a combination of end bearing and shear stress. The surrounding soil plays a key role in determining the degree to which stress-share will occur and as a result the settlement performance. The distribution of shear stress within the column and soil is a key indicator of the degree of stress-share.

5.5.1 Shear strains for an infinite array of stone columns

The distribution of shear strain for an infinite array of columns with lengths 2.4, 6.0 and 14.5 m is shown in Figures 5.19(a), 5.19(b) and 5.19(c) respectively. Evidence for punching as the dominant mode of deformation can be observed in Figure 5.19(a) with the majority of shear stress occurring at the base of the column at 2.4 m depth. The uniform distribution of the shear stress in Figure 5.19(a)(i), bridging from the edge of the unit cell across the base of the column to the other edge of the unit cell at low area ratio of 3.5, suggests behaviour which is consistent with block failure as described by Black (2007). With increasing area ratio in Figures 5.19(a)(ii-iii) it can be observed that column punching becomes more focused on the column as it takes more of the stress.

For 6 m long floating columns the mode of deformation can be observed in Figure 5.19(b) as a combination of punching and bulging modes of deformation. It can be seen in Figure 5.19(b)(i) that bulging is evident in the upper column just below the base of the Upper Carse clay in the lower Carse clay but the strain occurs laterally. Shear strain occurs to a lesser extent at the base of the column but is uniform in distribution across the column and soil which suggests behaviour associated with block failure at low area ratios. For increased area ratios of 8.0 and 14.2 a change in the mode of deformation is

evident in Figures 5.19(b)(ii) and 5.19(b)(iii). Bulging failure is evident in the upper region of the column just below the base of the upper Carse clay in the less competent lower Carse clay. As the area ratio increases the distribution of shear strain within the column increases due to the loss of lateral confinement and the increased applied stress adsorbed by the column with increased column spacing.

For a 14.5 m long end bearing column resting on a rigid stratum no punching failure can occur. Bulging occurs for all area ratios below the upper Carse clay in the less competent lower Carse clay. The increase in the distribution of shear strain associated with increased area ratio is due to the loss of lateral confinement and increased applied stress adsorbed by the column.

5.5.2 Shear strains for a single stone column

The distribution of shear strains for single columns with lengths 2.4, 6 and 14.5 m is shown in Figures 5.20(a), 5.20(b) and 5.20(c) respectively. It can be observed that for a column length of 2.4 m the development of shear strain within and beneath the column is relatively low. This is due to the development of localised shear zones as a result of the displacement continuity between the small pad foundation and soil near the surface. A small degree of straining is observed at the base of the column.

The distribution of shear strain for 6 m floating columns is shown in Figure 5.20(b). It can be observed that for a low area ratio that the strain between column and soil is negligible. For area ratios of 8.0 and 14.2, Figures 5.20(b)(ii) and 5.20(b)(iii), the shear strain can be observed to develop along the side and base of the column. This suggests that for an area ratio of 8.0 that bulging is the dominant mode of deformation compared to an area ratio of 14.2 which indicates that both bulging and punching failure are significant.

The distribution of shear strain for a 14.5 m end bearing stone column is shown in Figure 5.20(c) and it can be observed that bulging failure does not occur at a low area ratio of 3.5. With increasing area ratios of 8.0 and 14.2, Figures 5.20(b)(ii) and 5.20(b)(iii) shear strain can be observed to develop as bulging deformation near the top of the lower Carse clay.

5.5.3 Shear strains for three column strip of stone columns

The distribution of shear strain for a 1x3 group of columns at lengths of 2.4, 6 and 14.5 m is shown in Figures 5.21(a), 5.21(b) and 5.21(c). It can be seen that the majority of shear strain develops beneath the base of columns in Figure 5.21(a) which indicates that punching is the dominant mode of deformation for 2.4 m columns. As the area ratio increases punching becomes more localised within columns which behave individually for ratios of 8.0 and 14.2 in Figures 5.21(a)(ii) and 5.21(a)(iii). The uniformity of shear strain beneath the columns and surrounding soil suggests that for an area ratio of 3.5 (Figure 5.21(a)(i)) that block failure is occurring.

The distribution of shear strain for 6 m floating columns is shown in Figure 5.21(b). The uniformity of shear strain for an area ratio of 3.5 (Figure 5.21(b)(i)) suggests that block failure associated with punching is occurring with no evidence of bulging observed. As the area ratio increases the mode of deformation becomes dominated by bulging failure for ratios of 8.0 and 14.2 in Figures 5.21(b)(ii) and 5.21(b)(iii) respectively. Some punching is evident for a ratio of 8.0 but disappears for a ratio of 14.2. It is clear that as the ratio increases the columns are taking a greater proportion of the applied stress and in doing so are subject to greater shear stress. The bulging zone is associated with the top of the lower Carse clay just below the upper Carse clay which is the least competent depth in the soil profile.

The distribution of shear strain for 14.5 m end bearing stone columns is shown in Figure 5.21(c). It can be seen that no bulging failure occurs at a low area ratio of 3.5 (Figure 5.21(c)(i)). With increasing area ratios of 8.0 and 14.2, Figures 5.21(c)(ii) and 5.21(c)(iii), the shear strain can be observed to develop as bulging deformation near the top of the lower Carse clay. A minor increase in depth of bulging is observed for the central columns for these area ratios. This effect is associated with the mobilisation of the passive resistance of the soil which is bounded by the central and edge columns. Partial confinement is observed for the inward facing directions which forces bulging slightly deeper for the central column. Bulging for the edge columns will occur at shallower depth near the top of the lower Carse clay and will bulge more in the unrestrained directions (outward facing).

5.5.4 Shear strains for nine column raft of stone columns

The distribution of shear strain within a 3x3 group of stone columns arranged in a square grid configuration of equally spaced stone columns of lengths 2.4, 6 and 14.5 m shown in Figure 5.22(a), 5.22(b) and 5.22(c) respectively. It can be seen in Figure 5.22(a)(i) that for a low area ratio of 3.5 that the column and soil strain equally, with the magnitude of shear strain low beneath the columns. It is suggested that the columns are acting in block failure due to the uniformity of the strain between column and soil. Development of localised shear zones as at the edge of the foundation results in a displacement continuity between the small pad foundation and soil near surface which is less evident with increasing area ratio. As the area ratio increases from 8.0 to 14.2 it can be seen in Figures 5.22(a)(ii) and 5.22(a)(iii) that punching occurs beneath the base of the columns. As the area ratio increases the punching becomes more localised and the columns behave more individually.

The distribution of shear strain for 6 m floating columns is shown in Figure 5.22(b). Punching failure is evident for all area ratios with bulging failure identified as the dominant mode of deformation. Bulging occurs below the base of the upper Carse Clay near the interface with the lower Carse clay. The fact that bulging occurs at this depth suggests that the columns are efficient in transferring the applied stress from the foundation to depth bypassing the stiffer crust and upper Carse clay. The uniformity of stress concentration within the columns and soil at a low ratio of 3.5 (Figure 5.22(b)(i)) suggests a degree of block failure is occurring. As the area ratio increases from 8.0 to 14.2 it can be seen in Figures 5.22(b)(ii) and 5.22(b)(iii) that columns at higher ratios tend to bulge and act more independently. The bulging zone becomes more evident with increased area ratio.

For a 14.5 m long end bearing columns resting on a rigid stratum no punching failure can occur. Bulging occurs for all area ratios below the upper Carse clay in the less competent lower Carse clay. The magnitude of shear stress within the column is higher than that observed for a single column or strip foundation but lower than that of the unit cell. While the lowest area ratio columns of 3.5 (Figure 5.22(c)(i)) show a uniform depth of shear strain, with increased area ratio of 8.0 and 14.2, it can be seen in Figures 5.22(c)(ii) and 5.22(c)(iii) that the central column tends to bulge slightly deeper than the external columns. This is typical of groups of stone columns were an effect associated with mobilising of the passive resistance of the soil occurs when columns are bounded

by the central and external column. This in turn increases the lateral resistance while enhancing the confinement and also forces the bulging deeper. Bulging for the external columns however occurs at the shallower depth near the top of the lower Carse clay which bulge outwardly due to the lack of confinement.

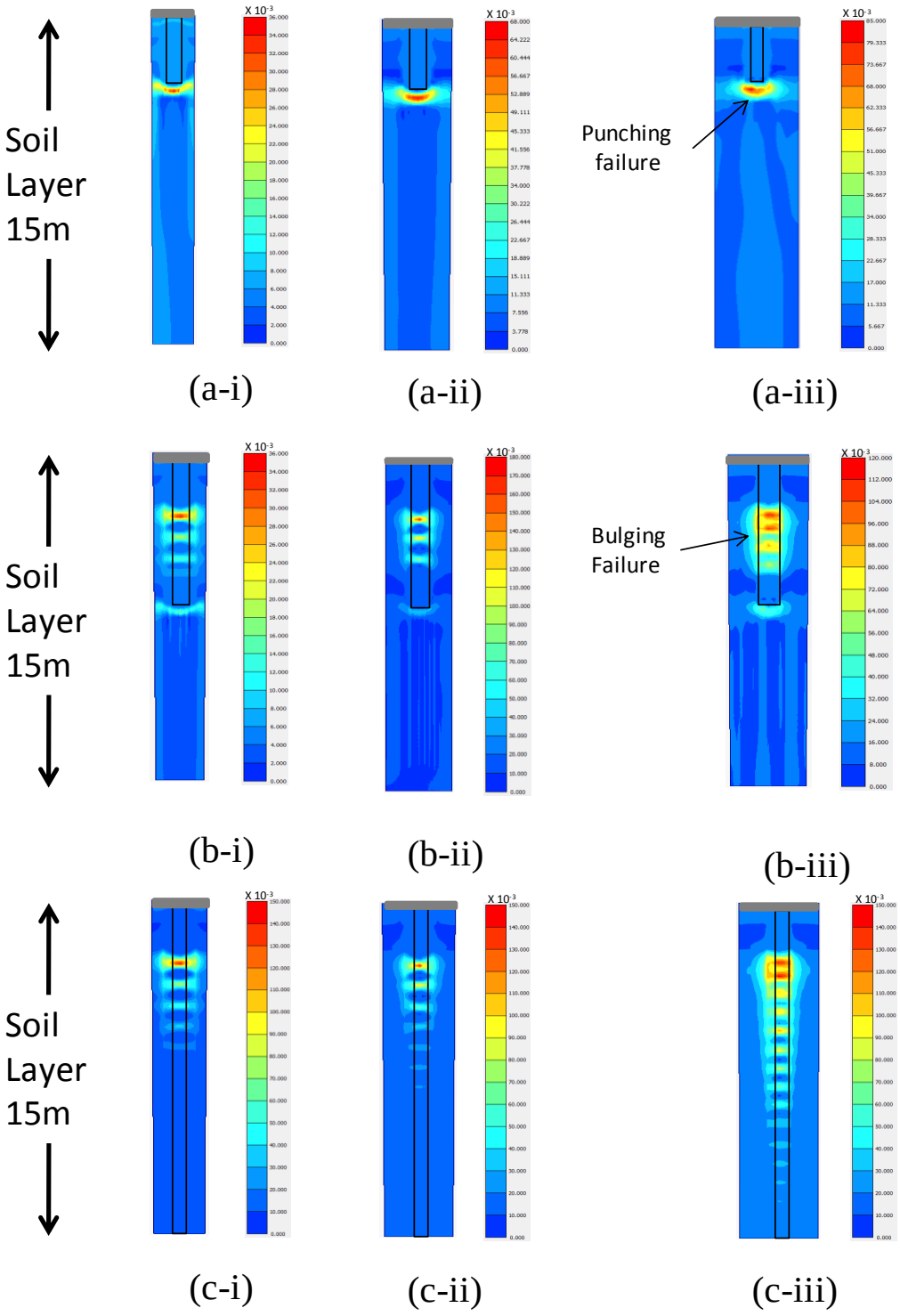

Figure 5.19 Shear strains for an infinite grid of stone columns with length (a) 2.4m, (b) 6.0m and (c) 14.5 and area ratios (i) 3.5, (ii) 8.0 and (iii) 14.2

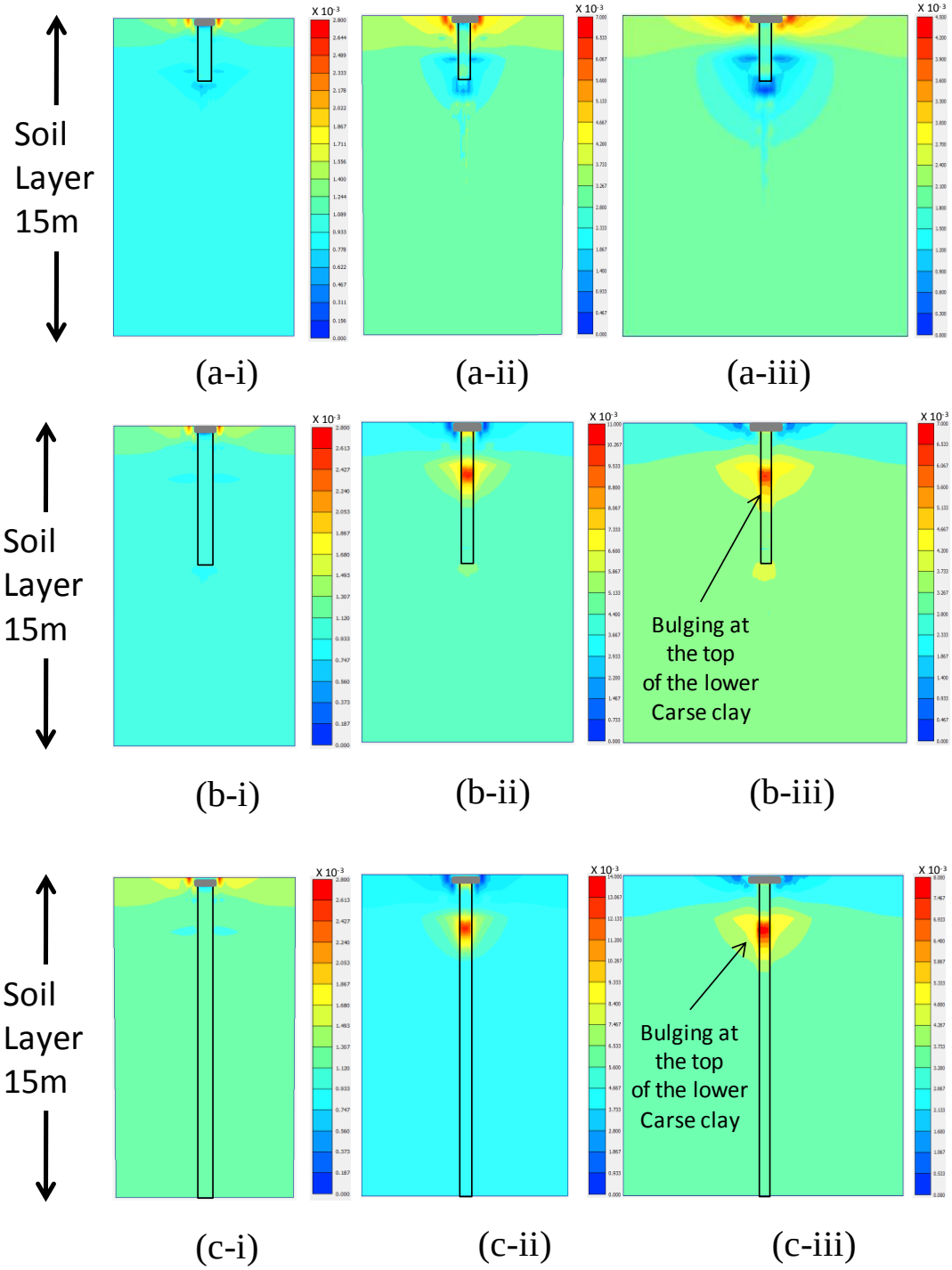

Figure 5.20 Shear strains for a single stone column with length (a) 2.4m, (b) 6.0m and (c) 14.5 and area ratios (i) 3.5, (ii) 8.0 and (iii) 14.2

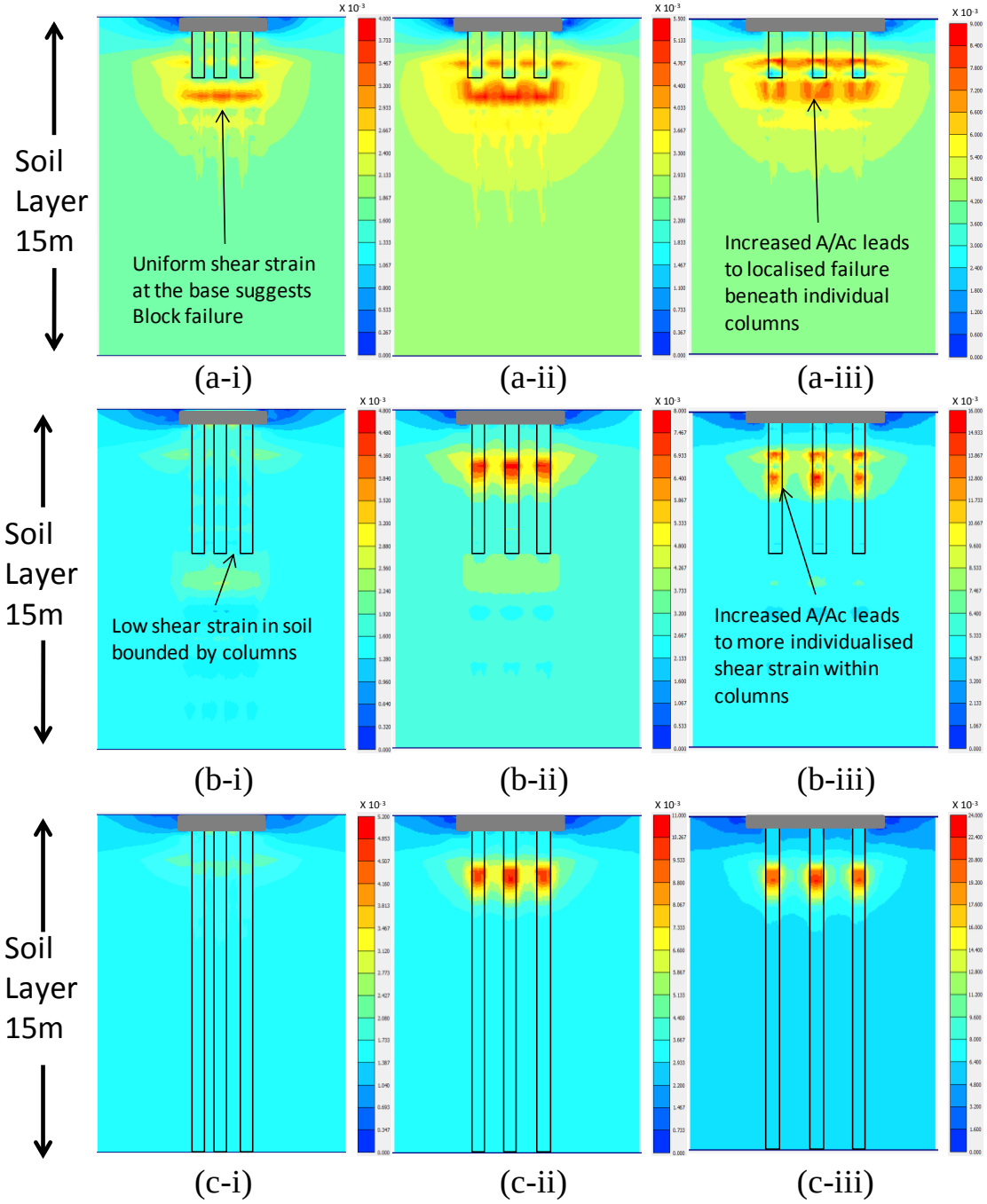

Figure 5.21 Shear strains for a three column strip with stone columns of lengths (a) 2.4m, (b) 6.0m and (c) 14.5 and area ratios (i) 3.5, (ii) 8.0 and (iii) 14.2

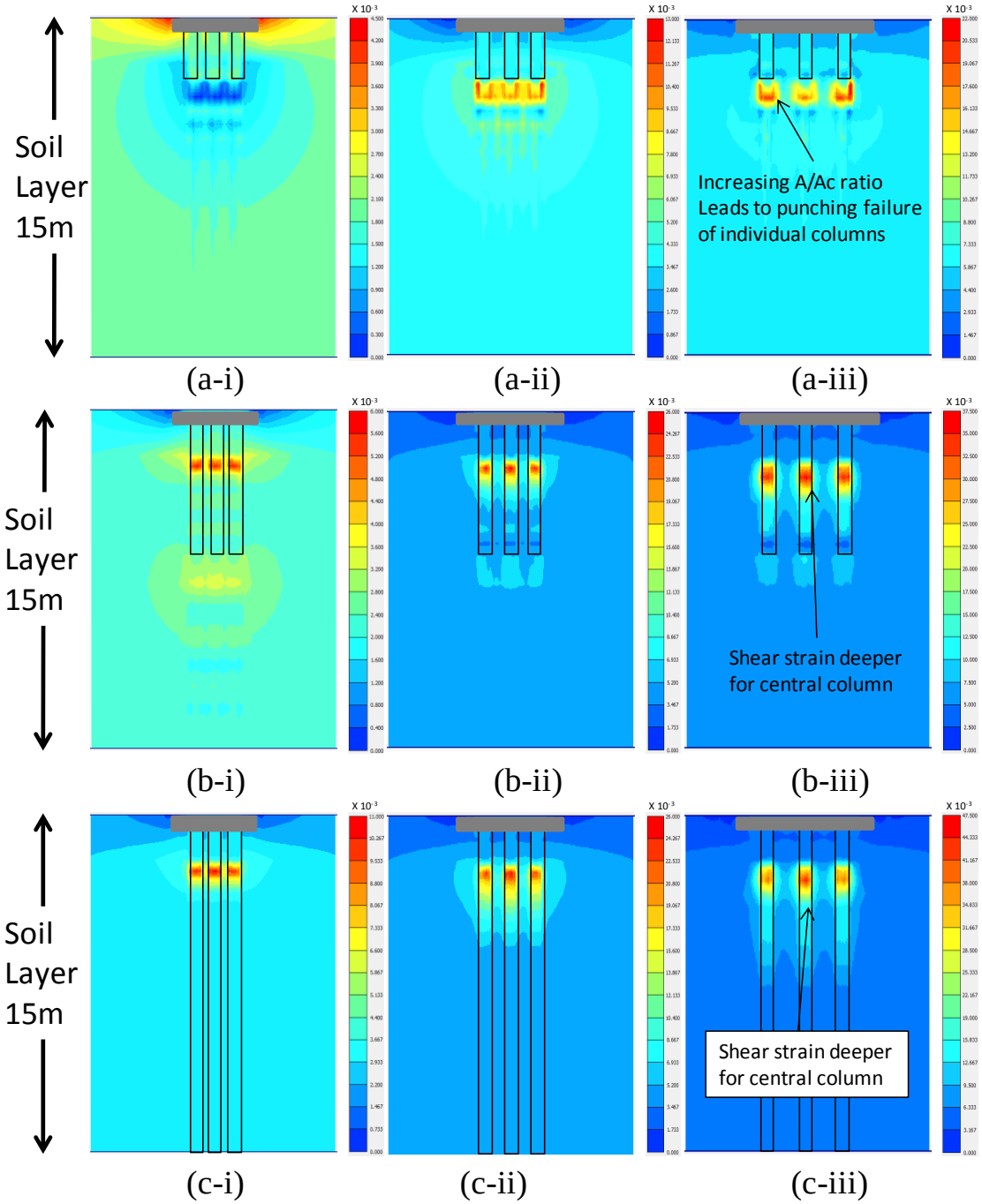

Figure 5.22 Shear strains for a nine column raft with stone columns of lengths (a) 2.4m, (b) 6.0m and (c) 14.5 and area ratios (i) 3.5, (ii) 8.0 and (iii) 14.2

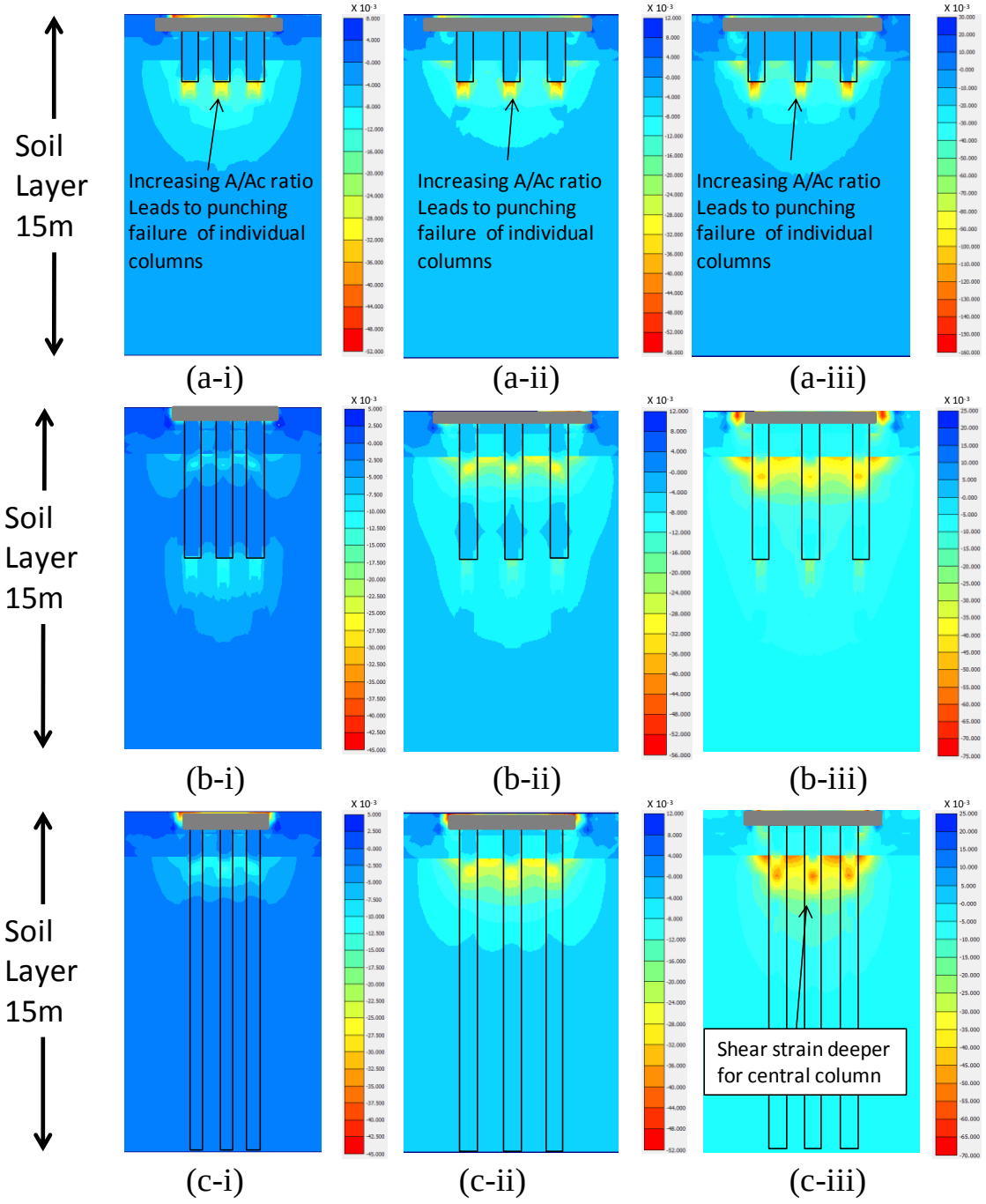

Figure 5.23 Shear strains for a nine column raft with stone columns of lengths (a) 2.4m, (b) 6.0m and (c) 14.5 and area ratios (i) 3.5, (ii) 8.0 and (iii) 14.2 for cross section corner to corner B-B'

5.6 Characteristic column behaviours

Stone columns have been shown to exhibit specific behaviours associated with their mode of deformation. The distribution of horizontal and vertical strain associated with column length is now examined for 2.4 m, 6.0 m and 14.5 m stone columns. The effect of confinement is observed by comparing the central column from a 3x3 raft and 3x1 strip with the unit cell and single column. The magnitude of vertical and horizontal strain appears to be related to area ratio with the highest strain values observed for the highest area ratios of 14.2 for all column lengths (Figure 5.24). This is to be expected due to the reduced lateral confinement and increased load absorbed due to increased foundation size.

5.6.1 Infinite array

The distribution of vertical and horizontal stress with depth for an infinite array of stone columns is shown in Figure 5.24. It can be observed that for a column of 2.4m length, regardless of area ratio, that the vertical strain (Figure 5.24(a)(i)) and horizontal strain (Figure 5.24(b(i)) are lowest between a depth interval of 0.0 m to 3.0 m. However, at 3.0 m the vertical and horizontal strain are highest which corresponds to the base of the column. As described earlier (Section 5.4 and 5.5) the base of the columns is where punching occurs. For columns of 6.0 m length it also appears that vertical strain is occurring at the base of the column which is suggestive of punching failure. For a low area ratio of 3.5 (Figure 5.24(a)(ii)) the vertical strain along the column length is relatively small compared to that observed for area ratios of 8.0 and 14.2. The horizontal strain (Figure 5.24(b)(ii)) appears to show the highest values at mid column height with some strain at the base of the column which suggests punching and bulging failure is occurring simultaneously. This is comparable to the observations of settlement inferred deformation ratios (Section 5.4) and total shear strain plots (Section 5.5) which suggest that bulging and punching occur simultaneously for columns of length 6.0 m. As the column length is increased to 14.5 m (Figure 5.24(a)(i) and 5.24(b)(i)) it is clear that deformation occurs at a depth of 2.0 m - 3.0 m for both vertical and horizontal strain which is considered to be due to bulging failure. Similarly, like 6.0 m this is also comparable to the observations made in Sections 5.4 and 5.5 of bulging failure occurring at a depth of 2.0 m - 3.0 m. It is clear from the observations of each column length examined that deformation occurs between 2.0 m and 3.0 m at the base of the upper Carse clay and lower Carse clay which corresponds to the weakest depth in the Bothkennar soil profile.

5.6.2 Single column

The distribution of the vertical and horizontal strain for single columns of length 2.4 m, 6.0 m and 14.5 m is shown in Figure 5.25. Similar to the infinite array, the single columns suggest punching failure is occurring at the column base at 2.9 m for both vertical strain (Figure 5.25(a)(i)) and horizontal strain (Figure 5.25(b)(i)). For a column length of 6.0 m the vertical strain (Figure 5.25(a)(ii)) and horizontal strain (Figure 5.25(b)(ii)) columns indicate that two modes of deformation are present at 2.9 m and 6.5 m which correspond to the earlier identified bulging and punching failure in Sections 4.4 and 4.5. The end bearing columns of length 14.5 m appear to suggest bulging failure has occurred at 2.9 m depth while below this depth the column suggests negligible vertical strain (Figure 5.25(a)(iii)) and horizontal strain (Figure 5.25(b)(iii)).

5.6.3 3x1 Column strip

The distribution of the vertical and horizontal strain for a 3x1 column strip with columns of length 2.4 m, 6.0 m and 14.5 m is shown in Figure 5.26. Vertical strain (Figure 5.26(a)(i)) and horizontal strain (Figure 5.26(b)(i)) are at their maximum at a depth of approximately 2.9 m. This is comparable to the observations made earlier in Sections 5.4 and 5.5 which suggest punching is the dominant mode of deformation. With increasing area ratio the stain increases both vertically and horizontally due to the reduced support provided by nearby columns. In a strip setting the columns are only restrained in the inward facing direction so are susceptible to bulging in the outwards directions perpendicular to the strip length. For a column length of 6.0 m the columns indicate that two modes of deformation are present at 2.9 m and 6.5 m which are observed as increased vertical strain (Figure 5.26(a)(ii)) and horizontal strain (Figure 5.26(b)(ii)). These increases in strain correspond to the earlier identified bulging and punching failure in Sections 4.4 and 4.5. The magnitude of vertical and horizontal strain is greatest at 2.9 m which suggests that bulging failure is the dominant mode of deformation. Similar to the infinite array the end bearing columns of length 14.5 m appear to suggest bulging failure has occurred at 2.9 m depth while below this depth the column suggests negligible vertical strain (Figure 5.26(a)(iii)) and horizontal strain (Figure 5.26(b)(iii)) decreasing with depth to negligible levels at a depth of 6.0 m. The area ratio appears for all column lengths to influence the magnitude of strain.

5.6.4 3x3 Column raft

The distribution of the vertical and horizontal strain are shown in Figure 5.27(a) and 5.27(b) respectively for a 3x3 column raft with columns of length 2.4 m, 6.0 m and 14.5 m. For column lengths of 2.4 m the vertical strain appears to develop beneath the base (Figure 5.27(a)(i)) which suggests punching is the dominant mode of deformation. As the area ratios increases from 3.5 to 14.2 the vertical strain increases. By increasing the A/Ac ratio the restraint provided by the neighbouring columns reduces and columns are able to deform more easily. Horizontal strain appears to be linked to vertical strain with the largest magnitude observed at a depth of 2.9 m which corresponds to the base of the column and the weakest point of the soil profile at the top of the lower Carse clay.

The distribution of vertical and horizontal strain with depth for a 6.0 m long column in Figure 5.27(a)(ii) and 5.27(b)(ii) respectively. The highest magnitude of vertical and horizontal strain occurs at a depth of 2.9 m which corresponds to the weakest point of the soil profile and hence bulging failure. It is clear from the vertical strain that at the base of the column (at a depth of 6.5 m) punching failure is evident. It appears that although some punching is evident, bulging is the dominant mode of failure for this length of column.

The distribution of vertical and horizontal strain with depth for a 6.0 m long column is shown in Figure 5.27(a)(iii) and 5.27(b)(iii). The highest magnitude of vertical and horizontal strain occurs at a depth of 2.9 m which corresponds to the weakest point of the soil profile (indicates bulging failure). With increasing depth, strain decreases to negligible levels. Punching cannot occur due to the end bearing nature of the columns. As the area ratio increases from 3.5 to 14.2 the vertical and horizontal strain increase due to the reduction in column to column restraint and the load taken by the column due to the increased foundation size.

It is clear from the results that the vertical and horizontal strain for each column length confirm the identified modes of deformation in Sections 5.4 and 5.5. For a column length of 2.4 m punching failure is evident. For a column length of 6.0 m bulging and punching failure are observed, with bulging confirmed as the dominant mode of failure. For columns of length 14.5 m bulging failure was observed.

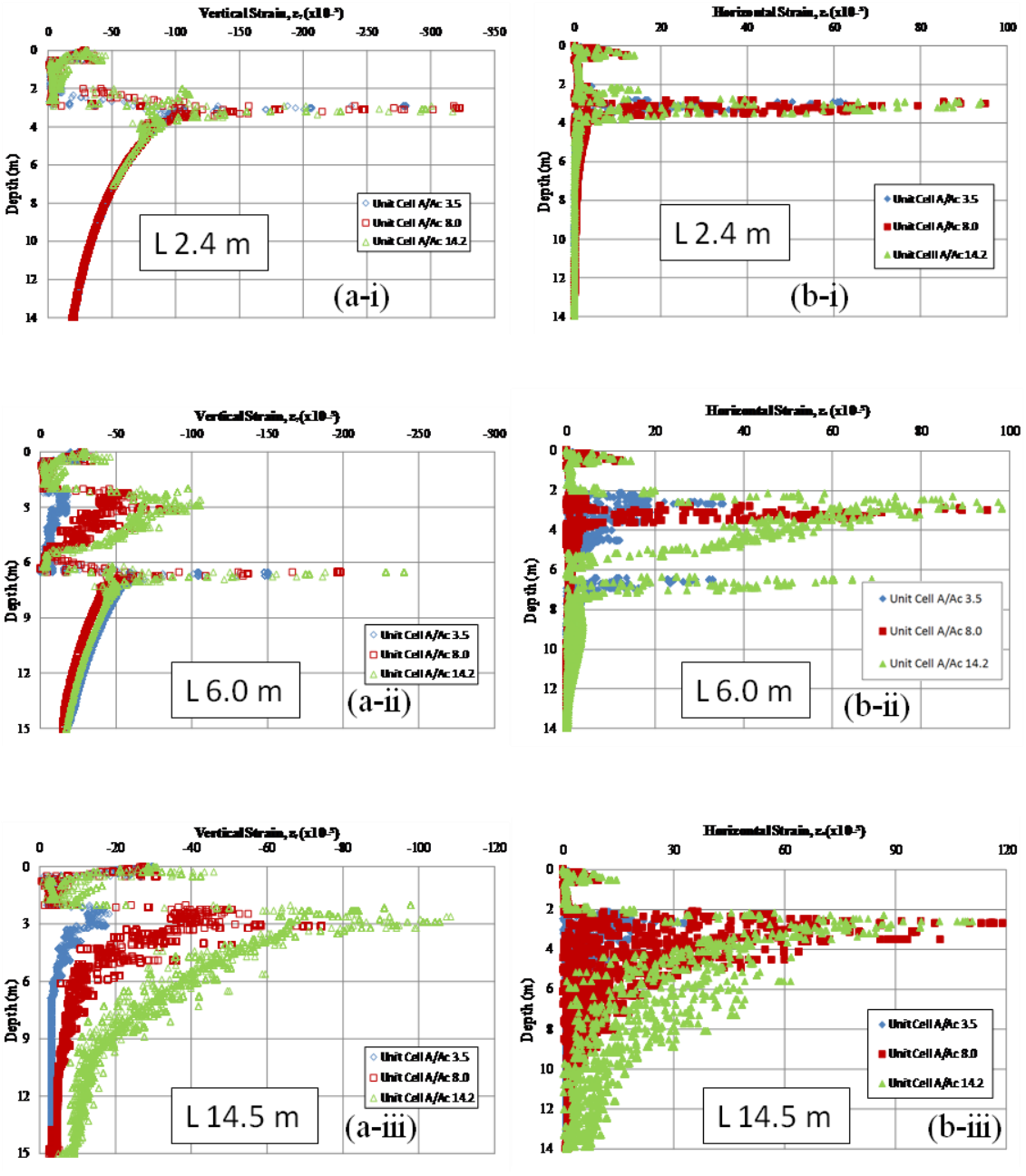

Figure 5.24 Horizontal and Vertical Strain for a unit cell of stone columns of lengths 2.4 m, 6.0 m and 14.5 m

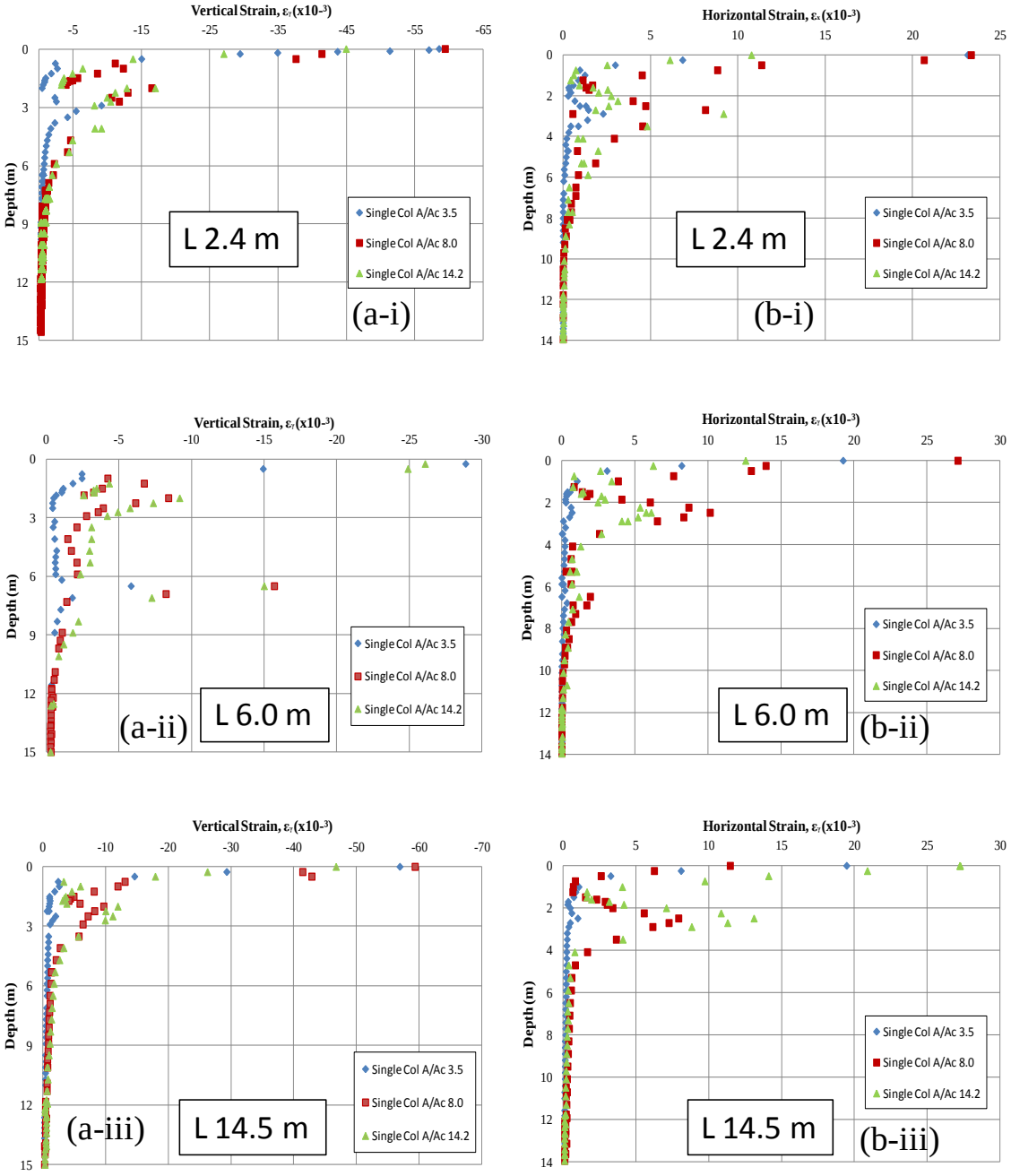

Figure 5.25 Horizontal and Vertical Strain for a single stone column of lengths 2.4 m, 6.0 m and 14.5 m

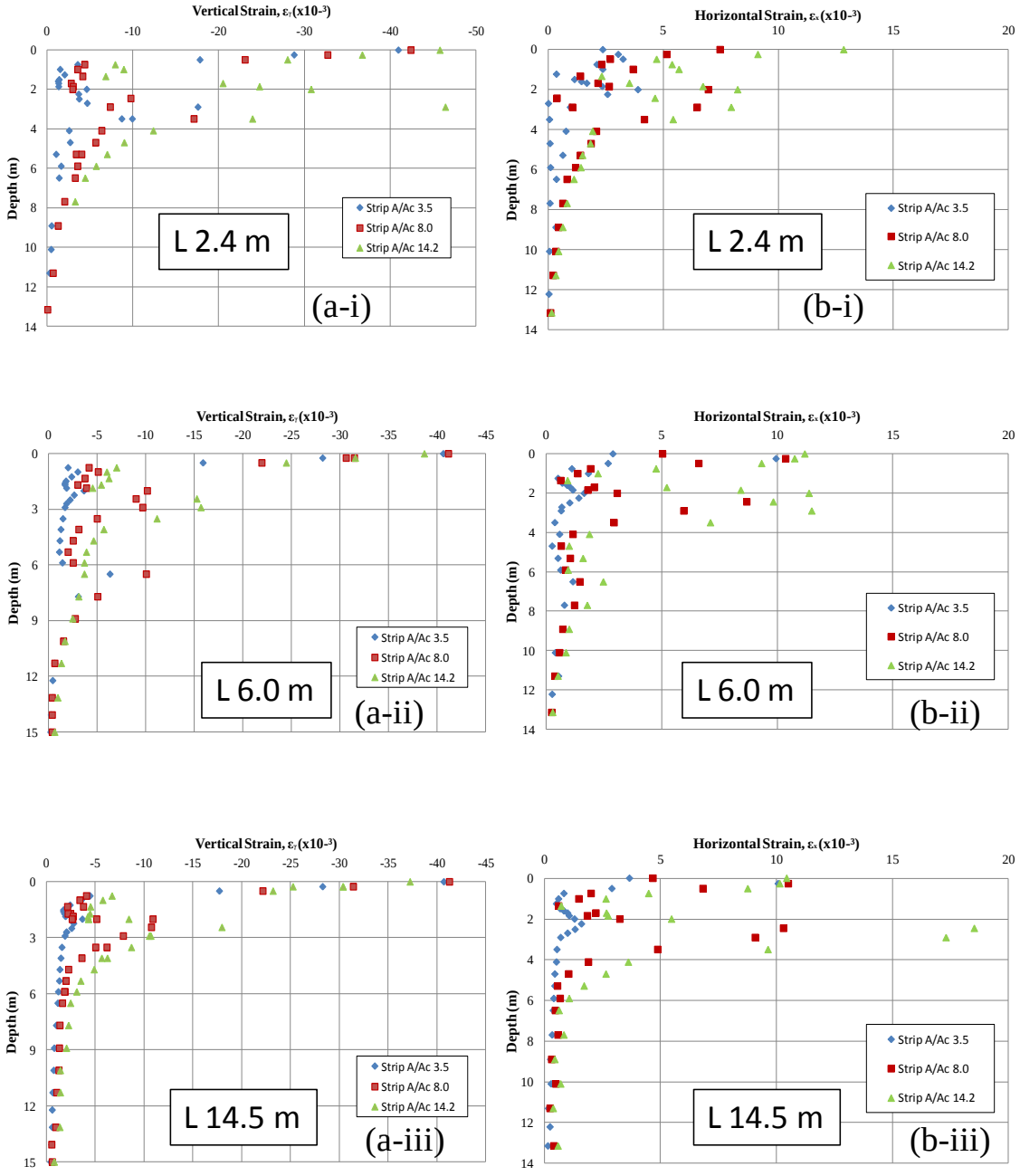

Figure 5.26 Horizontal and Vertical Strain for a three column strip of lengths 2.4 m, 6.0 m and 14.5 m

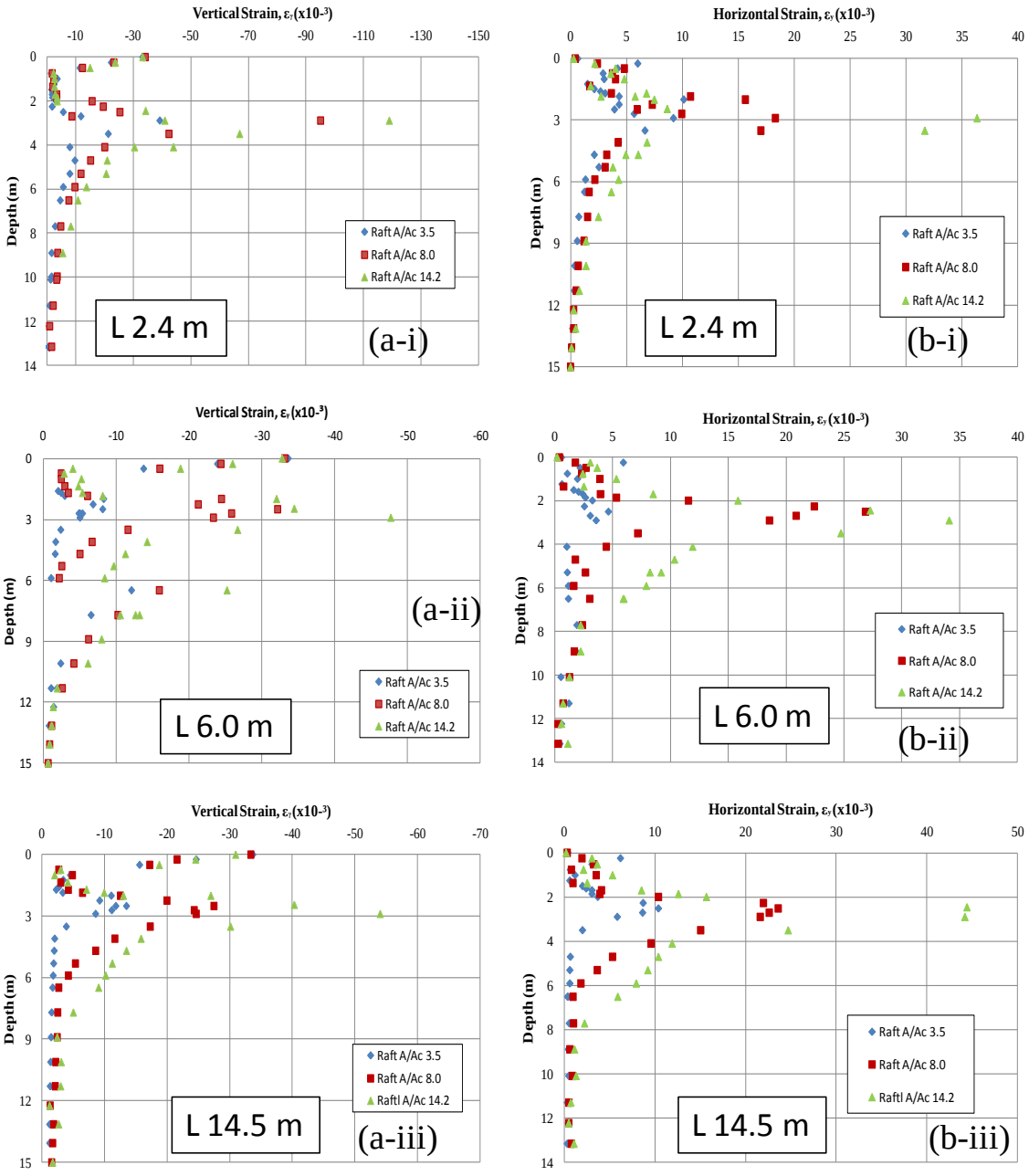

Figure 5.27 Horizontal and Vertical Strain for a nine column raft of lengths 2.4 m, 6.0 m and 14.5 m

5.7 Conclusions

Four configurations of stone column were analysed for various column lengths and a range of area ratios consistent with current practice. The effect of column confinement, column strength, column compressibility, column installation effects and crust thickness on column performance was examined. The performance of the stone column configurations was assessed using the Bothkennar soil profile (Chapter 3) and a working load of 50 kPa.

5.7.1 Settlement performance

The settlement performance of stone columns was assessed using the basic improvement factor, *n*, described by Priebe (1995). This is expressed as a ratio of untreated settlement divided by treated settlement. The key findings in terms of settlement performance are summarised as follows:

- The stiff crust and upper Carse clay extend to a depth of 2m from surface which limits the settlement improvement by stone columns up to a length of 2.4m due to high stiffness values of the soil.
- The settlement improvement factor for a unit cell was found to increase from a value of 1.07 for a column length of 2.4m to values of 10.1, 2.75 and 1.7 for a column length of 14.5m with area ratios of 3.5, 8.0 and 14.2 respectively. This suggests that with increasing column length the settlement improvement increases for a unit cell with the highest improvement observed for the lowest area ratios.
- For all configurations of stone column foundation examined increasing the area ratio was found to reduce the settlement reduction benefit. For an area ratio of 3.5 and column length of 2.4m, the settlement improvement factor was found to be 1.26 regardless of foundation type but increased to 1.59, 2.03 and 2.38 for a 14.5m length of column in single column, strip and raft configuration respectively. For an area ratio of 8.0, the settlement improvement factor was found to be 1.15 regardless of foundation type but increased to 1.33, 1.50 and 1.69 for a 14.5m length of column in single column, strip and raft configuration respectively. For an area ratio of 14.2 which is equivalent to a column spacing of 2.0m, the settlement improvement factor was found to be 1.07 regardless of foundation type but increased to 1.20, 1.31 and 1.40 for a 14.5m length of column in single column, strip and raft configuration respectively. Increasing the

area ratio in the case of the strip and raft foundations reduces the restraint provided by neighbouring columns while increasing the absorbed loads hence the reducing improvement factor with increasing A/A_c. It is preferable when installing columns to found them on a stiff or rigid layer and the values for 14.5m columns are considered end bearing with the base of layer C (lower Carse clay) modelled as a hard substrate i.e. assumed to be the Bothkennar gravel.

- Increasing the stiffness of the stone column has been shown to reduce the settlement. Settlement improvement factors for a single stone column increase from 1.17-1.22 for a column of length 2.4m to 1.29-1.59 for column of length 14.5m with stiffness in the range of 30MPa-70MPa. For a strip and raft the settlement improvement factor at 2.4m depth of 1.20-1.26 increases as stiffness and column length is increases. For a strip with columns of length 14.5m the improvement factor is seen to increase to 1.63-2.03 for stiffness values in the range of 30MPa-70MPa. Similarly, a raft for column length of 14.5m suggests improvement factors of 1.91-2.38 as stiffness increases from 30MPa to 70MPa. Interestingly, for a column of length 14.5m as the stiffness increases in the range from 30MPa-70MPa the benefit is highest to the single column with an increase in settlement reduction of 14.6%, followed by a strip of 12% and raft of 10.4%. This is because the single column and strip have less confinement provided by neighbouring columns and benefit the most from increased stiffness.
- Column strength was increased in the range of 38°-50° to assess the impact on settlement reduction performance. For a single column much of the settlement improvement behaviour was similar until after a column length of 6.0m when it increased from 1.46 to 1.57-1.59 for a column of length 14.5m. Increasing the column friction angle for a 14.5m column represents an increase in settlement reduction of 0.8% which is small suggesting a lesser influence on this foundation type. For a strip and raft foundation a settlement improvement factor of 1.25 for a column of length 2.4m was observed. With increased column length of 14.5m for friction angles in the range 38°-50° the improvement factor was in the range of 1.68-2.08 and 1.77-3.20 for a strip and raft respectively. This suggests that for a strip and raft increasing the friction angle from 38° to 50° reduces the settlement by 11.4% and 25.3% respectively. The higher reduction for a raft is a result of the highest confinement provided by adjacent columns in the group.

- The coefficient of lateral earth pressure, k_0 , was found to influence settlement behaviour. The effect of increasing the value from 0.75 to 1.0 had the largest effect but increasing to 1.25 had minimal impact on the settlement improvement factor. Generally the settlement improvement factor increases with increasing length with the highest values seen for values of 1.00 and 1.25. For a column of length 14.5m which is longest column examined increasing the value from 0.75 to 1.00 for a single column, strip and raft foundation increased the settlement reduction by 4.1% (n value increase of 1.59 to 1.70), 0.3% (n value increase of 2.01 to 2.02) and 4.8% (n value increase of 2.38 to 2.69).
- The thickness of the stiff crust had earlier been noted to effect foundation settlement performance (Chapter 4). With stone columns present the thickness of the crust impacts the performance of stone columns. With the thinnest crust of 0.5m the highest improvement was seen for all foundation types with settlement improvement factors of 2.29, 3.58 and 3.0 for a single column, strip and raft respectively with columns of length 14.5m. By comparison for the thickest crust the improvement factors were lower with values of 1.53, 1.76 and 2.23 for a single column, strip and raft with columns of length 14.5m. This is to be expected because the less competent lower Carse clay which is thicker for a crust thickness of 0.5m was able to benefit the most from the introduction of stone columns. The thickest crust of 1.5m results in the lowest improvement as the stiff crust and upper Carse clay layers are more competent and as such less improved.

5.7.2 Settlement inferred deformation ratios

The deformation of stone columns was examined by the use of two ratios termed punching and compression ratios. Columns which punch into the underlying soil transfer most of the applied load to the base. This mode of deformation is characterised by high punching ratios and low compression ratio. Columns which suffer bulging failure tend to bulge laterally into the soil stress-share with the surrounding soil while failing to transfer load to the base of the column. Typically, bulging failure is characterised by high compression ratio and low punching ratios. Use was made of these ratios to define the mode of failure for different configurations of stone columns.

This research has observed two modes of deformation by numerical analysis, punching and bulging failure. In addition a sub-type of punching failure defined by Black (2007) as 'Block failure' has also been observed. Punching failure is seen for all short columns

(length less than 2.4 m) which is observed as an increase in punching ratio coupled with low compression ratios. For columns with a low area ratio of 3.5 low punching and compression ratios were observed with increasing column length. 'Block' failure occurs when both the column and soil act as a single unit and punch uniformly, which accounts for the low compression ratios. Beyond a length of 2.4 m the punching ratio reduces and the compression ratios increase as the mode of deformation transitions from punching to bulging failure which is observed for longer columns with area ratios of 8.0 and 14.2. It has been noted that the configuration of columns does not affect the mode of deformation rather this is influenced by the area ratio and column length. The influence of the other examined parameters on deformation ratios are summarised as follows:

- With increasing column stiffness the columns absorb more of the applied load. This is seen for the highest value of stiffness which has the highest punching ratios and the lowest compression ratios for all configurations of columns. The increased stiffness was found to increase the compression ratio while the punching ratio reduced below 2.4 m.
- Increasing column strength (friction angle) was found to have no effect for single column configurations. For 1x3 strip and 3x3 raft configurations increasing column strength was found to increase the maximum punching ratio. Increasing strength had the effect of reducing column compression ratio. It is suggested that the columns absorb more of the applied load when column strength is increased from 38° to 50°.
- The coefficient of lateral pressure was found to have a negligible influence on the deformational behaviour i.e. punching and compression ratios for 3x3 raft configurations. This is consistent with the findings of the numerical study conducted by Kirsch (2006) and Killeen (2012).
- The stiff crust thickness was found to influence the deformational behaviour of stone columns. The highest punching and compression ratios were noted for the thinnest thickness of crust 0.5m. The thickness of the crust was found to influence the depth at which maximum punching occurred. For a 0.5 m thick crust this occurred at 2.4 m and for a 1.5 m thick crust this occurred at 3.6 m. This is because the thickness of the crust alters the depth to which punching can occur. The more competent crust supports the column allowing it to transfer stress to depth. The compression ratios were found to be highest for a 0.5 m

crust and lowest for a 1.5 m crust. A reduced crust thickness reduces the depth of the lowest lateral restraint. This then allows the column to bulge closer to the surface.

5.7.3 Shear strain behaviour

The use of settlement ratios allowed for the identification of two modes of deformation, bulging and punching (including 'block' failure). The ratios themselves do not confirm the actual mode of deformation so in order to confirm this cross sections of shear strain with depth were examined. Three column lengths of 2.4 m, 6.0 m and 14.5 m were chosen to illustrate the different modes of deformation. 2.4 m long columns were chosen to illustrate punching failure, 6.0 m long columns to illustrate the change from punching to bulging failure and 14.5 m columns to illustrate bulging failure as the columns are end bearing and founded on a rigid stratum.

The punching mode of deformation was seen for short columns of 2.4 m length. Shear strain was seen to have developed at the base of the column and partially along column length. 'Block' failure was observed for columns with low area ratios of 3.5 with uniform shear strain occurring across the base of columns and soil bound by the columns. The columns and soil are considered to act as a single unit punching into the underlying soil. Bulging failure was seen for columns with area ratios of 8.0 and 14.2 within columns of lengths 6 m and 14.5m. It was not observed for low area ratios. The increased depth of the bulging for the central columns is considered comparable to the findings of Hu (1995) and Muir-Wood *et al.* (2000) who suggested that central columns bulge at a deeper depth.

5.7.4 Characteristic column behaviours

The distribution of vertical strain and horizontal strain were examined for column lengths of 2.4 m, 6.0 m and 14.5 m. It was difficult to identify bulging or punching modes of deformation from the data. It appears that for columns there is evidence of both modes of deformation occurring simultaneously. The stress concentration ratios were found to be influenced by the distribution of vertical and horizontal strain within the columns. Upper sections of columns suggest large magnitude vertical strains which are in a state of plasticity which limits their ability to absorb large vertical loads. As a result stress concentration ratios are lower in these regions.

Chapter 6

Laboratory testing

This chapter summarises the shear box and unconfined compressive testing of binder/ gravel composites for this research carried out at the geotechnical and structural laboratories in the School of the Built Environment, Heriot-Watt University.

6.1 Introduction

The numerical simulations in Chapter 5 examined the settlement and deformational behaviour of stone column configurations beneath pad, raft and strip foundations. By increasing the stiffness of the column material it was found that the settlement reduced. One of the potential methods of increasing the stiffness of a stone column is to add a 'binder' material to it in order to increase its stiffness. In this Chapter the use of potential binders is examined and discussed. The void ratios of gravels are examined to determine the volumes of binder required for a full field trial. The friction angle of aggregates and gravels is also examined in terms of their friction angle for various normal loads. The dependency of the friction angle on load is considered since the friction angle and confinement of a column control the bearing capacity of a stone column.

6.2 Shear box analysis of aggregates and gravels

6.2.1 Overview

The use of aggregates and gravels in the construction industry for the formation of granular (stone) columns in ground improvement is common in Europe and North America. The wide variation in soil types has led to the evolution of specialist techniques which can be summarised as falling into two main categories, bottom and top feed installation systems. The use of a particular technique is site dependent and based upon client requirements. The use of top feed systems use grain sizes of 40-75 mm and bottom feed typically use 20-40 mm grain sizes. In the United Kingdom dry bottom feed systems are common due to their low spoil creation and their deeper treatment depth. The vibroflot in the bottom feed technique can also overcome potential borehole failure as stone is delivered to the tip and compacted without the need to withdraw the tool. Withdrawal in soft soil can risk cave-in.

In soft clays the compaction of stone is difficult due to the inability of the weak soil to restrain the column leading to larger diameters. The use of normal compaction pressures in soft clay requires larger volumes of stone and so creates a larger diameter of column raising costs significantly. In order to examine the effect of confining pressure on friction angle bottom feed aggregates are tested in a large shear box. The results are examined and discussed in the context of this research. For completeness gravel used in the composite test samples is also tested in a small shear box to determine the friction angle and to understand the change in stiffness when the mix material is added.

6.2.2 Principles and applications of the shear box test

The shear box is a tool extensively used in geotechnical engineering to assess the shear strength of materials such as aggregates and soil. Other materials and multi layered samples may also be tested. The materials tested in this research are tested according to British Standard BS1377: Part 7: 1990 unless otherwise specified. All aggregates and gravels are tested under drained conditions.

The shear box, unlike triaxial systems where the failure plane is allowed to develop naturally and in a random orientation, relies on the development of shear stress along a controlled horizontal plane. The shear box apparatus can be used to determine the angle of shear resistance of materials but can also be used to assess the change in void ratio as a result of compaction in the apparatus. Two variants of shear box are used in this research: The first is a standard large shear box of dimensions 300mm by 300mm by 175mm deep. The advantage of this apparatus is that it can be used to perform shear strength tests on coarse materials like aggregates which are too large for triaxial tests. The rate of displacement was set at 2.5mm per minute equating to a strain rate of 0.01 per minute. The maximum size of aggregate grain sizes suitable for testing is 37.5mm; the second is the small shear box with dimensions 100mm by 100mm by 25mm. Commonly sands and gravels below 20mm are tested using this apparatus. The rate of displacement was set at 0.66mm per minute equating to a strain rate of 0.0066 per minute.

Shear box analysis for geomaterials (aggregates and gravels) and composites relies on an established theory of material failure. Coulomb (1776) developed an understanding of the shear behaviour of materials. The shear strength at a point on a particular plane is expressed by the general relationship between the maximum shearing resistance, τ_f, and

normal stress, σ_n, for soils. The assumption being that shear stress in a soil can be resisted only by the skeleton of solid particles. Therefore expressing shear strength as a function of effective normal stress at failure, σ'_f :

$$\tau_f = c' + \sigma'_f * tan\varphi' \quad [6.1]$$

Where τ_f = maximum shearing resistance

σ'_f = effective normal stress

c' = effective cohesion

φ' = angle of friction

Figure 6.1 highlights the principal features of the shear box test. The top section is displaced at a set rate laterally along the interface. The rate of displacement is set by material type according to the relevant British Standard. As the top portion slides laterally the material contained within the top and bottom sections is subjected to a normal force from the top of the upper box at an angle normal to the controlled shear plane (horizontal) and restraint provided by the framework of the shear box sides and bottom. With increasing displacement horizontal shearing force is applied and increases over the duration of the test until the material reaches a critical point at which shear failure occurs.

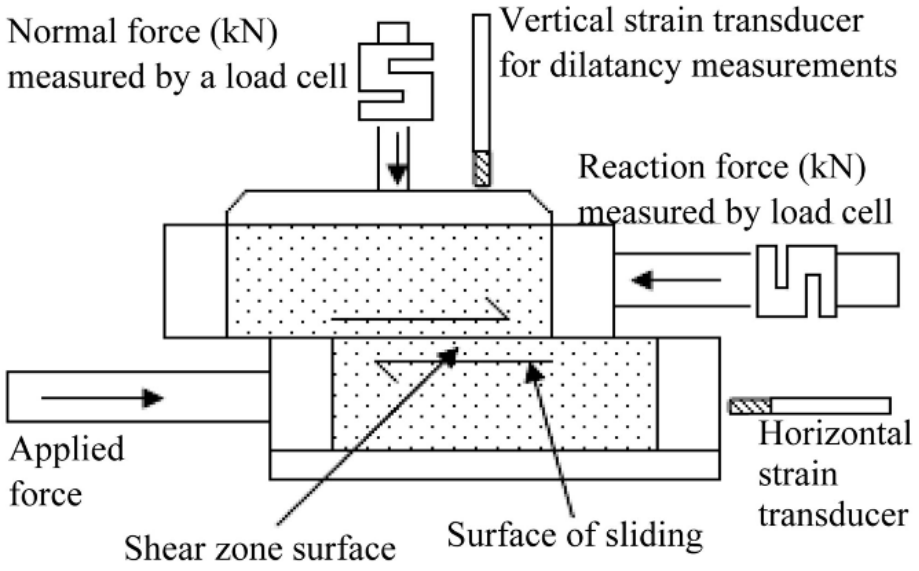

Figure 6.1 Schematic of a typical shear box (Wijeyesekera *et al.* 2013)

The shear box although widely used has some drawbacks. The soil specimen is only permitted to fail along a pre-determined shear failure plane. This leads to a non-uniform distribution of stresses on the shear failure plane. In a field situation the failure plane would be undefined and the distribution of stresses related to the failure. The ultimate deformation applied to the soil is limited by the maximum travel of the shear box. It is also limited in that the pore pressures in the sample for undrained conditions cannot be measured during testing. Although the shear box has limitations its cost effectiveness, simplicity, ease of sample preparation & installation and quick interpretation of the behaviour of the material are advantageous. The large shear box represents the most practical means of testing the shear behaviour of aggregates which would otherwise be too large in the standard triaxial test.

6.2.3 Results of the angle of repose, specific gravity and initial void ratio

The angle of repose represents an approximation of the friction angle of a granular material in a very loose state at low confining pressure. It is easily obtained by forming the sample into a heap, the angle of repose can then be found. The height of the heap and half the width of the heap can be used assuming they are at right angles to each other. The slope can be considered the hypotenuse. Equation 6.2 can be used to calculate the angle of repose, θ.

$$\tan\theta = \frac{heap\ height}{heap\ width*0.5} \qquad [6.2]$$

Table 6.1 shows the values of the angle of repose obtained for the aggregates and gravels. Values of 33.2°, 39.1° and 41.3° were obtained for the friction angle of 5.0 mm to 6.3 mm, 6.3 mm to 10 mm and 20 mm to 40 mm, respectively. Hartmann (1992) states that typical values for the angle of repose for gravel termed 'run of the bank' and screened samples is 38° and 40° respectively. Kleinhans *et al.* (2011) suggests that loose dry gravel has an angle of repose in the range of 30°-45°. It is suggested therefore that the results are within an acceptable range for gravels.

The specific gravity and initial void ratios were measured for granular material of grain sizes in the ranges 5.0mm-6.3mm; 6.3mm to 10.0mm; and 20.0mm to 40.0mm (Table 6.2) and were found to be 2.6, 2.5 and 2.0 respectively. The lower value of 2.0 is considered a result of experimental error and is discounted. Nemati (2014) states that typical specific gravities for sands and gravels are in the range of 2.4 to 2.9. Bell (2007) states that typical specific gravities for gravel are in the range 2.5 to 2.8. The lower than

expected specific gravity for the river bed gravel (20 mm-40 mm) is considered due to the presence of a variable rock types and experimental error.

The measured void ratios for the gravel sizes 5 mm - 6.3 mm; 6.3 mm - 10 mm and 20 mm - 40 mm are 0.63, 0.59, and 0.5. Das (2008) suggests that typical void ratios for gravel are between 0.3 and 0.60 across the range of typical gravel sizes. Das (2008) and the Swiss Standard (2013) suggests that for gravelly sands with little or no fines void ratios can be in the range of 0.29 to 0.74. The results are considered acceptable.

Grain Size (mm)	Test Number	Width of Mound (mm)	Height of Mound (mm)	Angle of Repose (°)	Average Angle of Repose (°)
5	1	17	5.3	31.96	33.2
	2	16.5	5.3	32.7	
	3	14	4.9	34.99	
6.3	1	14	6	40.59	39.1
	2	15	5.5	36.24	
	3	14	6	40.59	
20 - 40	1	35	15.3	41.16	41.3
	2	34	15.5	42.35	
	3	35.1	14.9	40.33	

Table 6.1 Angle of repose for selected aggregates and gravels

Grain Size (mm)	Test Number	Mass of Stone (kg)	Mass of Water (kg)	Specific Gravity, Gs	Average Gs	Void Ratio, e	Average e
3.35 - 5	1	2.314	0.633	2.47	2.5	0.68	0.67
	2	2.310	0.633	2.47		0.67	
	3	2.357	0.621	2.48		0.65	
5 - 6.3	1	2.502	0.603	2.59	2.6	0.62	0.63
	2	2.439	0.614	2.55		0.64	
	3	2.451	0.608	2.55		0.63	
6.3 - 10	1	2.495	0.591	2.55	2.5	0.60	0.59
	2	2.474	0.588	2.52		0.60	
	3	2.424	0.570	2.42		0.57	
10-20	1	2.281	0.620	2.4	2.5	0.65	0.69
	2	2.300	0.635	2.46		0.68	
	3	2.310	0.670	2.57		0.74	
20 - 40	1	43.900	10.100	2.02	2.04	0.47	0.5
	2	43.100	10.800	2.05		0.51	
	3	43.100	10.900	2.06		0.52	

Table 6.2 Specific Gravity and initial Void ratios

6.2.4 Results of the horizontal shear stress and displacement

The testing of the river bed gravel (20 mm - 40 mm) in the large shear box was carried out under different normal stresses ranging from 13.8 kN/m² to 1111.11 kN/m². The results of horizontal shear stress and displacement indicate that the higher the normal load the higher the shear stress on the sample (Figure 6.2). The shear and normal stress at failure for various normal stresses was plotted and a line of best fit drawn through the

origin (Figure 6.3) (cohesion, c = 0 for granular material). The gradient of the slope was then interpreted to calculate the average friction angle for the river bed gravel and a value of 41.3° obtained. Marshal (1967) reported that friction angles for river bed gravel varied between 42.2°-52.7° as a function of shear stress in the range of 1000 kN/m² - 40 kN/m² when tested in a large shear box. Yasuda *et al.* (1997) reported that

for a river bed gravel the friction angle varied between 44.8°-49.6° as function of shear stress for values in the range of 290 kN/m² - 50 kN/m². The lower friction angle obtained in this study is comparable to the values discovered by other researchers. The effect of grain size, sorting and levels of compaction will affect the friction angle obtained.

The testing of the 5 mm and 6.3mm gravels was performed in the small shear box. The intention in testing the gravel is to provide an understanding of the initial friction angle before combining with mix materials. The horizontal shear stress and displacement results are plotted in Figures 6.4 and 6.5 for gravels 5mm and 6.30mm respectively. During testing the small shear box suffered from a failure of the belt drive and upper platen ball bearing. It is considered that the test results were affected by the replacement of the upper platen which appeared to show a stiffer response during testing of the 5mm to 6.3mm gravel. The highest normal stress tests and two of the lowest normal load tests were completed prior to failure of the apparatus. The tests with applied stress that are considered affected are one of the 18.66kN/m² tests and the three 28.47kN/m² tests. The friction angles were calculated using the same method described earlier with the gradient of the straight line used from the normal and shear stress plot (Figure 5.6). The calculated friction angles for the 5.0 mm to 6.30 mm and 6.3 mm to 10.0 mm gravels were 63° and 43° respectively. The results for the 5.0 mm gravel are considered erroneous due to issues with the shear box apparatus i.e. replacement of the belt on the drive system and repair of the ball bearing in the upper platen. However, the value obtained for a 6.3 mm - 10.0 mm gravel compares well with the range of 32° to 44° quoted by the Swiss Standard (2013).

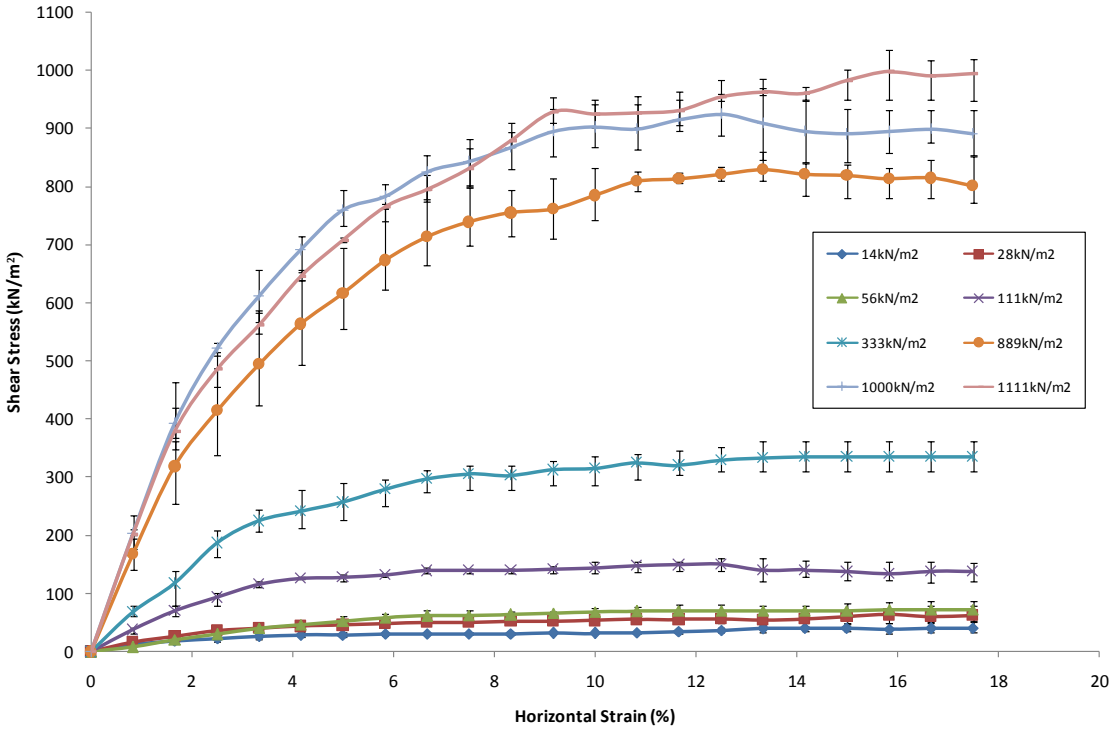

Figure 6.2 Horizontal shear stress and horizontal strain for river bed gravel deposit

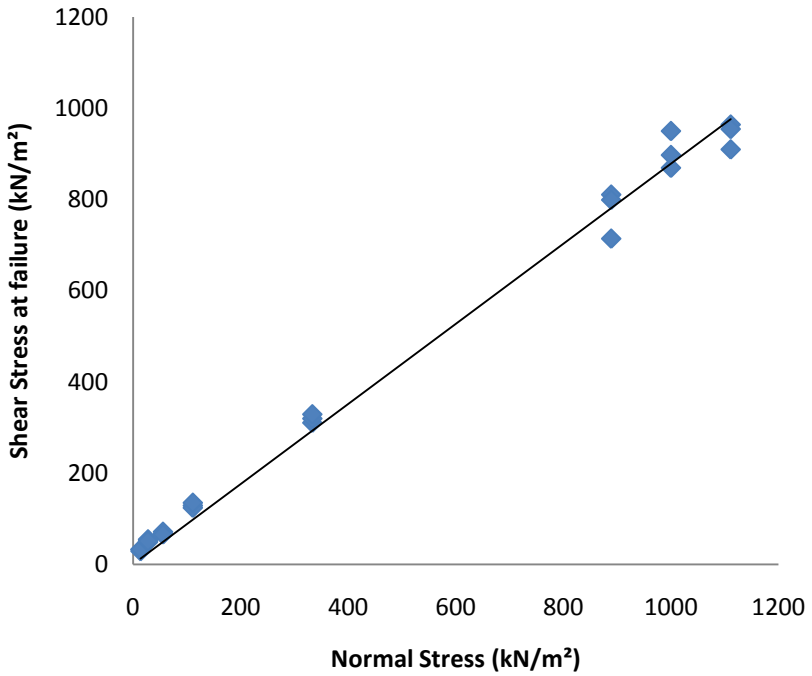

Figure 6.3 Plot of shear stress at failure and normal stress for river bed gravel

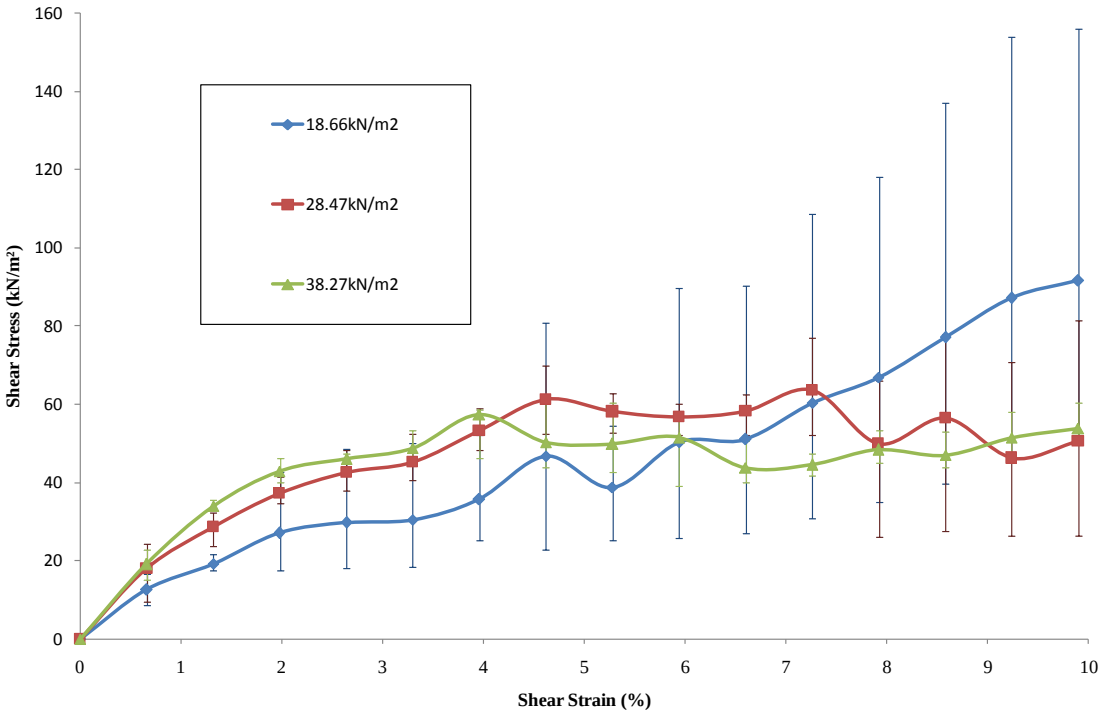

Figure 6.4 Horizontal shear stress and horizontal displacement for 5.0 mm gravel

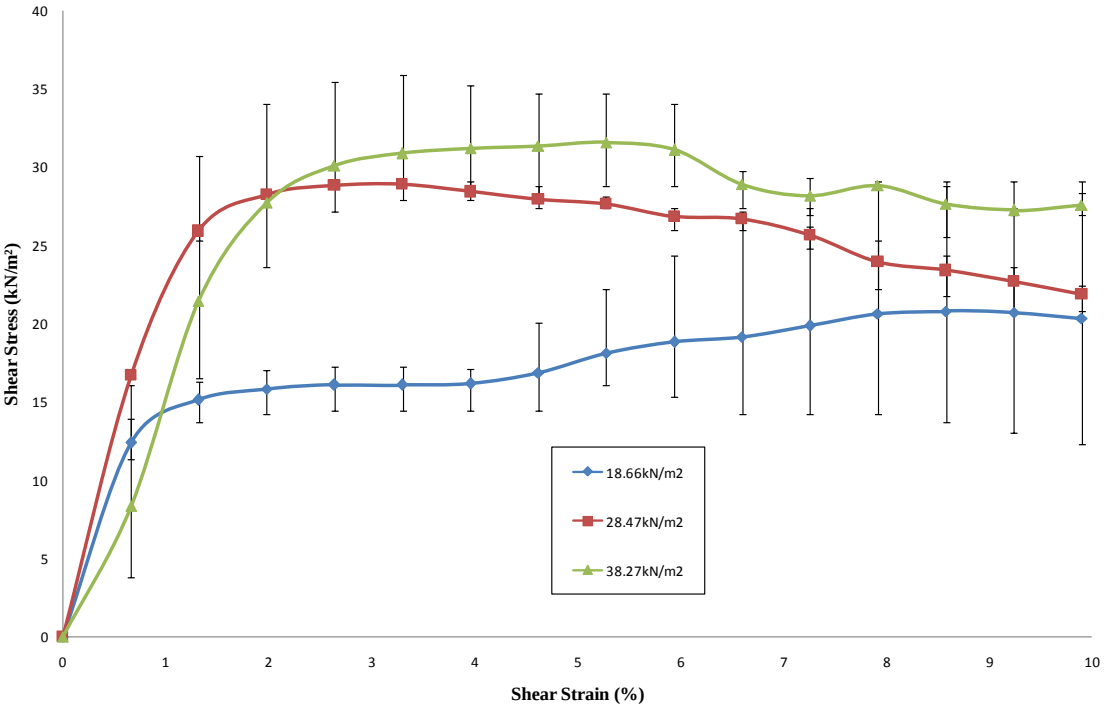

Figure 6.5 Horizontal shear stress and displacement for 6.3 mm gravel

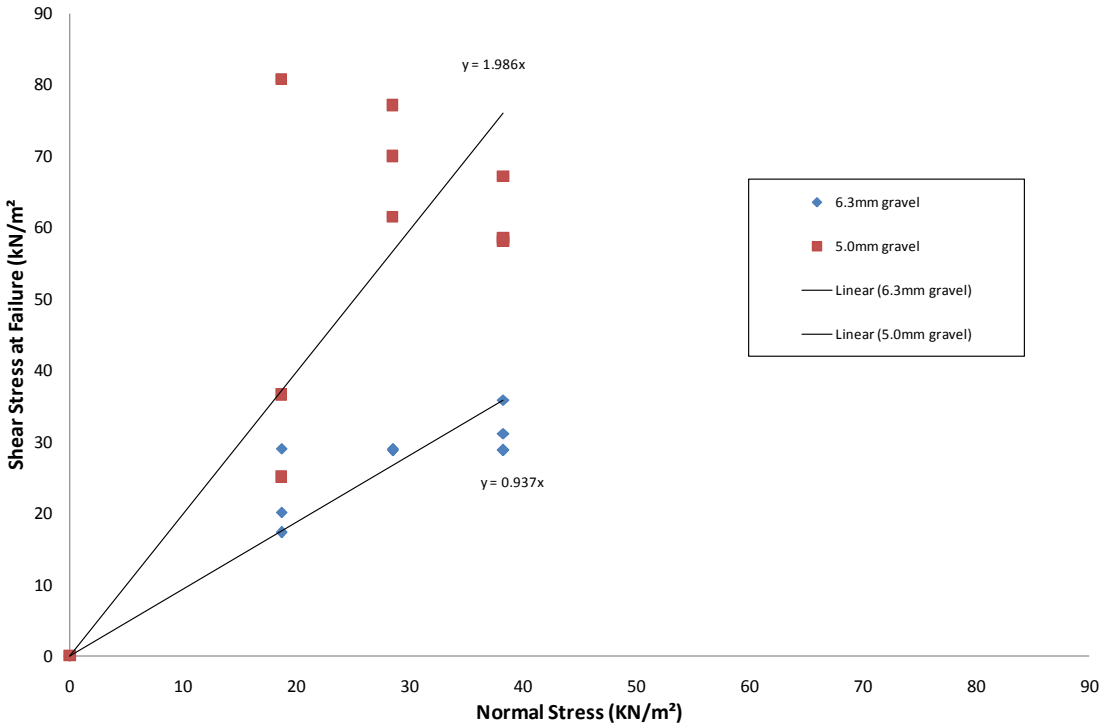

Figure 6.6 Plot of shear stress and normal stress with interpreted friction angle for 5 mm and 6.3 mm gravels

6.2.5 Results of volumetric strain and particle size distribution

The testing of the 20 mm to 40mm gravels revealed differences in dilatancy behaviour dependent upon the level of normal stress applied (Figure 6.7). The shear box is somewhat limited in the sense that the failure plane and orientation are controlled by the horizontal displacement. However, the results suggest that for normal stresses in the range of 14 kN/m² to 111 kN/m² the sample indicates positive volumetric strain which is indicative of sample expansion (dilation). For normal stresses in the range of 333kN/m² to 1111kN/m² negative volumetric strain was recorded. This suggests the samples are contractive and evidence of crushing was recorded when comparing the particle sieve analysis for the samples before and after a normal stress of 888-1111kN/m² was applied (Figure 6.8). The particle D_{50} reduces from 25-28 mm to 20-24mm post testing and the D_{90} values reduce slightly from 37.5mm to 35mm. The largest reduction was observed for D_{10} values with a change in particles passing from 19-25 mm to 12-14mm. However, for lower loads comparable to foundation stresses applied to stone columns in the range of 25kN/m² to 50kN/m², deformation of the column material due to crushing was observed to be insignificant. Changes in particle size distribution were observed for instances where sample dilation occurred due to the effect of crushing.

The volumetric strain of the 5.3 mm - 6.3 mm and 6.3 mm - 10.0 mm gravel was found to be positive indicating sample expansion (Figures 6.9 and 6.10). The volumetric strain appears to be highest for the 5.0 mm - 6.3 mm samples tested. During particle sieve analysis of the material (before and after testing) no evidence was found of crushing or a change to the profile, so deformation of the gravel/ crushing is ruled out for the range of applied stresses tested (Figure 6.11).

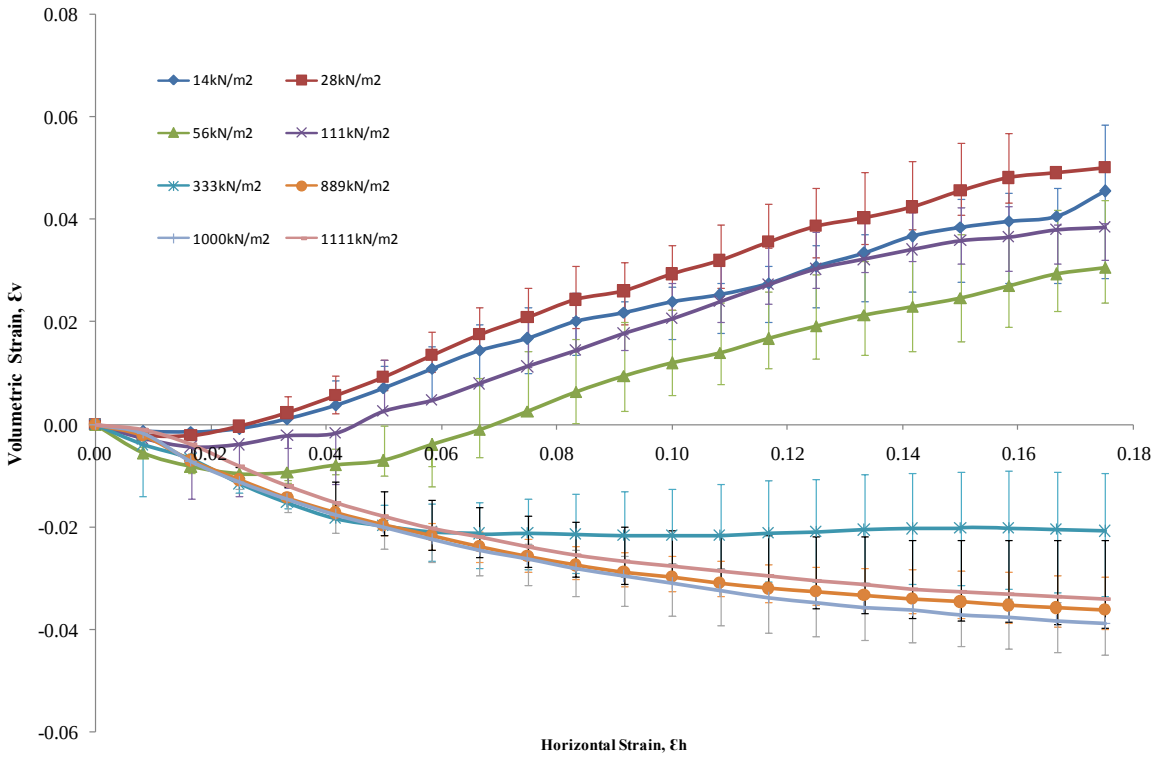

Figure 6.7 Volumetric strain and horizontal displacement for river bed gravel

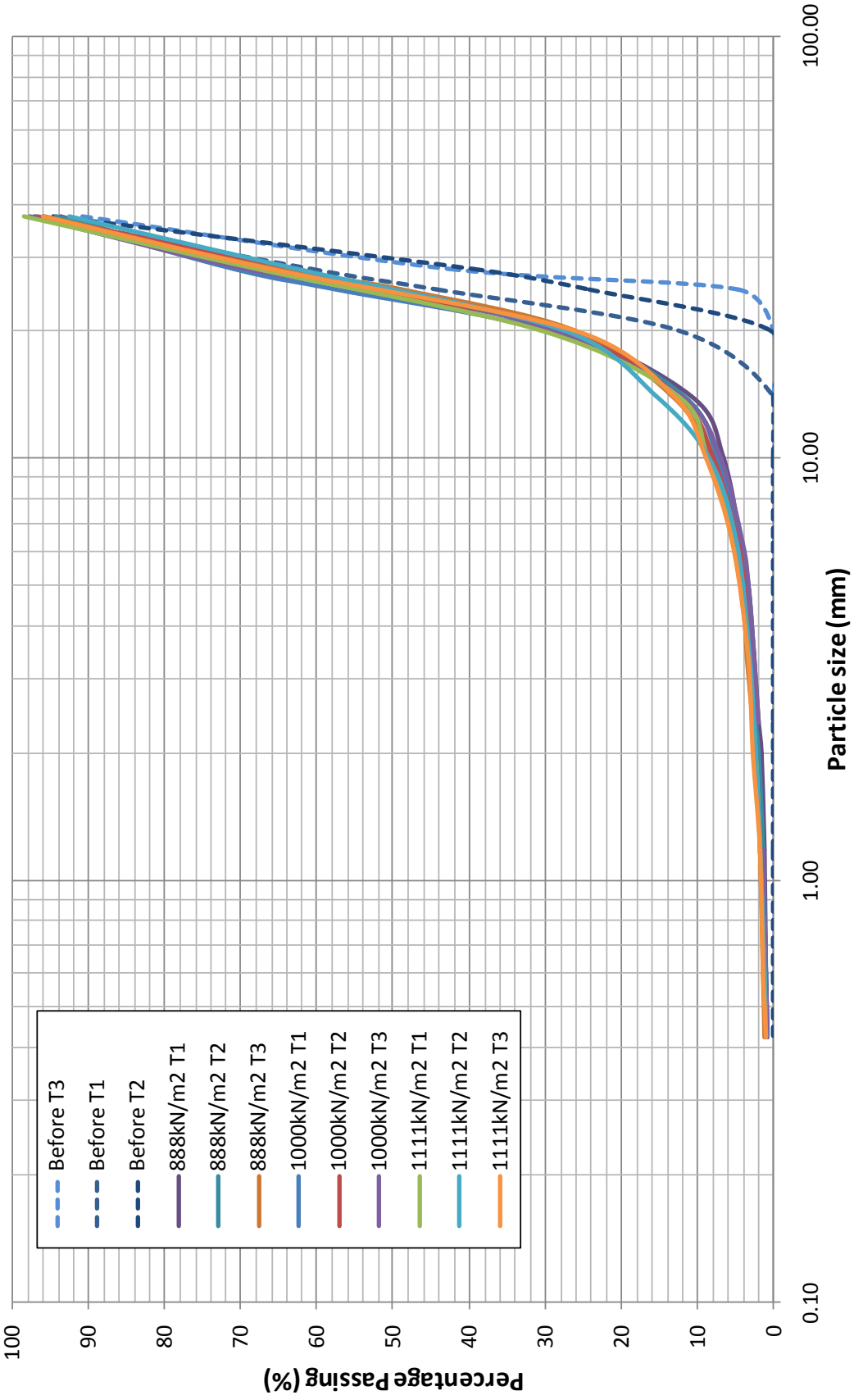

Figure 6.8 Particle sieve analysis of river bed gravel prior to and after shear box testing

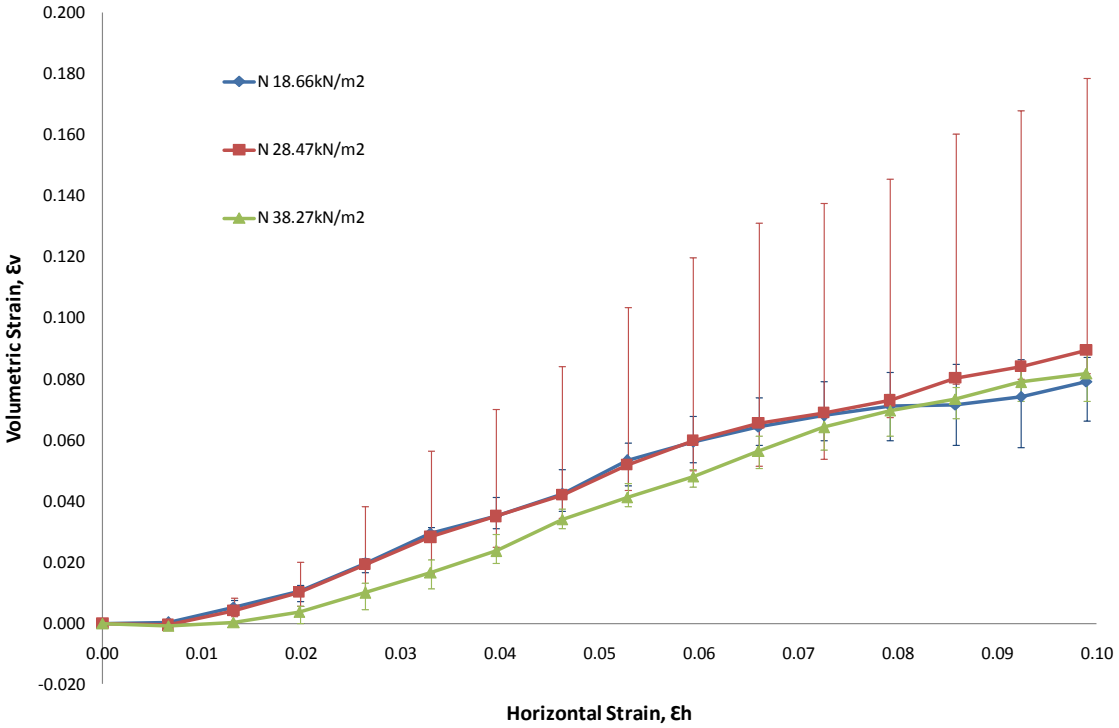

Figure 6.9 Volumetric strain and horizontal displacement for 5 - 6.3 mm gravel

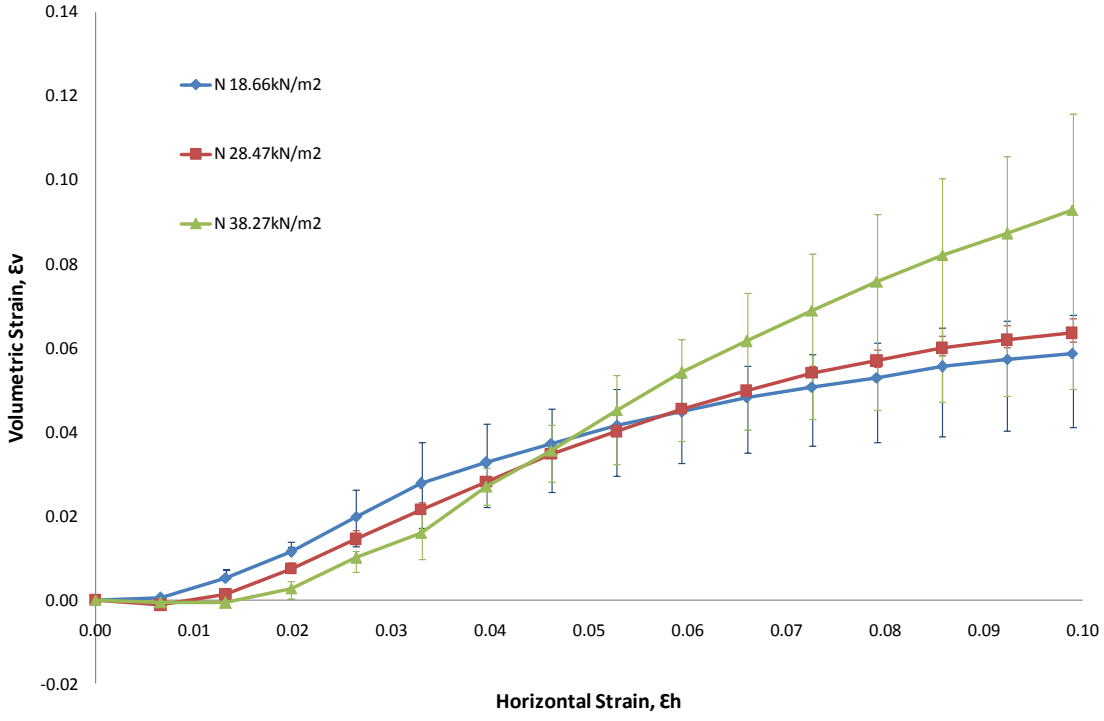

Figure 6.10 Volumetric strain and horizontal displacement for 6.3 - 10 mm gravel

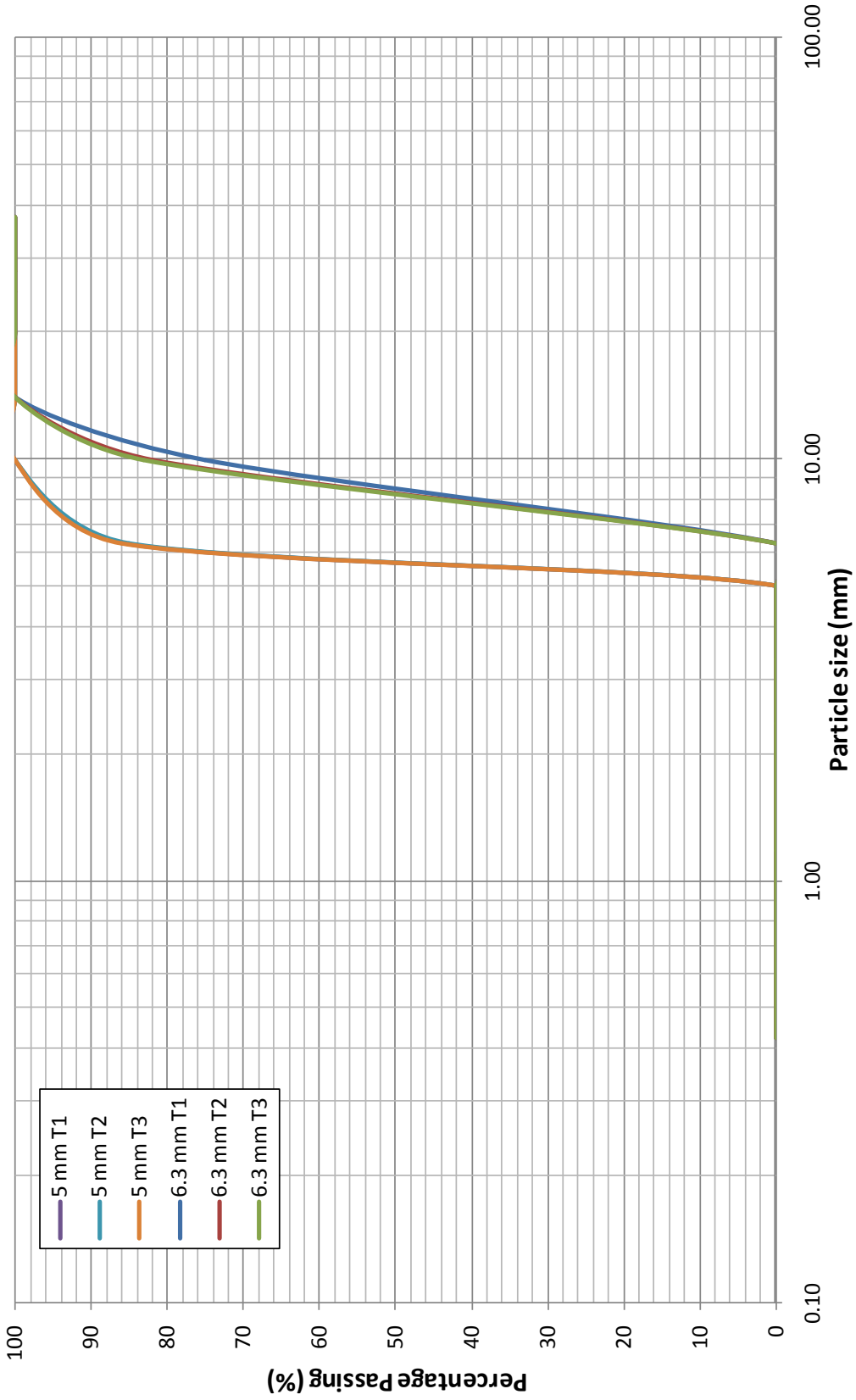

Figure 6.11 Particle sieve analysis of 5 mm - 6.3 mm and 6.3 mm - 10 mm gravels

6.2.6 Conclusion

The testing of gravels in the ranges of 5 - 6.3 mm, 6.3 - 10 mm and 20 - 40 mm reveals that grain size affects the angle of repose, void ratio, and friction angle. The effect of increasing grain size was an increase in angle of repose. The results were found to be comparable to the range of values specified in the literature for gravels. The void ratio of the gravels was found to decrease with increasing grain size, with the values found to be acceptable within the range of values quoted for gravels. The friction angle results for typical river bed gravels was found to be 41.3° this value is close to the angle of repose of 41.7°.

The volumetric strain of the river bed gravel was found to be positive for loads typically applied to stone columns suggesting that the effect can be considered minimal. The degree of crushing of river bed gravel was found to be significant for applied normal loads of 888kN/m² or greater. For stone columns, applied loads to the foundation are typically in the range of 25kN/m² to 50kN/m² so the effect of crushing is not considered significant.

The void ratio obtained for river bed gravel has been used to estimate the volumes of mix material required for the creation of field columns. To allow for a margin of error (and waste) field columns will be assumed to require a volume equivalent to a 0.55 void ratio. Typically for a stone column of length to diameter ratio of 10 and installed diameter of 0.6m, this will equate to a volume of 0.93 m³ or 0.16 m³ of mix per metre assuming void saturation for a wet volume of binder.

6.3 Mix selection, testing and analysis

6.3.1 Introduction

It is recognised that the properties of the soil cannot often be altered and therefore focus is placed upon improving the cohesion and stiffness of granular columns installed in soft clays by the addition of a binder material. This section summaries the methodology used in the identification of binder material and subsequent laboratory testing which was carried out to identify the Young's modulus and cohesion of the material. The stiffness of the material only permitted testing in an Instron testing rig in unconfined compressive strength mode. The composite material was modelled in Plaxis 2D to simulate a triaxial cell to assess the effect of axial and radial pressure on the composite of gravel and binder.

6.3.2 Mix selection criteria

Prior to selecting a potential binder material enquires were made with stone column contractors Pennine Vibropiling to understand the potential challenges in forming a composite stone column composed of gravel and a 'binder' material. Commonly in the United Kingdom bottom feed vibroflotation systems are used due to their ability to deliver material to the tip of the vibroflot, minimise spoil and the potential for cave-in of the borehole. In the specific case of soft clay, maintaining the integrity of the borehole before and during stone placement is crucial to ensuring the integrity of the stone column. The use of the bottom feed system was selected for the construction of composite stone columns for the reasons described earlier and also because the system allows for the injection of fluid to the tip of the vibroflot. Pennine Vibropiling proposes to inject the 'binder' via a modified line attached to the Tremie tube which will allow delivery to the tip of the vibroflot. The 'binder' would need to have a low enough viscosity to be pumped at a low pressure of 1 bar.

The following criteria were devised on an ideal scenario basis following discussions with Pennine Vibropiling. The criteria were applied to all potential materials and used to screen for potential materials. The criteria are as follows:

- The material must bind to the column and offer settlement control by reducing settlements in comparison to a field column.
- The material must not gain significant strength over time (undesirable UCS of 18GPa) as it would behave as a stiff reinforced pile which could require a different foundation type.
- The material must deform elasto-plastically and not suffer from brittle failure under normal stone column working loads of 25kN/m² - 50kN/m².
- The material must not harm the environment or be composed of material components which when broken down in a soluble or water suspended state could cause harm. The material must either have current compliance with on site application regulations or be capable (by its composition) of obtaining such compliance.
- The material must be of sufficient viscosity when in fluid form as to permit saturation of the void spaces between grains. The material must be water based requiring no oil or solvent additive which could harm human health and the environment.

- The material must be chemically stable over time and not be susceptible to acid attack or erosion by exposure to groundwater.
- The material must be economically viable to install as part of a granular column.

6.3.3 Materials identified as potential binders

A number of material suppliers were identified during the initial search for materials which could be used as a binder. Based on the above criteria a number of materials were identified for inclusion in testing.

6.3.3.1 Bitumen

This material has been successfully used as a cohesive material in backfill and surfaces for roads. It has been observed to behave elasto-plastically (Krishnan and Rajagopal, 2003; Hens, 2012). It can show some strength gain over time but can be chemically controlled. The material is commonly used on roads but could pose environmental issues if groundwater is in contact. The material can be fluid when installed and potentially could fill void spaces between grains. The long term stability of the material is unknown and would be composition dependent. The material itself is not expensive but plant and other associated costs could make its use expensive. It was therefore rejected.

6.3.3.2 Cement

This material when added to a column can act as a binder and offer settlement control. The material is considered to have a high strength gain when in pure form, but mixing with additives such as sand to form 'grout' will reduce its strength. The material is known to suffer brittle failure in a pure form, but with additives, this behaviour may be modified. The material is in wide use in foundations and is considered environmentally safe for use, it could also fill the void spaces. It could be subject to chemical degradation but with the addition of further chemicals the susceptibility to acid attack could be reduced. It is in plentiful supply and not expensive to produce. In addition it is easy and cost effective to mix on site without the need for extra equipment. The material is a key component of Protomix and hence was selected for further testing. The cement used in the study was Portland Cement which fully complies with BS EN 197. This material was supplied by the main sponsor of this research, Balfour Beatty Ground Engineering (BBGE).

6.3.3.3 Protomix

The material is a cement-bentonite slurry with other key components which are known to include Pulverised Fuel Ash (PFA). The material is currently used for slurry trench cut-off walls and is subject to on-going confidential development. The material, if able to bind with stone, could offer settlement control. It is known to have strength gain based upon composition and water content (information supplied by Castle Cement). It has been shown to display elasto-plastic behaviour during in-house Castle Cement testing. It is environmentally safe and has a certificate for site use from the manufacturer. It has the potential for flow as demonstrated in laboratory tests. It can saturate voids and is chemically stable. Its cost is within acceptable limits although the requirement of a high shear mixer could add to plant costs. It was therefore selected for further testing and was supplied by Castle Cement.

6.3.3.4 Polymers

Due to the complex nature of the material no reference material was available. The material is known to have been applied in the United States however further information was not obtainable from Vibroflotation companies in this respect due to commercial sensitivities. It became clear that the costs of obtaining materials for testing was beyond the budget of this research. In terms of the above criteria, further consideration was not given as the likely site cost and the lack of information ruled out its consideration. It was therefore rejected on cost grounds.

6.3.3.5 Pulverised fuel ash

Pulverised Fuel Ash (PFA), also known as a fly ash, is a by-product created by the burning of coal at electric power plants (Senol *et al.* 2006). The fine particles which rise with flue gases are termed fly ash whereas coarser particles which do not rise are termed bottom ash. Fly ash is captured by electrostatic precipitators or other particle filtration equipment before flue gases reach the chimney stacks of coal fired power plants. Depending upon the chemical composition of the coal burned (i.e. anthracite, bituminous and lignite) the components of fly ash can vary considerably. Toxic constituents depend on the coal bed composition and tend to be present in trace quantities up to hundreds of parts per million (ppm). Scotash (2007) suggests that fly ash particles are similar in appearance and chemistry as it contains the same basic oxides but in differing proportions and mineralogy. It displays pozzolanic properties in

concrete i.e. it reacts with the lime contained in Portland cement to create cementitious hydrates. PFA has greater pumpability and could potentially be used to pump the mixes directly to the end of the vibroflot without the need for pre-mixing.

Fly ash generated by coal combustion is generally classed in three categories by European Standard BS EN450. Three classes of fly ash are permitted which are characterised by their loss on ignition (LOI): category A LOI not more than 5%; category B LOI between 2 % and 7 %; and category C LOI between 4% and 9%. Categories A and B are permitted for use in concrete in the United Kingdom but category C is not as the LOI upper limit in BS 8500 is 7 %. The fineness of the material utilised in the research is category N which stipulates that no more than 40 % is retained by 45 micron sieves.

This material was discussed at length with Scotash. It is currently used as backfill for roadways, used as a partial replacement for cement in concrete (Siddique, 2003), and some contractors such as Minard use the material in Constant Modulus Columns (CMC). The replacement for cement tends to be in small fractions usually no more than 25 % - 40 % of the dry weight of cement (Scotash, 2007). Lime is required in small amounts to chemically activate the PFA (Siddique, 2003; Venkatarama Reddy and Gourav, 2011). Strength gain of the material over time is dependent upon blend composition i.e. the lower the amount of cement and PFA the lower the strength gain. PFA when combined with small amounts of lime has been known to behave like an elasto-plastic material in roadway applications (as suggested by Scotash in briefing presentation to Pennine Vibropiling). It is deemed not to present an environmental hazard if category A and B (Scotash, 2007) is used and is certified for on-site use. It is water based when mixed with dry components and the viscosity can be controlled, which offers the potential for void saturation between grains. The material is chemically inert with its base component being fly ash. The cost of the material is comparable to cement and was supplied by Scotash free of charge for laboratory testing.

Of the above materials of cement; protomix and PFA a number of added materials were also used to assess their effect in terms of performance. These materials were:

- Lime: added to PFA to activate the material
- Sand: added to cement to form grout
- Gravel: added to form composites with the binder material

6.3.4 Initial testing of potential composite stone column materials

6.3.4.1 Initial testing of the cementitious samples

Initial testing of the 'binder' material was performed in the Avery-Denison compression machine to assess the initial strength of the material. This was to ensure the material strength did not exceed the maximum load capacity of the 100kN Instron compression machine and damage the testing apparatus. Cylindrical composite samples of 100 mm by 200 mm gravels (20 mm – 40 mm) and 'binder' materials of cement, grout, and protomix were created to assess their potential. Initial curing periods of 7, 14, 28, 60 and 90 days were selected for testing. All samples were created with the same water to cement ratio of 0.64. All gravel materials were prepared in accordance with British Standard BS 1377. Testing of the composite samples in the Avery-Denison was carried out in accordance with British Standard BS 1881. The Cement was found to increase in unconfined compressive strength (UCS) from 12 MPa to 17 MPa from an age of 7 to 28 days. Neville and Brooks (1997) suggests that for a water to cement ratio of 0.6 to 0.7 values of compressive strength for 7 and 28 days are 24-32 MPa and 35-44 MPa for concretes made with standard gravel (gravel sizes mostly below 10mm and in accordance with BS EN 12620). Sahin *et al.* (2003) suggests that the strength of concrete is dependent upon the type of aggregate material used in the material. Ozturan and Cecan (1997) suggest that for concretes formed with the same type of paste but with a variable type of aggregate with different shapes, mineralogy and strength, that the strength of concrete varied. It is suggested that with increasing gravel size and the variable composition of river bed gravel, the strength of concrete varies so the values obtained during this initial testing are considered acceptable. The results of the displacement controlled compression testing suggested that both the cement and grout composites were gaining cohesion and strength at a significant rate such that they would act as a stiff pile over time (Table 6.3). By contrast the gain in cohesion and strength of the Protomix over time was much less suggesting that the material could be used as a potential binder material. The Protomix were selected for further testing.

6.3.4.2 Initial PFA samples

Following further discussions with Pennine Vibropiling after the initial cementicious samples were tested, PFA material was identified as a potential binder material. Discussions with Scotash took place to identify potential blends of PFA which could be used during testing. Four types of material which were recommended by Scotash

material engineers in order that the effect of processing by the suppliers could be examined. It is during this processing that the material taken straight from Longannet power station is de-carbonised and sorted according to particle size distribution before packing. The material supplied was as follows:-

- Post-use: This material was supplied in an air tight container with no de-carbonisation or sifting
- Post-decarbonisation: This material was supplied in an air tight container with no sifting
- Post sifting: This was a material supplied in an air tight container with minimal stage 1 sifting which removes the biggest particles. It has a coarse to medium grade particle size.
- Post-final sifting: This was packaged for sale PFA, known as SV-80. It has a uniform particle size distribution of less than 25 microns on average.

The use of PFA tends to be as a replacement for cement. It requires the addition of lime to activate the material chemically. In order to evaluate the potential for the material to be used in a stone column as a 'binder' for each of the four types of PFA supplied four mix ratios were selected (Table 6.4). The binder material was formed with a water to cement ratio of 0.64. The results suggested that for four dry weight ratios of PFA to lime of 2:1, 5:1, 10:1 and 20:1 none of the samples were able to bind to the gravels for the three selected curing periods and as such no viable samples were obtained for testing in the Instron. In order to overcome the issue of sample failure an additional number of samples were created with a cement fraction of 2.5 %, 5 % and 10 % (Table 6.4). The samples with cement contents of 2.5 % and 5 % were found to fail in the same manner as the earlier PFA samples once the mould was removed. The 10% cement fraction samples were removed from the moulds and were initially stable until they were moved from the base of the mould at which point they collapsed. It was noted that during the four curing periods examined of 7, 14, 28 and 90 days that the inability of the PFA to bond to the gravel would present significant challenges in determining both composite material properties and obtaining confidence that the material could obtain sufficient strength longer term. Typically, stone columns are ready for foundation construction after installation. Any delays in gaining strength would severely impact the usability of the material and a composite column technique.

Further examination of composite pieces (PFA and gravel) for all four PFA types of the air cured; water cured and samples with cement fraction beneath the microscope revealed that unlike the earlier cementacious samples there appeared to be no real binding to the gravel. Handling of the initial mixes had indicated that the Post-use and Post-Decarbonisation materials were much weaker than the other samples. Also there was some concern that the presence of carbon could have an effect on obtaining certification for safe environmental use and as such they were discontinued. The SV80 PFA had shown some promise. It appeared to bind better than the earlier PFA samples but its inability to bind to the gravel led to the PFA testing being discontinued. It was decided after further discussion with Scotash that the material would be unsuitable as binder material in a granular column.

	Unconfined Compressive Strength (kN/m²)		
	7	14	28
Cement Slurry	12,688	16,590	17,634
3 to 1 Grout	6,493	8,455	13,550
4 to 1 Grout	2,043	3,575	6,293
Protomix	240	350	609

Table 6.3 Initial testing of cementitious samples

Description of mix	Composition (% of sample)			Granular	Test by Curing periods (3 samples)		
Composition tested	PFA	Lime	Cement	component	7	14	28
2 parts PFA to one part Lime	66.6%	33.3%	0.0%	6.3mm	Failed	Failed	Failed
5 parts PFA to one part Lime	83.0%	16.0%	0.0%	6.3mm	Failed	Failed	Failed
10 parts PFA to one part Lime	91.0%	9.0%	0.0%	6.3mm	Failed	Failed	Failed
15 parts PFA to one part Lime	93.7%	6.3%	0.0%	6.3mm	Failed	Failed	Failed
20 parts PFA to one part Lime	95.2%	4.7%	0.0%	6.3mm	Failed	Failed	Failed
2 parts PFA to one part Lime, 2.5% cement	65.0%	32.5%	2.5%	6.3mm	Failed	Failed	Failed
2 parts PFA to one part Lime, 5% cement	63.3%	31.6%	5.0%	6.3mm	Failed	Failed	Failed
2 parts PFA to one part Lime, 10% cement	60%	30%	10.0%	6.3mm	Failed	Failed	Failed

Table 6.4 Pulverised fuel ash mixes description

Group	Batch Code	Sample Codes	Description of Samples	Curing (days)	Water to Cement Ratio
1	G1-1	G1-1/1 to G1-1/9	3.35 mm gravel-protomix composite	7, 14, 28	0.54
	G1-2	G1-2/1 to G1-2/9	5.00 mm gravel-protomix composite	7, 14, 28	0.54
	G1-3	G1-3/1 to G1-3/9	6.30 mm gravel-protomix composite	7, 14, 28	0.54
	G1-4	G1-4/1 to G1-4/9	10.0 mm gravel-protomix composite	7, 14, 28	0.54
2	G2-1	G2-1/1 to G2-1/9	6.30 mm gravel-protomix composite	7, 14, 28	0.65
	G2-2	G2-2/1 to G2-2/9	6.30 mm gravel-protomix composite	7, 14, 28	0.54
	G2-3	G2-3/1 to G2-3/9	6.30 mm gravel-protomix composite	7, 14, 28	0.50
3	G3-1	G3-1/1 to G3-1/9	All chosen grain sizes	14	0.50
	G3-2	G3-2/1 to G3-2/9	All chosen grain sizes	14	0.44

Table 6.5 Protomix composites description

6.3.5 Final mix testing

The initial mix testing showed that of the examined materials of cement, grout, PFA and Protomix, that only one material would be suitable according to the aims of the research. The cement and grout was found to increase in strength leading towards a stiff pile. The PFA appeared to fail to bind to the granular material to such an extent that the gravel could be washed and the PFA removed. The Protomix did behave similarly to the cement and grout but with a lower degree of gain in stiffness making further consideration of the material possible.

Three trial groups were developed with a view to assessing how the Protomix might behave when combined with gravel. The availability of moulds was such that the 2:1 moulds were chosen, i.e. the size of the samples was 200mm long by 100mm in diameter.

The three trial groups had different objectives. Group 1 was designed to assess the effect of grain size on Protomix. Group 2 was designed to assess the effect of water content on Protomix. Group 3 was designed to assess the effect of multiple grain sizes scaled to be proportionate in terms of composition to a field column range of sizes. Table 6.5 summaries the group tests performed.

6.3.6 Testing methodology and data interpretation

The samples tested during the final mix testing were composed of gravel and Protomix. During initial testing in the Avery-Denison compression machine the compressive strength of the material was greater than the 5kN load limit of the triaxial cell in the Geotechnical laboratories. As a consequence the Instron machine with a maximum load limit of 100kN in the Structures laboratory was selected. The Instron unconfined compression tests were carried out under displacement control according to British Standard BS 1881. Values for applied vertical load (kN) and displacement (records in inches and later converted to metric) were recorded by the Instron computer. The Instron computer system is pre-programmed by default to use pre-load which is designed to remove any slack in a specimen before testing starts (Instron, 2005). From previous testing no change in the sample height was noted at low loads of 1 kN so re-calibration of the system was not performed to record values of load and displacement. The 100 kN load cell is compliant with BS1610 Part 1 1992 and BS EN ISO 7500 and

has an accuracy of 0.5% of the 100kN rating. Two displacement transducers were placed at mid height of the sample to record any changes in diameter of the sample.

Values for applied stress were calculated from the area of the sample in contact with the platen and the strain calculated from the reduction in sample length compared to original length. Where appropriate displacement transducer data was used to account for changes in effective area. The data was then plotted on a stress-strain graph with the elastic domain and yield point identified. The Instron only captures data above the minimum pre-load force which is approximately ~1kN.

To obtain a value for the elastic modulus the procedures outlined in British Standard BS 1881 and ASTM (2002) were consulted. The sample initial length, L_0, and the changing sample length, ΔL, with displacement is used to calculate the strain, ε. The strain is used to compute the effective sample cross sectional area, *A'*. This is done by division of the original sample cross sectional area, A_0, by 1 minus the strain. The stress applied to the sample is calculated by dividing the force reading from the Instron (in kN) by the effective sample cross-sectional area. A plot is then generated for the applied stress (kPa) and strain. The gradient of the line prior to the yield point is used to determine the chord modulus for the samples. Although pre-loading has been used by the Instron system it does not affect calculation of the chord modulus for each sample. The calculation of Young's modulus and Poisson's ratio is from equations 6.3 and 6.4 respectively:

$$\textit{Chord Modulus, } E = ((S_2 - S_1)/(\varepsilon_2 - 0.000050))*6.894757 \qquad [6.3]$$

where E = chord modulus of elasticity (kPa)
S_2 = stress corresponding to 40% of the ultimate load
S_1 = stress corresponding to a longitudinal strain, ε_1, of 50 micro-strain
ε_2 = longitudinal strain produced by stress S_2

$$\text{Poisson's ratio, } \nu = (\varepsilon_{t2} - \varepsilon_{t1})/(\varepsilon_2 - 0.000050) \qquad [6.4]$$

where ν = Poisson's ratio
ε_{t2} = transverse strain at mid-height of the specimen produced by stress s_2
ε_{t1} = transverse strain at mid-height of the specimen produced by stress s_1

6.3.7 Group 1 testing: effect of grain size

During discussions with Pennine Vibropiling the issue of clogging of the Tremie Tube had been identified which can affect the installation times of stone columns. This can lead to longer construction times and potentially a greater disturbance to the soil. Sand columns have a considerably reduced grain size when compared to stone columns, described by Aboshi *et al.* (1979), and in clays had proven successful in reducing settlements which suggested finer grained gravels could be used. An assessment was made of the cohesion, stiffness and strength characteristics to determine if a gravel and Protomix composite in the bulging zone could reduce column deformation and reduce settlement. The effect of gravel size on mix strength and stiffness behaviour was assessed using grain sizes in groupings of 3.35mm to 5.00mm; 5.00mm to 6.30nm; 6.30mm to 10mm and 10mm to 14mm samples. The samples were prepared using a water to cement ratio of 0.54 which had been identified by earlier testing as a suitable viscosity so as to allow mixing with the different grain sizes. The samples were cured according to testing requirements of 7, 14 and 28 days. During this period the samples gained sufficient strength to allow testing. However, the 14 day samples for G1-1 (Table 6.5), and the 14 and 28 day samples for G1-4 were damaged in the curing tank. Due to lack of material the tests could unfortunately not be repeated.

Figures 6.12 to 6.19 show the applied stress versus strain plots for Group 1 samples. The tests were interpreted to obtain values for stiffness and cohesion of the composite material for each gravel type and curing age. The interpreted results are shown in Table 6.6. The cohesive strength was plotted against grain size as show in Figure 6.20. It is observed for 7 day curing that with increasing grain size the cohesion reduces. From Figure 6.20 the equation suggests the relationship for the cohesion:

$$\text{Cohesion, } C = -21.154g + 457.63 \qquad [6.5]$$

where g is the grain size. This implies that if the relationship holds for a field column of say 20mm, the cohesive strength could become 34.55kPa. The 14 day curing samples indicate no significant increase or decrease in cohesive strength with grain size. The 28 day samples show a general decrease in strength with increasing grain size. However, it is suggested that the conditions in the curing tank may have affected the results. Figure 6.21 shows a plot of stiffness and grain size. The stiffness data does not clearly show a relationship between stiffness and grain size. For samples of 7 day curing it is suggested that with increasing grain size the stiffness is reduced. The data for 14 day

and 28 day curing does not illustrate a clear relationship between grain size and stiffness. Sample movement was not detected by the displacement transducers placed at opposing sides of the sample at mid-height. The transducers have a calibrated accuracy of 0.5mm. It is possible that the samples were moving at other positions not detected by the displacement transducers due to placement.

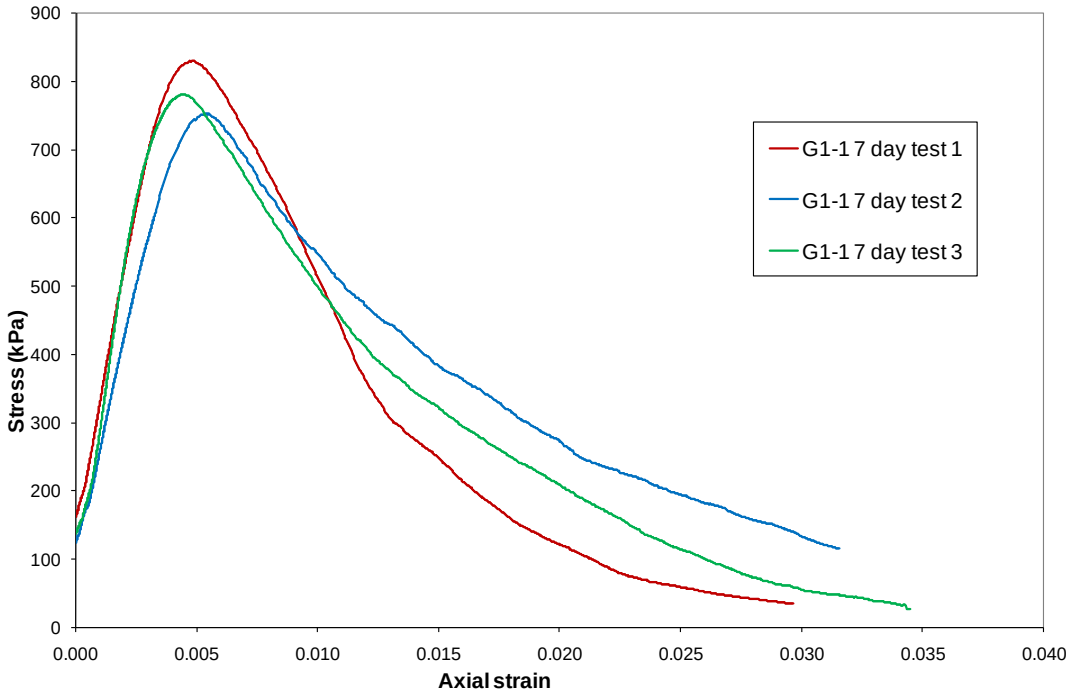

Figure 6.12 G1-1 7 day Protomix tests

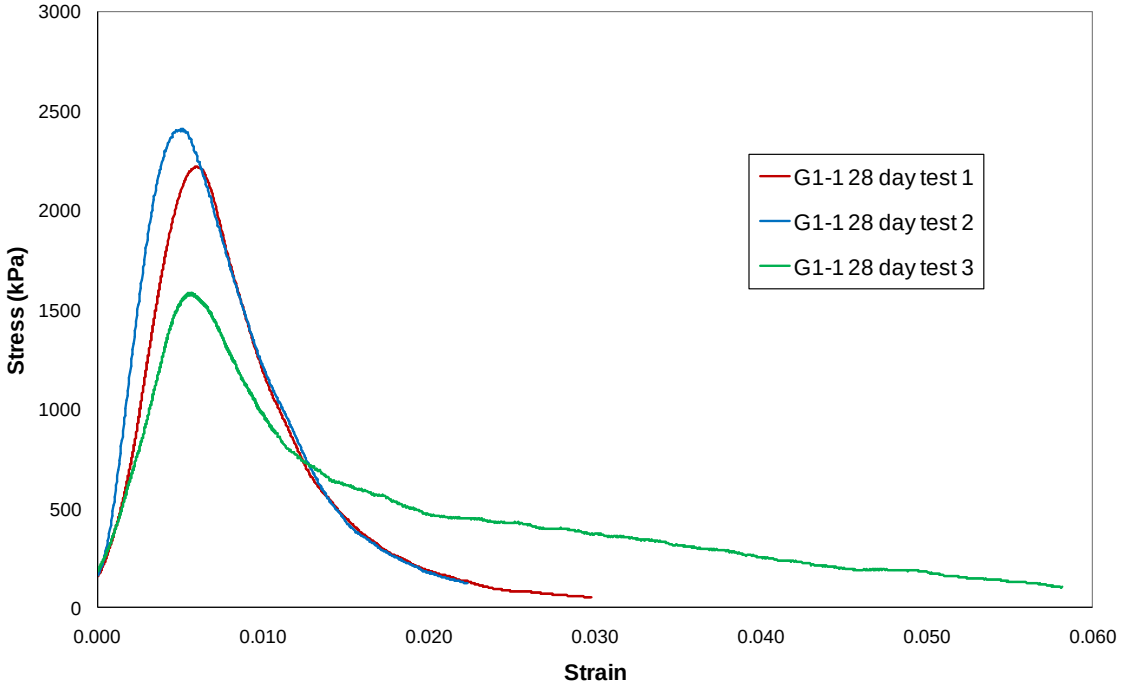

Figure 6.13 G1-1 28 day Protomix tests

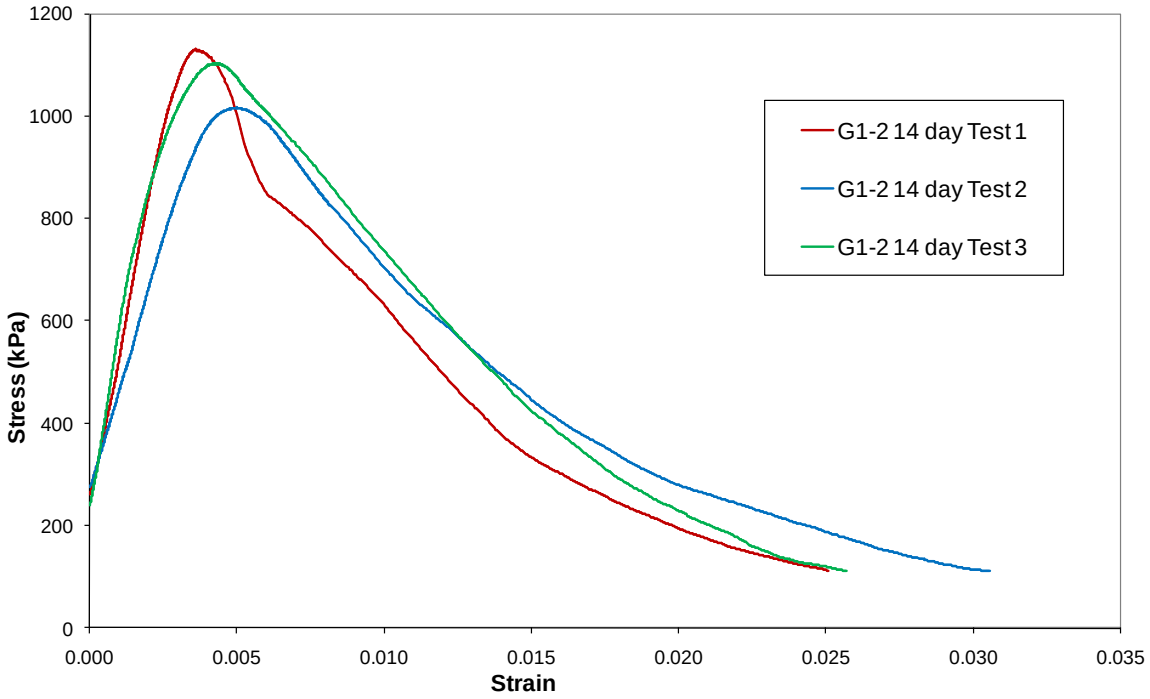

Figure 6.14 G1-2 14 day Protomix tests

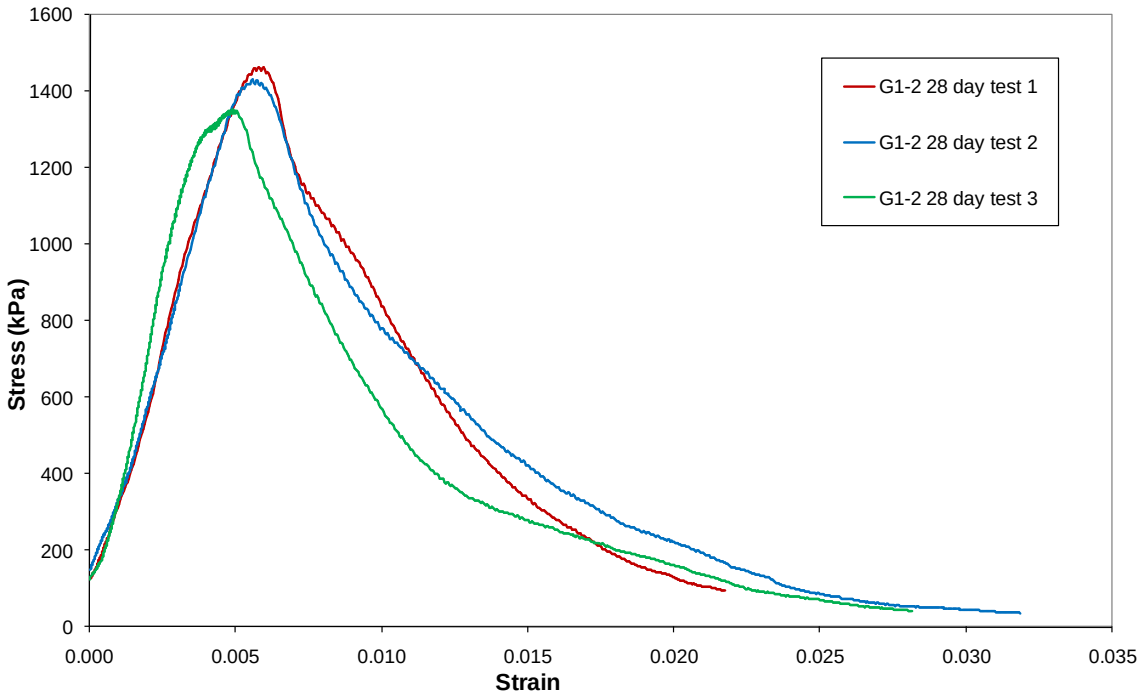

Figure 6.15 G1-2 28 day Protomix tests

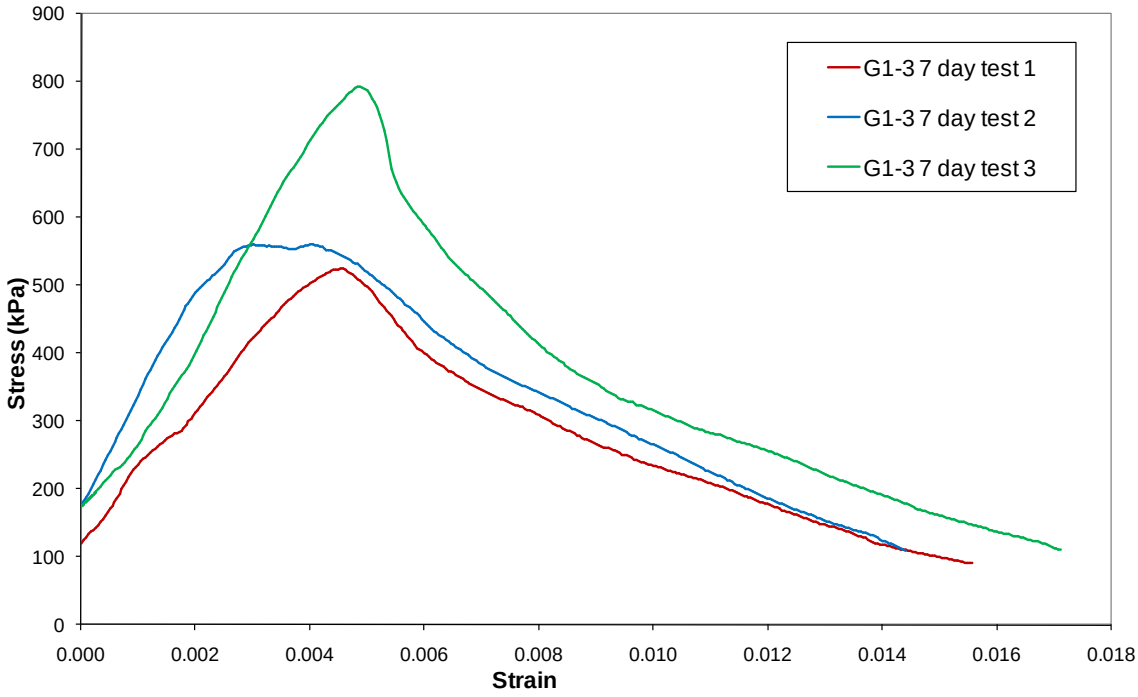

Figure 6.16 G1-3 7 day Protomix tests

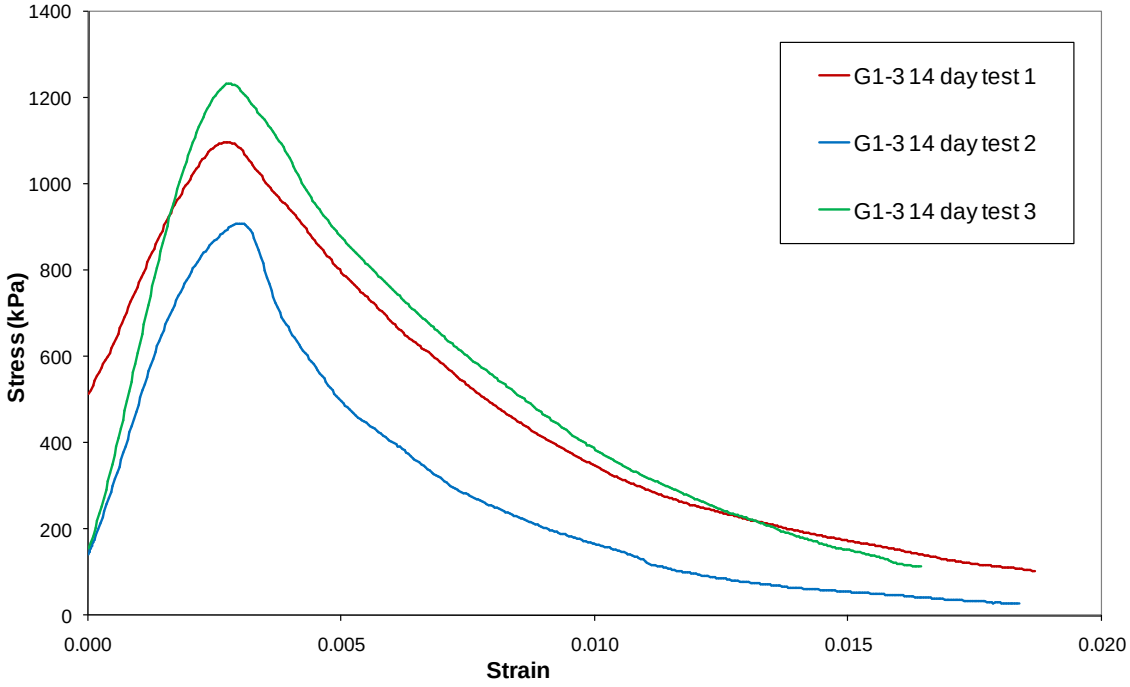

Figure 6.17 G1-3 14 day Protomix tests

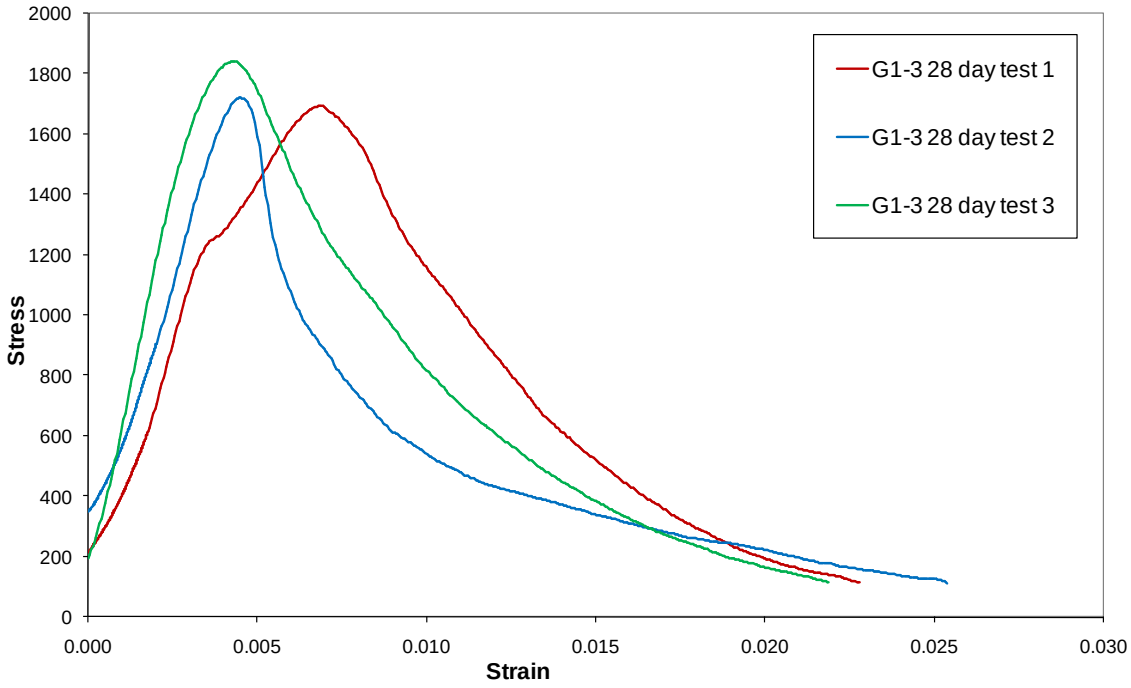

Figure 6.18 G1-3 28 day Protomix tests

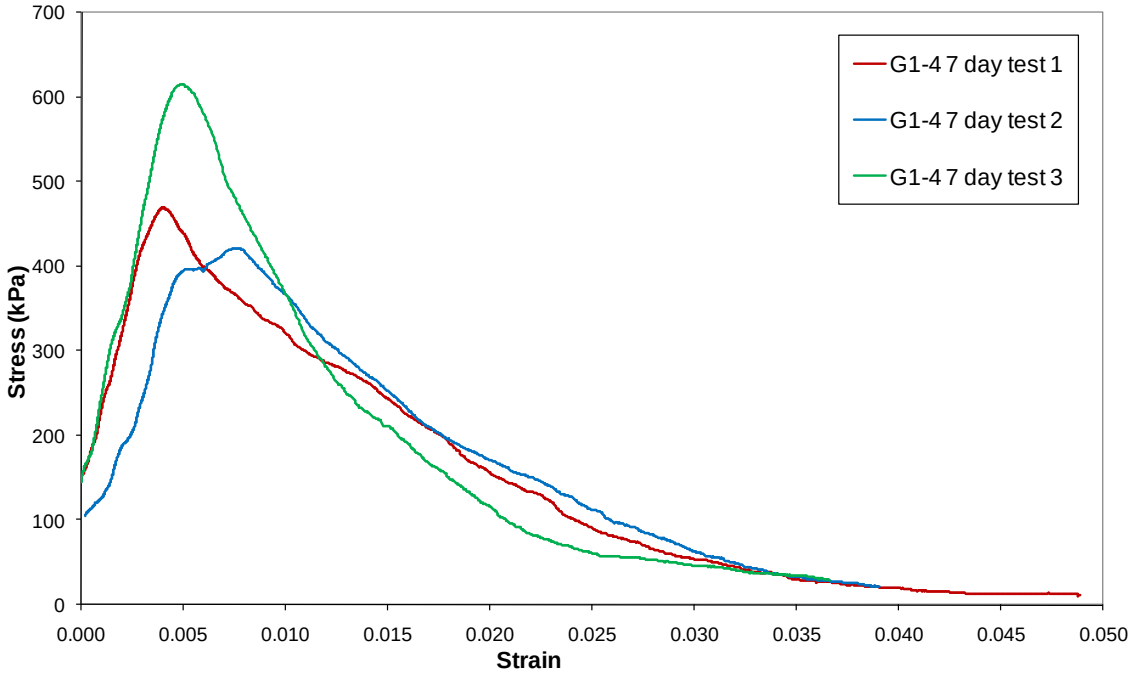

Figure 6.19 G1-4 7 day Protomix tests

Group	Batch Code	Water to Cement Ratio	Curing (days)	Young's Modulus (kN/m²)			Cohesion (kPa)		
				Minimum	Maximum	Average	Minimum	Maximum	Average
1	G1-1	0.54	7	187,969	235,017	203,651	375	414	393
	G1-1	0.54	28	309,981	620,397	516,780	792	1,207	1,036
	G1-2	0.54	14	249,391	353,510	271,672	509	562	541
	G1-2	0.54	28	289,097	317,533	298,576	675	732	708
	G1-3	0.54	7	94,382	144,913	122,859	262	397	313
	G1-3	0.54	14	284,785	366,819	337,597	454	617	540
	G1-3	0.54	28	270,514	744,030	521,890	847	921	876
	G1-4	0.54	7	76,003	95,026	88,685	211	308	251

Table 6.6 Group 1 interpreted results

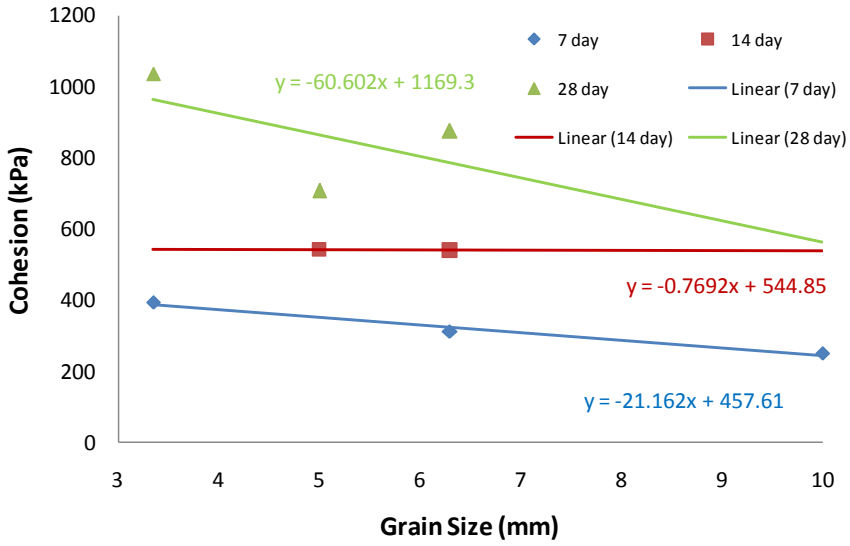

Figure 6.20 Comparison of the effect of grain size on cohesion of composite samples

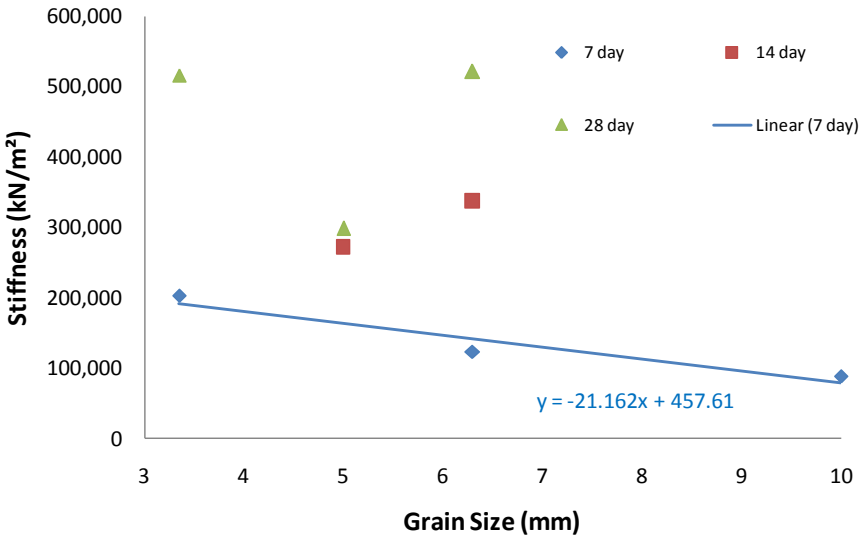

Figure 6.21 Comparison of the effect of grain size on stiffness of composite samples

6.3.8 Group 2 testing: effect of water to cement ratio

The effect of water to cement ratio on mix strength and stiffness behaviour was assessed using a grain sizes of 6.30mm to 10mm. This gravel size was selected as it was considered by Pennine Vibropiling to offer the optimum size and was readily available for use in a future field trial. Gravels of 3.35mm to 5.00mm and 5.00mm to 6.30mm were difficult to obtain in sufficient quantity to permit further testing. This testing will also assess the strength of the proposed column during the construction period. It is accepted that with time Protomix composites will gain strength. Typically installed stone columns can be built on within a few days of construction. It is therefore crucial to understand what potential cohesive strength and stiffness properties the columns are likely to have during the foundation construction period.

The samples were formed using three water to cement ratios to assess the effect on stiffness and cohesive strength. The values chosen represent the upper and lower bounds at which the Protomix is useable for sample formation. The water to cement ratios trialled were 0.64; 0.54 and 0.5. The composite samples were cured according to testing requirements of 7, 14 and 28 days and during this period they gained strength to allow testing.

Figures 6.22 to 6.30 show the applied stress versus strain plots for Group 2 samples. The tests were interpreted to obtain values for stiffness and cohesion of the composite material for each water to cement ratio and curing age. The interpreted data is shown in Table 6.7. The cohesive strength is plotted against curing age for each test batch in Figure 6.31. It can be observed that with increasing curing there is a strength gain for all water to cement ratios. The water-cement ratio of 0.64, Group 2-1, appears to show the lowest gain. From Figure 6.31 Group 2-1 has a cohesion which is related to curing time, *t*, by the relationship:

$$\text{Cohesion, } C = 12.64t + 163.78 \qquad [6.6]$$

If a linear trend was maintained beyond a period of 365 days the cohesive strength would be approximately 4777 kPa. For a water to cement ratio of 0.54, Group 2-2 appears to closely follow the trend of Group 2-3.

This group has a water to cement ratio of 0.54. It is suggested that below a water to cement ratio of 0.54 the differences in cohesion are minimal with curing time. In group 2-2 the cohesion, can be related by the curing time, t through the equation:

Cohesion, C= 25.44t+154.58 [6.7]

In group 2-3 the cohesion can be related by the curing time, t by the equation:

Cohesion, C= 26.709t+120.85 [6.8]

For a period of 365 days, assuming cohesion follows a linear trend, the cohesion can be approximated for groups 2-2 and 2-3 to 9440kPa and 9869kPa respectively. It is suggested that post installation of the Protomix/ gravel composite in the bulging zone that sufficient strength will exist 7 days later such that foundation construction can commence. The unconfined compressive strength is much lower than that of concrete which will allow the use of this material without the need for pile specific foundations. From the results of Group 1 it is clear that with increasing grain size, 7 day cohesive strength appears to reduce. If the Protomix material is used with a larger grain size the cohesive strength gain could potentially reduce. If the issues with the Tremie tube can be overcome by a future re-design of the vibroflot then a larger grain size could be used.

Figure 6.33 illustrates a plot of cohesion and water to cement ratio for three curing periods. It can be seen that for all curing periods a decrease in water to cement ratio indicates a higher cohesive strength. The three water to cement ratios represent the upper and lower limits of the Protomix material when added to granular material in the size range 6.3mm to 10.00mm.

Figure 6.34 illustrates a plot of stiffness with time for three different water to cement ratios as defined earlier. The data suggests that stiffness is reducing with reducing water to cement ratio which is considered due to the composition of the Protomix material. The material contains a high fraction of clay and if a low water to cement ratio is used the clay present will have a larger effect on stiffness as the cement is not fully hydrated. Interestingly the 14 day curing period indicates a close correlation between stiffness values. The group G2-3 appears to show a reduction in stiffness strength gain beyond the 14 day period with a water to cement ratio of 0.5. The trends for groups G2-1 and G2-2 illustrate a linear gain in strength with time suggesting an increase in stiffness with time. For the different test groups the stiffness relationship, Y, can be related to curing time for each water-cement ratio as shown in Figure 6.34. It should be noted that the 90 day samples were damaged during a tank move and insufficient material was available to recreate the samples. The material was found to dry out when exposed to air conditions over a two day period. A leak fault of one of the two curing

tanks caused the tank to drain and leave the samples exposed to air which impacted their curing behaviour. Sample movement was not detected by the displacement transducers placed at opposing sides of the sample at mid-height. The transducers have a calibrated accuracy of 0.5mm. It is possible that the samples were moving at other positions not detected by the displacement transducers.

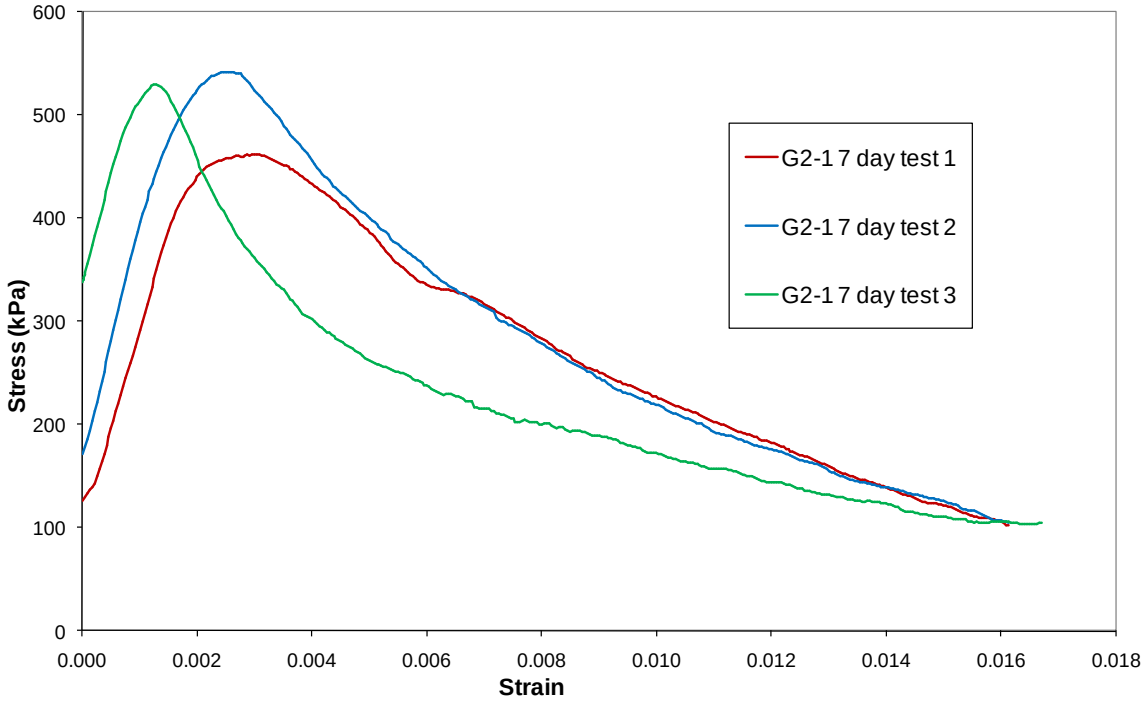

Figure 6.22 G2-1 7 day Protomix tests

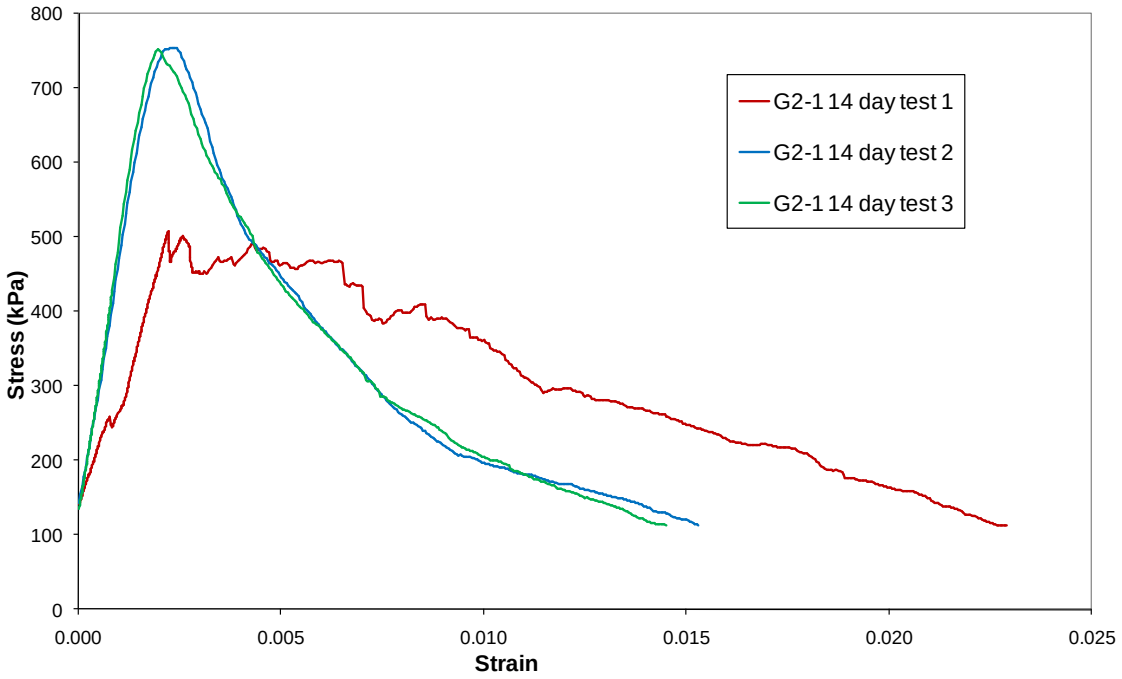

Figure 6.23 G2-1 14 day Protomix tests

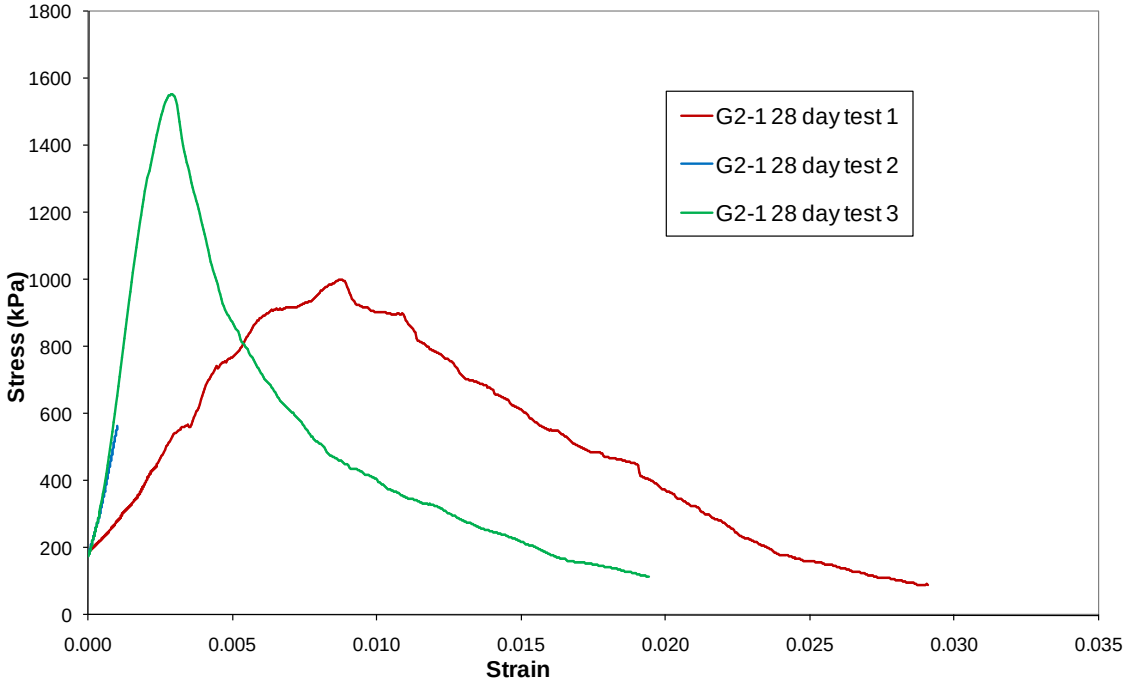

Figure 6.24 G2-1 28 day Protomix tests

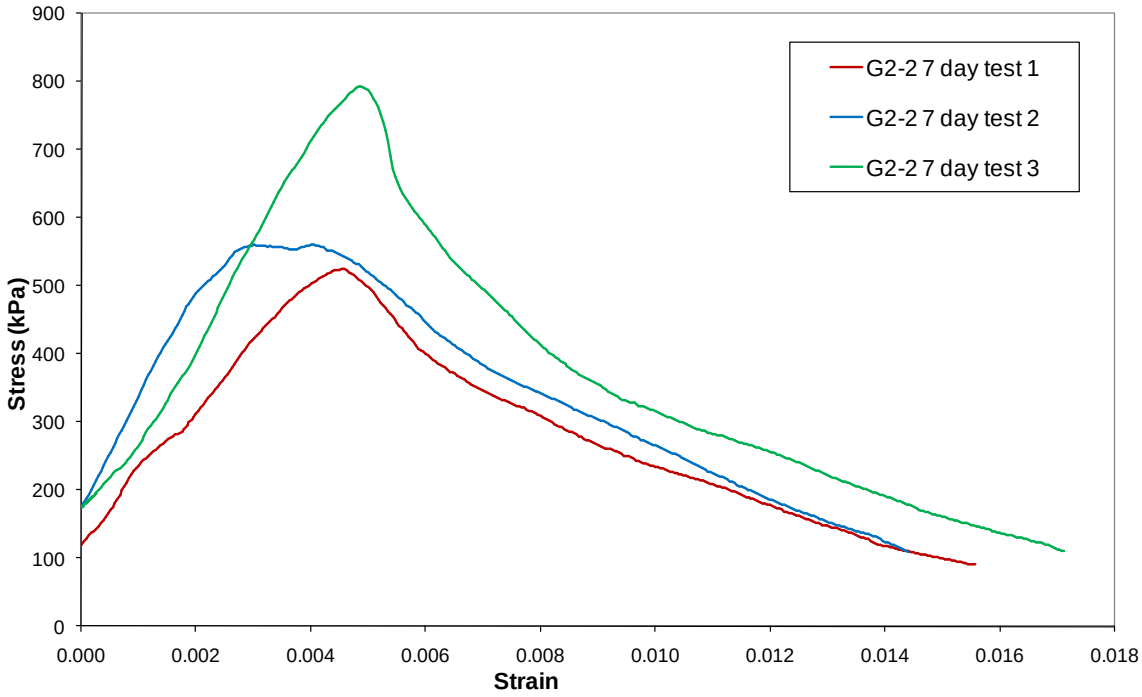

Figure 6.25 G2-2 7 day Protomix tests

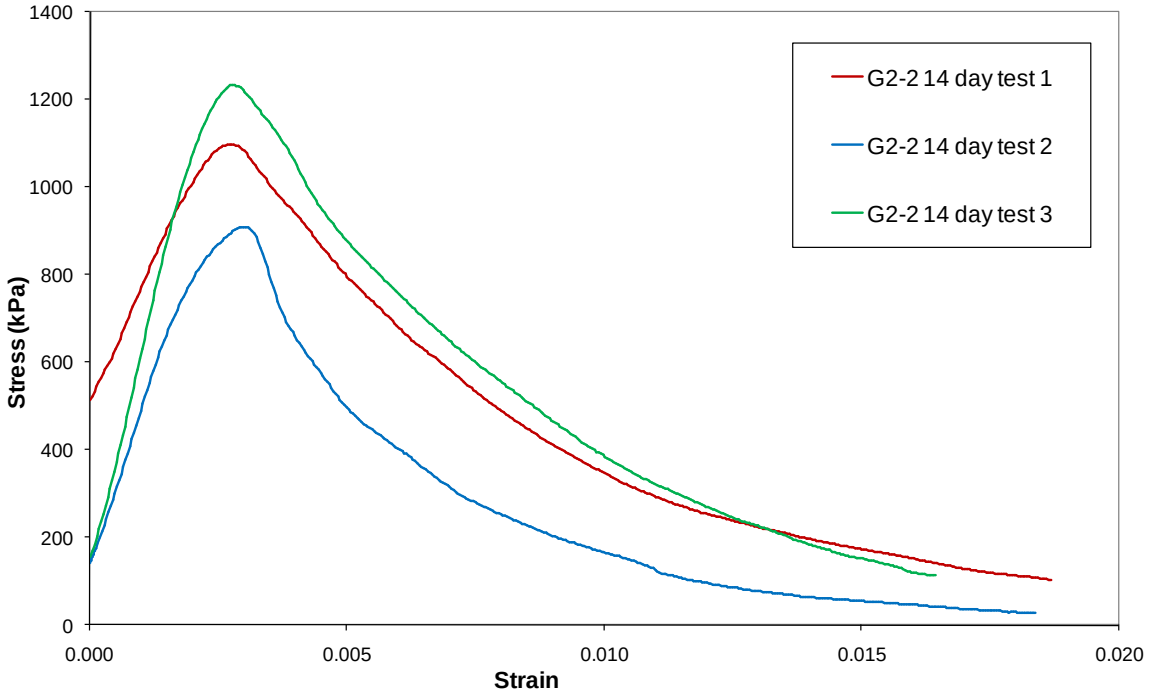

Figure 6.26 G2-2 14 day Protomix tests

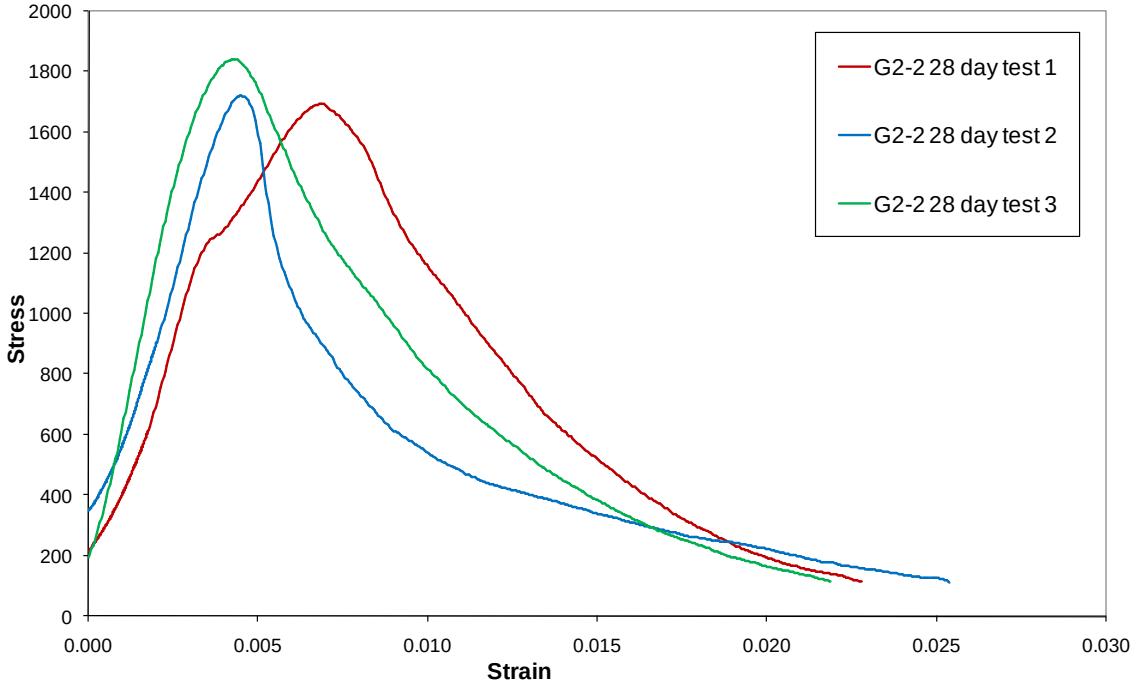

Figure 6.27 G2-2 28 day Protomix tests

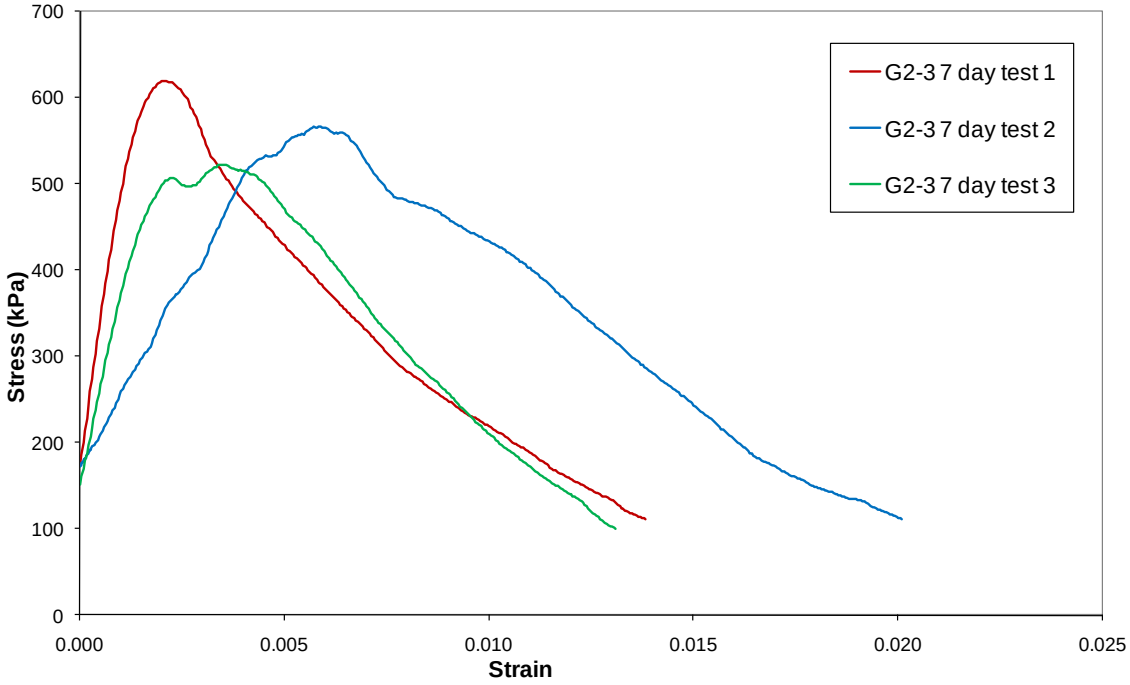

Figure 6.28 G2-3 7 day Protomix tests

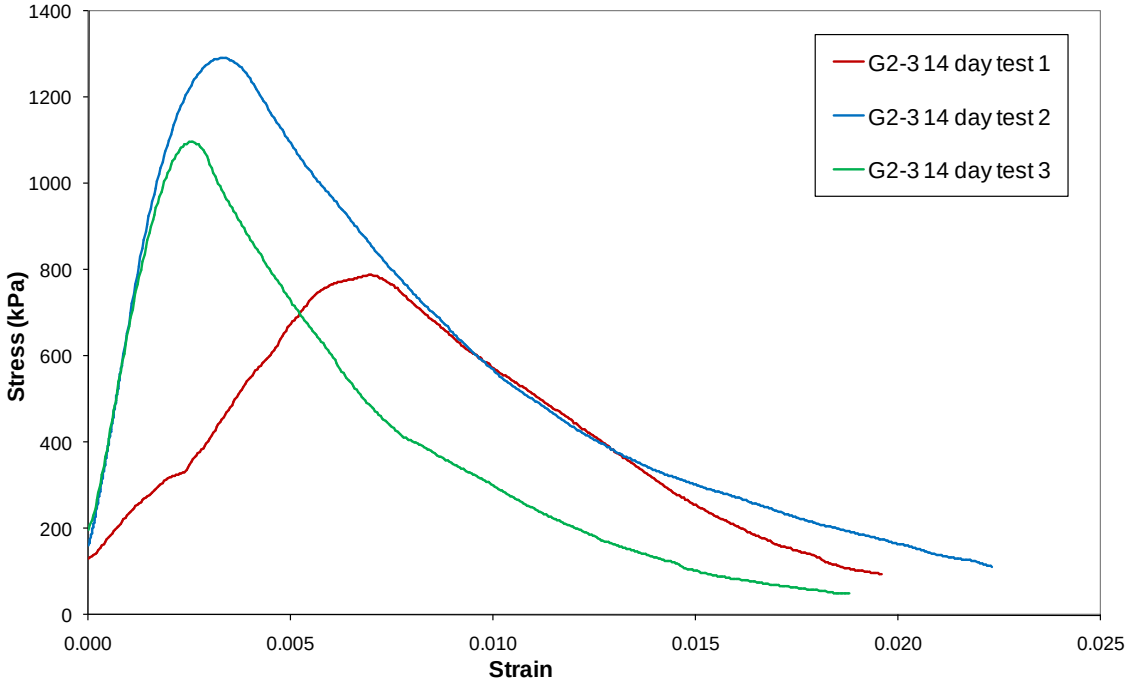

Figure 6.29 G2-3 14 day Protomix tests

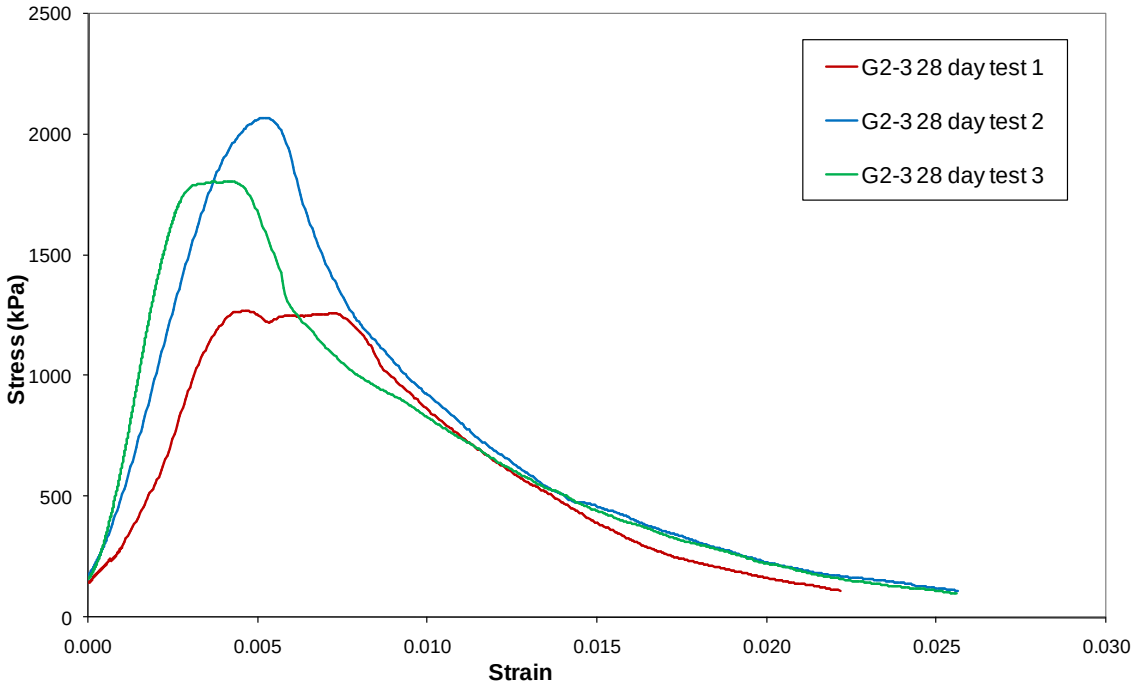

Figure 6.30 G2-3 28 day Protomix tests

Group	Batch Code	Water to Cement Ratio	Curing (days)	Young's Modulus (kN/m²)			Cohesion (kPa)		
				Minimum	Maximum	Average	Minimum	Maximum	Average
2	G2-1	0.65	7	191,222	191,222	191,221	231	271	256
	G2-1	0.65	14	162,158	360,288	294,245	254	377	336
	G2-1	0.65	28	98,639	706,737	448,731	282	777	519
	G2-2	0.54	7	94,382	144,913	122,859	262	397	313
	G2-2	0.54	14	284,785	366,819	337,597	454	617	540
	G2-2	0.54	28	270,514	744,030	521,890	635	1,035	857
	G2-3	0.50	7	85,644	304,024	180,617	261	310	285
	G2-3	0.50	14	102,934	493,547	363,342	394	646	529
	G2-3	0.50	28	302,587	477,121	368,736	635	1,035	857

Table 6.7 Group 2 interpreted results

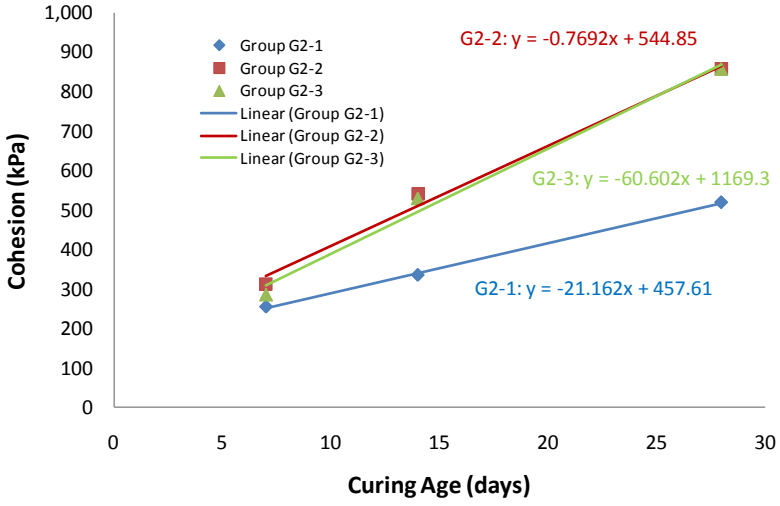

Figure 6.31 Comparison of the effect of curing age on Cohesion of composite samples

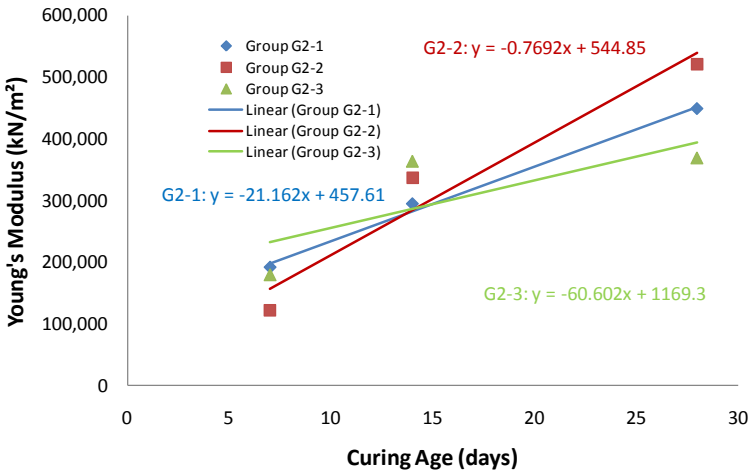

Figure 6.32 Comparison of the effect of curing age on Stiffness of composite samples by group

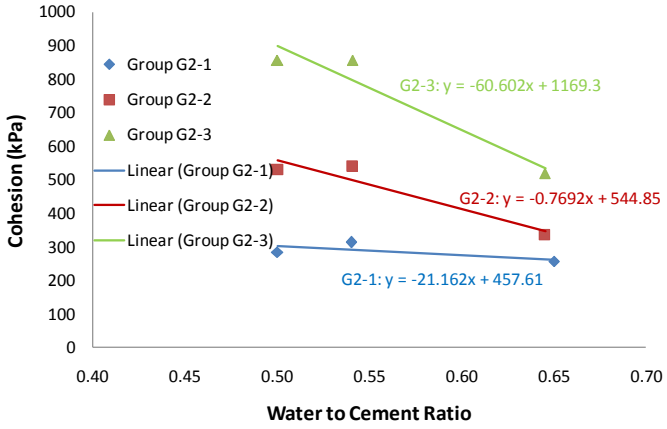

Figure 6.33 Comparison of the effect of water cement ratio on cohesion of composite samples by water to cement ratio

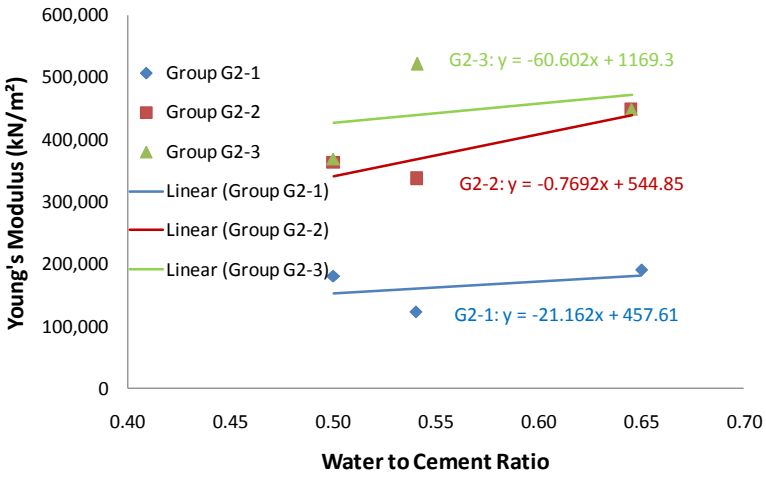

Figure 6.34 Comparison of the effect of water cement ratio on stiffness of composite samples by water to cement ratio

6.3.9 Group 3 testing: scaled column

This group of tests on gravel-Protomix composites examined the effect of variable grain size on sample behaviour. The samples contained scaled gravels representative of different sizes of aggregates normally found in a bottom fed 20-40mm field column to replicate the PSD curve shape. The samples were formed with the intention that all grain sizes should be as uniformly mixed as possible. The four grain sizes of 3.35mm; 5.00mm; 6.30mm and 10.00mm were pre-mixed by hand before being added to the main mix and then mixed in by hand. Due to the limited supply of gravel sizes, samples were formed only for 14 and 28 day curing periods. The 28 day period samples collapsed during removal from the curing tank while held in a mould. Two water to cement ratios were trialled in order to assess if the material would have the same increase in strength with different grain sizes. Water to cement ratios of 0.5 and 0.44 were trialled. A value of 0.44 was considered during formation to be very close to the lower bounds of sample formation with Protomix, and in order to ensure gravel to gravel contact the material was lightly compacted and the sample topped up before applying the top cap to the mould. The earlier testing of Group 2 had examined the effect of water to cement ratio on column stiffness and cohesion. The results suggested an increase in cohesion with a decrease in water to cement ratio. Given the potential difficulty of mixing materials on site the effect of decreasing the ratio was examined i.e. making the material 'water hungry'.

The results of Group 3-1 are shown graphically in Figure 6.35. The 14 day tests reveal a considerable variation between samples in terms of stiffness. Across the three samples the range of stiffness values is 99,393 to 246,785 kN/m² with a mean value of 148,524 kN/m². The range of values would seem to indicate considerable variation in behaviour due to grain size variations. The cohesion values for the three samples were in the range 544 to 708 kPa with an average cohesion value of 609 kPa.

The results of Group 3-2 are shown graphically in Figure 6.36. The 14 day tests reveal considerable variation between samples in terms of stiffness with values in the range of 50,000 to 197,370 kN/m² (Table 6.8). The average stiffness value is 113,855 kN/m². The cohesion was found to be in the range of 388 to 546 kPa with an average cohesion value of 454 kPa (Table 6.8). It is clear from the data that in terms of average stiffness and cohesion the G3-2 samples, with a lower water to cement ratio, appear to have lower values than the G3-1 samples.

The displacement transducers have a calibrated accuracy of 0.5 mm and were placed at opposing sides of the sample at mid-height. No sample movement was recorded by the transducers. It is possible that sample movement occurred at other positions not measured by the displacement transducers.

The results suggest that there is considerable variation in the composite properties when grain size is varied. When using river bed gravels for conventional stone columns there will be a variation in grain sizes i.e. no two columns will have the exact same grain sizes. This creates potential issues since the above results indicate cohesion and stiffness varies with composition within a sample which has been graded and formed with the same particle size distribution. Within a field column, with a range of grain sizes between 20 mm and 40 mm, the effect will be potentially greater. A field trial is required to confirm this finding.

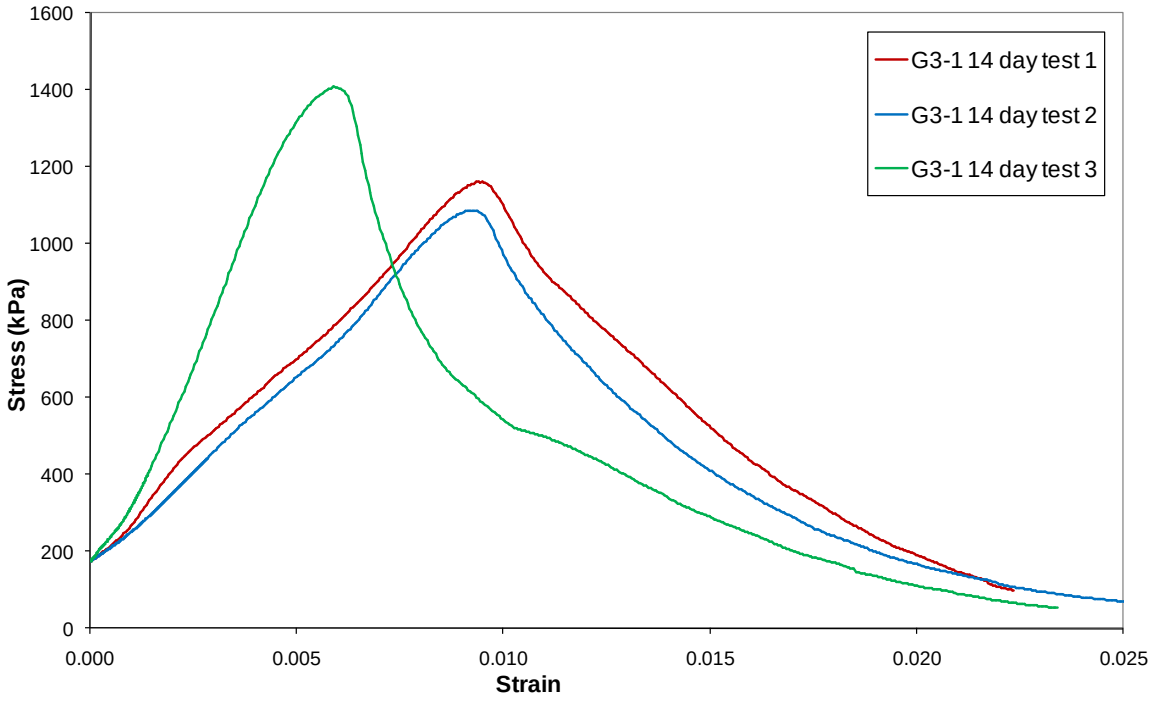

Figure 6.35 G3-1 14 day Protomix tests

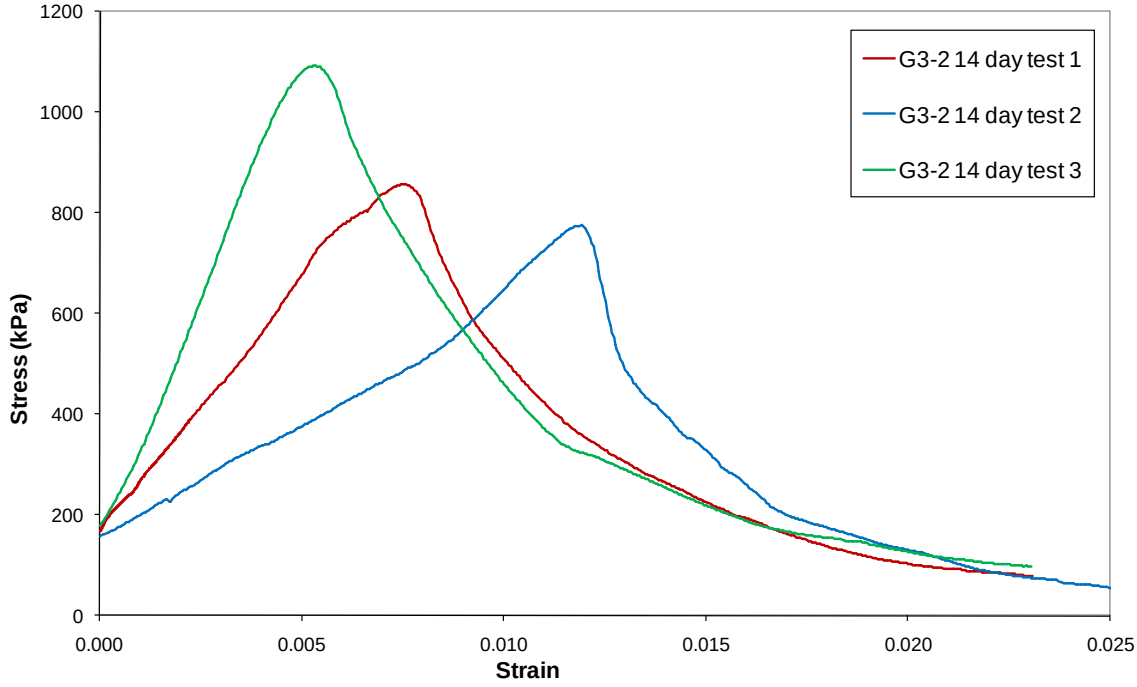

Figure 6.36 G3-2 14 day Protomix tests

Group	Batch Code	Water to Cement Ratio	Curing (days)	Young's Modulus (kN/m²)			Young's Modulus (kPa)		
				Minimum	Maximum	Average	Minimum	Maximum	Average
3	G3-1	0.50	14	99,394	246,786	148,525	544	704	609
	G3-2	0.44	14	50,000	197,370	113,855	388	546	454

Table 6.8 Group 3 interpreted results

6.4 Conclusion

The mix selection, testing and analysis had sought to screen and identify potential materials which could be combined with gravel to form a composite column. This composite column would be used as a partial replacement for a stone column in the bulging zone while preserving the consolidation and drainage benefits of the column below this zone. The testing identified a number of potential materials which could be used to bind the column. Initial testing of cement, grout, and PFA ruled them out as potential binders. In the first two cases of cement and grout they were deemed to be too stiff a material. PFA was found unable to bind to the gravel material. Initial testing of the Protomix material revealed that it had the potential to bind together gravel while having a relatively low stiffness compared to other cement based 'binders'.

Final mix testing of the Protomix material sought to identify the main parameters which were likely to affect composite material performance. The effect of grain size, water to

cement ratio and variable grain size composition were examined. Testing suggests that with increasing grain size the cohesion, stiffness and unconfined compressive strength reduced. Decreasing the water to cement ratio was found to increase the cohesion, but below a water to cement ratio of 0.54 the cohesion did not increase significantly for the cases examined. Stiffness and unconfined compressive strength was found to descrease with increasing water to cement ratio. Utilising samples in Group 3 which had a similar variability in grain size range to the column were found to show significant variation in composite behaviour. It is suggested that the composite column requires that the grain size of material for the composite be more uniform. After a review of the results the values of cohesion and stiffness from the 6.33 - 10 mm composite samples has been taken forward for numerical modelling of a triaxial test. The use of this grain size overcomes the potential issues with the Tremie tube clogging with river bed gravel sizes in the range of 20 - 40 mm and allows for pre-mixing of the material which will improve the binder/ gravel contact helping to form a more uniform bond. A friction angle, θ, of 20° is specified for the numerical models going forward until a field trial and plate load test can further clarify material behaviour in terms of ground improvement.

Chapter 7

Behaviour of composite stone columns in soft soils for small raft and strip foundations

7.1 Introduction

This Chapter examines the behaviour of small groups of composite columns installed beneath small pad, raft and strip foundations in soft soils. A novel type of column termed 'Composite' column is now proposed for use in ground improvement. It was identified from the studies of stone columns earlier in this thesis (Chapter 5) that columns fail by two main modes of deformation, punching and bulging failure in soft soils. The focus of this research was to examine a means by which the bulging failure could be reduced by the introduction of a binder material in the bulging zone. It is inferred from the results of the numerical models that (typically) bulging failure occurs at the top of the lower Carse clay in the Bothkennar soil profile to a maximum depth of 4.0 m. This is to be expected since this is the least competent interval in the soil profile below the stiff crust and upper Carse clay.

A sensitivity analysis was performed using area ratio, column confinement and column length to allow comparison of the performance of composite columns to stone columns. The settlement performance, settlement inferred deformation ratios and shear strain distribution is examined and discussed below.

7.2 Composite stone column specification

From the sensitivity analysis in Chapter 5 for a 1.0 m thick crust the bulging zone exists to a maximum depth of 4.0 m in the Bothkennar soil profile. The composite column concept uses a normal stone column with composite material added between 1.7 m and 4.0 m depth. Both above this depth and below, the remaining lengths of column are specified with normal stone column material. By applying normal stone above and below the composite the drainage and consolidation properties of the column are maintained as far as possible. The composite material is specified with stiffness of 191 MPa, Poisson's ratio = 0.3, cohesion = 256 kPa, friction angle = 20° and dilation angle = 0° based upon properties from Table 6.7 for seven day strength of a composite with water to cement ratio of 0.65. It is a assumed that over time the column will increase in strength. In the absence of a field trial composite stone columns are numerically

modelled in the same manner as stone columns. It is anticipated that a field trial will allow the parameters to be revised.

7.3 Settlement performance of composite columns

The performance of composite columns is evaluated for a typical working load of 50 kN/m² for the foundations. The settlement behaviour for the three types of foundation (single column, small raft, and strip) is defined by the basic settlement improvement factor, n, which is defined as the ratio of the settlement of the untreated foundation to the settlement of the treated foundation described previously in Chapter 5. An assessment was made of the effect of column confinement using a single column, 1x3 column strip and a 3x3 column raft adopting a standard square column placement as applied in Chapter 5 (See Figure 5.1).

The influence of the column length and confinement on the settlement improvement factor is shown in Figure 7.1(a). It can be seen that for columns length of 2.4 m or less, the column behaviour is similar due to the restraint provided by the stiff crust and upper Carse clay. Beyond a column length of 2.4m the composite column appears to improve the settlement improvement factor for all foundation types (Figure 7.1a) compared to stone columns (Figure 7.1b). The introduction of the composite column into the bulging zone appears to reduce the settlement significantly. The largest increases are observed for strip and raft foundation configurations with end bearing values of settlement improvement factor increasing from 2.03 to 2.4 and 2.38 to 3.45 respectively for an area ratio of 3.5. Similar increases are seen for strips with area ratios of 8.0 and 14.2 for end bearing stone columns with settlement improvement factors increasing from 1.5 to 2.1 and 1.31 to 1.77. For a raft foundation with area ratios of 8.0 and 14.2 the increase in settlement improvement factors is from 1.69 to 2.56 and 1.4 to 2.1. Interestingly, composite columns with area ratios of 8.0 (Figure 7.1(a-ii)) indicate that the same improvement factor can be achieved as stone columns with area ratio of 3.5 (Figure 7.1(b-i)). The single columns by contrast show significantly higher settlement improvement factors which is attributed to the significant increase in stiffness and lower applied loads absorbed by the pad foundations i.e. applied load is transferred from the base of the foundation to the columns.

A comparison of the area ratio and column confinement for end bearing composite and stone columns of length 14.5 m is shown for different foundation types in Figure 7.2. Increasing the area ratio reduces the settlement improvement factor. It can be seen that

the composite columns offer a considerable reduction in settlement compared to stone columns. The use of composite columns suggests an increase in settlement improvement factor of up to 0.7 and 0.5 for a raft and strip respectively.

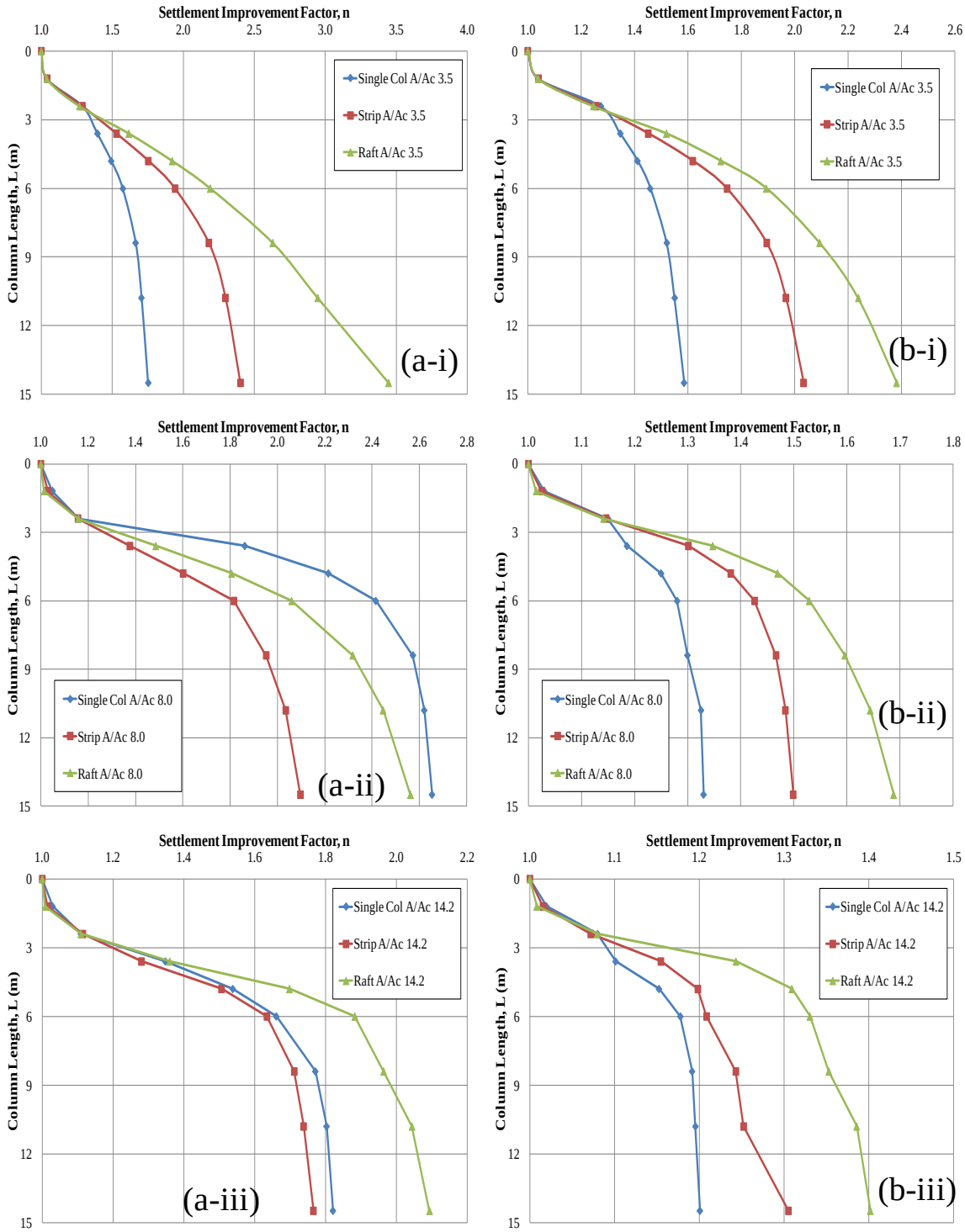

Figure 7.1 Influence of area ratio on settlement improvement factors for (a) composite stone columns, (b) stone columns for area ratios (i) 3.5, (ii) 8.0 and (iii) 14.2

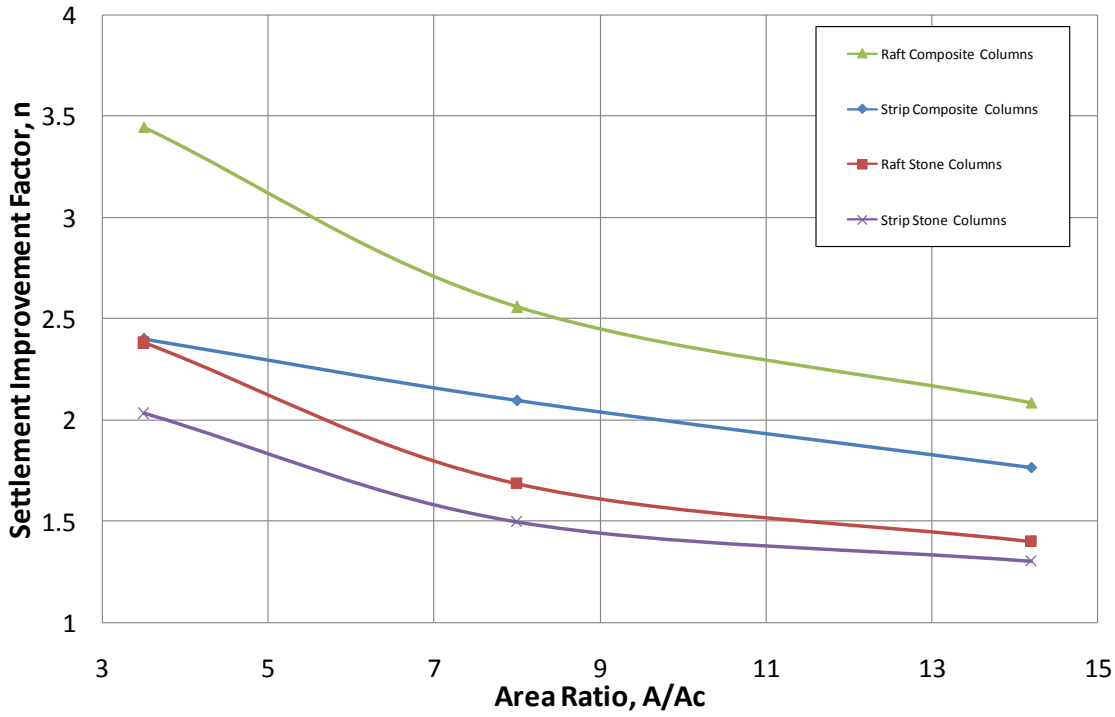

Figure 7.2 Comparison of the influence of area ratio for end bearing composite columns and stone columns

7.4 Settlement inferred deformation ratios

The settlement inferred deformation ratios of punching and compression as described earlier in Section 5.4 were used to describe the behaviour of the composite columns. As discussed for stone columns two modes of deformation, bulging and punching, were observed. In addition a sub-type of punching failure known as 'block' failure described by Black (2007) was also identified for strip and rafts with low area ratios of 3.5. An assessment of the results for composite columns beneath pad, 1x3 column strip and 3x3 small raft configurations is now made with comparison to stone columns as appropriate.

7.4.1 Deformation ratios of a single composite stone column

The influence of area ratio and column length on the punching ratio for a single composite column is shown in Figure 7.3(a-i). It can be seen that increasing the area ratio has the effect of increasing the magnitude of the punching ratio. Interestingly, the maximum depth of the highest value of punching ratio is 3.6m which is similar to a single stone column (Figure 7.3b-i) but the magnitude of punching increases. Above a depth of 3.6 m the punching ratio is lower as the stiff crust and upper Carse clay restrain the column. The punching ratio increases below 3.6 m for area ratios of 8.0 and 14.2. Increasing the area ratio leads to a wider width of pad foundation which will increase

the applied stress from the foundation. The increased stiffness of the column allows more of the applied load to be absorbed and transferred to the base of the column which is observed as a higher punching ratio and shear stress at the column base.

The increased stiffness of the composite column in the bulging zone has an effect on the compression ratio at depths less than 3.6 m in Figure 7.4(a-i). With increasing area ratio the compression ratio reduces above 3.6 m. The compression ratios for the single column are lower than those of a stone column (Figure 7.4(b-i)) which suggests that the composite material has reduced the bulging potential. The increased punching ratios coupled with reduced compression ratios with depth suggest that for a single column punching is a more dominant mechanism. However, when contrasted with settlement improvement factors for a single column (Figure 7.1) the increased punching ratio has a positive effect on settlement reduction. This increased punching would be expected to be seen as increased shear stress at the base of the column.

7.4.2 Deformation ratios of composite stone columns beneath a strip foundation

The variation in punching ratio for the central column with column length for a 1x3 group of stone columns beneath a strip foundation is shown in Figure 7.3(a-ii). Punching ratios increase with length to a maximum of 3.6 m which is similar to a single composite column and raft regardless of area ratio. Interestingly, the depth of maximum punching ratio for a composite column is deeper for an area ratio of 3.5 than for an equivalent stone column (7.3(b-ii)). It is suggested that this is due to increased column cohesion of the composite column allowing for deeper punching into the underlying soil while still providing a higher settlement reduction than a stone column due to improved column cohesion. Increasing the area ratio has the effect of increasing the punching ratio which reflects the individual behaviour of the columns at this ratio and also the increased column cohesion. The punching ratios are higher than stone columns for this reason. The increase in punching ratios is coupled with low compression ratios (Figures 7.3(a-ii) and 7.b(a-ii)). The low compression ratios suggest that column cohesion is increased; columns are not deforming along their length but are transferring their load to the column base due to the use of the composite in the bulging zone.

The variation in punching and compression ratios for individual columns (centre, edge and corner) is shown in Figures 7.5(a) and 7.6(a) for a 1x3 column strip foundation. For all column lengths and area ratios punching ratios are highest for the centre columns and

lowest for the corner columns. Punching ratio is highest for an area ratio of 14.2 (Figure 7.5(a-iii)) and lowest for the lowest area ratio of 3.5 (Figure 7.5(a-i)). This suggests that the composite columns are behaving in a similar manner to stone columns as a greater area ratio leads to more independent behaviour of the columns. The increased magnitude of punching ratios with composite columns is attributed to the increased stiffness and cohesion of the column within the bulging zone with allows the column to transfer more applied stress to the base of the column which can be observed as higher punching ratios.

7.4.3 Deformation ratios of composite stone columns beneath a raft foundation

The variation in punching ratio for the central column for a 3x3 group of stone columns is shown in Figure 7.5(a-iii). The increase in punching ratios is coupled with low compression ratios, as seen in Figure 7.6(a-iii). This suggests that columns do not deform along their length but rather they are transferring their load to depth down to the column base. This would imply that punching failure is the dominant mode of deformation for short composite columns.

The increase in magnitude of the punching ratios with increasing area ratio is considered partially due to increased column cohesion/ stiffness and partly due to the loss of lateral confinement by other columns. As the foundation width and area ratio is increased the applied stress transferred from the foundation to the composite column increases which leads to higher punching ratios. The increased cohesion/ stiffness increases the depth of punching as the columns are able to carry more applied stress to the base of the column. The compression ratios for the columns, regardless of area ratio, are much lower than those observed for stone columns for column lengths between 2.4m and 4.8 m. This is due to the composite column providing a higher level of cohesion and stiffness so the potential for bulging is reduced. For an area ratio of 8.0 and 14.2 the maximum depth of punching is 3.6 m whereas for a ratio of 3.5 the depth is 2.4 m. The shallower depth of punching failure is due to 'block' failure which is indicated by low punching (Figure 7.5(a-i)) and low compression ratio (Figure 7.6(a-i)). Punching ratios reduce with depth (Figure 7.5(a-iii)) while compression ratios increase with depth (Figure 7.6(a-iii)) which indicates a change in mode of deformation from punching to bulging failure with increasing column length. The reduction in compression ratios of composite columns (Figure 7.6(a-iii)) in comparison to stone columns (Figure 7.6(b-iii)) suggests that the composite is effective in reducing the

magnitude of bulging failure while offering increased settlement reduction (Figure 7.6 (a-iii)).

The variation in punching ratio and compression ratio for individual columns within a 3x3 group is shown in Figure 7.5 and 7.6 for different area ratios. For all column lengths and area ratios punching ratios are highest for the centre columns, followed by the edge and highest for the corner columns. This suggests that the columns are behaving in a similar manner to stone columns. The lowest punching ratios occur for the lowest area ratio (Figure 7.5(a-i)) and the highest for the highest area ratios of 14.2 (Figure 7.5(a-iii)). The low punching ratios and associated low compression ratios are considered consistent with 'block failure' which is seen in the shear stress plots in Figures 7.13-7.15 as uniform shear stress within the soil and columns which punch as a block. Columns which are punching transfer shear stress to the surrounding soil which tends to drag the columns downwards. Similar behaviour was also observed for composite columns beneath strip foundations and strip/ raft configurations of stone columns at low area ratios.

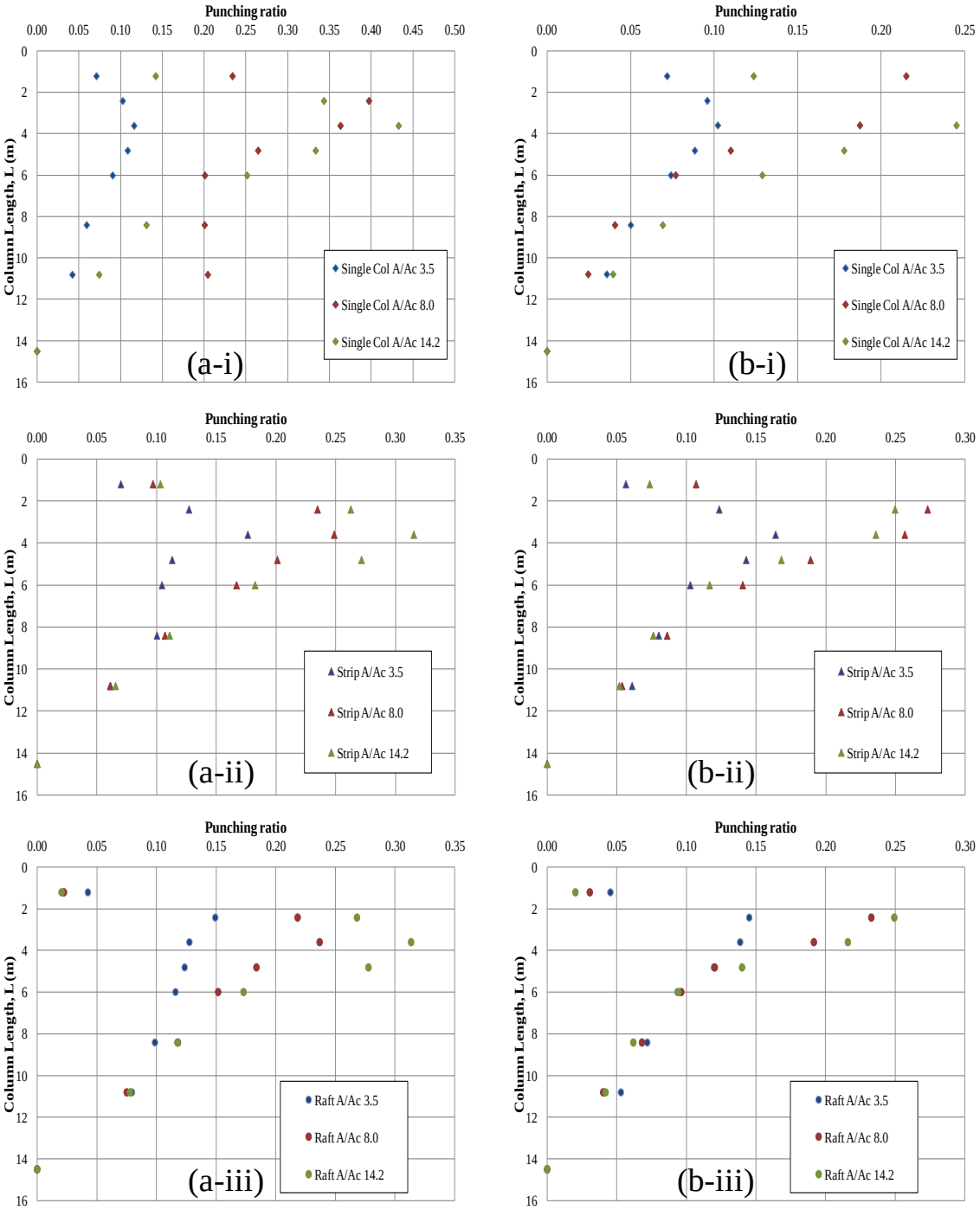

Figure 7.3 Punching ratios for a three column strip and nine column raft for central, edge and corner columns area ratios of (i) 3.5, (ii) 8 and (iii)14.2 for (a) composite stone columns and (b) stone columns

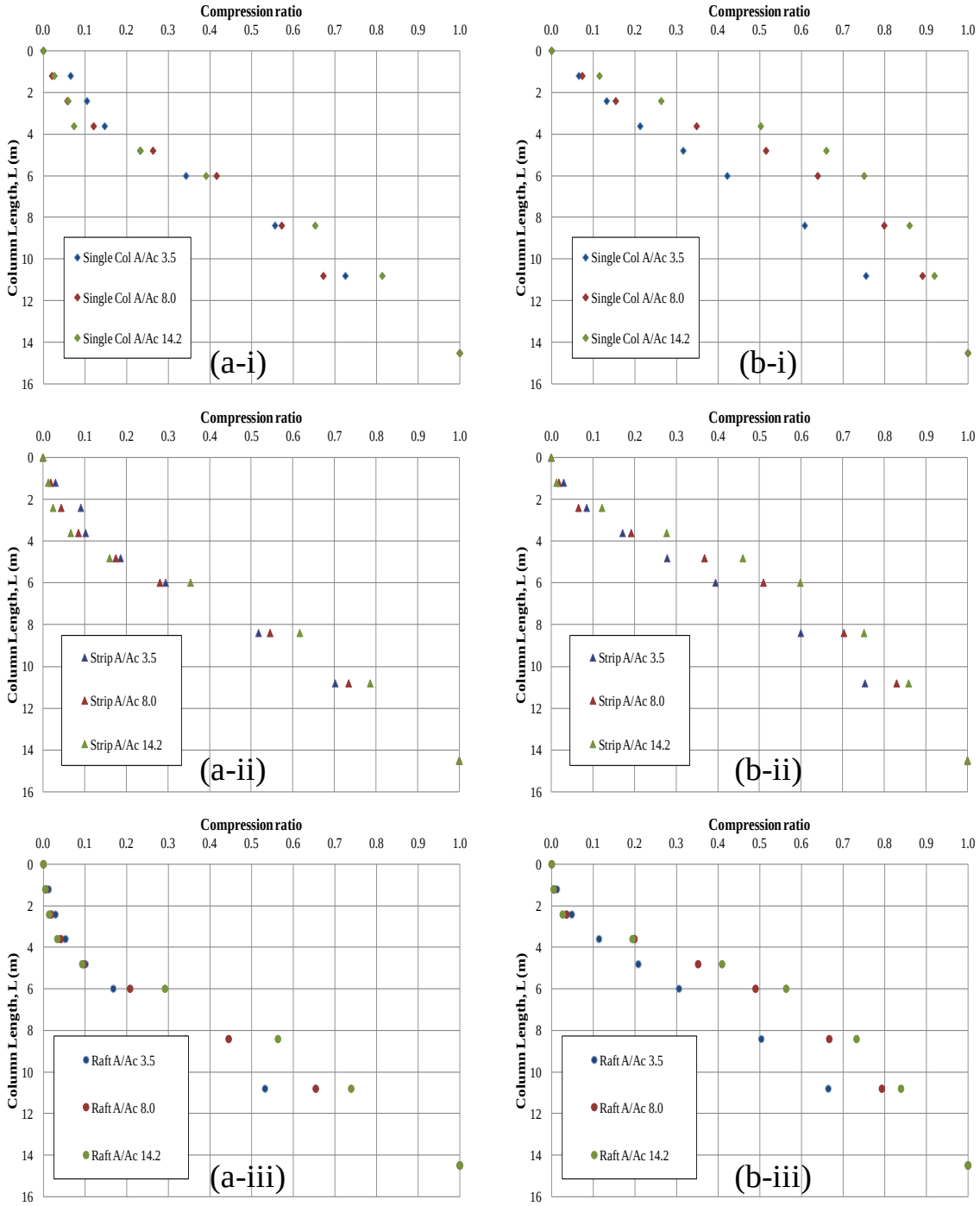

Figure 7.4 Compression ratios for a three column strip and nine column raft for central, edge and corner columns area ratios of (i) 3.5, (ii) 8 and (iii)14.2 for (a) composite stone columns and (b) stone columns

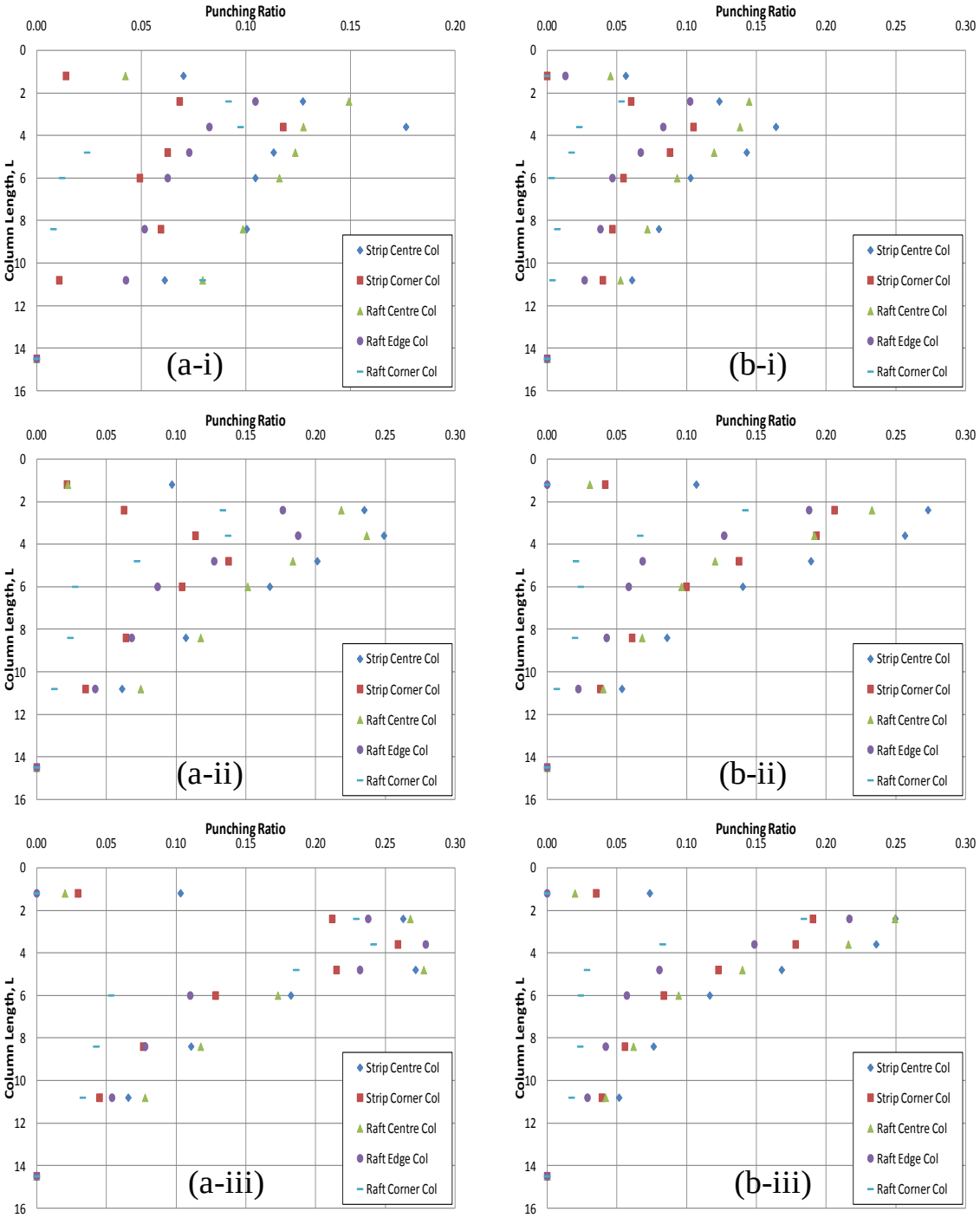

Figure 7.5 Punching ratios for a three column strip and nine column raft for central, edge and corner columns area ratios of (i) 3.5, (ii) 8 and (iii)14.2 for (a) composite stone columns and (b) stone columns

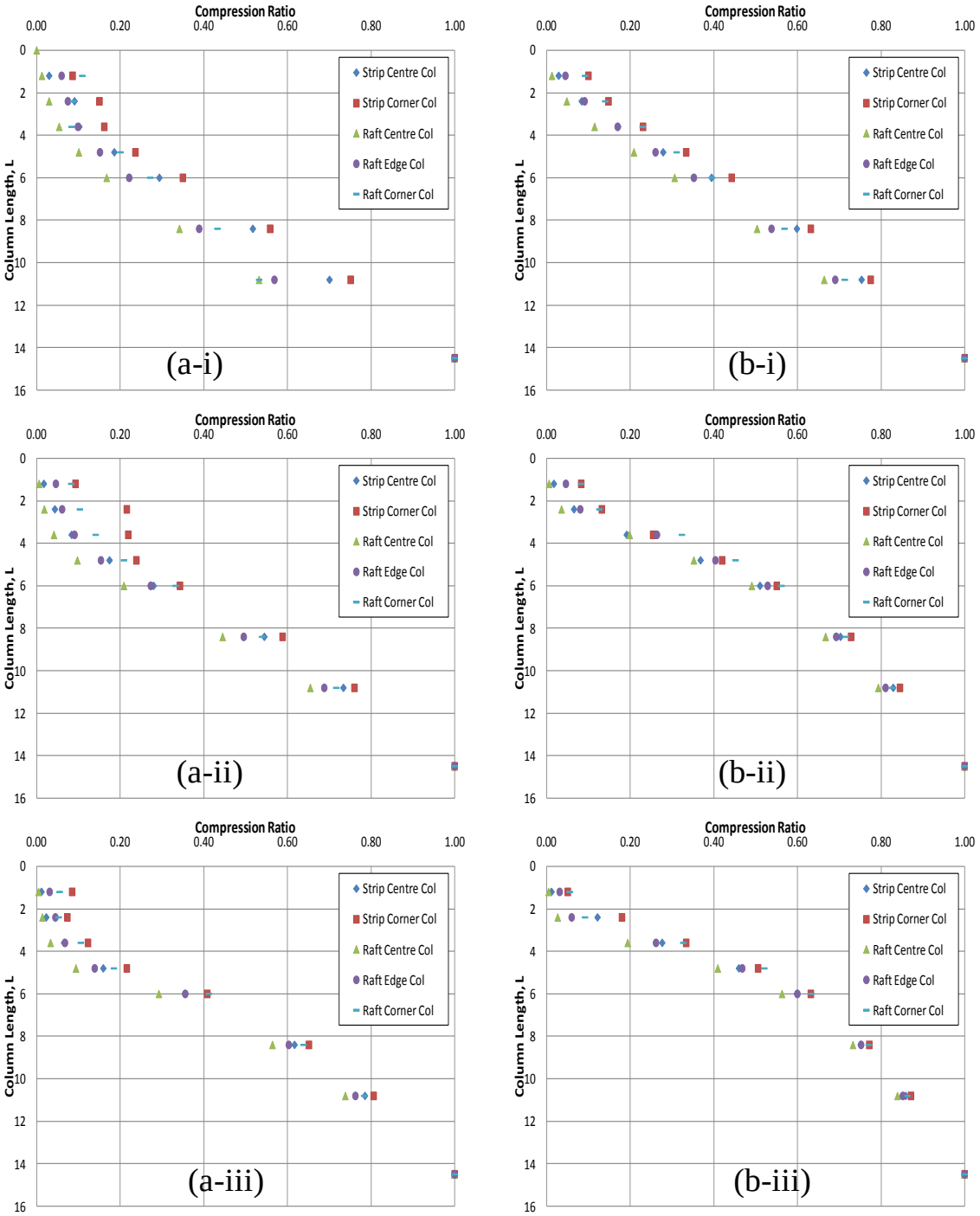

Figure 7.6 Compressibility ratios for a three column strip and nine column raft for central, edge and corner columns area ratios of (i) 3.5, (ii) 8 and (iii)14.2 for (a) composite stone columns and (b) stone columns

7.5 Distribution of shear strains

Three column lengths of composite column are selected to compare to stone columns and to examine the specific modes of deformation and the associated distribution of shear strains: 2.4 m long columns are chosen to investigate punching; 6 m long columns are chosen to investigate the failure modes of punching and bulging; and 14.5 m end bearing columns are chosen to investigate bulging failure since punching does not occur due to the base of the column being founded on a rigid stratum. Columns, although composed of the composite in the bulging zone, would still be expected to show similar behaviour to stone columns if the technique was successful in reducing the potential for bulging failure alone.

7.5.1 Shear strains for a single composite stone column

The distribution of shear strains for single columns with lengths 2.4, 6 and 14.5 m is shown in Figures 7.7 to 7.9. For a column length of 2.4 m (Figure 7.7(a)) increasing the area ratio has the effect of increasing the magnitude and size of the zone of shear strain observed along column length and at the base of the column. At a low area ratio of 3.5 the development of shear strain is negligible.

The distribution of shear strain for a 6 m floating column is shown in Figure 7.8(a). For a low ratio of 3.5 the strain between the column and soil is negligible. For higher area ratios of 8.0 and 14.2 in Figures 7.8(a-ii) and 7.8 (a-iii) respectively shear strains can be observed to develop within the column and at the base. Interestingly, unlike the stone columns no significant shear strain develops within the column for an area ratio of 8.0 which would be suggestive of bulging failure. It is therefore suggested that punching failure is most likely to be the mode of deformation. For an area ratio of 14.2 increased shear strain is observed around the column and within the column. The increase in shear strain within the column is considered evidence of the composite column transferring applied load to depth and the development of bulging below the composite column treated depth of 4.1m. The composite column (Figure 7.8(a-iii) reduces the potential for bulging failure above 4.1 m when compared to the results for an equivalent length and area ratio of stone column (Figure 7.8(b-iii)). Bulging is considered the dominant mode of failure with some punching evident at the base of the column.

The distribution of shear strain for a 14.5 m end bearing composite column is shown in Figure 7.9(a) and it can be observed that bulging failure does not occur for area ratios of

3.5 and 8.0. This is encouraging since stone columns with an area ratio of 8.0 (Figure 7.9(b-ii)) show evidence of the development of bulging failure. For an area ratio of 14.2 bulging appears to occur at the top of the lower Carse clay which was also observed for an equivalent stone column (Figure 7.9(b-iii)).

7.5.2 Shear strains for three column strip of composite stone columns

The distribution of shear strain for a 1x3 group of columns of lengths 2.4, 6 and 14.5 m is shown in Figures 7.10 to 7.12. For columns of length 2.4 m uniform shear strain was seen beneath the columns in Figures 7.10(a-i) and 7.10(a-ii) for area ratios of 3.5 and 8.0 respectively. This is evidence of 'block' failure which occurs when the column and soil punch into the soil below as one 'unit'. This behaviour was also observed for stone columns of the same length and area ratios in Figures 7.10(b-i) and 7.10(b-ii). It is suggested that the composite columns exhibit typical stone column behaviour for short columns of length 2.4 m. With increased area ratio of 14.2 (Figure 7.10(a-iii)) columns were seen to develop localised failures beneath the base of each column which suggests punching failure.

The distribution of shear strain for a 6 m floating composite column is shown in Figure 7.11(a). For an area ratio of 3.5 the shear strain within the column and soil is the same with small uniform strains observed at the base of the column. This is suggestive of 'block' failure associated with punching with no evidence of bulging seen. For an area ratio of 8.0 the uniform shear train at the base of the columns suggests 'block' failure is occurring. As the area ratio is increased to 14.2 individualised shear strains develop within the columns close to the top of the lower Carse clay. The applied load is not being transferred to the base of the column instead stress-share is occurring by bulging failure expressed as the observed shear strain. Interestingly, the shear strain is occurring at a similar depth to the stone columns (Figure 7.11(b-iii)) with the central column having a slightly larger shear strain. It is clear that as the ratio increases the composite columns absorb a greater proportion of the applied stress and as such are subject to a greater shear stress. This is also seen with stone columns.

The distribution of shear strain for a 14.5 m end bearing column is shown in Figure 7.12(a). No bulging failure occurs for an area ratio of 3.5 (Figure 7.12(a-i)). Columns with ratios of 8.0 and 14.2 develop shear strains at depths below the composite column treated 'bulging' zone. This suggests that the column is transferring stress to depth and the concentration of shear stress below this depth is suggestive of bulging failure being

transferred to depth. Given the increased restraint with depth and the increase in settlement improvement factor (Figure 7.1) it is considered that the composite material improves the performance of the column compared to a stone column. The central column appears to show shear strain at a slightly deeper level and intensity compared to the edge columns. Partial confinement is considered responsible for this deepening effect. Similar behaviour was observed for a stone column (Figure 7.12(b-iii)).

7.5.3 Shear strains for nine column raft of composite stone columns

The distribution of shear strain within a 3x3 group of stone columns of lengths 2.4, 6.0 and 14.5 m is shown in Figures 7.13 to 7.18. For columns of length 2.4 m uniform shear strain was seen beneath the columns in Figures 7.13(a-i) and 7.13(a-ii) for area ratios of 3.5 and 8.0 respectively. Uniform strain is considered evidence of 'block' failure. Similar behaviour was observed for the strip configuration in Figure 7.10(a-i) and 7.10(a-ii). This behaviour was observed for stone columns of the same length and area ratios in Figures 7.10(b-i) and 7.10(b-ii). It is suggested that the composite stone columns are behaving in a similar manner to stone columns. With an increased area ratio of 14.2 (Figure 7.10(a-iii)) shear strain expressed as 'punching' failure is seen below the individual columns which suggests the columns are acting independently. This behaviour was also seen for a 3x3 raft of stone columns.

The distribution of shear strain for 6 m floating columns is shown in Figure 7.14(a). Punching failure is seen for all area ratios. 'Block' failure is evident for area ratios of 3.5 and 8.0 with uniform shear strain observed below the columns. Evidence of shear strain within the column is observed for an area ratio of 8.0 at a depth below 4.1 m which is the base of the composite treated part of the column. It is considered that bulging is occurring beneath the treated zone which suggests the increased cohesion of the upper column is able to stress transfer to depth. Although the column is bulging the settlement improvement factor is increased suggesting that the column is effective in reducing settlement. The stone column (Figure 7.14(b-ii)) by comparison bulges as a shallower depth. The dominant mode of deformation appears to be both bulging and punching in this case unlike a stone column which indicates bulging failure is the dominant mode of deformation (Figure 7.14(b-ii)). As the area ratio increases from 8.0 to 14.2 it can be seen in Figures 7.14(a)(ii) and 7.14(a)(iii) that columns at higher ratios tend to bulge and act more independently. However, unlike a stone column the

composite has some punching occurring at the column base. The dominant mode of deformation for this area ratio and length appears to be bulging failure.

For a 14.5 m long end bearing column resting on a rigid stratum no punching failure can occur (Figure 7.15). It is not clear for a column with ratio of 3.5 which mechanism of deformation occurs. Within the treated zone between 1.7 m and 4.1 m the shear stress is low. Below the outer edges of the foundation it appears some development of a shear plane has occurred but not sufficient enough to cause failure. As the area ratio is increased to 8.0 and 14.2 it is clear that shear strain develops within the column at a depth below the composite treated part of the column. The composite column appears to transmit the applied load to depth with bulging failure occurring at a deeper depth. The lateral restraint provided at a deeper level in the soil is sufficient so as to reduce the magnitude of bulging such that the settlement is reduced. This is evident when comparing the settlement improvement factors (see Section 7.3). The central column can be seen to have a higher concentration of shear stress at a slightly deeper level which suggests that the edge and corner columns are providing restraint. This effect is typical of groups of stone columns which is associated with the mobilising of passive resistance of the soil which is bounded by the central and external column. This in turn increases the lateral resistance while enhancing the confinement and forces the bulging deeper. However, bulging for the external columns occurs at a shallower depth which bulge outwardly due to the lack of confinement.

The influence of restraint is seen in Figures 7.16 to 7.18 for corner columns. The left and right most columns represent a section B-B' taken through the two corner and outer edge columns (defined in Figure 5.1). The columns at the outer edge appear to have significant differences in shear strain behaviour compared to the central column. For column lengths of 2.4 m regardless of area ratio they appear to show punching failure (Figure 7.16(a)) which is similar to stone columns (Figure 7.16(a)). No evidence of block failure appears evident for an area ratio of 3.5 compared to the central column (Figure 7.13). This is due to less restraint being observed for columns along section B-B' compared to the central column in line A-A' (Figure 5.1). Composite corner columns (Figure 7.17(a)) of length 6.0m, regardless of area ratio, suggest that the outer columns show less bulging than the central columns (Figure 7.14(a)) but show a similar depth of deeper bulging compared to stone columns (Figure 7.17(b)). For columns of length 14.5m the magnitude of shear strain observed for area ratios of 8.0 and 14.2 is reduced (Figure 7.18) compared to the central columns (Figure 7.15). The depth of bulging is

deeper than for stone columns (Figure 7.18(b)). The concentration of stress in the column is controlled not just by the column composition but also the restraint provided by the soil and surrounding columns. Central columns are more restrained and therefore are able to carry a higher amount of stress which is observed as a greater degree of bulging than corner columns.

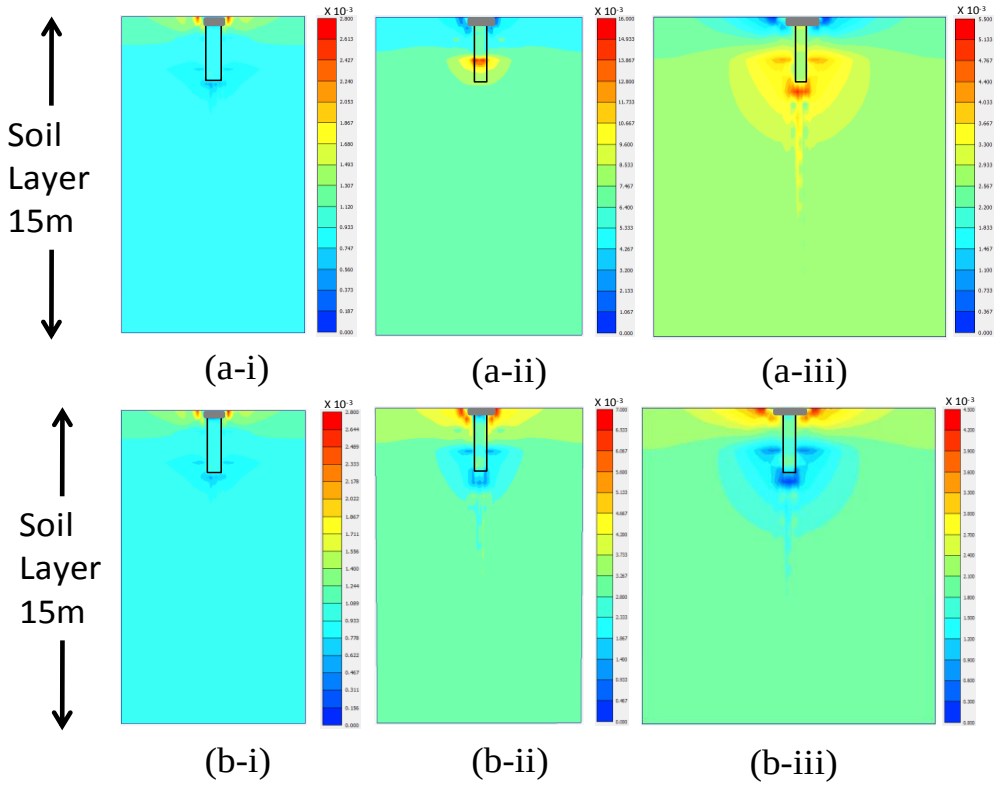

Figure 7.7 Shear strains for a single (a) composite stone column and (b) stone columns with length 2.4m and area ratios (i) 3.5, (ii) 8.0 and (iii) 14.2

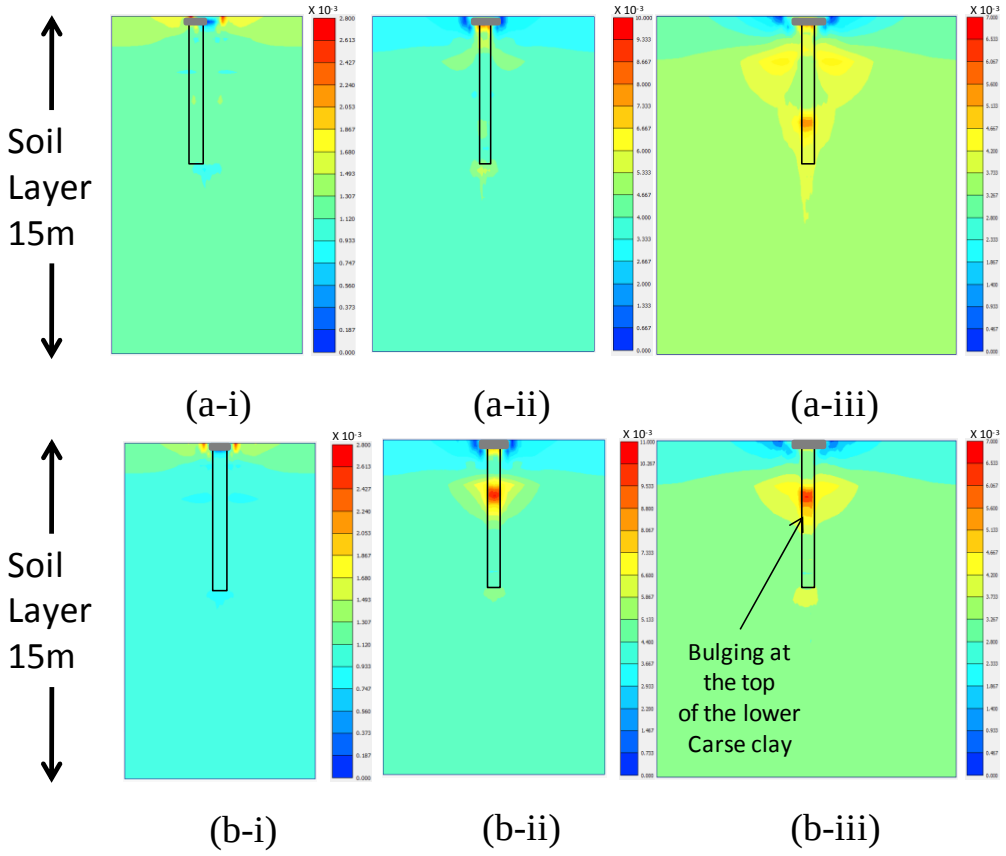

Figure 7.8 Shear strains for a single (a) composite stone column and (b) stone columns with length 6.0m and area ratios (i) 3.5, (ii) 8.0 and (iii) 14.2

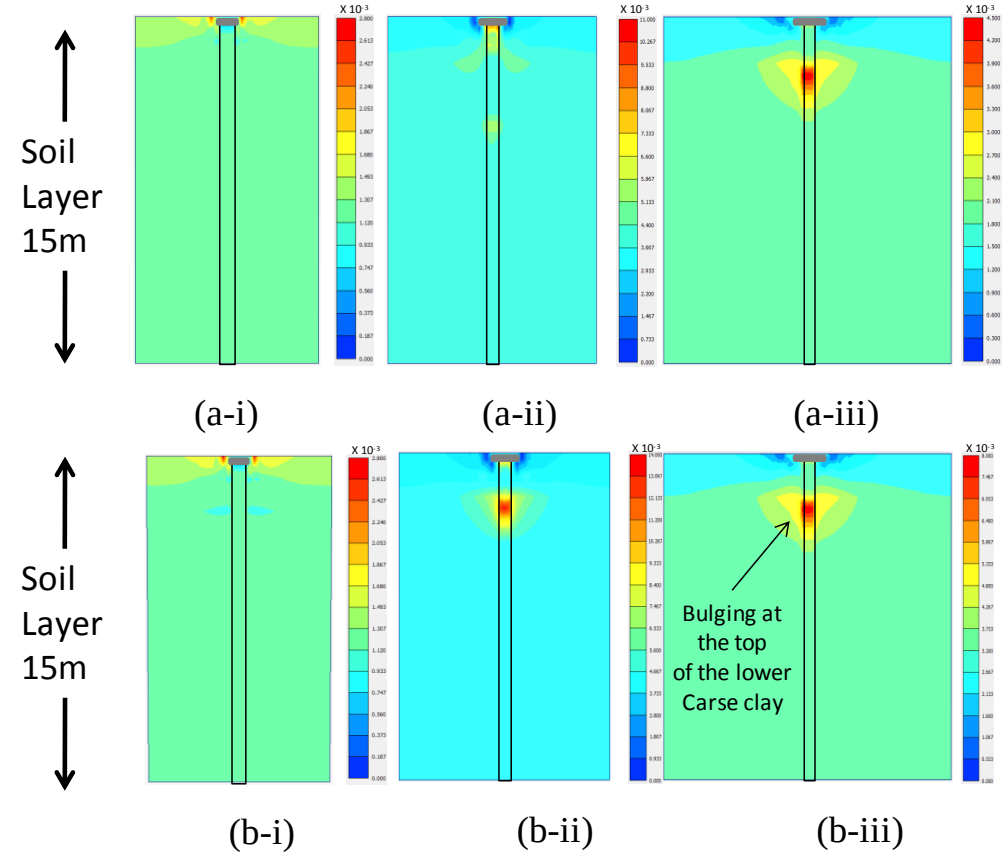

Figure 7.9 Shear strains for a single (a) composite stone column and (b) stone columns with length 14.5m and area ratios (i) 3.5, (ii) 8.0 and (iii) 14.2

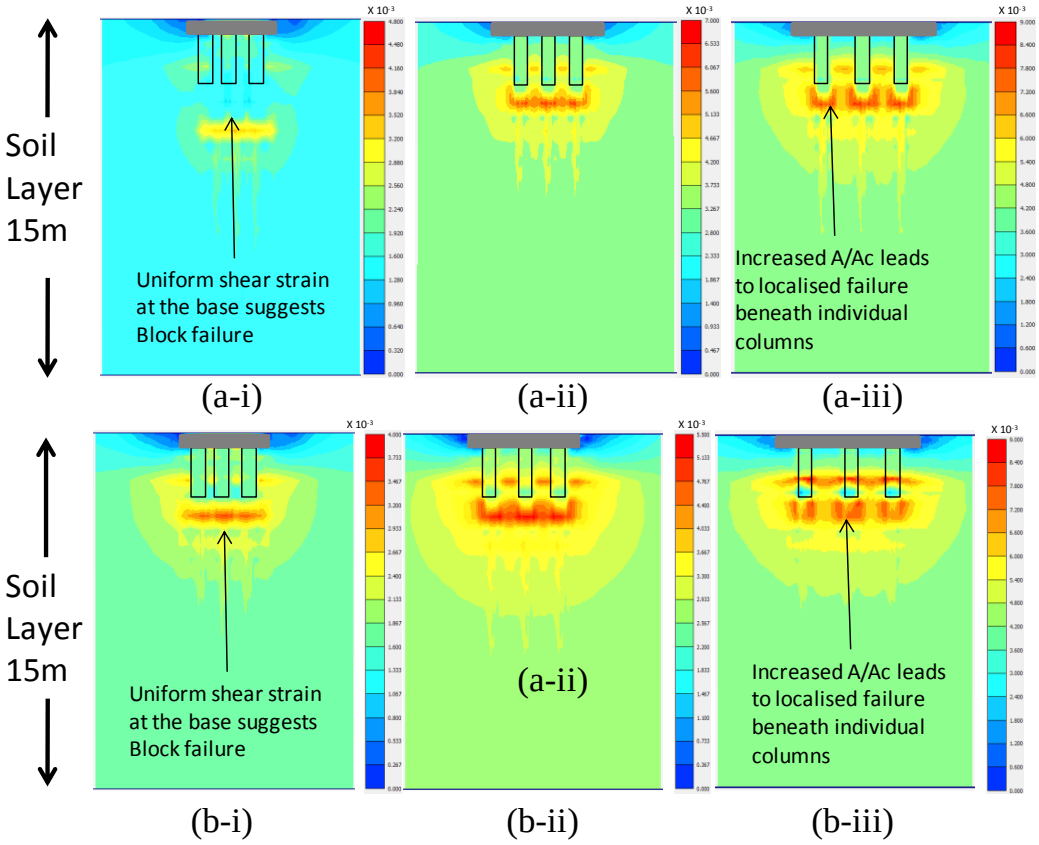

Figure 7.10 Shear strains for a three column strip (a) composite stone column and (b) stone columns with length 2.4m and area ratios (i) 3.5, (ii) 8.0 and (iii) 14.2

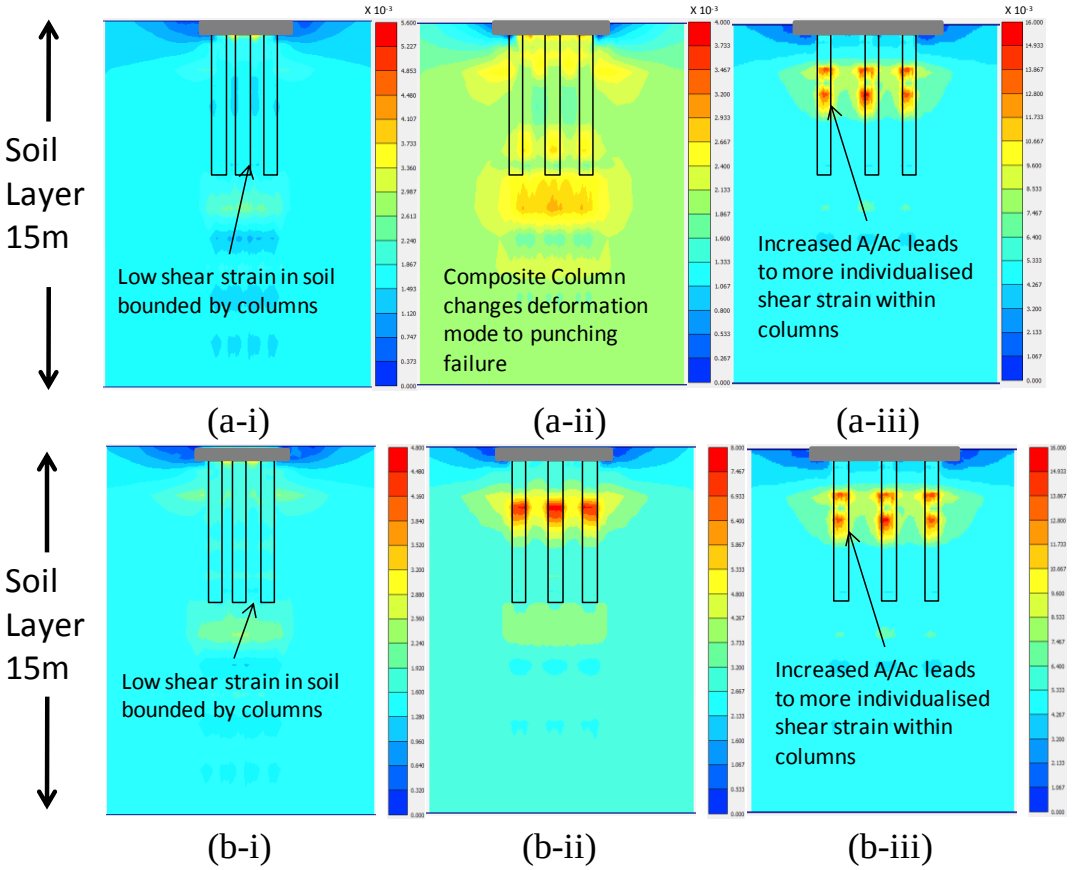

Figure 7.11 Shear strains for a three column strip (a) composite stone column and (b) stone columns with length 6.0m and area ratios (i) 3.5, (ii) 8.0 and (iii) 14.2

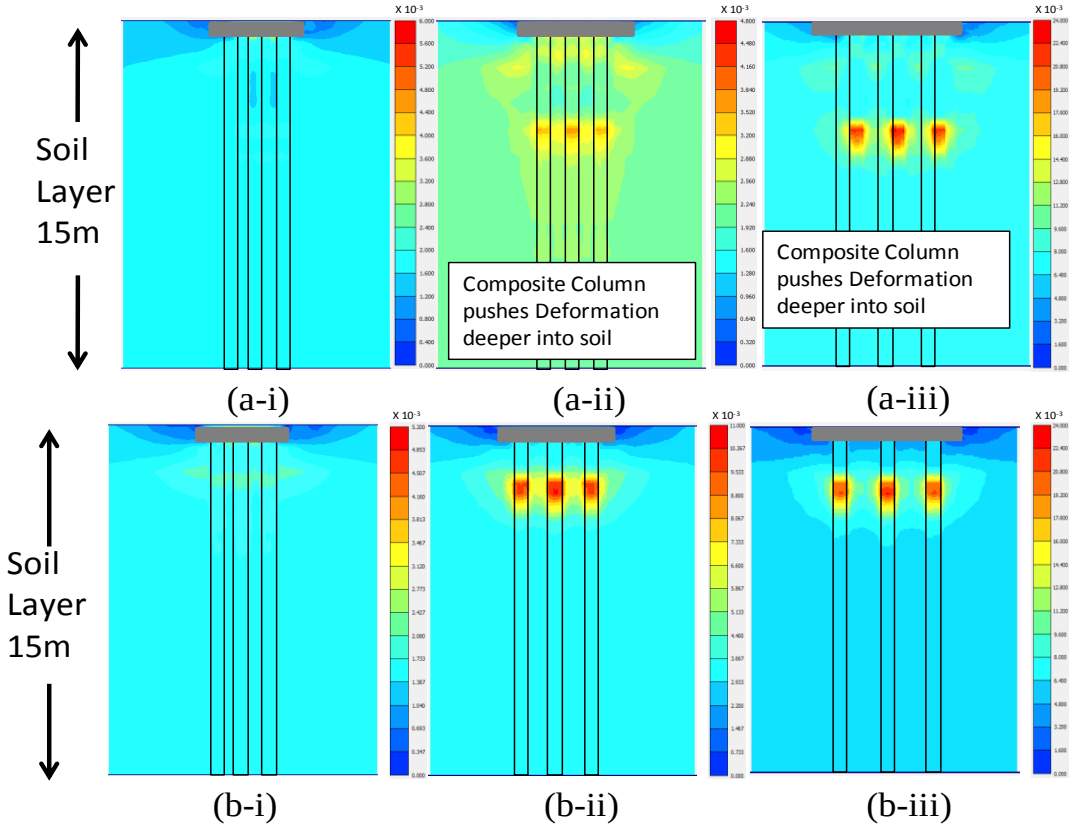

Figure 7.12 Shear strains for a three column strip (a) composite stone column and (b) stone columns with length 14.5m and area ratios (i) 3.5, (ii) 8.0 and (iii) 14.2

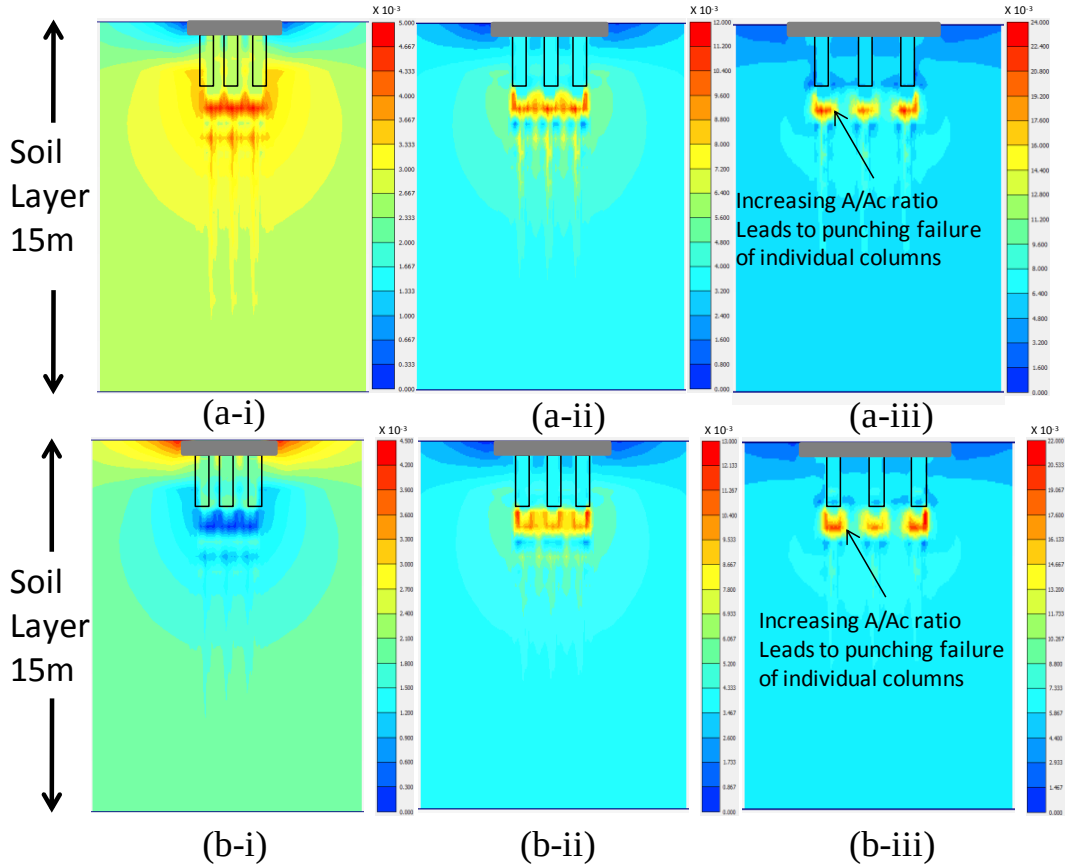

Figure 7.13 Shear strains for a nine column raft (a) composite stone column and (b) stone columns with length 2.4m and area ratios (i) 3.5, (ii) 8.0 and (iii) 14.2

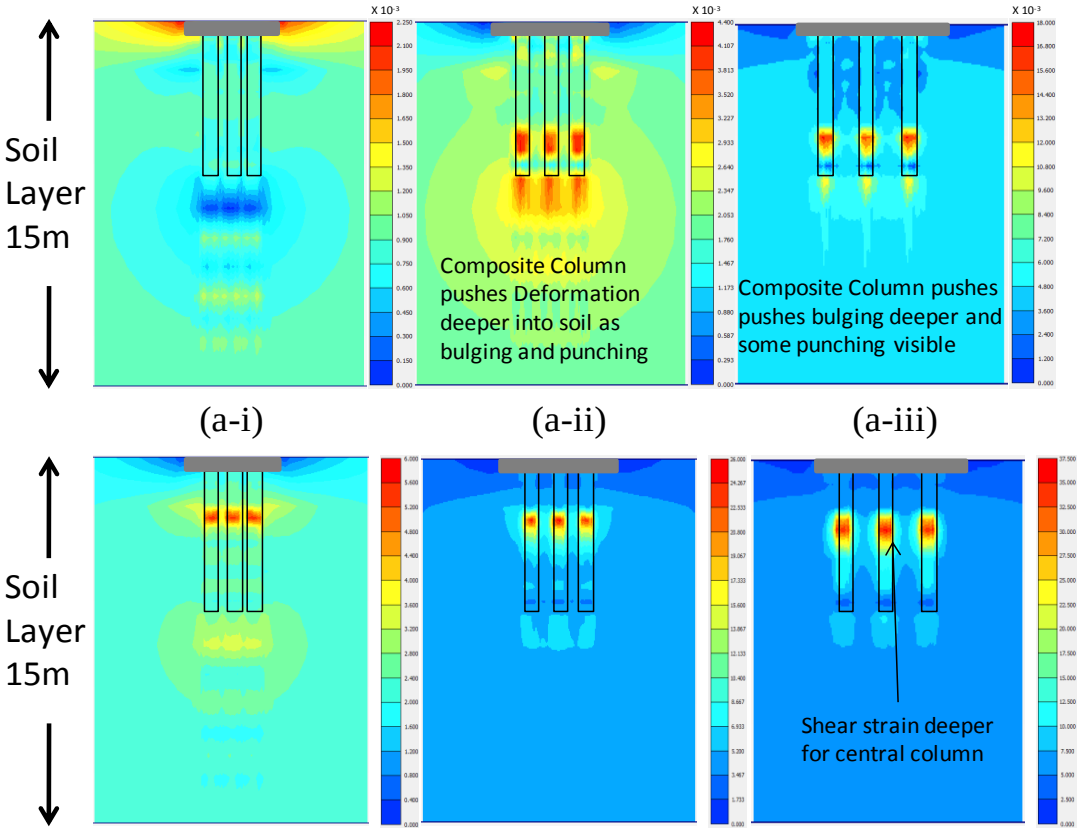

Figure 7.14 Shear strains for a nine column raft (a) composite stone column and (b) stone columns with length 6.0m and area ratios (i) 3.5, (ii) 8.0 and (iii) 14.2

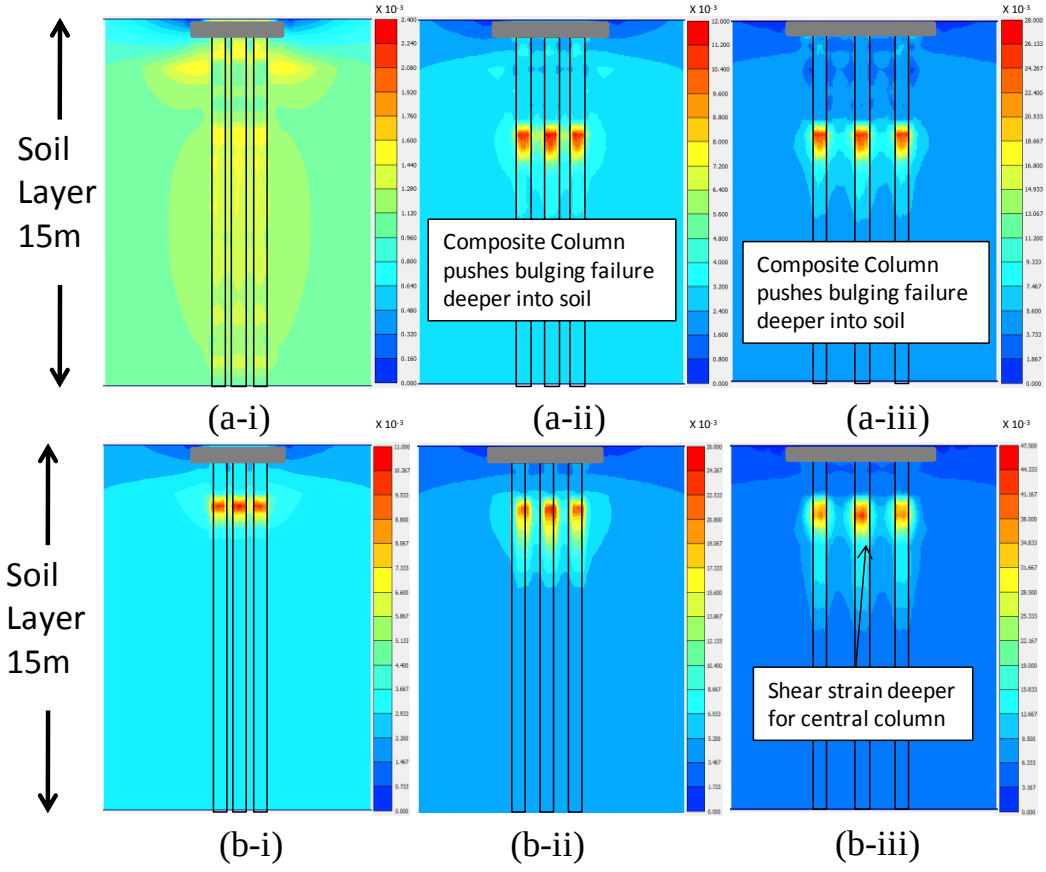

Figure 7.15 Shear strains for a nine column raft (a) composite stone column and (b) stone columns with length 14.5m and area ratios (i) 3.5, (ii) 8.0 and (iii) 14.2

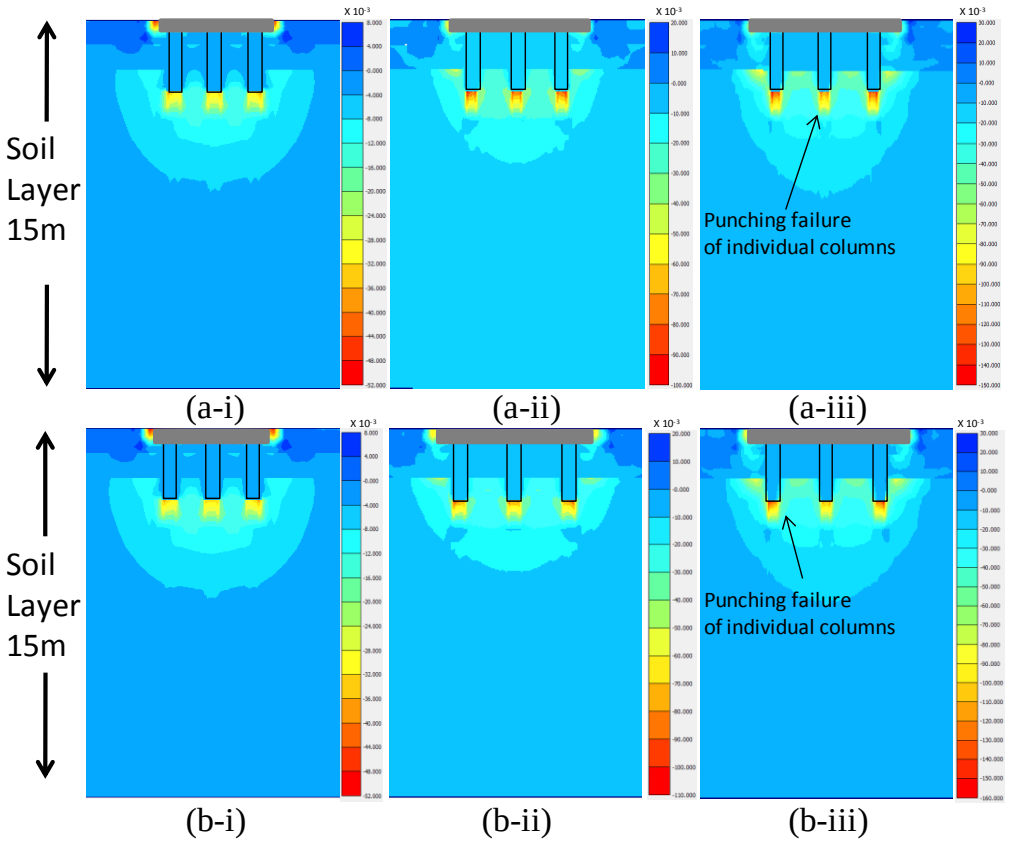

Figure 7.16 Shear strains for a nine column raft (a) composite stone column and (b) stone columns with length 2.4m and area ratios (i) 3.5, (ii) 8.0 and (iii) 14.2 for cross section corner to corner B-B'

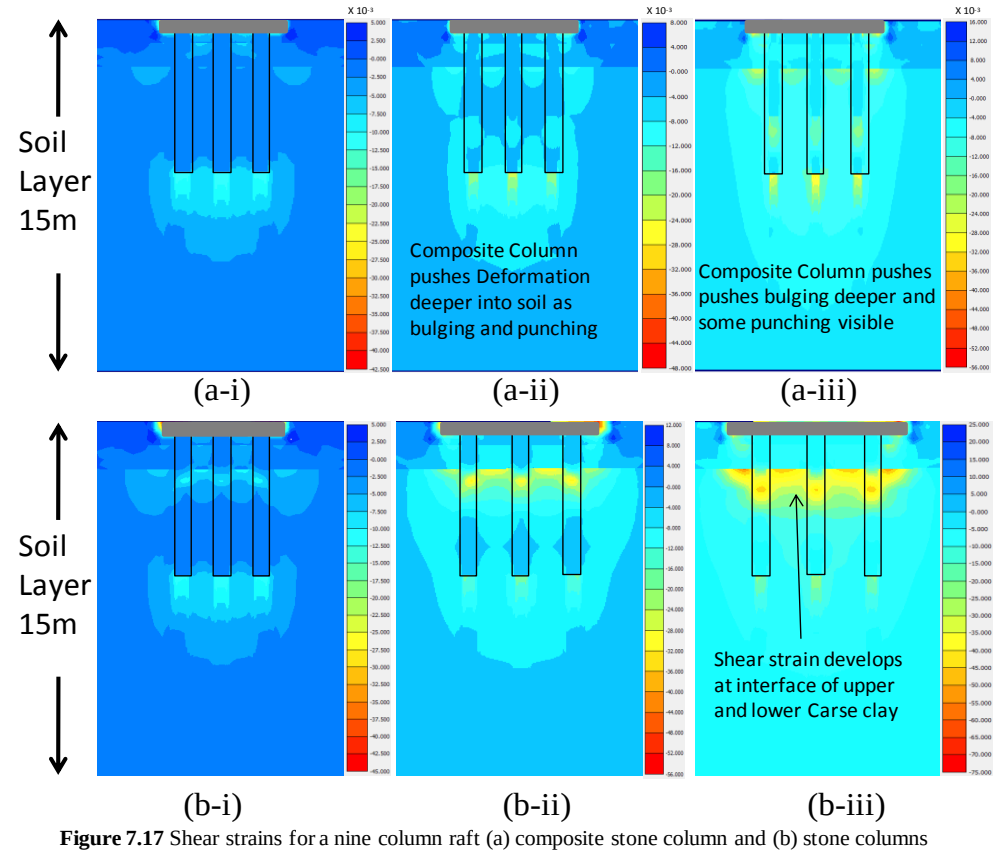

Figure 7.17 Shear strains for a nine column raft (a) composite stone column and (b) stone columns with length 6.0m and area ratios (i) 3.5, (ii) 8.0 and (iii) 14.2 for cross section corner to corner B-B'

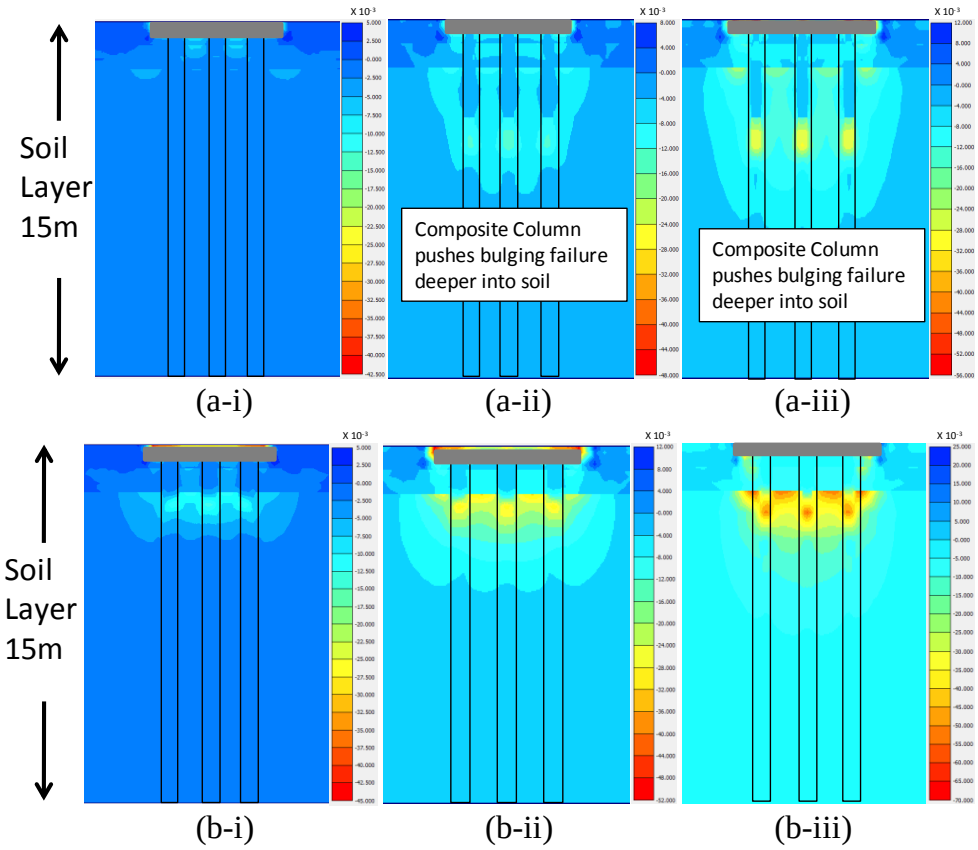

Figure 7.18 Shear strains for a nine column raft (a) composite stone column and (b) stone columns with length 14.5m and area ratios (i) 3.5, (ii) 8.0 and (iii) 14.2 for cross section corner to corner B-B'

7.6 Characteristic column behaviours

Stone columns were found to exhibit specific behaviours associated with their mode of deformation in Section 5.6. Composite columns by contrast contain a binder material in the bulging zone. As discussed in order for such columns to be used they must display behaviours consistent with stone columns. Three column configurations were examined consisting of a single column, 3x1 column strip and 3x3 column raft to compare the vertical and horizontal strain behaviour. Increasing the area ratio for all column configurations was found to increase the magnitude of the vertical and horizontal strain which was also observed for stone columns.

7.6.1 Single column

The distribution of the vertical and horizontal strain for single columns of length 2.4 m, 6.0 m and 14.5 m is shown in Figure 6.8. For a column length of 2.4 m it can be observed that the highest magnitude of vertical strain (Figure 7.19(a)(i)) and horizontal strain (Figure 7.20(a)(i)) occur at the same depth of 2.9m which is the same depth at which punching occurs for stone columns (Figures 7.19(b) and 7.20(b)) and consistent

with the punching identified by settlement inferred deformation ratios (Section 7.4) and shear strain plots (Section 7.5). This behaviour is expected to be the same as stone columns since 2.4 m columns are composed mostly of stone rather than composite. For a column of length 6.0 m the vertical (Figure 7.19(a)(ii)) and horizontal strain (Figure 7.20(a)(ii)) suggest that like stone columns two modes of deformation are present at depths of 2.9 m and 6.5 m. The column appears to bulge in the upper part of the column above the composite treated zone with punching occurring at the column base. Interestingly the composite column appears to have reduced bulging with a significant reduction in horizontal strain observed compared to stone columns. Both modes of deformation appear to be significant. The presence of both modes of deformation is confirmed by settlement inferred deformation ratios (Section 7.4) and shear strain plots (Section 7.5). Similarly to stone columns the vertical strain (Figure 7.20(a)(ii)) and horizontal strain (Figure 7.20(b)(ii)) of end bearing columns of length 14.5 m, appear to suggest bulging failure has occurred at 2.9 m depth while below this depth the column suggests negligible strain. The horizontal strain suggests that for composite columns that bulging is significantly reduced.

7.6.2 3x1 Column strip

The distribution of the vertical and horizontal strain for a 3x1 column strip with columns of length 2.4 m, 6.0 m and 14.5 m is shown in Figures 7.21 and 7.22. For various lengths of composite column it was found to be consistent with the observed behaviour of settlement inferred deformation ratios (Section 7.4) and shear strain plots (Section 7.5). Columns of length 2.4 m were found to punch at 2.9m depth as suggested by the vertical strain (Figure 7.21(a)(i)) and horizontal strain (Figure 7.22(a)(i)) plots. Columns of 6.0 m length suggest some degree of bulging in the upper zone close to the top of the lower Carse clay which is the weakest depth of the soil profile (Figures 7.21(a)(ii) and 7.22(a)(ii)). Interestingly, bulging appears to be reduced between 3.0 m and 6.5 m suggesting that the composite treated section is effective in reducing settlement. A degree of punching exists at the base of the column. For a column of length 14.5 m the vertical strain (Figure 7.21(a)(iii)) and horizontal strain (Figure 7.22(a)(iii)) appear reduced compared to stone columns. The behaviour of composite stone columns beneath a strip is therefore considered to be similar to stone columns (Figures 7.21(b) and 7.22(b)).

7.6.3 3x3 Column raft

The distribution of the vertical and horizontal strain for a 3x3 column strip with columns of length 2.4 m, 6.0 m and 14.5 m is shown in Figure 7.23 and 7.24. For various lengths of composite column considered the observed behaviour of settlement inferred deformation ratios (Section 7.4) and shear strain plots (Section 7.5). Composite columns of various lengths were found to show consistent behaviour of settlement inferred deformation ratios (Section 7.4) and shear strain plots (Section 7.5). Columns with length 2.4 m bulged at a depth of 2.9 m which is consistent with the vertical strain (Figure 7.23(a)(i)) and horizontal strain (Figure 7.24(a)(i)) plots. Columns with length of 6.0 m suggest a degree of bulging in the upper zone close to the top of the lower Carse clay which is the weakest depth of the soil profile (Figures 7.23 (a)(ii) and 7.24(a)(ii)). The magnitude of bulging appears significantly reduced within the treated composite column zone. Composite columns with length of 14.5 m appears to indicate lower vertical strain (Figure 7.23(a)(iii)) and horizontal strain (Figure 7.24(a)(iii)) compared to stone columns (Figures 7.23(b) and 7.24(b)). Bulging occurs at a deeper depth than for stone columns which is related to the use of the composite material in the bulging zone. Composite stone column behaviour beneath a raft is therefore considered to be similar to stone columns.

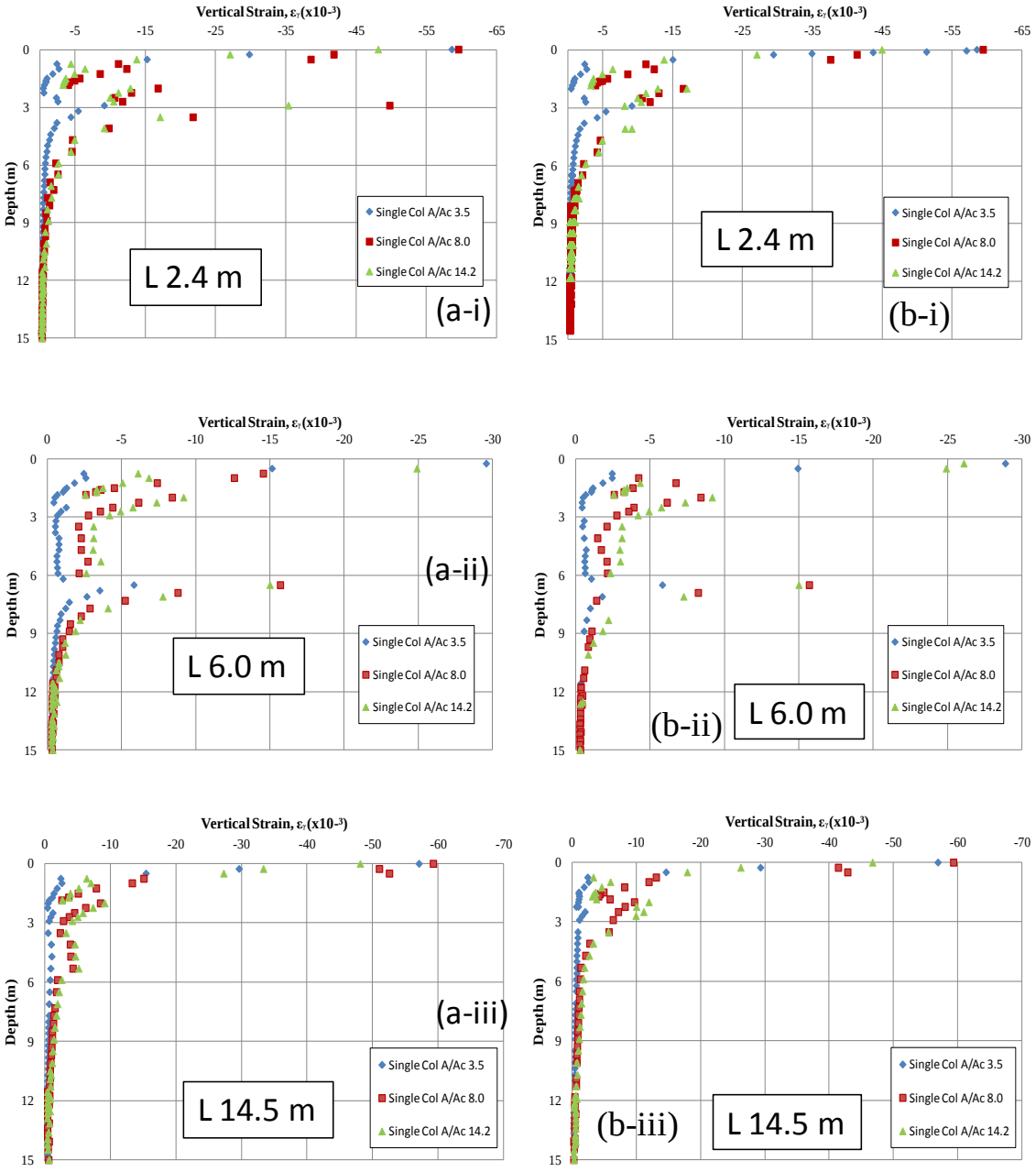

Figure 7.19 Vertical strain for a single (a) composite stone column and (b) stone column of lengths 2.4 m, 6.0 m and 14.5 m

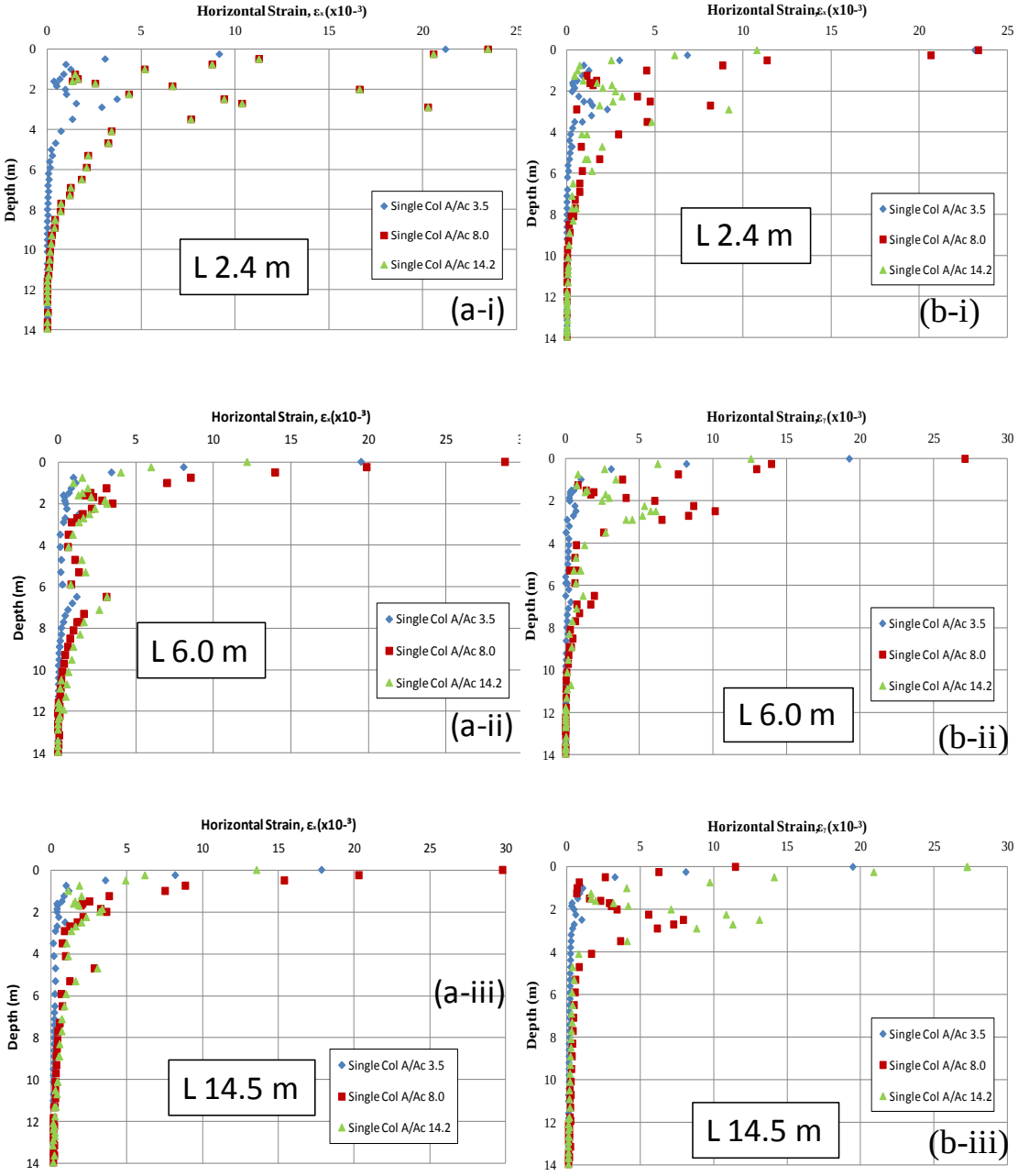

Figure 7.20 Horizontal strain for a single (a) composite stone column and (b) stone column of lengths 2.4 m, 6.0 m and 14.5 m

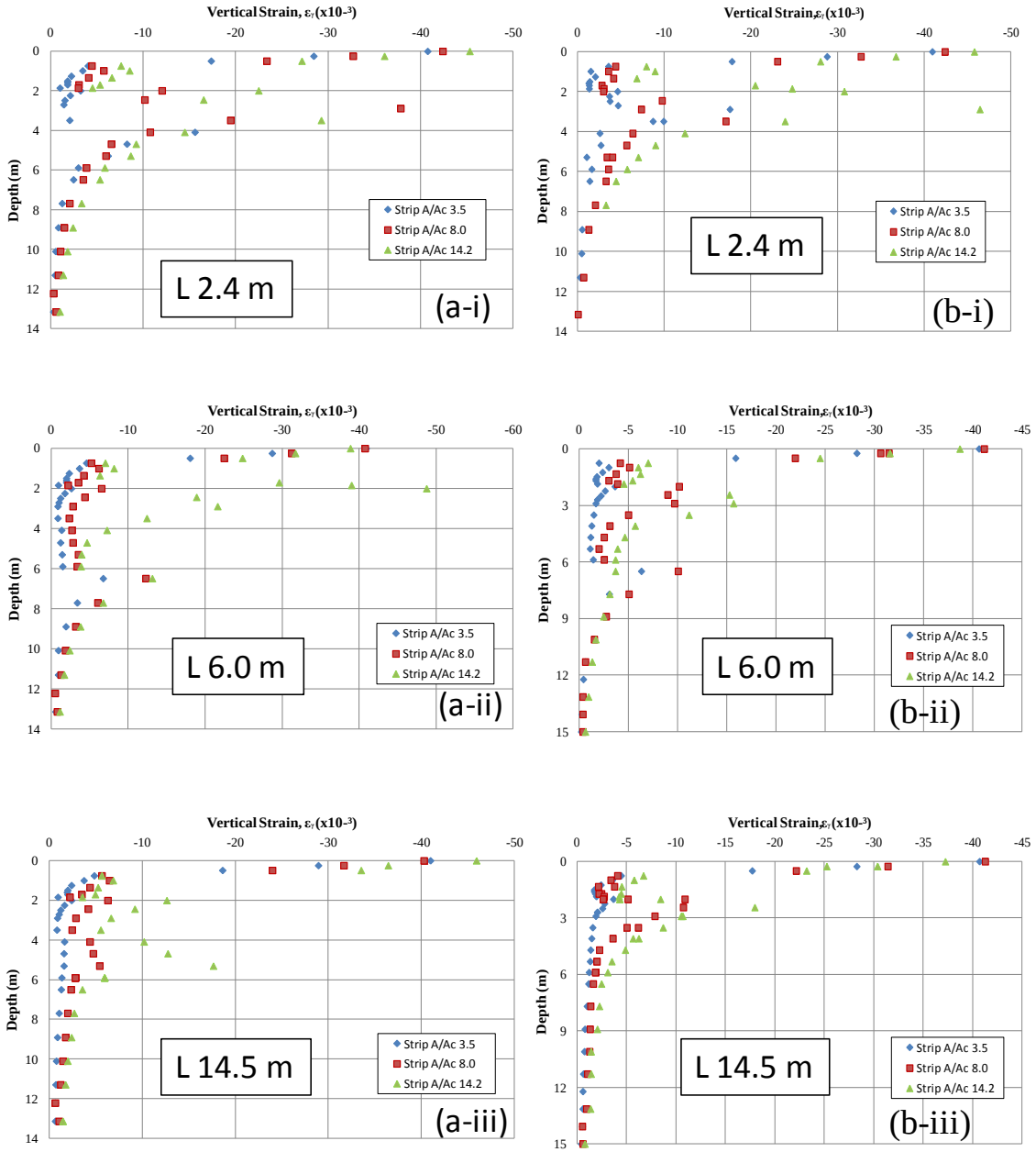

Figure 7.21 Vertical strain for a three column strip with (a) composite stone column and (b) stone column of lengths 2.4 m, 6.0 m and 14.5 m

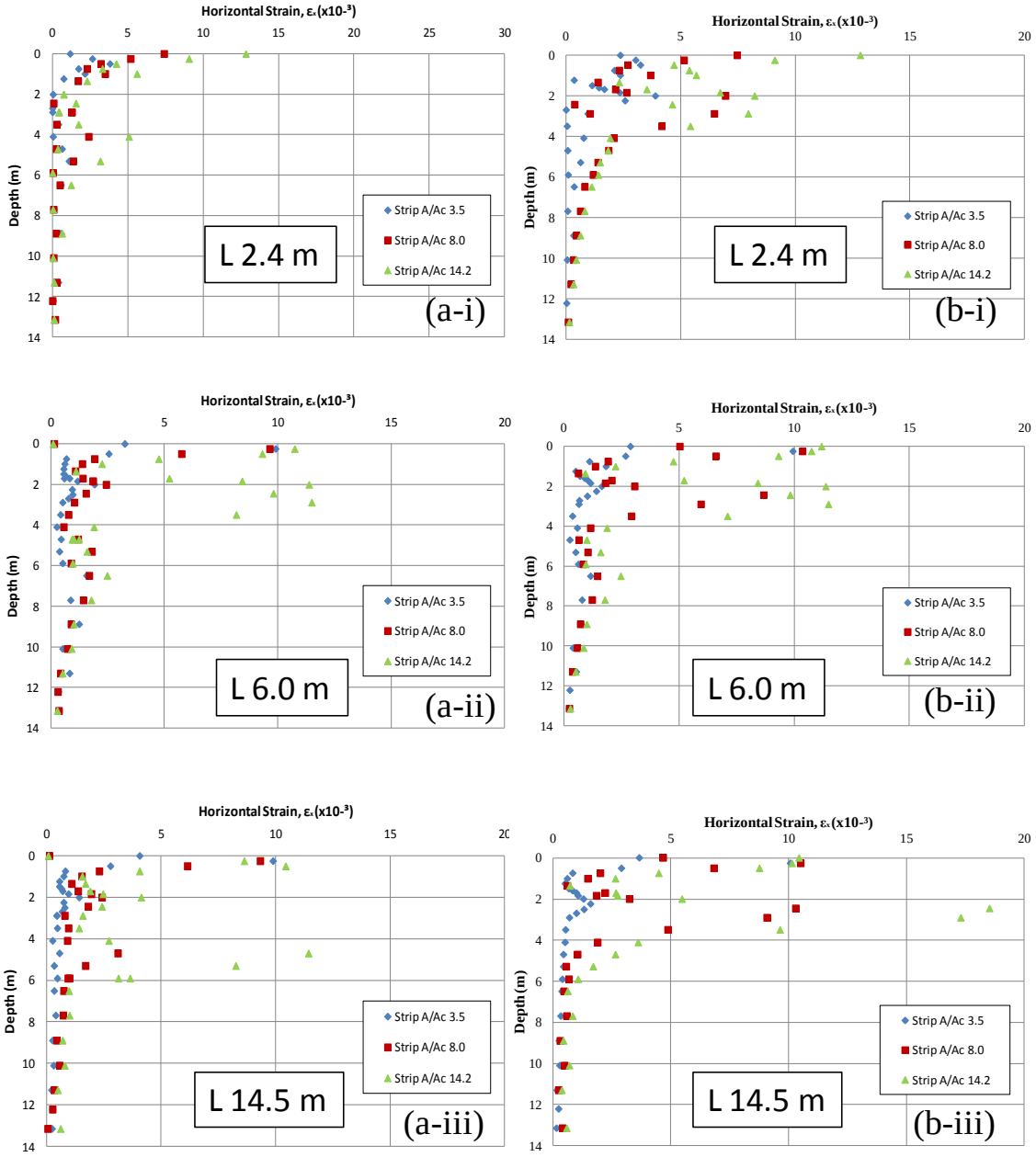

Figure 7.22 Horizontal strain for a three column strip with (a) composite stone column and (b) stone column of lengths 2.4 m, 6.0 m and 14.5 m

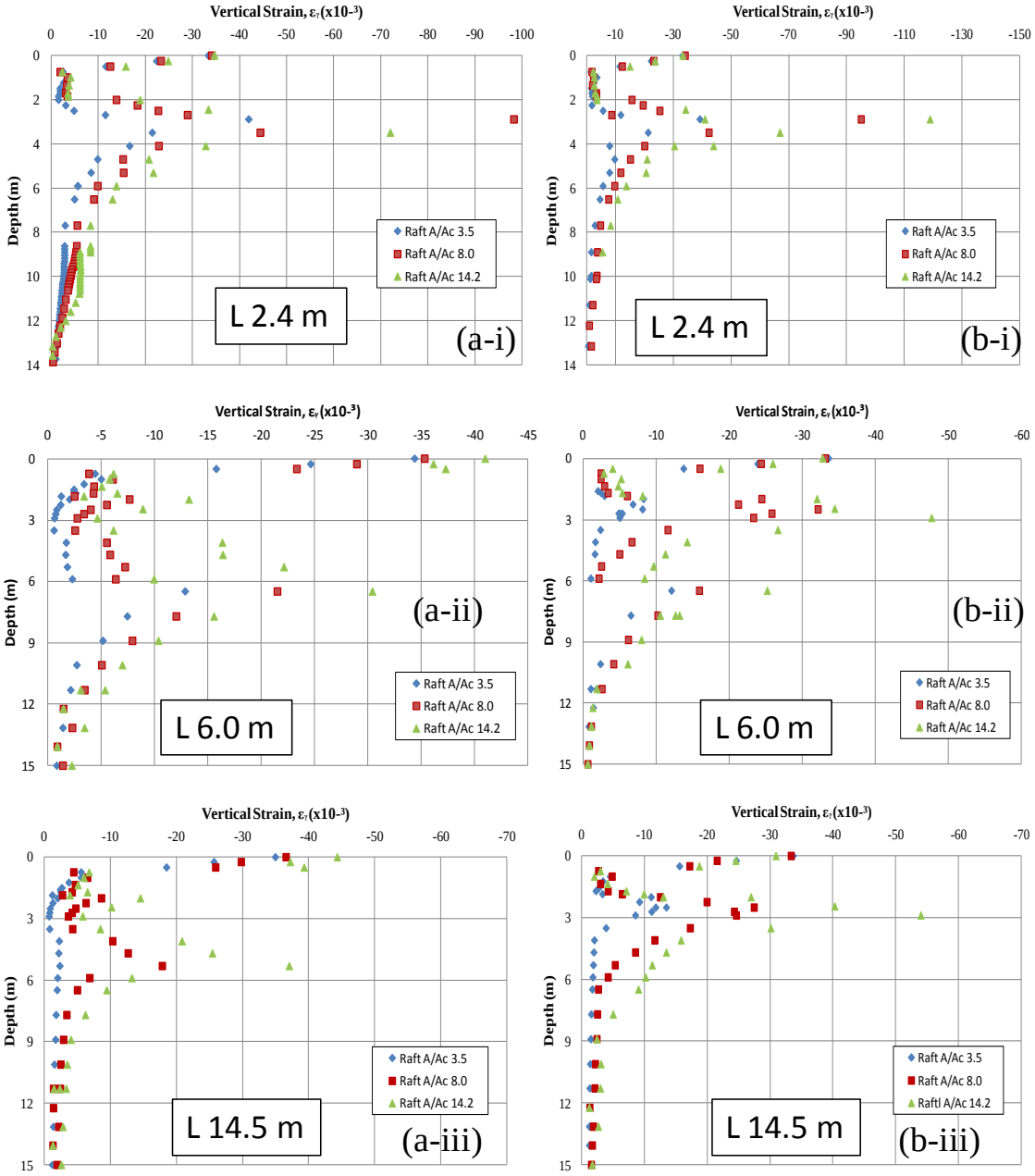

Figure 7.23 Vertical strain for a nine column raft with (a) composite stone column and (b) stone column of lengths 2.4 m, 6.0 m and 14.5 m

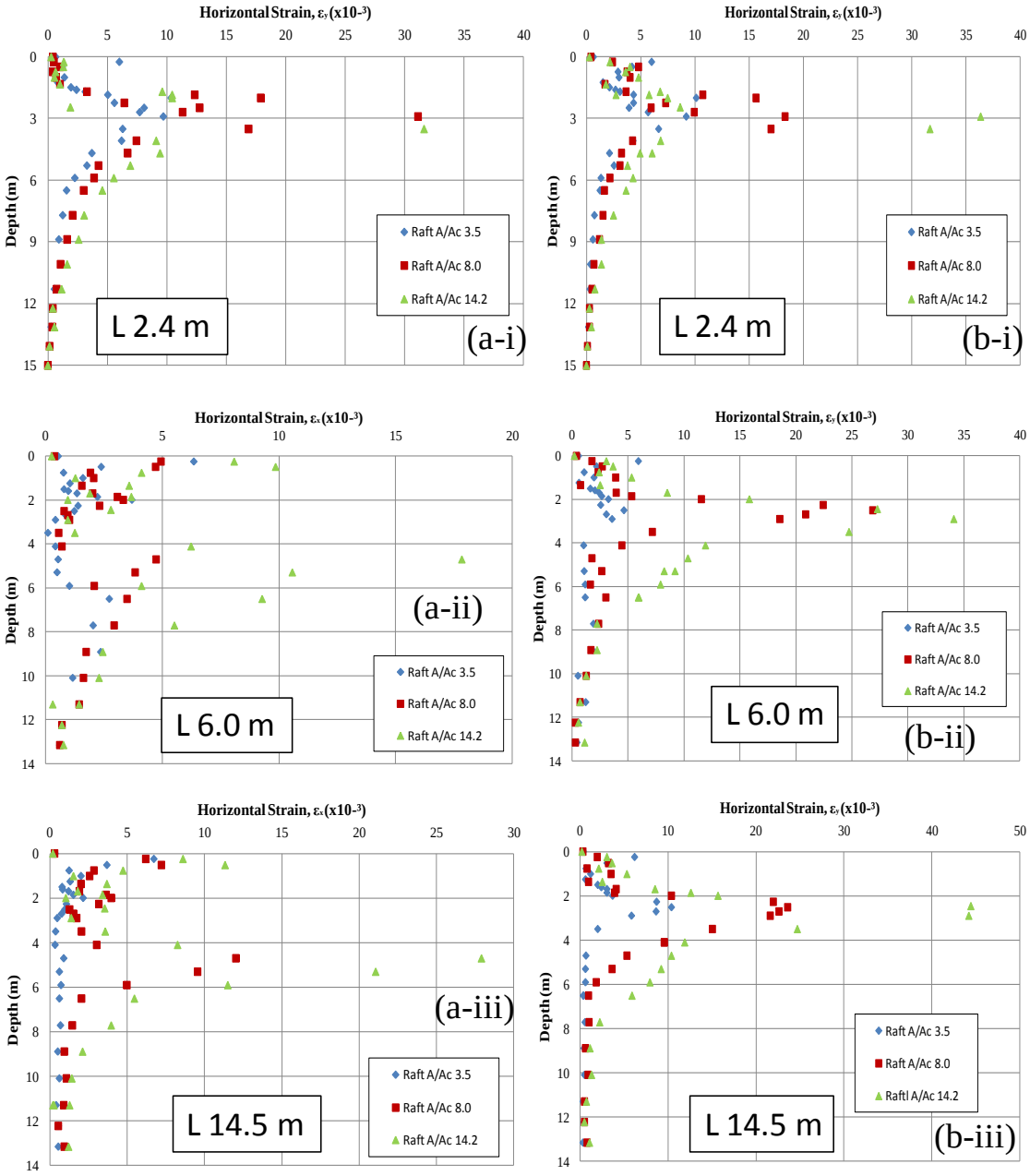

Figure 7.24 Horizontal strain for a nine column raft with (a) composite stone column and (b) stone column of lengths 2.4 m, 6.0 m and 14.5 m

7.7 Conclusions

7.7.1 Settlement performance

The settlement performance of composite columns was assessed by applying the basic improvement factor described by Priebe (1995). This factor is a ratio of untreated settlement to treated settlement. The introduction of the composite columns into the Bothkennar soft soil profile was found to reduce the settlement for all foundation configurations, area ratios and column lengths. The key findings in terms of settlement performance and their implication for the design of composite stone columns are summarised as follows:

- The stiff crust and upper Carse clay extend to a depth of 2m from surface which limits the settlement improvement for stone columns. For the case of composite columns a similar effect is seen such that until a column length of 2.4m is exceeded the columns have the same settlement improvement factor regardless of area ratio. For area ratios of 3.5, 8.0 and 14.2 the settlement improvement factor was found to be 1.27, 1.16 and 1.11 regardless of foundation type. The use of the CSC increases the settlement improvement factor by 0.01 for area ratios of 3.5 and 8.0 with an increase of 0.04 for A/A_c of 14.2. This effect is considered marginal for this column length.
- As the column length is increased to 14.5m for an area ratio of 3.5 the settlement improvement factors become 1.75, 2.40 and 3.45 for a single column, strip and raft foundation. The use of composite stone columns represents an increase in settlement improvement factors of 0.16, 0.37 and 1.07 for a single column, strip and raft foundation suggesting a significant benefit in utilising this type of column.
- Utilising an area ratio of 8.0 and column length of 14.5m the settlement improvement factor was 2.65, 2.10 and 2.56 which represents an increase of 1.32, 0.60 and 0.87 for single column, strip and rafts with CSC compared to stone columns.
- With the largest area ratio of 14.2 and columns of length 14.5m the settlement improvement factor was 1.82, 1.77 and 2.09 which represents an increase of 0.62, 0.46 and 0.69 for single column, strip and rafts with CSC compared to stone columns. The lowest improvement like stone columns is observed for

configurations with the highest area ratio. This is to be expected since at this area ratio columns are spaced 2.0m apart and act independently.

- From the analysis of the results it can be suggested that utilising composite stone columns rather than stone columns improves the settlement reduction as columns increase in length. For the longest column lengths of 14.5m with area ratios between 3.5-14.2 the increase in settlement reduction is in the range of 6%-28% for single columns, 8%-20% for strip and 13%-24% for raft foundations. Therefore, it is suggested that in terms of settlement this type of column reduces bulging in the weakest zone of the soil profile between 1.7m-4.0m.

7.7.2 Settlement inferred deformation ratios

An assessment was made of the influence of introducing the composite material into stone columns using the punching and compression ratios described earlier in Chapter 5. Two main modes of deformation, bulging and punching, were observed in Chapter 5 for stone columns. Columns which punch into the underlying soil transfer most of the applied load to the base. This mode of deformation is characterised by high punching ratios and low compression ratios. Columns which suffer bulging failure tend to bulge laterally into the soil stress-share with the surrounding soil while failing to transfer load to the base of the column. Typically, bulging failure is characterised by high compression ratios and low punching ratios.

Examination of the results of punching and compression ratios suggest that composite stone column are exhibiting behaviour consistent with stone columns. This suggests that the benefits of stone column behaviour maybe retained with composite columns while allowing for settlement reduction particularly in the bulging zone. The main modes associated with composite columns are described as follows:

- *Punching failure:* was observed for all area ratios of the composite column foundations. The depth of maximum punching was recorded as 3.6 m for A/Ac ratios of 8 and 14.2 which is deeper than the stone columns. As the A/Ac ratio increased the magnitude of bulging increased which suggests that the composite nature, i.e. increased cohesion in the bulging zone of the new proposed column, leads to a higher concentration of the applied load. This is supported by the cross sections of shear strain which suggest a higher magnitude is observed at

the base of the columns for the composite case. It is suggested that punching mode of failure is dominant for short columns.

- *Block failure:* was seen for the lowest area ratio of 3.5 with punching occurring at a depth of 2.4 m. This was identified by low punching and low compression ratios.
- *Bulging failure:* Compression ratios were much smaller in magnitude between 2.4 m and 4.8 m column lengths than with stone columns. It is suggested that bulging failure occurs below this depth which was seen as reducing punching ratios and increasing compression ratios.

7.7.3 Shear strain behaviour

Three column lengths of composite column were examined to compare to stone columns and examine the specific modes of deformation and the associated distribution of shear strains: 2.4 m long columns to examine punching; 6 m long columns to illustrate the change from punching to bulging failure and 14.5 m columns to illustrate bulging failure as the columns are end bearing and founded on a rigid stratum. The main observations for composite column behaviour are summarised as follows:

- For short column single column lengths of 2.4 m, increasing the area ratio has the effect of increasing the magnitude and size of the zone of shear stress observed along the column and at its base. For a low area ratio of 3.5 the development of shear strain appears negligible. For single columns of length 6 m the strain between column and soil is negligible. As the area ratio increases shear strain develop within the column and at its base. For a A/Ac ratio of 8 no significant shear strains develop within the column which suggests that punching is the dominant mode of failure. For a A/Ac ratio of 14.2 the highest magnitude of shear strain, i.e. bulging failure, develops at a deeper depth than that observed for stone columns. This is potential evidence of the composite column transferring applied load to depth. For a column length of 14.5 m the column does not develop bulging failure for A/Ac ratios of 3.5 and 8 which is encouraging since stone columns have been shown to develop bulging failure (Chapter 5). For a A/Ac ratio of 14.2 bulging appears to occur at the top of the lower Carse clay which is at a similar depth to a stone column.
- For a 1x3 column strip and a 3x3 column raft, 'block' failure was observed for an area ratios of 3.5 and 8.0 with column lengths of 2.4 m and 6.0 m. With

increasing A/Ac ratio the mode of deformation became punching failure for 2.4 m columns and bulging failure for 6 m columns.

- For end bearing columns of 14.5 m length no bulging failure was noted for strip or raft foundations for A/Ac ratio of 3.5. For an A/Ac of 8 and 14.2 shear strain developed in the columns below the bulging zone for the strip and raft. This suggests that the column is transferring stress to depth and the concentration of shear stress below this depth is suggestive of bulging failure being transferred to depth.

7.7.4 Characteristic column behaviours

The distribution of vertical strain and horizontal strain were examined for column lengths of 2.4 m, 6.0 m and 14.5 m. It was difficult to identify bulging or punching modes of deformation from the results. It appears that for columns there is evidence of both modes of deformation occurring simultaneously. The stress concentration ratios were found to be influenced by the distribution of vertical and horizontal strain within the columns. Upper sections of columns suggest large magnitude vertical strains which are in a state of plasticity, which limits their ability to absorb large vertical loads. As a result stress concentration ratios are lower in these regions.

Chapter 8

Discussion of results for stone and composite stone columns

8.1 Introduction

The research conducted into the settlement performance, settlement inferred deformation ratios, and stress concentration ratios for the different column group configurations examined in Chapters 5 and 7 are now discussed in the context of previous stone column research.

This research has examined the settlement behaviour of stone columns in terms of the column configuration and confinement for end bearing and floating stone columns. The results of end bearing FEM in PLAXIS 3D Foundation is compared to previous research and design methods.

This research has identified two modes of deformation from settlement inferred deformation ratios and total shear stress analysis which were seen for stone columns and composite stone columns installed using the Bothkennar soil profile and numerical analysis. The profile was constructed from data sourced from the literature and modelled using the Hardening soil model to attempt to capture the effect of increased stiffness of the soil due to increased confining stress. The columns were represented by Mohr-Coulomb Perfect Plasticity due to their stiff nature. The two modes of failure were bulging failure and punching failure. A sub-type of punching failure was also identified for closely spaced columns. The deformation modes observed are compared to laboratory studies conducted by Hu (1995), Muir-Wood *et al.* (2000), McKelvey *et al.* (2004), Black (2006), and numerical studies by Killeen (2012).

The novel composite stone columns are now compared to stone columns and their behaviour compared where practicable to the previous research. Justification is given for the design approach to using these new columns to reduce settlements. At the end of the Chapter new design equations are proposed based on numerical results.

8.2 Settlement analysis of stone columns

This research has examined the complex behaviour of unit cell, single column, 1x3 column strip and a 3x3 column raft numerically by FEM analysis in Chapter 5. Key design parameters were examined to determine their influence on column performance and it was noted that area ratio and column length had a significant effect on settlement.

The different configurations reveal that columns which are not restrained by neighbouring column suffer higher settlements. The lowest settlements were observed for columns which were restrained in an infinite array and 3x3 raft configurations.

8.2.1 Comparison of the settlement ratio for end bearing stone columns from PLAXIS to Priebe (1995)

The design method of Priebe (1995) is based on analytical calculations which attempt to approximate the reduction in vertical stress with increasing depth beneath a unit cell. The method was designed for use in homogeneous soils so careful subdivision of the soil profile must be made during the design process. The method does not directly use the area of the foundation in the calculation but instead uses the area ratio, A/Ac. It is explicitly assumed that columns are end bearing and are founded on a stiff stratum which prevents end bearing failure. Any bulging of the column is assumed to occur over its entire length which is a simplification since most research (including this thesis) have identified bulging as occurring in the upper regions of the column.

The three ground improvement factors of Priebe (1995) attempt to account for different characteristics of column behaviour. The basic factor, n_0, assumes that the column is composed of incompressible material with bulk densities of the column and soil ignored. It is assumed that the column suffers from plastic shear from the onset of loading and the soil behaves elastically. It is also assumed that k_0 = 1 for the soil to account for installation effects and Poisson's ratio of 1/3 to represent drained state of the material. The factor, n_1, attempts to account for column compressibility by increasing the area ratio A/Ac to $\Delta(A/Ac)$. This is necessary since the n_0 factor ignores the pressure difference between the column and soil which causes the bulging behaviour of columns. Bulging behaviour depends solely on the distribution of the applied foundation load and this method considers bulging to be constant over the entire length. The final factor, n_2, attempts to account for the fact that the column and soil weight may exceed external loads and that with increasing overburden the columns have better lateral support.

Priebe (1995) presented a design chart (Figure 2.31) which relates the settlement of groups of columns beneath pad footings to the settlement of stone columns beneath an infinite area (s_∞). The curves are considered to account for the stress distribution beneath footings but consider a reduced bearing capacity for columns on the edge. The author states that the footing area must be calculated from the area ratio, A/A_c, to

compensate for footing size since larger footing areas have higher A/A_c ratios which give lower improvement factors for settlement. The curves are considered to be valid for area ratios up to 10.

This research has examined the behaviour of stone columns beneath a unit cell, small pad, 1x3 column strip and 3x3 column raft. It was found that the column confinement and settlement improvement factor is influenced by the number of columns, area ratio and column length. The design method of Priebe (1995) uses the settlement ratio S/S_{uc} to relate the depth to diameter ratio, d/D, to the number of columns. The depth to diameter ratio is equivalent to the column length to diameter ratio, L/d, for end bearing columns. The results of this research are compared to Priebe (1995) in Figure 8.1. It can be seen that an increase in the number of columns leads to a higher S/S_{uc} ratio. With an increasing number of columns from a single column to a nine column raft the confinement increases which leads to higher levels of vertical stress with depth. Vertical stress also increases with footing area. As the number of columns increase the S/S_{uc} ratio increases towards a value of 1 which represents boundary conditions similar to unit cell conditions. The area ratio, *A/Ac*, of 3.5 is similar for PLAXIS and Priebe (1995). Beyond an area ratio of 3.5 PLAXIS and Priebe (1995) solutions diverge.

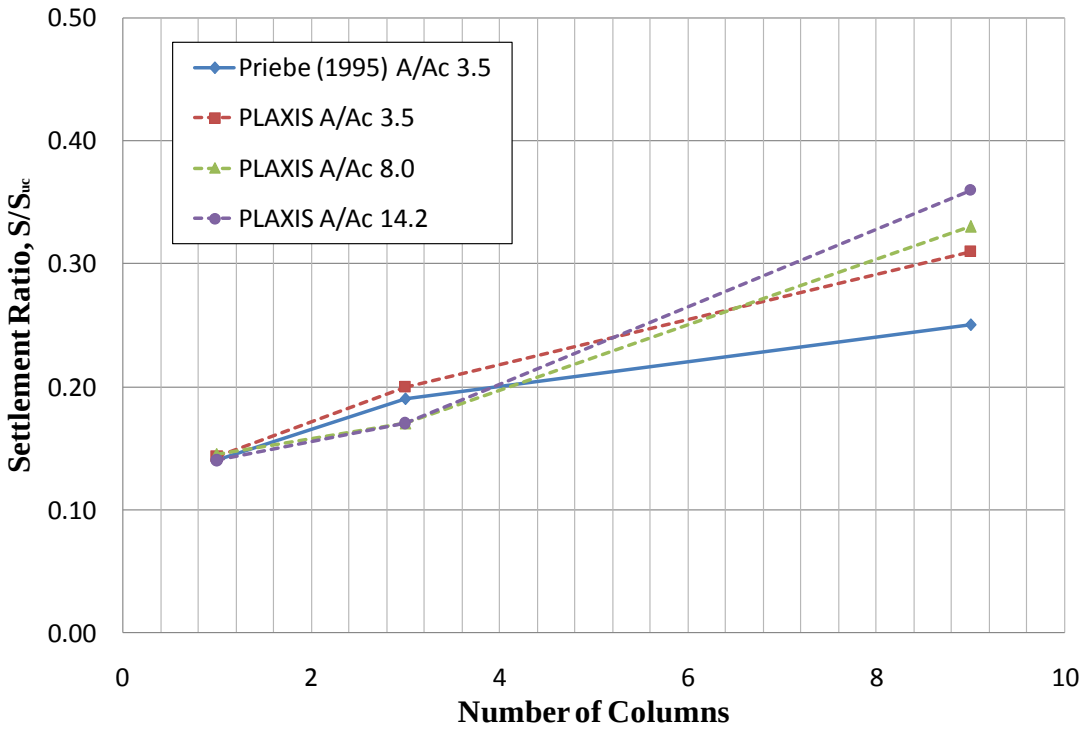

Figure 8.1 Comparison of settlement ratios for groups of stone columns from Priebe (1995) and PLAXIS 3D Foundation

8.2.2 Comparison of the results for end bearing stone columns to McCabe *et al.* (2009)

McCabe *et al.* (2009) complied a column settlement database from twenty case studies which consisted of a series of data points representing settlement improvement factors. The authors plotted the improvement factor data points against the basic improvement factor curve of Priebe (1995) with a friction angle of 40° for the column material. The majority of the data points related to wide spread loading with three of these case studies relating to pad and strip footings. The authors suggest that Priebe (1995) maybe too conservative and in fact higher friction angles may be achieved. The results of the PLAXIS 3D Foundation simulations are plotted against the database for unit cell, single pad, 1x3 column strip and 3x3 column raft in Figure 8.2. The simulations appear to follow the general trend of the field data. Given that the strip and raft data display similar trends to the field data, it is suggested that the PLAXIS results are representative of field behaviour. Interestingly, McCabe *et al.* (2009) states that the friction angle of 40° is too conservative for stone column design and that higher values can be achieved. The PLAXIS results suggest that for a friction angle of 45° the settlement improvement for small groups is much lower. This is due to the soft soil nature of the lower Carse clay in the Bothkennar soil profile.

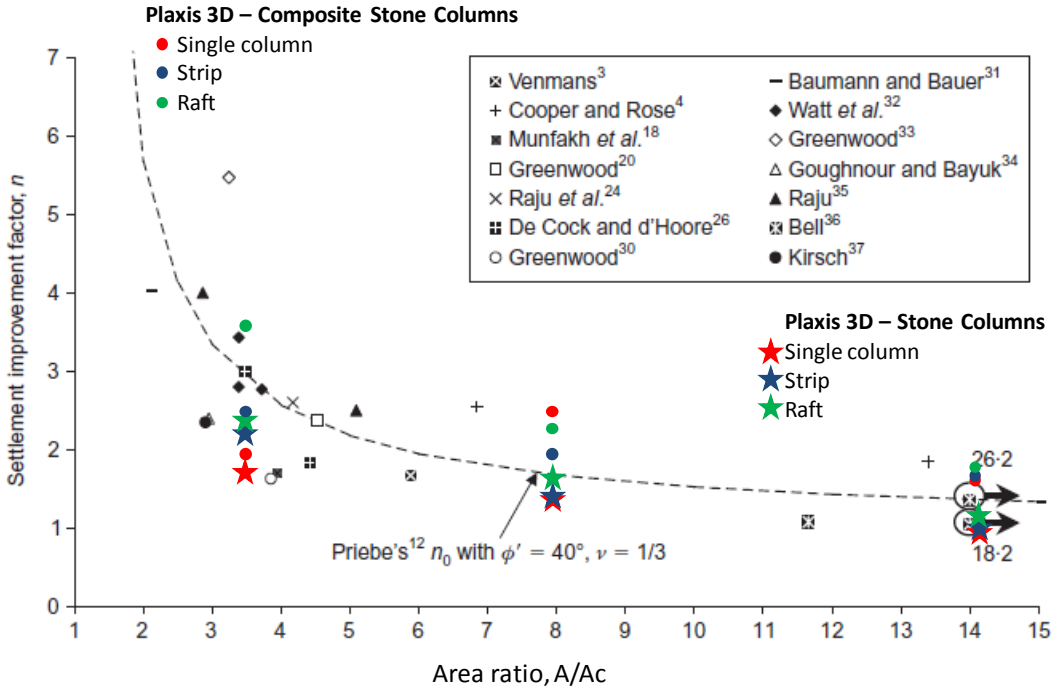

Figure 8.2 Settlement improvement factors plotted against area ratio for various field installations compared to PLAXIS 3D Foundation results (modified from McCabe *et al.* 2009)

8.3 Deformational behaviour and settlement inferred deformation ratios

8.3.1 Overview

This research has utilised PLAXIS 3D Foundation to examine the deformational behaviour and settlement of stone columns as investigated in Chapter 5. The results of that analysis are now compared to the findings from other studies into stone column deformational behaviour.

8.3.2 Key findings from PLAXIS 3D Foundation FEM analysis

The FEM analysis in Chapter 5 examined the deformational behaviour of stone columns beneath four foundation configurations: unit cell, small pad with single column, 1x3 column strip and a 3x3 column raft. The influence of key design parameters was examined for each foundation configuration to determine how these configurations impacted the column confinement and deformational behaviour. In order to better understand deformational behaviour two ratios were defined, compression and punching. Both ratios had been successfully used in other studies to help define deformation behaviour from relating foundation, base of column and soil near the base of the column settlement. The ratios were used to identify two different modes of deformation, bulging and punching. Interestingly, a sub-type of punching failure first observed by Black (2007) termed 'block failure' was seen. The deformation modes (including 'block' failure) were then verified by comparing the shear strain across sections in Chapter 5. It was noted that the area ratio and column length are significant controls on the mode of deformation seen. The two main deformation modes and sub-type can be described as follows:

Bulging failure:

- Observed for high area ratios, not observed for low A/Ac.
- Defined by high compression ratios and low punching ratios.
- Occurred at the point of lowest lateral restraint in the Bothkennar soil profile from the top of the lower Carse clay to a depth of approximately 4.1 m. Below 4.1 m the soil was able to provide sufficient restraint. Considered that the stiff crust and upper Carse clay being competent restrained the column assisting in the transfer of stress to depth.

- Bulging weakens the ability of the column to transfer stress to depth which is observed by low punching ratios and shear strain in the upper column region on total strain profiles

Punching failure:

- Observed for short columns and all area ratios
- Defined by low compression ratios and high punching ratios
- Shear stress development is highest at the base of columns. With increasing A/Ac the columns act independently increasing the degree of punching.

Block failure (sub-type of punching failure):

- Sub-type of punching failure and shares similar characteristics.
- Observed for columns with low A/Ac ratios. Columns and soil act together as one unit and punch into the underlying soil.
- As columns and soil punch together as one unit, low differential settlement between them results in low compression and low punching ratios being observed.
- Shear stress appears uniform beneath the columns base. Shear stress in the columns and in the soil between the columns is uniform.

8.3.3 Comparison of key findings to Hu (1995) and Muir-Wood *et al.* (2000)

Muir-Wood *et al.* (2000) reported and discussed a series of scaled laboratory tests on rigid strip footings by Hu (1995). Model stone columns were installed beneath the footings in soft kaolin clay to examine the effect of area ratio, length of column and method of installation on deformational behaviour under drained conditions. The study was reviewed in Chapter 2 Section 2.3.2. A summary of the key findings of Muir-Wood *et al.* (2000):

- Column behaviour in a strip foundation was found to be different from single column behaviour as described by Hughes and Withers (1974), i.e. deepening of a conical wedge failure was observed for a strip with the central column representing the deepest point of the wedge. For example, bulging failure could be pushed deeper for the central column than the lateral columns due to the lateral restraint by other columns. Kelly (2014) observed conical wedge failure beneath a strip footing pushing the deformation mechanism deeper.

- Stiffness of the reinforced homogeneous clay was found to increase with increasing length of column which reduced the settlement.
- Four modes of deformation were observed: bending, bulging, punching and shearing. The mode of deformation was found to be dependent upon column and foundation configuration.
- The bulging was found to follow the conical slip surface. The degree of bulging was found to increase and the depth of bulging was found to decrease with increasing area ratio.
- Punching failure was observed for short columns. If the column length was less than or equal to the footing diameter then the columns will transfer load to depth and develop punching simultaneously with bulging failure.
- For columns which have a length of one and a half times the footing diameter the penetration phenomenon of 'punching' at the column base is insignificant. Beyond 1.5 diameters punching does not occur and a critical column length is proposed.
- The area ratio was found to be an important parameter in controlling the overall performance of the composite foundation.

8.3.4 Comparison of key findings to McKelvey *et al.* (2004)

McKelvey *et al.* (2004) examined the group behaviour of single and groups of columns beneath a circular foundation installed in soft clay under drained conditions. The study was reviewed in Chapter 2 Section 2.3.2. A summary of the key findings are as follows:

- It was discovered that bulging occurred in both short columns (L/d = 6) and long columns (L/d = 10). In short columns bulging occurred over the entire column length. In longer columns bulging occurred in the upper region with no significant deformation recorded in the lower region.
- The results revealed that the short columns provided less resistance to loading (as they punch into the soft clay below) compared to the longer columns which show resistance to punching.
- Close column spacing was found to increase the confining stress field in the upper portions of the columns. It is considered that it moves friction support to greater depths where smaller settlements are observed. Increasing column spacing increases the area ratio for a constant diameter of column.

McKelvey *et al.* (2004) identified bulging and punching failure as occurring for short columns (L/d = 6) and long columns (L/d = 10). This would be equivalent to PLAXIS column lengths of 3.6 m and 6.0 m for L/d = 6 and L/d = 10 respectively. For the case of 3.6 m punching failure was seen at the base of the columns. For a 6.0 m column bulging failure was observed as the main mode of deformation with some punching visible at the column base. This suggests good agreement between this research and McKelvey *et al.* (2004). The effect of the stiff crust in the PLAXIS Bothkennar soil profile and the homogeneous soil samples of McKelvey *et al.* (2004) appear not to affect the type of deformation observed in this case. The increase in A/Ac ratios in PLAXIS and increased column spacing in McKelvey *et al.* (2004) suggest that the same effect is seen whereby increases in A/Ac and spacing cause higher stress concentrations in the upper portions of the column and ultimately bulging failure.

8.3.5 Comparison of key findings to Black (2007)

Black (2007) examined the group behaviour of single and groups of columns beneath a circular foundation installed in soft clay under drained conditions. The study was reviewed in Chapter 2 Section 2.3.2. The study findings are:

- Closely spaced groups of columns were found to under-perform in comparison to single columns. This is due to 'block failure' in which the columns and soil act together to punch into the underlying soil.
- The mode of deformation was found to be dependent upon column length and configuration. Columns with L/d ratios of between 3 and 5 punched into the underlying soil regardless of configuration. Single columns with L/d ratios of between 7 and 10 were found to display bulging failure whereas closely spaced groups of columns displayed 'block failure' behaviour.
- The critical length at which the mode of failure changes from punching to bulging failure is L/d = 8 under drained conditions. This was also confirmed by Kelly (2014) for strips and small rafts in which laboratory studies on stone columns indicated similar results.

The compression ratios for a single column from PLAXIS are compared with the results of compression ratios computed from penetration data from Black (2007) using Equation 5.2 in Figure 8.3. The compression ratios from Black (2007) are much higher than those obtained from PLAXIS. In PLAXIS the Bothkennar soil profile accounted for the presence of a stiff crust and the upper Carse clay which is not present in the

homogeneous clay tested by Black (2007). The stiff crust and upper Carse clay act to confine the column whereas in a homogeneous soil the potential for bulging is much higher as observed with the higher compression ratios. Figure 8.4 highlights a comparison of the stiff crust thickness of 1.0 m and 0.5 m compared to Black (2007). It is evident that the crust does have an effect on column performance which is not accounted for in laboratory studies using homogeneous samples.

This research sought to examine the influence of key design parameters on settlement performance at working load levels. The results from modelling stone columns in PLAXIS suggest that punching can be observed for floating columns which are short and/or have with low A/Ac ratios. Increasing the length of column was found to reduce settlements with the effects of punching reducing with depth. No evidence was observed that a critical length exists for stone columns in comparison to Black (2007) and Kelly (2014) who considered this existed at a ratio of L/d = 8. In both cases the laboratory studies utilised idealised homogeneous soil samples which does not reflect real soil conditions.

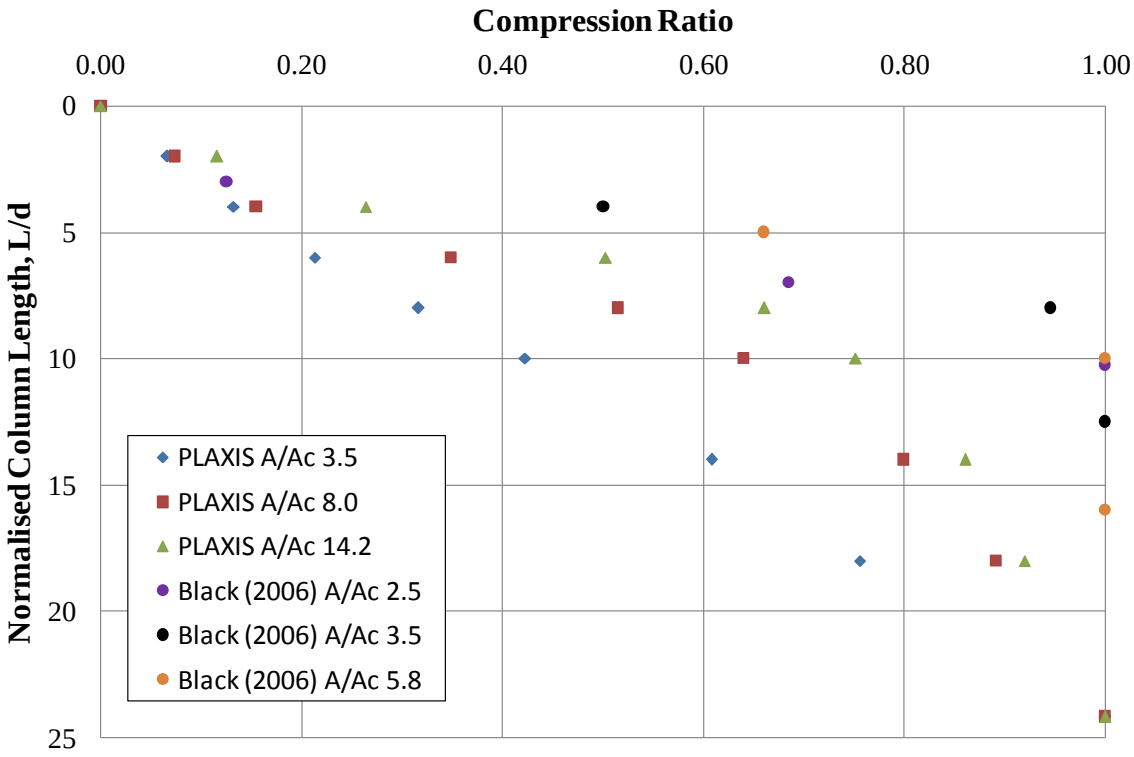

Figure 8.3 Comparison of the results of compression ratios for a single stone column in PLAXIS to Black (2007)

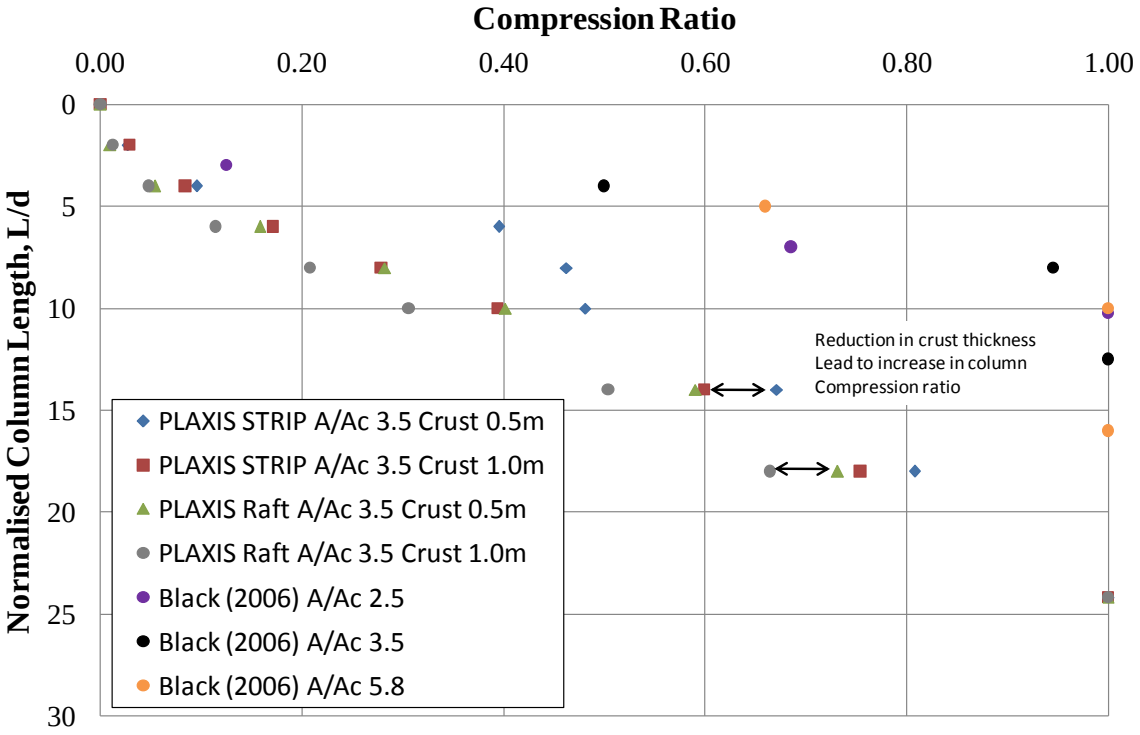

Figure 8.4 Comparison of the results of compression ratios for different crust thickness a 1x3 column and 3x3 column raft from PLAXIS to Black (2007)

8.3.6 Comparison of key findings to Killeen (2012)

Killeen (2012) examined the group behaviour of single and groups of columns beneath a circular foundation installed in soft clay under drained conditions. The study was reviewed in Chapter 2 Section 2.5.3. The study findings are:

- A/Ac ratio and column length were found to have a significant effect on settlement performance. At low area ratios column length was found to have the greatest effect. Increasing the number of columns, and hence confinement, reduced settlements.
- Compression and punching ratios were defined to describe three distinct mechanisms: punching, block failure and bulging. The presence of these mechanisms was identified by analysing the distribution of shear strain within columns and soil.
- Examination of the deformational behaviour showed that a combination of bulging and punching can occur simultaneously. One of the mechanisms will be more dominant depending upon the area ratio and column length.
- When a crust is present it is suggested that a unique critical length for columns in a small group does not exist. The presence of a stiff crust in most soft clays,

which is absent in laboratory studies, is considered to have significant effect on the deformational behaviour of stone columns. As such the observation of critical length in the laboratory studies of homogenous clay beds is considered in part due to the absence of the stiff crust as columns are more likely to bulge in the upper regions of the column and cannot transfer their load to the base of the column.

The research of Killeen (2012) examined column behaviour for small groups of stone columns arranged in configurations of single column, 2x2, 3x3, 4x4, and unit cell numerically in PLAXIS 3D Foundation. In this research PLAXIS was also used but for column configurations of single column, 1x3, 3x3 and unit cell configurations. In the FEM analysis of Chapter 5 the influence of column length and area ratio were found to be significant in the development of specific modes of deformation. Bulging failure was found to occur for high area ratios and characterised by high compression and low punching ratios. The results were validated against total shear strain cross sections which confirmed the presence of bulging failure at the top of the lower Carse clay which represented the weakest point in the Bothkennar soil profile. Bulging weakens the ability of the column to transfer stress to depth which is observed by low punching ratios and end bearing stress on total strain profiles. Killeen (2012) also noted similar behaviour with bulging occurring at the weakest point in the soil profile for high A/Ac ratios regardless of foundation configuration. A stiff crust thickness of 1.5 m was used compared to the 1 m thickness in this research although the observations around bulging failure are similar. Killeen (2012) noted that punching failure occurred for short columns with low compression and high punching ratios with shear stress development occurring at the column base and sides. It was also reported that block failure was observed for column configurations with low A/Ac ratios with uniform shear stress seen beneath columns. Such observations on punching and block failure were also made for strip and raft foundations in this research which validates the observations made in Chapter 5 regarding deformation modes.

8.4 Use of composite stone columns in soft soils

Composite stone columns (CSC) is the name proposed for a new novel stone column variant. By installing a composite material consisting of Protomix and granular material in the area associated with stone column bulging, the settlement behaviour can be improved. In this research the behaviour of stone columns installed in the

Bothkennar soil profile was examined in Chapter 5 and the main modes of deformation identified. The depth at which bulging occurred was identified. An analysis was then conducted on the potential binder material (Chapter 6) and a sensitivity analysis carried out utilising the Bothkennar soil profile for key design parameters. The goal was to assess the settlement and modes of deformation that occur with the new composite stone columns. This FEM analysis confirmed that the new variant of stone column behaves in a similar manner to traditional stone columns which allows for similar approaches to their use in terms of foundation design and treatment.

8.4.1 Settlement performance

The settlement performance of composite stone columns (CSC) was assessed using key design parameters of area ratio and column length which had been identified by the stone column analysis (Chapter 5) as being significant. The key findings of the settlement analysis are described in detail in Chapter 7 and are now summarised below:

- CSC were found to significantly reduce the settlement of composite foundations compared to traditional stone columns for all foundation types and area ratios with column lengths greater than 2.4 m. The highest improvement was observed for end bearing CSC.
- For CSC lengths of 2.4 m or less the settlement improvement factor was found to be similar to stone columns. This is due to the influence of the stiff crust and upper Carse clay which have low settlement improvement ratios due to their stiff competent nature which provides column restraint.
- Beyond a column length of 2.4 m increasing the A/Ac ratio was found to reduce the settlement improvement factor as columns act independently and are not restrained by nearby columns.
- The application of CSC with an A/Ac ratio of 8 was able to achieve the same improvement factor as stone columns with an A/Ac of 3.5. This would suggest that composite stone columns could offer an economic advantage as well as settlement control compared to traditional stone columns.

The results of the CSC settlement improvement factors for end bearing columns from PLAXIS are plotted in Figure 8.2 from McCabe *et al.* (2009). It can be seen that the CSC outperform traditional stone columns and appear to follow the general trend of Priebe (1995).

8.4.2 Settlement inferred deformation ratios

The deformation behaviour of CSC was examined using settlement inferred ratios. Previous studies in Chapter 5 had identified two main modes of deformation, bulging and punching (including 'block failure') associated with stone columns. If CSC were to be utilised in current practice with existing technology for installing stone columns then the modes of deformations should be similar. Additionally, if CSC were indeed altering the bulging behaviour at the weakest depths of the soil profile then the ratios should also change to account for the reduction in settlement. The key findings of the settlement analysis are described in detail in Chapter 7 and are now summarised with comparisons to previous research:

- The two main modes of deformation, bulging and punching (including 'block failure') were observed for CSC which suggested the columns are performing in a similar manner to stone columns. This allows for current foundation designs associated with stone columns to be used without the need for reinforced foundations that are associated with pile foundations.
- *Punching failure:* was observed for all A/Ac ratios by low compression ratios and high punching ratios. For A/Ac ratios of 8 and 14.2 the highest punching ratio was observed at 3.6 m in contrast to 2.4m observed for A/Ac 3.5. As the A/Ac ratio increased the applied load from the foundation increased leading to higher stress concentration ratios in the column. The enhanced cohesion of the composite column allows it to absorb more of the load which leads to punching occurring at a deeper depth than traditional stone columns. This is verified by the cross sections of total shear strain and this is considered the main mode of deformation for short columns.
    - *Block failure:* was observed for the lowest A/Ac ratio of 3.5 with punching occurring at a depth of 2.4 m. It was suggested by low punching, low compression ratios and confirmed by the total shear strain cross sections.
- *Bulging failure:* Compression ratios were much smaller in magnitude between 2.4 m and 4.8 m column lengths than with stone columns. It is suggested that bulging failure occurs below this depth which was seen as reducing punching ratios and increasing compression ratios. This is supported by the cross sections of shear stress which indicate that a deeper deformation occurs which is considered to be bulging failure.

The punching failure associated with short columns was observed by Muir-Wood *et al.* (2000), McKelvey *et al.* (2004), Black (2007) and Kelly (2014). Black (2007) observed block failure for closely spaced columns and suggested that the mode of deformation is dependent upon L/d ratio. Punching occurred for L/d = 3-5 and Bulging for L/d = 7-10. In this research a CSC length of 3.6 m indicated the highest degree of punching which represents a L/d ratio = 4. Bulging as the dominant mode of deformation was observed in this research for a length of 6.0 m which represents a L/d ratio of 10 which is comparable to Black (2007). It is therefore suggested that CSC behave like traditional stone columns by their mode of deformation.

8.4.3 Shear strains

Three column lengths were chosen to allow comparison of the specific modes of deformation and the associated distribution of shear strains of composite stone columns to stone columns: 2.4 m long columns to examine punching; 6 m long columns to illustrate transition from punching to bulging failure and 14.5 m columns to illustrate bulging failure as the columns were end bearing founded on a rigid stratum. The main observations for composite column behaviour and how it relates to stone columns is summarised as follows:

- For short columns of 2.4 m for a low area ratio of 3.5 the development of shear strain appears negligible. Increasing the A/Ac ratio from 8 to 14.2 leads to an increased magnitude and size of the zone of total shear stress observed along the column and at its base.
- For columns of length 6 m the strain between column and soil is negligible for strip and raft. Bulging failure is not observed for an A/Ac ratio of 8 however for a ratio of 14.2 the highest magnitude of shear strain i.e. bulging failure, develops at a deeper depth than that observed for stone columns. It is suggested that the composite zone of the column allows for the transfer of bulging failure to a deeper depth.
- For columns of length 14.5 m the absence of bulging failure for A/Ac ratios of 3.5 compared to traditional stone columns suggests that the composite has reduced or eliminated bulging failure. The A/Ac ratio appears to allow for sufficient restraint from neighbouring columns for both strip and raft. For an A/Ac ratio of 14.2 bulging appears to occur at the top of the lower Carse clay which is at a similar depth to a stone column. The column is considered to be

acting independently and therefore cannot benefit from mutual restraint from neighbouring columns.

- For a 1x3 column strip and a 3x3 column raft 'block' failure was observed for an area ratios of 3.5 and 8.0 with column lengths of 2.4 m and 6.0 m. With increasing A/Ac ratio the mode of deformation became punching failure for 2.4 m columns and bulging failure for 6 m columns.
- For end bearing columns of 14.5 m length no bulging failure was noted for strip or raft foundations for A/Ac ratio of 3.5. For an A/Ac of 8 and 14.2 shear strain developed in the columns below the bulging zone for the strip and raft. This suggests that the column is transferring stress to depth and the concentration of shear stress below this depth is suggestive of bulging failure being transferred to depth.

The shear strain results are consistent with the previously discussed modes of deformation of punching, block failure and bulging identified by Black (2006), Killean (2012) and Kelly (2014). It is therefore confirmed that CSC behaviour is similar to traditional stone columns which allow established construction methods to be adopted.

8.4.4 Designing composite stone columns: considerations and challenges

The simple design method proposed by Killean (2012) is similar in nature to the definitions used by Balaam *et al.* (1977) and Balaam *et al.* (1985). All approaches suggest a relationship which links column length, L, thickness of soil layer, H, and breadth of the foundation, B. In order to develop a similar method the approach of Killean (2012) is used to derive a simple equation for stone column behaviour. Killean (2012) assumed a stiff crust thickness of 1.5 m compared to a thickness of 1.0 m in this study. It would be expected that although similar the design methods would vary in terms of constants in the equations.

(i) Derivation of the stone column design equation

The design method of Priebe (1995) has indicated a good prediction for stone column settlement behaviour to the simulated response of a unit cell (Chapter 4). Priebe (1995) uses a settlement ratio to relate the settlement of a small group of stone columns to the settlement of an infinite array for end bearing stone columns. In this study stone columns of various lengths have been analysed for different foundation types (Chapter

5). The settlement results of five column lengths of 2.4 m, 3.6 m, 6.0 m, 10.8 m and 14.5 m from the unit cell and small raft were selected to derive the design equation.

The settlement ratio of settlement of a small raft to settlement of a unit cell S/S_{uc}, is plotted against the normalised footing width, B/L in Figure 8.5 and 8.6. Figure 8.5 highlights that for different A/A_c ratios different S/S_{uc} ratios occur. The lowest values of S/S_{uc} represent the highest settlement reductions. From the plot it appears that data points follow a linear trend for points which have the same column length to depth ratio, L/H. With increasing L/H ratio the S/S_{uc} ratio increases. An increase in L/H represents a reducing thickness of soil below the base of the column. The settlement of a column within the unit cell S_{uc} is higher than a small group due to the loading conditions and constant stress with depth. As a result reducing L/H for a unit cell leads to higher settlement and as a result lower S/S_{uc} ratios. Increasing the area ratios for a given L/H, will increase the S/S_{uc} ratio (Figure 8.5). This suggests that increasing the S/S_{uc} ratio signifies an increasing amount of settlement for both the unit cell and small group of columns.

From Figure 8.5 it is clear that for a small group of columns that columns with the same L/H ratio lie on a linear trend. It can be reasonably argued that a relationship therefore exists for each of these ratios between S/S_{uc} and B/L. The points are re-plotted in Figure 8.6 and it can be observed that a best fit line can be applied assuming that the S/S_{uc} and B/L are directly proportional for each L/Hratio. For each L/Hratio the equation of the best fit line is noted. A relationship can be derived as follows:

$$S/S_{uc} = \alpha\,(B/L) \qquad [8.1]$$

α describe the gradient of the slope of the line for each L/Hratio. The R^2 values suggest a good correlation for L/H ratios of 0.41 or less. This suggests that for most values the relative predictability of the model for column length to diameter ratios, *L/d*, of 10 is reasonable with caution shown for columns approaching end bearing lengths. The gradient of the slope is plotted against L/H ratio in Figure 8.7. The equation of the best fit line through the points relating α and $L/H$is:

$$\alpha = 0.882(L/H)^3 - 0.434(L/H)^2 + 0.611(L/H) + 0.003 \qquad [8.2]$$

Equations 8.1 and 8.2 can be combined to provide a single design equation which relates S/S_{uc} , B/L and L/Hratios:

$$S/S_{uc} = (0.882(L/H)^3 - 0.434(L/H)^2 + 0.611(L/H) + 0.003) * (B/L) \quad [8.3]$$

Equation 8.3 is proposed as a simple design equation that can allow design engineers to use the Priebe (1995) method and apply Equation 8.3 to determine the settlement of a small group of stone columns. However this method will require rigorous comparison to field trials. This equation has been derived from data produced by numerical analysis but will allow a quick calculation of settlement when compared to time consuming and complex numerical analysis.

(ii) Derivation of the composite stone column equation

The design of composite stone columns is complicated by the presence of the binder material in the bulging zone which makes it difficult to provide a universal equation which can be used for any soft soil. For the specific case of the Bothkennar soil profile an equation is proposed with an assumption that the bulging zone occurs from 1.7 m to 4.1 m and that between these depths the composite material is present. A minimum design length of 6.0 m and column diameter of 0.6 m is assumed which represents a length to diameter ratio of 10. This is to allow the base of the column to act like a stone column rather than a pile which would be the tendency if the base of the column was composed of composite material. Similarly to the stone column equation, the ability to predict settlement beyond a column length of 6.0m and length to diameter ratio of 10 is limited. The settlement results of five column lengths of 2.4 m, 3.6 m, 6.0 m, 10.8 m and 14.5 m from the unit cell and small raft were selected to derive this design method.

The settlement of a small raft relative to a unit cell is expressed as the ratio, S/S_{uc}, is plotted against normalised footing width, B/L in Figure 8.8 and 8.9. Figure 8.8 suggests a similar behaviour to SC for CSC. Similarly to stone columns, the lowest values of S/S_{uc} represent the highest settlement reductions and lowest area ratios. The data points follow a linear trend where points have the same column length to depth ratio, L/H. Similar behavioural characteristics are observed as seen with stone columns. With increasing L/H ratio the S/S_{uc} ratio increases. The influence of area ratio, A/A_c , appear to be that with increasing area ratios for a given L/H the S/S_{uc} ratio increases (Figure 8.8). This suggests that increasing S/S_{uc} ratio signifies an increasing amount of settlement for both the unit cell and small group of CSC.

The derivation of a design equation is complicated for CSC due to the presence of a binder and should only be used for columns of 4.1 m or greater. From Figure 8.8 it is clear that for various ratios of *L/H* points appear to lie on a linear trend in a similar way to stone columns. This suggests a relationship exists for each value of *L/H* between S/S_{uc} and B/L. Re-plotting the points in Figure 8.9 and assuming a best fit line through the origin and points, an equation for each line can be derived which assumed that the S/S_{uc} and B/L ratios are directly proportional for each L/Hratio. For each L/Hratio the equation of the best line is noted and it is clear a relationship can be derived as follows (in the same manner as stone columns):

$$S/S_{uc} = \alpha\,(B/L) \qquad [8.4]$$

α describes the gradient of the slope of the line for each L/H ratio. The R^2 values suggest a good correlation for most L/H ratios of 0.41 or less. This suggests that for most values the relative predictability of the model for column length to diameter ratios of 10 is reasonable with caution shown for columns approaching end bearing lengths. The gradient of the slope is plotted against L/Hratio in Figure 8.10. The equation of the best fit line through the points relating α and $L/H$is:

$$\alpha = 0.514(L/H)^3 - 0.126(L/H)^2 + 0.272(L/H) + 0.056 \qquad [8.5]$$

Equations 8.4 and 8.5 can be combined to provide a single design equation which relates S/S_{uc} , B/L and L/Hratios:

$$S/S_{uc} = (0.514(L/H)^3 - 0.126(L/H)^2 + 0.272(L/H) + 0.056) * (B/L) \qquad [8.6]$$

Equation 8.6 is proposed as a simple design equation that can allow design engineers to use the Priebe (1995) method and apply Equation 8.3 to determine the settlement of the small group of composite stone columns. Caution must be exercised as the equation is based solely on numerical analysis and requires verification through field trials.

(iii) *Use of the Design equations for stone and composite stone columns*

The design methods for stone columns and composite columns are somewhat similar in terms of application, both are referenced to a stone column in a unit cell. Initially, the engineer must calculate the settlement of the unit cell with the desired length of column using the method of Priebe (1995). Once the unit cell settlement, S_{uc}, is known the Length of column, L, thickness of soil layer, H, and foundation breadth, B, the

settlement can be calculated for the case of columns installed beneath a small raft foundation.

For stone columns the design Equation 8.3 can be re-arranged to give the form:

$$S = [(0.882(L/H)^3 - 0.434(L/H)^2 + 0.611(L/H) + 0.003) * (B/L)] * S_{uc} \quad [8.7]$$

Where S = settlement of the stone column beneath the raft

S_{uc} = settlement of a stone column in a unit cell calculated from Priebe (1995)

B = breadth of the foundation

L = length of the column

H = thickness of the soil layer

For composite stone columns the design Equation 8.6 can be re-arranged to give the form:

$$S = (0.514(L/H)^3 - 0.126(L/H)^2 + 0.272(L/H) + 0.056) * (B/L)] * S_{uc} \quad [8.8]$$

Where S = settlement of the composite stone column beneath the raft

S_{uc} = settlement of a stone column in a unit cell calculated from Priebe (1995)

B = breadth of the foundation

L = length of the column

H = thickness of the soil layer

(iv) Settlement design example of a stone column

For an end bearing stone column with length 14.5 m, diameter 0.6 m and area ratio of 3.5 installed in the Bothkennar soil profile the unimproved settlement is calculated as 753 mm (See Chapter 4). The analytical methods of Priebe (1995) and Pulko & Majes (2005) suggest settlements of 155 mm and 44 mm respectively. The foundation breadth of nine column raft is 3.0 m, and the soil layer thickness, H, beneath the foundation 14.5 m. The column length, L, is 14.5 m and diameter 0.6 m. Utilising Equation 8.7 and analytical solution for S_{uc} of Pulko & Majes (2005):

$$S = [(0.882(L/H)^3 - 0.434(L/H)^2 + 0.611(L/H) + 0.003) * (B/L)] * S_{uc} \quad [8.7]$$

$= [(0.882*(14.5/14.5)^3 - 0.434*(14.5/14.5)^2 + 0.611*(14.5/14.5) + 0.003)* (3/14.5)]*44$

$= [(0.882 - 0.434 + 0.611+0.003)*0.207]*44$

$= 9.63$ mm

Utilising Equation 8.7 and analytical solution for S_{uc} of Priebe (1995):

$$S = [(0.882(L/H)^3 - 0.434(L/H)^2 + 0.611(L/H) + 0.003) * (B/L)]*S_{uc} \quad [8.7]$$

$= [(0.882(14.5/14.5)^3 - 0.434(14.5/14.5)^2 + 0.611(14.5/14.5) + 0.003) * (3/14.5)]*155$

$= [(0.882 - 0.434 + 0.611+0.003)*0.207]*155$

$= 34.1$ mm

The calculated settlement for stone columns present suggests a range of 9.63 mm to 34.1 mm method dependent. The numerical solution suggests a settlement of 39 mm. This suggests that the analytical method which uses Priebe (1995) overestimates the settlement by 12%. It should be noted that the numerical solution for the settlement of a unit cell with column length of 14.5 m was 66.6 mm suggesting the method of Priebe (1995) overestimated the settlement by 132 %. The proposed Equation 8.7 is considered acceptable until a field trial is carried out on site to refine the method.

(v) Settlement design example of a composite stone column

The key assumption in the design of composite stone columns is that columns will have a minimum length of 6.0 m and that between 1.7 m and 4.4 m below the base of the foundation the column will be composed of composite material. A traditional stone column in a unit cell has length 14.5 m, diameter 0.6 m and area ratio of 3.5. Utilising the Bothkennar soil profile the settlement for a unit cell utilising traditional stone columns was calculated utilising the methods Pulko & Majes (2005) and Priebe (1995) which suggested 44 mm and 155 mm respectively. This calculated settlement is utilised in Equation 8.8 to calculate the settlement for a composite stone columns. The foundation breadth of nine composite column raft is 3.0 m, and the soil layer thickness, H, beneath the foundation 6.0 m. The column length, L, is 6.0 m and diameter 0.6 m.

S = (0.514$(L/H)^3$ -0.126$(L/H)^2$ + 0.272(L/H) + 0.056) * (B/L)]*S_{uc} [8.8]

= [(0.514$(6/14.5)^3$ -0.126$(6/14.5)^2$ + 0.272$(6/14.5)$ + 0.056) * $(3/14.5)$]*44

= 1.66 mm

S = (0.514$(L/H)^3$ -0.126$(L/H)^2$ + 0.272(L/H) + 0.056) * (B/L)]*S_{uc} [8.8]

= [(0.514$(6/14.5)^3$ -0.126$(6/14.5)^2$ + 0.272$(6/14.5)$ + 0.056) * $(3/14.5)$]*155

= 5.88 mm

The calculated settlement for composite stone columns utilising the method of Pulko & Majes (2005) and Priebe (1995) suggest values of 1.66 mm and 5.88 mm respectively. The numerical solution suggested a settlement of 34.4 mm. This suggests that the analytical method which uses Priebe (1995) underestimates the settlement by 82%. A field trial is required to refine the equation.

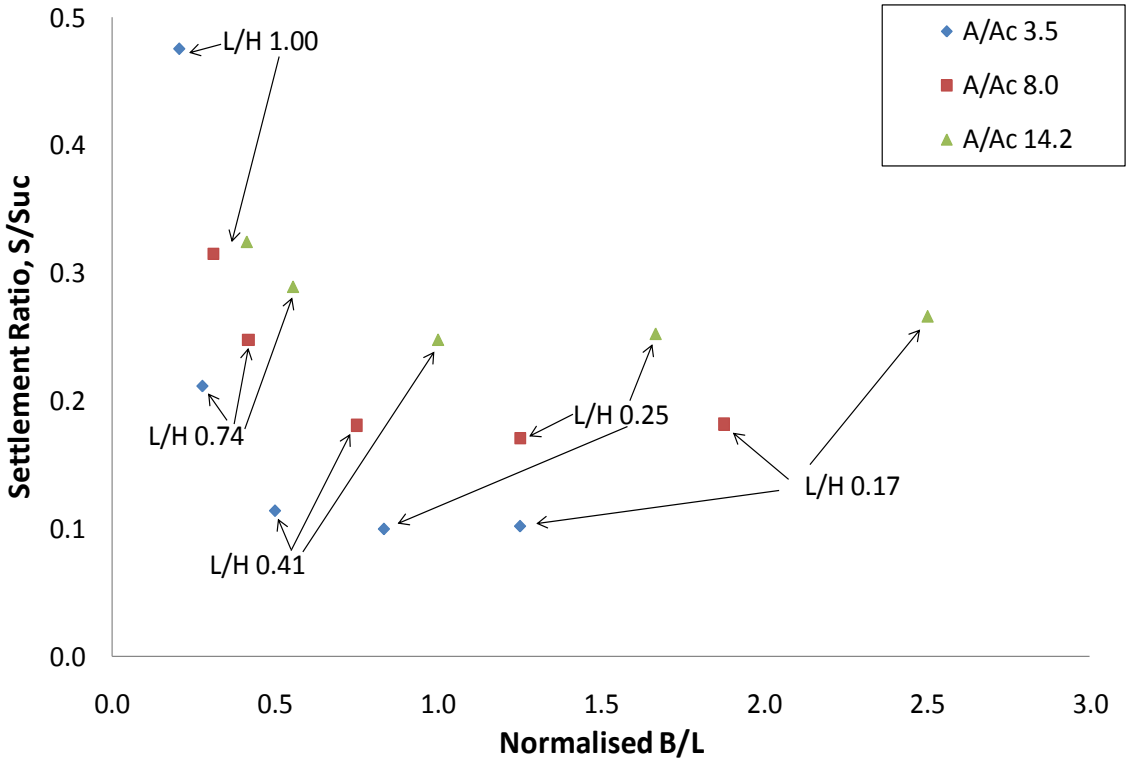

Figure 8.5 Effect of normalised foundation width, B/L, and column length to depth ratio, L/H, on settlement ratio, S/S_{uc}

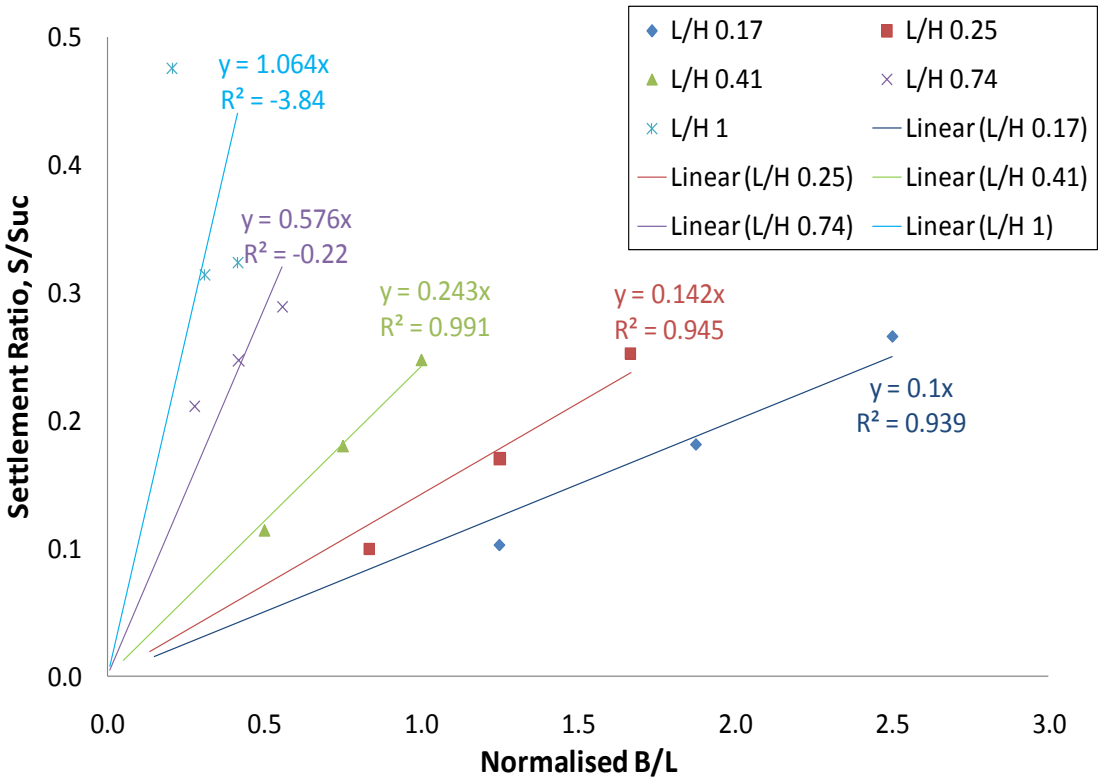

Figure 8.6 Effect of normalised foundation width, B/L, and column length to depth ratio, L/H, on settlement ratio, S/S_{uc}

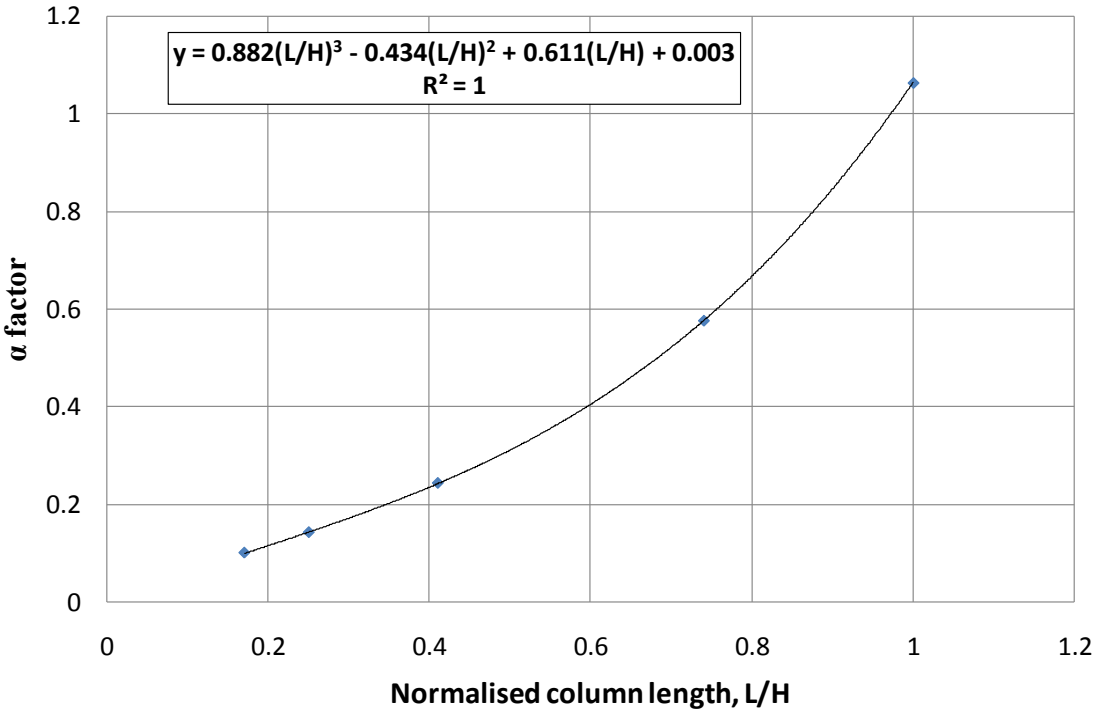

Figure 8.7 Relationship when Δ factor and normalised column length

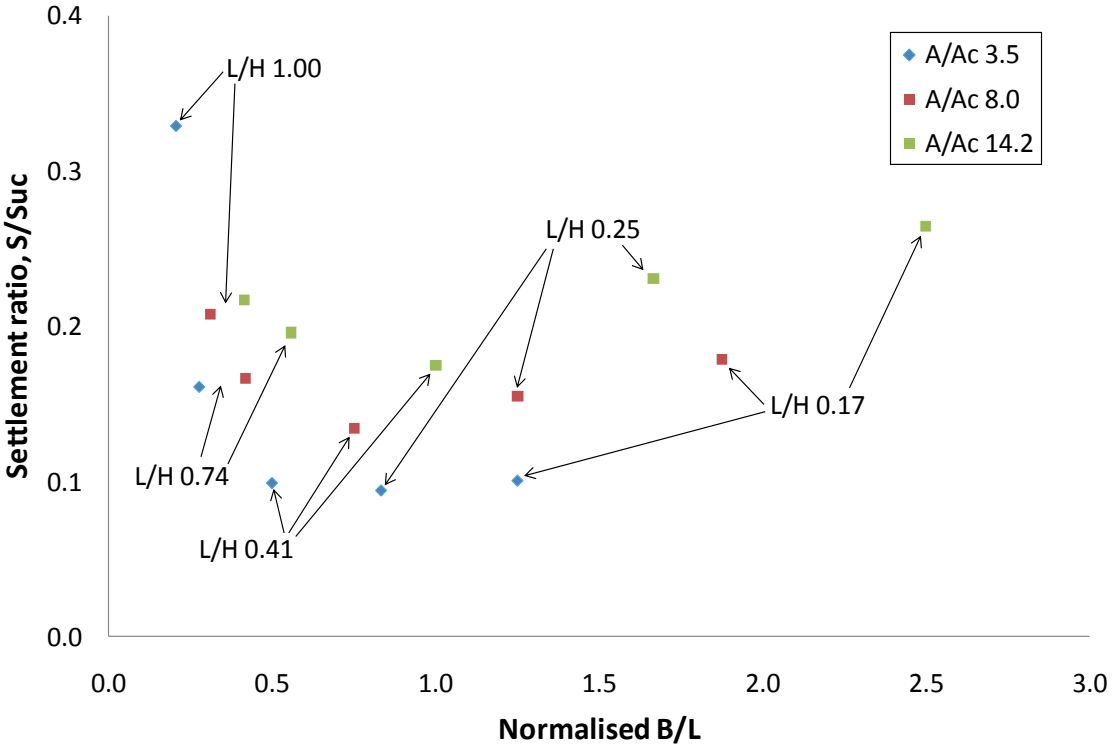

Figure 8.8 Effect of normalised footing width, B/L, and column length to depth ratio, L/H, on settlement ratio

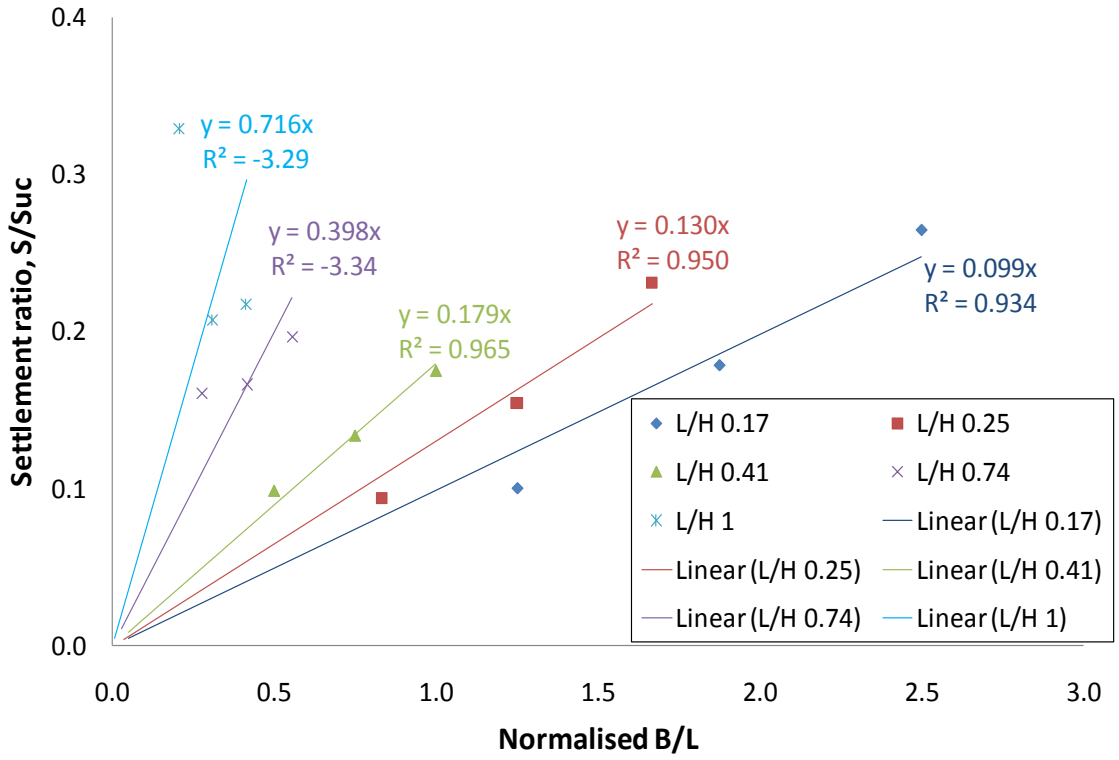

Figure 8.9 Effect of normalised foundation width, B/L, and column length to depth ratio, L/H, on settlement ratio, S/S_{uc}

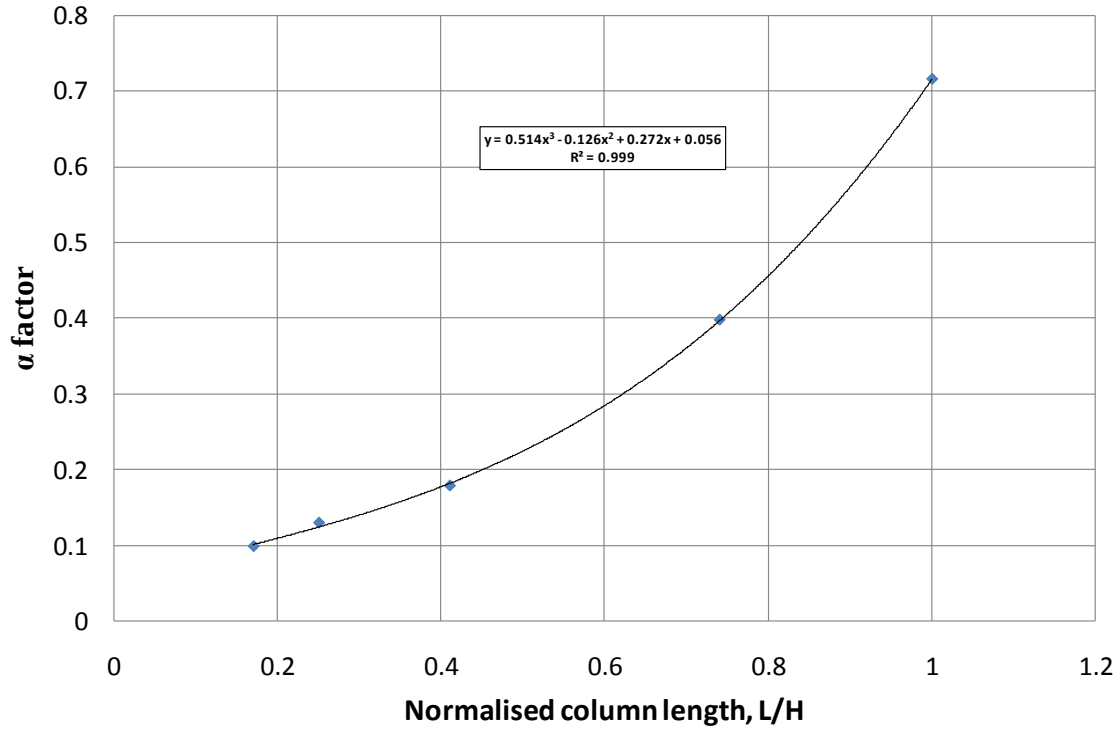

Figure 8.10 Relationship between α factor and normalised column length

Chapter 9

Conclusions

9.1 Introduction

This research examined the settlement and deformational behaviour of stone columns using Finite Element Analysis (FEA) for four foundation arrangements: unit cell, single column, 3x1 column strip and 3x3 column raft. PLAXIS 3D Foundation was used in this research with the Mohr-Coulomb perfect-plasticity and advanced elasto-plastic Hardening soil models to simulate the behaviour of stone columns and the Bothkennar soil profile. The soil profile was constructed from the available literature on the well characterised Bothkennar test site. The influence of key stone column design parameters including the area ratio, column length, column confinement and arrangement, column stiffness, column strength, installation effects and the effect of stiff crust thickness was examined.

In addition consideration was given to a method of reducing the potential for lateral column deformation or bulging by the use of a novel composite column. The deformational characteristics of a stone column were identified and also a composite of granular and the experimental Protomix material. Laboratory testing was carried out to gain an understanding of the cohesive, stiffness and unconfined compressive strength properties of the composite before simulation studies were performed on key design parameters of area ratio, column length, column confinement and arrangement.

9.2 Numerical modelling approach

In order to represent the behaviour of stone columns general published literature on the subject was reviewed and different modelling approaches considered to represent the behaviour in soft soils. The initial modelling studies identified were:

- The long term settlement behaviour of stone columns was found to be accurately modelled by drained analysis in PLAXIS 3D Foundation. The results of an initial sensitivity strongly suggested that the results were similar to an undrained-consolidation analysis. The undrained-consolidation analysis took significantly longer to run and hence the drained analysis was chosen as it would look at the long term behaviour in a shorter timeframe.
- The use of interfaces was examined for a 3x1 strip of stone columns and a 3x3 stone column raft with and without interfaces. The settlement behaviour was

considered to be similar with and without interfaces. This was consistent with studies by Balaam and Booker (1985) and Killeen (2012) interfaces were therefore not included in subsequent analysis. Balaam *et al.* (1985) suggested that modelling of the interface is unnecessary as the most significant yielding occurs within the column and little in the surrounding clay.

- Plaxis was able to model the behaviour of stone column installed in a unit cell. The settlement behaviour was found to be comparable to one dimensional consolidation theory. The Bothkennar soil profile was used in the study for validation.
- Plaxis was able to capture the field trial settlement behaviour of Jardine *et al.* (1985) and Watts and Serridge (2000) for a pad foundation and a strip improved by stone columns respectively for the Bothkennar soil profile. The Bothkennar soil profile was therefore considered validated for further use in stone column and composite stone column modelling in Plaxis 3D.

9.3 Stone columns

The influence of key design parameters was conducted for stone column foundations. The effect of area ratio, column length and area ratio, column stiffness, column strength, installation effects and stiff crust thickness on the settlement improvement using stone columns was examined.

9.3.1 Settlement performance

Investigation of the settlement performance of small groups of stone columns was conducted using the Bothkennar soil profile. The field trial of Jardine *et al.* (1995) had identified the bearing capacity of the Bothkennar soil to be 138 kPa, as such adopting a factor of safety of 2.5 to 3, the working load was considered to be in the range of 46 - 55 kPa. Therefore to examine column behaviour under working load a value of 50 kPa was selected. The key findings in terms of settlement performance are summarised as follows:

- The stiff crust and upper Carse clay to a depth of 2.0m limits the settlement improvement by stone columns to a length of 2.4m. This is due to the high stiffness of these layers compared to the lower stiffness of the lower Carse clay.
- For all configurations of stone column foundation examined increasing the area ratio was found to reduce the settlement improvement factor. For a single

column, three column strip and nine column raft the reduction in settlement improvement factor was 0.39, 0.72 and 0.98 as the area ratio increases from 3.5 to 14.2 for a column of length 14.5m. Optimal spacing would therefore 1.0m column centre to centre equivalent to an area ratio of 3.5. Hughes and Withers (1974) suggest that columns which are spaced 1.5 column diameters apart act independently. In this case an area ratio of 14.2 has a column spacing of 2.0 m or 3.3 diameters.

- Increasing the column length for the lowest area ratio of 3.5 was found to offer the highest settlement improvement factors for all foundation configurations with the highest recorded for unit cell configuration which has the highest lateral restraint. For a column of length 2.4m installed in a unit cell configuration the improvement factor was 1.07 for all area ratios. Extending the column length to 14.5m the settlement improvement factor increased to 10.1, 2.75 and 1.7 for area ratios of 3.5, 8.0 and 14.2 respectively. It is suggested that as the area ratio is increased the columns act more independently.
- Increasing the stiffness of the columns i.e. Young's modulus has been shown to reduce the settlement and increase the settlement improvement factor. The highest improvement is observed for an end bearing stone column of length 14.5m as the stiffness is increased from 30MPa to 70MPa. An increase in settlement reduction of 14.6%, 12.0% and 10.4% is observed for a single column, three column strip and nine column raft. The single column benefits the most from increased stiffness as prior to this the column is fully independent i.e. not restrained by neighbouring columns.
- The effect of increasing the column strength was examined by increasing the friction angle from 38° to 50°. The effect on a single column was found to be minor with an increase in settlement reduction of 0.8% observed as column length increased from 6.0m to 14.5m. Increasing the friction angle for a strip and a raft foundation was found to have the highest settlement reduction for columns of 14.5m. Increasing the friction angle from 38° to 50° saw reduction in settlement of 11.4% and 25.3% for a strip and raft respectively. The higher reduction observed for the raft is a result of enhanced confinement provided by neighbouring columns due to an increase in column strength.
- The coefficient of lateral earth pressure, K_o, was found to influence settlement behaviour. Increasing the value from 0.75 to 1.00 had the highest impact for all foundation configurations. However increasing the value to the highest value of

1.25 had minimal impact on settlement performance. For a column of length 14.5m increasding the value from 0.75 to 1.00 for a single column, strip and raft foundation increased the settlement reduction by 4.1% (n value increase of 1.59 to 1.70), 0.3% (n value increase of 2.01 to 2.02) and 4.8% (n value increase of 2.38 to 2.69).

- The stiff crust thickness was examined due to the effect observed earlier on settlement performance in Chapter 4. The highest increases in settlement reduction factor are seen for a crust of thickness 0.5m compared to the lowest for a crust thickness of 1.5m. For a column length of 14.5m the difference is 0.76, 1.82 and 0.77 for a single column, strip and raft foundation. The higher settlement improvement factors seen for the thinnest crust (Section 5.7.1) are to be expected since the thicker lower Carse clay in the thin crust case will improve more than the thicker crust since there is less lower Carse to improve and the stiffer layers are already competent.

9.3.2 Settlement inferred deformation ratios and total shear strains

The deformation of stone columns was examined by the use of settlement inferred deformation ratios termed punching and compression ratios. Columns which punch into the underlying soil transfer most of their applied load to the base of the column which is typically seen as a high punching ratio and low compression ratio. A sub-type of punching failure defined by Black (2007) termed 'block' failure is seen as low punching and low compression failure in closely spaced columns. Compression ratios can be used to infer the potential bulging of stone columns and is characterised by a high compression ratio and low punching ratio. In this research the ratios were utilised with observations of settlement improvement factor and total shear strain observations to assess modes of deformation. It has been noted that the configuration of columns does not affect the mode of deformation rather this is influenced by the area ratio and column length. The foundation configuration was found to have little influence on the mode of deformation and consideration was given as to how the mode of deformation and ultimately settlement could be influenced by the development of a composite stone column.

Characteristic behaviours were identified from the deformation ratios and verified by analysis of the total shear strain distribution within the columns for various configurations:

- *Punching failure:* was observed for all short columns with lengths of 2.4 m or less. This mode of failure was typified by high punching ratio, low compression ratio and the highest distribution of shear strain at the base of the column. Punching failure was evident for all area ratios examined. Total shear strain analysis suggests that as area ratio increases the columns act more independently and punch with greater intensity into the underlying soil. This is due to the increased applied load from the increased foundation area and lack of restraint provided by neighbouring columns.
- *Block failure:* a sub-type of 'punching' failure first identified by Black (2007) was observed in both settlement inferred deformation ratios and total shear strain plot analysis. For columns with a low ratio block failure was identified from low punching and low compression ratios. Total shear strain analysis suggests uniform strain across the base of the columns and in the soil which is also considered evidence of block failure. No shear strain was observed between the central zone of the column and soil. During block failure columns and soil act as a single unit and punch uniformly into the underlying soil which leads to low punching ratios as such ratios are defined by the settlement of the column relative to the settlement of the surrounding soil.
- *Bulging failure:* as column length increases the dominant mode of deformation and failure changes from punching to bulging. This change occurred for columns of length to diameter ratio of 4 or greater and was typically seen for area ratios greater than 8.0. This mode of deformation was identified by reducing punching ratios and increasing compression ratios. The development of bulging was found to be dependent upon the area ratio with the highest total shear strains observed for the largest area ratios. Typically bulging occurs at the shallowest zone of least competent soil which in this research was associated with the top of the lower Carse clay. The competent layers of the stiff crust and upper Carse clay showed no evidence of bulging which, it is suggested, is due to the restraint they provide to the column.

From further analysis of the total shear strain results, the effect of area ratio and column length identified that one or more modes of deformation can occur simultaneously

within a stone column foundation. From the 3x1 column strip and 3x3 column raft it was noted that for column lengths of 6 m or greater that bulging and punching modes of deformation occurred simultaneously. As the area ratio increased the intensity of total shear stain increased at the base of the column however the total shear strain concentration was highest at the top of the lower Carse clay layer which suggests that bulging failure is the dominant mode of deformation.

The influence of other design parameters on column inferred deformation ratios can be summarised as follows:

- Increasing column stiffness and strength allows the columns to absorb more load. The highest values of stiffness were found to be associated with the highest punching ratios and the lowest compression ratios for all configurations of columns. The increased stiffness was found to increase the compression ratio while the punching ratio reduced below 2.4 m. Increasing column strength (friction angle) was found to have no effect for single column configurations. For 1x3 strip and 3x3 raft configurations increasing column strength was found to increase the maximum punching ratio. Increasing strength had the effect of reducing column compression ratio with increasing length.
- The coefficient of lateral earth pressure was found to have negligible effects on punching and compression ratios for 3x3 column rafts. This suggests that the effect of column installation is minimal. This is consistent with the findings of the numerical study conducted by Kirsch (2006) and Killeen (2012).
- The effect of crust thickness was examined to determine the influence on the deformational behaviour of stone columns. The thickness of the crust was found to influence the depth at which maximum punching occurred. It was noted that the highest punching and compression ratios occurred for the thinnest crust. The deepest punching ratio was also found for the thinnest crust thickness. This is to be expected since the restraint provided by the stiff crust and upper Carse clay is weakest for this soil profile. A reduced crust thickness reduces the depth of the lowest lateral restraint. This then allows the column to bulge closer to the surface.

9.4 Composite stone columns

The use of a composite stone column is proposed as a solution which can be adopted to reduce the potential for bulging failure in soft soils. By the addition of a composite

material of gravel and protomix into the 'bulging' zone the cohesion of the column can be increased. This allows for the transfer of applied load to depth thereby reducing the settlement and potential for failure associated with stone columns. Three column configurations were examined for a range of ratios and various column lengths to allow comparison with stone column behaviour (Chapter 4). The performance of the composite stone column configurations was assessed using the Bothkennar soil profile (Chapter 3) and a working load of 50 kPa.

9.4.1 Settlement performance

Composite stone columns were found to reduce the settlement of the foundation than stone columns for all area ratios and column lengths greater than 2.4 m for the pad, 3x1 column strip and 3x3 column raft. The presence of the composite material within the bulging zone is considered to be the reason for the increased settlement improvement factors. The settlement improvement applies to both floating and end bearing composite columns. In addition to the improved settlement performance the following observations was also noted:

- The stiff crust was found to impact the settlement performance in the same manner as stone columns. The improvement is marginal for columns of length 2.4m as the stiff crust and upper Carse clay are competent prior to column installation.
- For the case of a single composite stone column improvement factors of 1.75, 2.65 and 1.82 were seen for area ratios of 3.5, 8.0 and 14.2 for a 14.5m column. This represents an increase of 0.16, 1.32 and 0.62 compared to stone columns.
- For a three column strip settlement improvement factors of 2.40, 2.10 and 1.77 were seen for ratios of for area ratios of 3.5, 8.0 and 14.2 for a 14.5m column. This represents an increase of 0.37, 0.60 and 0.46 compared to stone columns.
- For the case of a raft the settlement improvement factors seen were 3.45, 2.56 and 2.09 representing an increase of 1.07, 0.87 and 0.69 compared to stone columns.
- Composite stone columns provide a significant benefit compared to stone columns. For a column length of 14.5m and area ratios between 3.5-14.2 the settlement reduction is in the range of 6%-28% for single columns, 8%-20% for a strip and 13%-24% for raft foundations. It is therefore concluded that in terms

of settlement this type of column reduces the bulging and therefore settlement in the weakest zone of the soil profile between 1.7m-4.0m.

9.4.2 Settlement inferred deformation ratios

The effect of introducing a composite material into the bulging zone was assessed using the punching and compression ratios described in Chapter 4. Previously in stone column analysis it was identified that two main modes of deformation, punching and bulging affected column performance. Columns which punch into the underlying soil transfer most of the load to the base and can identified by high punching ratios and low compression ratios. A sub-type of punching failure was also seen for stone columns termed 'block' failure which describes a situation in which the column and soil act as a single unit punching into the underlying soil. This is typically observed by low punching and low compression ratio values. Bulging failure was seen previously as high compression ratios and low punching ratios. This type of failure occurs when the columns bulge laterally into the soil as the surrounding soil is unable to restrain the column. In such a case the column is unable to stress transfer to the base of the column instead stress-share occurs via lateral bulging.

Of the described behaviours of punching, 'block' and bulging failure all modes of deformation were observed for composite stone columns. This suggests that although the columns have been stiffened within the bulging zone they are still acting like stone columns rather than piles. This allows for current foundation designs associated with stone columns to be applied without the need for reinforced foundations that are associated with pile foundations. The main observations associated with composite stone columns in regards of failure types is summarised as follows:

- Punching failure: was observed for all area ratios. The maximum depth of punching was recorded as 3.6 m for ratios of A/Ac 8 and 14.2 which is deeper than equivalent stone columns which punched to 2.4 m in depth. As the A/Ac ratio increases the applied load from the foundation increases leading to a greater stress concentration in the column. The higher cohesion of the composite stone columns allows it to absorb more of the applied load which leads to punching occuring at a deeper depth. This is supported by the cross sections of total shear strain, which suggest a higher magnitude is observed at the base of the columns for the composite case. It is suggested that punching mode of failure is dominant for short columns.

- *Block failure:* was seen for the lowest area ratio of 3.5 with punching occurring at a depth of 2.4 m. This was identified by low punching and low compression ratios. The shear strain plots indicated the same stress state within the column and soil.
- *Bulging failure:* Compression ratios were much smaller in magnitude between 2.4 m and 4.8 m column lengths than with stone columns. It is suggested that bulging failure occurs below this depth which was seen as reducing punching ratios and increasing compression ratios. This is supported by the cross sections of total shear stress which indicate that a deeper deformation occurs which is considered to be bulging failure.

9.4.3 Shear strains

Three column lengths were chosen to allow comparison of the specific modes of deformation and the associated distribution of shear strains of composite stone columns to traditional stone columns: 2.4 m long columns to examine punching; 6 m long columns to illustrate transition from punching to bulging failure and 14.5 m columns to illustrate bulging failure as the columns were end bearing founded on a rigid stratum. The main observations for composite column behaviour and how it relates to stone columns is summarised as follows:

- For short columns of 2.4 m and a low area ratio of 3.5 the development of shear strain appears negligible. Increasing the A/Ac ratio to 8 and 14.2 leads to an increased magnitude and size of the zone of total shear stress observed along the column and at its base.
- For columns of length 6 m the strain between column and soil is negligible for strip and raft. Bulging failure is not observed for an A/Ac ratio of 8 however for a ratio of 14.2 the highest magnitude of shear strain i.e. bulging failure develops at a deeper depth than that observed for stone columns. It is suggested that the composite zone of the column allows for the transfer of bulging failure to a deeper depth.
- For columns of length 14.5 m the absence of bulging failure for A/Ac ratios of 3.5 and 8 compared to traditional stone columns suggests that the composite has reduced or eliminated bulging failure. The A/Ac ratio appears to allow for sufficient restraint from neighbouring columns for both strip and raft. For an A/Ac ratio of 14.2 bulging appears to occur at the top of the lower Carse clay

which is at a similar depth to a stone column. The column is considered to be acting independently and therefore cannot benefit from mutual restraint from neighbouring columns.

- For a 1x3 column strip and a 3x3 column raft, 'block' failure was observed for area ratios of 3.5 and 8.0 with column lengths of 2.4 m and 6.0 m. With increasing A/Ac ratio the mode of deformation became punching failure for 2.4 m columns and bulging failure for 6 m columns.
- For end bearing columns of 14.5 m length, no bulging failure was observed for strip or raft foundations for A/Ac ratio of 3.5. For A/Ac 8 and 14.2 shear strain developed in the columns below the bulging zone for the strip and raft. This suggests that the column is transferring stress to depth and the concentration of shear stress below this depth is suggestive of bulging failure being transferred to depth.

9.5 Design of composite stone columns

The behaviour of composite stone columns is complex and their behaviour is difficult to predict for different soil types. The FEM analysis results have been analysed and design equations produced to predict the behaviour of stone and composite stone columns over a finite area ratio of 3.5 to 14.2. This is equivalent to a spacing of 1.0 m to 2.0 m which is considered the maximum range for column application, since beyond a spacing of 1.5 diameters, columns act independently (Hughes and Withers, 1974). It should be noted that the design equations for stone and composite stone columns require validation via field trials to confirm their validity.

9.6 Recommendations for future research

Composite stone columns are proposed as a new novel type of column which can offer higher settlement reduction compared to traditional variants. The laboratory analysis derived values of cohesion and stiffness from testing the samples in unconfined compressive strength (UCS) testing rig. The material could not be tested in a triaxial testing system due to sample stiffness and the maximum load tolerated of 5 kN on the load frame being too low compared to the initial sample UCS determined in the UCS machine. Further investigation is required to determine the friction angle of the composite material by the use of a high pressure triaxial system. The current models make an assumption based on FEM triaxial simulation that the friction angle has minimal impact due to the high cohesion and stiffness of the composite material.

The behaviour of both column types has been performed by drained analysis which does not separate out the undrained and consolidation behaviours. Stone columns act as vertical drains allowing for the dissipation of pore water pressure and consolidation of the soil. During foundation loading the stress is mostly carried by the pore water during undrained conditions. As consolidation begins pore water dissipates and the soil compacts which transfers the vertical stress from the pore water to the soil as it drains. The limited information on permeability for the Bothkennar soil profile made undrained analysis difficult. The undrained consolidation behaviour of the Bothkennar soft soil should be examined to determine the change in stress in the columns and soil.

The analysis of the field trial of Watts and Serridge (2000) and the effect of column installation effects were examined using the FEM. Serridge and Sarby (2008) note that the vibroflot should not remain in the ground longer than is necessary which suggests installation in this case had negative effects. The simulation of column installation effects in this thesis was achieved by altering the earth pressure, k_o, which suggested higher values achieved due to column installation could lead to reduced settlement. It is clear than installing stone columns alters the stress regime in the soil and the displacing effects of the Vibroflot can cause stiffness changes which alters soil strength. It is recommended that a field trial be conducted to examine the installation of stone columns and composite stone columns in soft soils to assess the impact of this effect.

The application of composite stone columns to soft soils therefore requires this fully instrumented field test to validate the FEM analysis findings. The following aspects should be considered carefully during a field trial:

- The change from an undrained to drained state will see a re-distribution of stress as the initially incompressible soil consolidates transferring more stress to the column with time. This re-distribution of stress and how the load increments affect the rate at which this occurs needs further study.
- Assessment of earth pressure with construction: The effect of construction and disturbance to the soil fabric should be made by the installation of British Research Establishment miniature cells to measure horizontal earth pressure close to the toe and top of the column.
- It is unclear from the numerical analysis how drainage behaviour will be effected with a non-porous composite component. Therefore a field trial should measure the pore water at selected intervals along the length of column and at a

set distance radially. This should establish the drainage radius of the column both in the composite and stone column sections. Also it should allow an assessment to be made to ensure that there is no liquefaction risk due to elevated pore water pressures. The measurement of pore water can be performed by the installation of pneumatic piezometers in pre-drilled boreholes to monitor pre-construction, construction and post-construction pore-water behaviour.

- The field test should also include borehole sampling either by full size samples or core plugs to assess the porosity and permeability of the soil so that consolidation modelling of the field test can take place. Current data sources do not give sufficient detail for modelling.
- The current numerical analysis assessed the behaviour of stone columns beneath an infinite array, pad, raft and strip foundation for various lengths of column using drained analysis in PLAXIS 3D. The current modeling utilises a square configuration for stone columns (Figure 2.25). Further analysis should consider the effect of column arrangement with triangular and hexagonal columns beneath larger foundations to assess if a larger settlement reduction can be achieved using both stone and composite columns.
- The effect of the Bothkennar crust on the stone column settlement improvement was examined by varying the thickness of the crust and by adjusting the other layers so that a 15m depth of soil was achieved. In the laboratory studies homogeneous soil layers were created by consolidation in the large triaxial cells. Further numerical studies should look at the effect of a stiff crust on stone column behaviour.
- It is clear from the Watts and Serridge (2000) field trial that the columns underperformed due to the effects of the vibroflot being in the ground for too long during column forming. As such consideration should be given to modelling the weakening of the soil in the near column area so that future applications of the technique keep soil disturbance to the bare minimum.

10.0 References

Aboshi, H., Ichimoto, E., Enoki, M. and Harada, K. (1979), "The 'Compozer' – a method to improve characteristics of soft clays by inclusion of large diameter sand columns", Proceedings of the International Conference on Soil Reinforcement, Paris, Vol. 1, pp. 211-216.

Allman, M.A. and Atkinson, J.H. (1992), "Mechanical properties of reconstituted Bothkennar soil", Geotéchnique 42, No.2, pp289-301.

Ambily, A.P. and Gandhi, S.R. (2007), "Behaviour of Stone Columns based on Experimental and FEM analysis", Jour. of Geotechnical and Geoenvironmental Engineering, April 2007, pp. 405-415.

Andreou, P., Frikha,W., Frank, R., Canou, J., Papadopoulus, V., Dupla, J.-C. (2008), "Experimental study on sand and gravel columns in clay", Ground Improvement 161, Nov 2008, Issue G14, pp 189-198.

Andreou, P. and Papadopoulos, V. (2006), "Modelling stone columns in soft clay", Proc. 6th European Conf. on Numerical Methods in Geotechnical Engineering, Graz, pp 777-780.

ASTM (2002), "Standard method for static modulus of elasticity and Poisson's ratio of concrete in compression", C469-02

Azizi, F (2000), "Applied Analysis in Geotechnics", E & FN Spon, London

Bachus, R.C. and Barksdale, R.D. (1984), "The behaviour of foundations supported by clay stabilised by Stone Columns", Eighth European Conference on Soil Mechanics and Foundation Engineering, Helsinki, Vol. 1, pp. 199-204.

Balaam, N.P., Poulos, H.G., and Brown, P.T. (1977), "Settlement Analysis of soft clays reinforced with Granular Piles", 5th South-East Asian Conference on Soil Engineering, Bangkok Thailand, pp. 81-92.

Balaam, N.P. and Booker, J.R. (1981), "Analysis of Rigid Rafts supported by Granular Piles", Int. Jour. for Numerical and Analytical methods in Geomechanics, Vol. 5, Issue 4, pp. 379-403.

Balaam, N.P. and Booker, J.R. (1985), "Effect of Stone Column yield on settlement of Rigid foundations in stabilized clay", Int. Jour. For Numerical and Analytical methods in Geomechanics, Vol. 9, pp. 331-351.

Barksdale, R.D. and Bachus, R.C. (1983), "Design and construction of stone columns, Volume 1", Report No. FHWA/RD-83/026, Federal Highway Administration, U.S.A.

Barras, B.F (2000), "Some aspects of the geology and engineering properties of the holocene deposits at the Bothkennar soft clay research site", PhD thesis, Heriot-Watt University

Barras, B.F. and Paul, M.A. (1999), "Sedimentology and depositional history of the Claret Formation ('carse clay') at Bothkennar, near Grangemouth", Scottish Journal of Geology, 35, (2), pp. 131-144.

Baumann, V. and Bauer, G.E.A. (1974), “The performance of foundations on various soils stabilised by the vibro-compaction method”. Canadian Geotechnical Journal 2, Vol. 11, No. 4, pp. 509-530.

BBGE (2012), Figures for top and bottom feed stone column installation sourced from www.bbge.com.

Bell, A.L., Kirkland, D.A., and Sinclair, A. (1986), "Vibrated-replaced ground improvement at General Terminus Quay, Glasgow", Building on marginal and derelict land, Thomas Telford Ltd, London, pp 499-514.

Bell, F.G. (2007), "Engineering Geology", 2nd Edition, ISBN-9780080469522, Elsevier

Black, J.A. (2007), "The settlement performance of a footing supported on soft clay reinforced with vibrated stone columns", Queen's University of Belfast, Northern Ireland.

Black, J.A., Sivakumar, V. and Bell, A. (2011), "The settlement performance of stone column foundations", Geotéchnique, 61, No.11, pp. 909-922, Institution of Civil Engineers.

Bolton, M.D. (1986), "The strength and dilatancy of sands", Géotechnique 36, No.1, pp 65-78

Boussinesq, J. (1885), "Applications des Potentiels à L'étude de L'équilibrie et du Mouvement des Solides Élastiques, Gauthier-Villars, Paris, France.

Brinkgreve, R.B.J and Broere, Editors (2006), "Plaxis 3D Foundation Version 1.6", Manual, Plaxis B.V., Delft, Netherlands

Burd, H.J. (2005), "Introduction to the Hardening soil model", Numerical Methods in Geotechnical Engineering, 28th-30th June 2005 Stockport, Wilde FEA in-house training course.

Brinkgreve, R.B.J., (2007), "Plaxis: *Finite Element Code for Soil and Rock Analyses*", Plaxis manuals, Plaxis.

British Standard BS EN 197-1:2011 Cement. Composition, specifications and conformity criteria for common cements

British Standard BS EN 450- 1:2005 A1:2007, Fly ash for concrete Definition, specifications and conformity criteria

British Standard BS-1377 (1990) Part 7. Methods of Test for Soils for Civil Engineering purposes

British Standard BS-1610 Part 1 (1992) Materials testing machines and force verification equipment Specification for the grading of the forces applied by materials testing machines when used in the compression mode

British Standard BS EN ISO 7500-1:2004 Metallic materials. Verification of static uniaxial testing machines Tension/compression testing machines. Verification and calibration of the force-measuring system

British Standard BS EN 12620 Aggregates for Concrete

British Standard BS-1881 (1983) Part 120 Testing concrete method for determination of the compressive strength of concrete cores

British Standard BS-1881 (1983) Part 115 Specification for compressive testing machines for concrete

British Standard BS-8500 (2006) Concrete - Complimentary standard to BS EN206-1

Castro, J. (2007), "Pore pressure during stone column installation", Proceedings of the 18th European Young Geotechnical Engineers Conference, Ancona, Italy.

Castro, J. and Sagaseta, C. (2009), "Consolidation around stone columns. Influence of column deformation", Int. J. Numer. Anal. Meth. Geomech, 33, Issue 7, pp851-877.

Castro, C. & Karstunen, M. (2010), "Numerical simulations of stone columns installation", Can. Geotech. J., 47 (10), pp 1127-1138.

Charles, J.A. and Watts, K.S. (1983), "Compressibility of soft clay reinforced with granular columns", *In* Improvement of Ground: Proceedings of the 8th European Conference on Soil Mechanics and Foundation Engineering, Helsinki, 23rd - 26th May 1983, Vol. 1, pp. 347 – 352.

Choobbasti, A.J., Zahmatkesh, A., Noorzad, R. (2011), "Performance of stone columns in soft clay: numerical evaluation", Geotech. and Geol. Eng., Vol. 29, Issue 5, pp. 675-684.

Clayton, C.R.I., and Khatrush, S.A. (1986), "A new device for measuring local axial strains on triaxial specimens", Geotechnique, 36 (4), pp. 593-598.

Coulomb, C. A. (1776). Essai sur une application des regles des maximis et minimis a quelquels problemesde statique relatifs, a la architecture. Mem. Acad. Roy. Div. Sav., vol. 7, pp. 343–387

Cunze, G. (1985), "Ein Beitrag zur abschätzung des porenwasserüberdruckes beim rammen von verdrängungspfählen in bindigen böden. University of Hannover dissertation.

Das, B. (2008), "Advanced Soil Mechanics", 0203935845, Taylor & Francis, London & New York

Domingues, T.S., Borges, J.L. and Cardoso, A.S. (2007a), "Parametric study of stone columns in embankments on soft soils by finite element method", Applications of Computational Mechanics in Geotechnical Engineering V, Proceedings 5th Intl. Workshop, Guimaraes, pp281-291.

Domingues, T.S., Borges, J.L. and Cardoso, A.S. (2007b), "Stone columns in embankments on soft soils. Analysis of the effect of gravel deformability", 14th European conf. on Soil Mechanics and Geotechnical Engineering, Madrid, Vol. 3, pp 1445-1450.

Douglas, S.C. and Schaefer, V.R. (2012), "Reliability of the Priebe method for estimating settlements", Ground Improvement, Paper 1200012.

Duncan, J.M. and Chang, C.Y. (1970), "Non-linear analysis of stress and strain in soil", ASCE Journal of the Soil Mechanics and Foundation Division, Vol. 96, No. 5, pp.1629-1653.

Durgunoglu, H.T. and Mitchell, J.K. (1975), "Static penetration resistance of soils", Proceedings ASCE Conference on In-situ measurement of Soil properties, Raleigh N.C., Vol. 1, pp 151-188.

Egan, D., Scott, W. and McCabe, B.A. (2008), "Installation effects of vibro replacement stone columns in soft clay", Proc. 2nd Int. Workshop on the Geotechnics of soft soils, Glasgow, pp 23-30.

Ellouze, S., Bouassida, M., Hazzar, L., Mroueh, H. (2010), "On settlement of stone column foundation by Priebe's method.

Elshazly, H.A., Hafez, D. and Mossad, M.E. (2008), "Reliability of conventional settlement evaluation of circular foundations on stone columns", Journal of Geotechnical and Geological Engineering, Vol. 26, No. 3, pp 323-334.

Fayat (2013). Diagram of Vibro stone column installation rig, www.fayat.com, Accessed August 2008.

Gäb, M., Schweiger, H.F., Kamrat-Pietraszewska, D. and Karstunen, M. (2008), "Numerical analysis of floating stone column foundation using different constitutive models", Proceedings of the second international workshop on goetechnics of soft soils, Glasgow, Scotland 3rd to 5th September 2008, Volume 1.

Gerrard, C.M., Pande, G.N. and Schweiger, H.F. (1984), "Modelling behaviour of soft clay reinforced with stone columns", In-situ Soil and Rock Reinforcement Conference, Paris, pp. 145-150.

Gibson, R.E. and Anderson, W.F. (1961), "In-situ measurements of soil properties with the Pressuremeter", Civil Eng. and Pub. Works Rev., Vol. 56, No. 658, pp. 615-618.

Goughnour, R.R. and Bayuk, A.A. (1979:1), "Analysis of stone column-soil matrix interaction under vertical load", Proceedings of the International Conference on Soil Reinforcement, Paris, Vol.1, pp. 271-277.

Goughnour, R.R. and Bayuk, A.A. (1979:2), "A field study of long-term settlements of loads supported by stone columns in soft ground", Proceedings of the International Conference on Soil Reinforcement, Paris, pp. 279-285.

Goughnour, R.R. (1983), "Settlement of vertically loaded stone columns in soft ground", Proc. of the 8th conf. on Soil Mechanics and Foundation Engineering, Helsinki, Vol 1., pp 235-240.

Goughnour, R.R. (1997), "Stone Column construction by the rotary method", ASCE GSP No. 69, Ground improvement Ground reinforcement Ground treatment, Geol gen pp. 492 – 506.

Greenwood, D.A. (1970), "Mechanical improvement of soil below ground surface", Proceedings of Ground Engineering Conference, ICE, Vol. 1, June pp. 11-22

Greenwood, D.A. and Kirsch, K. (1984), "Specialist ground treatment by vibratory and dynamic methods", State of the art Report, Piling and Ground Treatment, Thomas Telford Ltd., London, pp. 17-45.

Guetif, Z., Bouassida, M. and Debats, J.M. (2007), "Improved soft clay characteristics due to stone column installation", Computers and Geotechnics, Vol. 34, Issue 2, pp 104-111.

Hartmann, H.L. (1992), "Appendix Table E: Material properties and characteristics", In SME Mining Engineering Handbook, 2nd Edition, Vol. 2 Littleton, CO: SME A32-A33

Hens, H.S.L.C (2012), "Performance based building design 1: From below grade construction to cavity walls", John Wiley & Sons, 7 Oct 2012

Herle, I., Wehr, J. & Arnold, M. (2008), "Soil Improvement with vibrated stone columns- influence of pressure level and relative density on friction angle", Proceedings of the second International Workshop on Geotechnics of Soft Soils, Glasgow, Scotland, 3-5th September 2008.

Hu, W. (1995), "Physical modelling of group behaviour of stone column foundations", Ph.D. thesis, University of Glasgow, Glasgow, U.K.

Hight, D.W., Bond, A.J. and Legge, J.D. (1992), "Characterization of the Bothkennar clay: an overview", Geotéchnique, 42, No 2, pp 303-347.

Hughes, J.M.O. and Withers, N.J. (1974) "Reinforcing of soft cohesive soils with stone columns", Ground Engineering, May, pp. 42-49.

Hughes, J.M.O., Withers, N.J. and Greenwood, D.A. (1975), “A field trial of the reinforcing effect of a stone column in soil”, Geotechniqué 25, 1, pp. 31-44.

Instron (2005) "Reference manual - Software", Instron supplied

Jaky, J. (1944), "The coefficient of earth pressure at rest", J. Soc. Hung. Eng. Arch., p 355-358

Janbu, J. (1963), "Soil compressibility as determined by oedometer and triaxial tests", Proc. Euro. Conf. on Soil Mechanics and Foundation Engineering, Wiesbaden, Vol. 1, pp 19-25.

Jardine, R.J., Fourie, A., Maswoswe, J. and Burland, J.B. (1985), "Field and laboratory measurements of soil stiffness", Proc. 11th Int. Conf. on Soil Mechanics and Foundation Engineering, San Francisco, 2, pp 511-514.

Jardine, R.J., Lehanem B.M., Smith, P.R. and Gildea, P.A. (1995), "Vertical loading experiments on rigid pad foundations at Bothkennar", Géotechnique 45, No. 4, pp 573 - 597

Kelly, P. (2014), "Soil structure interaction and group mechanics of vibrated stone column foundations", University of Sheffield, England.

Kennedy, K.C. (1959), Discussion: Journal Soil Mechanics Foundation Division, ASCE, Vol. 85, No. SM3, pp67-69.

Killeen, M. (2012), "Numerical modelling of small groups of stone columns", National University of Ireland, Galway.

Kimura, T., Nakase, A., Saitoh, K., and Takemura, J. (1983), “Centrifuge tests on sand compaction piles”, Proc. 7th Asian Regional Conference on Soil mechanics and foundation engineering, Vol. 1, pp. 255-260.

Kirsch, F. (2006), "Vibro stone column installation and its effect on the ground improvement", Int. Conf. on Numerical Simulation of Construction processes in Geotechnical Engineering for the Urban Environment, Bochum, pp 115-124.

Kirsch, F. (2008), "Evaluation of ground improvement by groups of vibro stone columns using field measurements and numerical analysis", Proceedings of the second international workshop on geotechnics of soft soils, Glasgow, Scotland, 3rd to 5th September 2008, pp. 241-247.

Klein, E.M. and Tobin, R.F. (1996), "Design & construction of Deep Stone Columns in Marine Clay at Spectacle Island", Civil Engineering Practice, Spring/Summer 1996.

Kleinhans, M.G., Markies, H., de Vet, S.J., in't Veld, A.C. and Postema (2011), "Static and dynamic angles of repose in loose granular materials under reduced gravity", Journal of Geophysical research, Vol 116, E11004, pp. 1-13.

Krishnan, J.M. and Rajagopal, K.R. (2003), "Review of the uses and modeling of bitumen from ancient to modern times", Appl. Mech. Rev. 56(2), pp 149-214

Lee, J.S. and Pande, G.N. (1994) “Analysis of stone column reinforced foundations”, Departmental Research Report CR/835/94, University College of Swansea.

Lee, J.S. and Pande, G.N. (1998), “Analysis of stone column reinforced foundations”, Int. Jour. for Numerical and Analytical methods in Geomechanics, 22 (12), pp. 1001-1020.

Leroueil, S., Lerat, P., Hight, D.W. & Powell, J.J.M. (1992), "Hydraulic conductivity of a recent estuarine silty clay at Bothkennar, Scotland", Géotechnique 42, No.2, pp 275 - 288

Lloyd, I.M. (1989), "The location and investigation of a test-bed site for research on soft clay", PhD thesis, University of Bristol.

Mar, A. (2002), "How to undertake finite element based geotechnical analysis", NAFEMS publication, No ISBN, pp. 1-47.

Marshal, R.J. (1967), "Large scale testing of rockfill", Journal of Soil Mechanics and Foundations Division, ASCE 93 (SM2), pp 27-43.

McCabe, B.A., Nimmons, G.J., Egan, D. (2009), "A review of field performance of stone columns in soft soils", Geotechical Engineering 162, Dec 2009, Issue GE6, pp. 323-334.

McKelvey, D., Sivakumar, V., Bell A., and Graham, J. (2004), “Modelling vibrated stone columns in soft clay”, Geotechnical Engineering, ICE, July 2004, Issue GE3, pp. 137-149.

Mitchell, J.K. Mitchell and Huber, T.R. (1983) “Stone column foundations for a wastewater treatment plant- A case history”, Geotechnical Engineering, Vol. 14, No.2., pp. 165-185.

Mitchell, J.K. and Huber, T.R. (1985), “Performance of a stone column foundation”, Jour. Of Geotech. Eng. ASCE Vol. 111, No.2, Feb. 1985, pp. 205-223.

Moreau, Neil and Mary (1835), “Foundations – employ du sable”, Annales des Ponts and Chaussees, Memoirs, No. 224, pp. 171-214.

Muir-Wood, D., Hu, W. and Nash, D.F.T. (2000), "Group effects of stone column foundations: model tests", Geotechnique 50(6), pp 689-698.

Munfakh, G.A. (1984), “Soil reinforcement by stone columns – Varied case applications”, International conference on insitu soil and rock reinforcement, Paris, pp. 157-162.

Narasimha Roa, S., Prasad, C.V., Prasad, Y.V.S.N., and Hanumanta Roa, V. (1992), “Use of stone columns in soft marine clays”, Proceedings of the 45th Canadian Geotechnical Conference, Toronto, Ont., pp. 9/1 – 9/7.

Nash, D.F.T., Powell, J.J.M. and Lloyd, I.M. (1992a), "Initial investigations of the soft clay site at Bothkennar", Géotechnique 42, No.2, pp163 - 181

Nash, D.F.T., Sills, G.C. and Davison, L.R. (1992b), "One-dimensional consolidation testing of the soft clay from Bothkennar", Géotechnique 42, No. 2, pp 241 - 256

Nemati, K.M. (2014), "CM425 Concrete Technology", University of Washington

Neville, A.M. and Brooks, J.J. (1997), "Concrete Technology", Prentice-Hall.

Özturan, T., ÇeÇen, C. (1997), "Effect of coarse aggregate type on mechanical properties of concrete with different strengths", Cem. Conr. Res. 27(2), pp 165-170

Pande, G.N., Lee, J.S. & Amaniampong, G. (1994), "A numerical model for stone-column reinforced foundations", Computer Methods and Advances in Geomechanics, Siriwardane & Zaman (eds), Balkema, Rotterdam.

Paul, M.A., Peacock, J.D. and Wood, B.F. (1992), "The engineering geology of the Carse clay at the National Soft Clay Research Site, Bothkennar", Geotéchnique, 42, No 2, pp 183-198.

Pennine (2001), "Design/ Tender Manual", Pennine Vibropiling

Potts, D.M. and Zdravkovic, L (1999), "Finite element analysis in geotechnical engineering: theory", Thomas Telford

Preece, D. (2007) Personal communication.

Priebe, H.J. (1991), "Vibro Replacement - Design Criteria and Quality Control", Deep Foundation improvements: Design construction and testing STP 1089, ASTM 1991.

Priebe, H.J. (1995), “The design of vibro replacement”, Ground Engineering, December 1995, pp. 31 – 37.

Randolph, M. F., Steenfelt, J.S. and Wroth, C.P. (1979), "The effect of pile type on design parameters for driven piles", Proc. 7th European Conf. on Soil Mechanics and Foundation Engineering, London, 2, pp 107-114.

Rowe, P.W. (1962), "The stress-dilatancy relation for static equilibrium of an assembly of particles in contact", Proceedings of the Royal Society A, 269, pp 500 - 527

Sahin, R., Demirboğ, R.A., Uysal, H., Gŭl, R. (2003), "The effect of different cement dosages , slumps and pumice aggregate ratios on the compressive strength and densities of concrete" Cem. Conr. Res. 33(8), pp 1245-1249

Sathishbalamurugan, M. and Muhunthan, B. (2008), "Modelling embankments reinforced with sand columns", Ground Improvement, 161, Issue G12, pp. 71-78.

Schanz, T., (1998), "Zur modellierung des mechanischen verhaltens von reibungsmaterialen", Heft 45, Habilitation, Stuttgart Universität.

Scotash (2007) "BS EN 450 Fly Ash: Sustainable solutions for construction specialists", Scotash/ Lafarge

Senol, A., Edil, T.C., Shafique, M.S.B., Benson, C.H. (2006), "Soft subgrades stabilization by using Fly Ashes", Resources, Conservation and Recycling, 46 (4); pp 365 – 376

Serridge (2006), Personal communication

Serridge, C.J. and Sarsby, R.W. (2008), "A review of the field trials investigating the performance of partial depth vibro stone columns in a deep soft clay deposit", Proceedings of the second International Workshop on Geotechnics of Soft Soils, Glasgow, Scotland, 3rd- 5th September 2008.

Siddique, R. (2003), "Effect of fine aggregate replacement with Class F fly ash on the mechanical properties of concrete", Cement and Concrete Research, No. 33 (4), pp 539 - 547

Sivakumar, V., McKelvey, D., Graham, J. and Hughes, D. (2004), "Triaxial tests on model sand columns in clay", Canadian Geotechnical Journal, 41, No.2, pp 299 – 312.

Sivakumar, V., Jeludine, D.K.N.M, Bell, A., Glynn, D.T., Mackinnon, P. (2011), "The pressure distribution along stone columns in soft clay under consolidation and foundation loading", Géotechnique 61, No.7, pp 613-620.

Sondermann, W., Wehr, W. (2004), "Deep vibro techniques", Ground Improvement, 2nd edition, Moseley & Kirsch, Spon Press, pp 57-92.

Stewart, B. & Hu, W. (1993), "Analysis of regularly inhomogeneous soils: Report on pilot tests. Technical report", Dept. of Civil Engineering, University of Glasgow, U.K.

Stewart, D.P. and Fahey, M. (1994), "An examination of the integrity of stone columns in soft clay", Centrifuge '94, Rotterdam, Rotterdam, Balkena, 1: pp 773 – 778.

Swiss Standard SN 670 010b (2013), "Characteristic Coefficients of soils" Association of Swiss Road and Traffic Engineers

Thorburn, S. and MacVicar, R.S.L. (1968), "Soil stabilisation employing surface and depth vibrators", The Structural Engineer, 46, No.10, pp. 309-316.

Tomlinson, M.J. (2001), "Foundation design and construction", 7th Edition, Pearson Prentice Hall.

Venkatarama Reddy, B.V. and Gourav, K. (2011), "Strength of lime-fly compacts using different curing techniques and gypsum additive", Materials & Structures, 44 (10), pp 1793-1808.

Vesic, A.S. (1972), "Expansion of cavities in infinite soil mass", Journal of the Soil Mechanics and Foundations Division, ASCE, Vol. 98, No. SM3, Proc. Paper 8790, Mar. 1972, pp. 265-290.

Watts, K.S. and Charles, J.A. (1991), "The use, testing and performance of vibrated stone columns in the United Kingdom", Deep foundation improvements: Design, construction, and testing, ASTM STP 1089.

Watts, K.S. and Serridge, C.J. (2000), "A trial of vibro bottom-feed stone column treatment in soft clay soil", In Grouting, soil improvement: geosystems including reinforcement (ed. Rath-Mayer), pp. 549-556, Helsinki: Building Information Ltd., Helsinki.

Wehr, J. (2004), "Stone columns - single columns and group behaviour", Proc. 5th Int. Conf. on Ground Improvement Techniques, Malaysia, pp 329-340.

Wehr, W.C.S. (2006), "Stone columns - group behaviour and the influence of footing flexibility", Proc. 6th European Conf. on Numerical Methods in Geotechnical Engineering, Graz, Vol. 1, pp 767-772.

Wijeyesekera, D.C., Siang, A.J.L.M, Yahaya, A.S.B. (2013), "Advanced statistical analysis for relationships between particle morphology (size and shape) and shear (static and dynamic) characteristics of sands", Dec 2013, International Journal of Geosciences, vol 4., No. 10A, pp 27-36

Yasuda, N., Ohta, N. and Takahashi, M. (1997), "Dynamic strength properties of undisturbed river bed gravel", Canadian Geotechnical Journal 34 (1), pp 726 - 736